Investigating the physiological and pharmacological effects of the gut hormone peptide YY (PYY)

A thesis submitted for the degree of Doctor of Philosophy at Imperial College London

Aldara Martin Alonso

2021

Section of Endocrinology & Investigative Medicine

Division of Diabetes, Endocrinology & Metabolism

Department of Metabolism, Digestion and Reproduction

Imperial College London

Supervisors: Dr Victoria Salem and Prof Kevin Murphy

Abstract

The obesity epidemic is a critical and global public health burden. Drugs that safely promote weight loss are urgently needed to halt the rising prevalence of obesity and its associated complications, such as type 2 diabetes (T2D). Gut hormones are important regulators in metabolism and have therapeutic potential as treatments for obesity and T2D. The gut hormone peptide YY (PYY) is released from the intestine after a meal. Exogenous $PYY_{3–36}$ suppresses food intake in both rodents and humans, including in the obese state. $PYY_{3–36}$ suppresses appetite by acting on its receptor, the Y2R. Y2R is expressed in brain appetite centres but also in the afferent vagus nerve, the main neuroanatomical link carrying information from the gut to the brain. However, the relevant contribution of the afferent vagus to the overall effects of $PYY_{3–36}$ is unknown. Chemogenetic activation of vagal afferent neurones results in reduced food intake (surpassing the effects of PYY) and might have altered the immune landscape of the gastrointestinal tract. To dissect the role of the Y2R expressed in the afferent vagus, we have developed a novel microsurgical technique in the mouse. Our work suggests that vagal Y2R mediates the anorectic effect of low dose and endogenous $PYY_{3–36}$ and that this vagal signalling pathway regulates short-term feeding. This anorectic effect was not caused by an aversive response. In vitro calcium imaging confirmed that $PYY_{3–36}$ directly activates vagal afferents. Chronic treatment of diet-induced obese (DIO) mice with a long-acting $PYY_{3–36}$ analogue, Y242, did not cause a significant body weight loss. Longitudinal tracking of individual islet function using a novel imaging platform allowed to study the effect of diet and Y242 treatment. Chronic Y242 did not improve or worsen islet function in obese mice. Therefore, PYY-based treatments might not be suitable as a single agent but have potential in combination with other gut-hormones. Vagus nerve neuromodulation has shown potential as an anti-obesity therapy and the work in this thesis adds to a better understanding of vagal afferent function which will help optimise therapeutic interventions.

Copyright declaration

Declaration of contributors

The majority of the work presented in this thesis was performed by the author. All collaboration and assistance are described below:

Chapter 2: All the flow cytometry work (tissue harvesting and processing, staining, and analysis) was performed in collaboration with Dr Noe Rodriguez Rodriguez (MRC Laboratory of Molecular Biology (LMB), Cambridge, UK). Reagents were also donated by Dr Noe Rodriguez Rodriguez. Phyllis Phuah helped with calcium imaging of neurons.

Chapter 3: All the animal models were established in collaboration with Dr SC Cork, who also helped in the feeding studies. Dr Victoria Salem and Prof Walter Distaso performed analysis of meal patterning. Radioimmunoassay was performed with the assistance of Prof Kevin Murphy and analysed with the help of Dr Georgia Franco Becker.

Chapter 4: All *in vivo* work was conducted with the assistance of Dr Kinga Suba and Dr Yat Patel. All *in vivo* imaging studies were conducted by Dr Victoria Salem and Dr Kinga Suba. The analogue was kindly donated by Prof Sir Steve Bloom.

Acknowledgements

Firstly, I would like to thank my main supervisor Dr Victoria Salem for giving me the opportunity to work on this exciting project as well as for all her support and patience. Special thanks to Prof Kevin Murphy for his expertise and guidance during my PhD. I am extremely grateful to Dr Simon Cork for all his invaluable advice, support and friendship.

I am very grateful for the help received from many members of the division and collaborators. I am particularly thankful to Dr M Norton, Dr Y Patel, P Phuah, Dr I Freitas, Dr K Suba and Dr Stolarczyk for all their help, expertise and friendship.

I would like to thank the Central Biomedical Services at Imperial College London for their advice and help.

And last, but not least, I would like to thank my parents for their unconditional support and confidence as well as to my partner and all the special people in my life that have supported me along the way.

Abbreviations

5-HT	5-hydroxytryptamine
α7nAchR	α7 subtype of the nicotinic acetylcholine receptor
α-MSH	α-melanocyte-stimulating hormone
AAV	Adeno-associated Virus
AC	Adenylate cyclase
ACE	Anterior chamber of the eye
ACh	Acetylcholine
ADP	Adenosine diphosphate
AF	Alexa Fluor™
AgRP	Agouti-related peptide
AP	Area postrema
APC	Allophycocyanin
ARC	Arcuate nucleus
Arg1	Arginase 1
ATP	Adenosine triphosphate
AUC	Area under the curve
BMI	Body mass index
BUV	Brilliant Ultraviolet™
BV	Brilliant Violet™
CAIP	Cholinergic anti-inflammatory pathway
cAMP	Cyclic adenosine monophosphate
CART	Cocaine- and amphetamine-regulated transcript
CasR	Calcium-sensing receptor
CB1	Cannabinoid type-1 receptor
CCK	Cholecystokinin
CCK-R	Cholecystokinin receptor
CD	Cluster of differentiation
cDNA	Complementary desoxyribonucleic acid
CeA	Central amygdala
CLAMS	Comprehensive Lab Animal Monitoring System
CGRP	Calcitonin gene-related peptide
CNO	Clozapine-N-Oxide

CNS	Central nervous system
Comp21	Compound 21
CTA	Conditioned taste aversion
CX3CR1	CX3C chemokine receptor 1
Cy	Cyanine
DA	Dopamine
DAG	Diacylglycerol
DC	Dendritic cell
DIO	Diet-induced obesity
DMEM	Advanced Dulbecco's Modified Eagle medium
DMH	Dorsomedial nucleus of the hypothalamus
DMX	Dorsal motor nucleus of the vagus
DNA	Desoxyribonucleic acid
DREADD	Designer Receptor Exclusively Activated by Designer Drugs
DRG	Dorsal root ganglia
DRN	Dorsal raphe nucleus
DVC	Dorsal vagal complex
EEC	Enteroendocrine cell
EGR-1	Early growth response-1
ENS	Enteric nervous system
Epac2	Exchange protein directly activated by cAMP 2
F	Calcium fluorescence signal
FACS	Florescence-activated Cell Sorting
FBS	Fetal bovine serum
FCS	Fetal calf Serum
FcεRI	Fc fragment of immunoglobulin E receptor
FDA	United States Food and Drug Administration
FFA	Free fatty acid
FI	Food intake
FITC	Fluorescein isothiocyanate
fMRI	Functional magnetic resonance imaging
Fox P3	Forkhead Box P3
FSC	Forward scatter
FSC-A	FSC - area
FSC-H	FSC - height

FWHM	Full width at half maximum
GABA	γ-aminobutyric acid
GATA3	GATA Binding Protein 3
GC	Genome copy
GCG	Glucagon
GCGR	Glucagon receptor
GDNF	Glia cell—derived neurotrophic factor
GFP	Green fluorescent protein
GHSR	Growth hormone secretagogue receptor
GLP-1	Glucagon-like peptide 1
GLP-1R	Glucagon-like peptide 1 receptor
GLUT	Glucose transporter
GPCR	G-Protein-coupled receptor
GSIS	Glucose-stimulated insulin secretion
HFD	High-fat diet
HKRB	HEPES-buffered Krebs-ringer bicarbonate
HPA	Hypothalamic-pituitary-adrenal
i.p.	intraperitoneal
i.v	intravenous
IBD	Inflammatory Bowel Disease
IC_{50}	Half maximal inhibitory concentration
ICS	Intracellular cytokine staining
IFN-γ	Interferon γ
IgA	Immunoglobulin A
IGLEs	Intraganglionic laminar endings
IL	Interleukin
ILC	Innate lymphoid cell
IMAs	Intramuscular arrays
INS5L	Insulin-like 5 peptide
IP	Intraperitoneal
IP_3	inositol triphosphate
IPGTT	Intraperitoneal glucose tolerance test
IPITT	Intraperitoneal insulin tolerance test
ITR	Inverted terminal repeats
KD	Knockdown

KO	Knockout
LepR	Leptin receptor
LH	Lateral hypothalamic area
LPS	Lipopolysaccharide
MC-R	Melanocortin receptors
ME	Median eminence
MHC	Major histocompatibility complex
MCHR1	Melanin-concentrating hormone receptor-1
MM	Muscularis Macrophages
mRNA	Messenger ribonucleic acid
MTA	Material Transfer Agreement
NAc	Nucleus accumbens
NCD	Non-communicable disease
NEFA	Non-esterified fatty acid
NG	Nodose ganglia
NMU	Neuromedin U
NPY	Neuropeptide Y
NTS	Nucleus tractus solitarii
OC	Optic chiasm
OFC	Orbitofrontal cortex
OGTT	Oral glucose tolerance test
OXM	Oxyntomodulin
P/S	Penicillin/Streptomycin
PBN	Parabrachial nuclei
PBS	Phosphate-buffered Saline
PCR	Polymerase chain reaction
PE	Phycoerythrin
PerCP	Peridinin chlorophyll
PFC	Prefrontal cortex
PI3K	Phosphatidylinositol-3-kinase
PI3Kγ	Phosphoinositide 3-kinase γ
PK	Protein kinase
PKA	Protein kinase A
PLC	Phospholipase C
POMC	Proopiomelanocortin

PP	Pancreatic polypeptide
PVN	Paraventricular nucleus
PYY	Peptide YY
RER	Respiratory exchange ratio
Rho	Ras homolog family
RhoGEF	Rho guanine nucleotide exchange factor.
RNA	Ribonucleic acid
ROI	Region of interest
RORγt	RAR (Retinoic acid receptor)-related orphan receptor γ
RPMI	Roswell Park Memorial Institute Medium
RT	Room temperature
RYGB	Roux-en-Y gastric bypass
s.c.	subcutaneous
SCFA	Short-chain fatty acid
SEM	Standard error of the mean
SGLT-1	Sodium-coupled glucose linked transporter 1
shRNA	Short-hairpin ribonucleic acid
SSC	Side scatter
SSC-A	SSC - area
SSC-H	SSC - height
T2D	Type 2 diabetes
TAE	Tris-acetate-EDTA
TCRβ	T-cell receptor β chain
TG	Trigeminal ganglia
T_H	Helper T Cell
TLR4	Toll-like receptor 4
TNF	Tumor Necrosis Factor
T_{reg}	Regulatory T-Cell
VDCC	Voltage-dependent calcium channels
VIP	Vasoactive Intestinal Peptide
VMH	Ventromedial nucleus of the hypothalamus
VNS	Vagus Nerve Stimulation
WHO	World Health Organisation
WT	Wild-type
Y2R	Y2 Receptor

Table of Contents

Index of figures

Index of tables

Chapter 1: General introduction

1.1. Obesity and diabetes

Obesity and overweight are defined by the World Health Organisation (WHO) as an abnormal or excessive accumulation of fat that may impair health. Although the causes are heterogenous, the fundamental cause is the energy imbalance between energy consumed and energy expended.
Clinically, obesity and overweight are mainly defined by body mass index (BMI), which is weight in kilograms divided by the square of height in meters (World Health Organization, 2020). Overweight is defined as a BMI greater or equal to 25 kg/m^2 while obesity is a BMI greater than or equal to 30 kg/m^2. Worldwide, the prevalence of obesity has nearly tripled since 1975. In 2016, the WHO reported that 39% of adults worldwide were overweight and 13% were obese (World Health Organization, 2020). With the current trend, 1 in 5 adults worldwide will be obese by 2025 (World Obesity, 2020). These increases have been driven by factors including easy accessibility to food and the shift to a more sedentary lifestyle. Obesity is a global health concern and does not only affect high-income countries. Many countries where undernutrition prevails are now facing a double burden of malnutrition.

Obesity is a major risk for the development of type 2 diabetes (T2D), a condition that causes high blood glucose levels due to a dysfunctional insulin release in the setting of peripheral insulin resistance, the complications of which remain the leading causes of blindness and renal failure (World Health Organization, 2016). High BMI is also a major risk factor for other common non-communicable diseases (NCD), such as cardiovascular disease and some cancers (World Health Organization, 2020).
Despite the high cost of obesity and its medical consequences on healthcare systems, compounded by the indirect costs, such as reduced productivity and quality of life, it has not yet been possible to develop an effective and safe weight-loss drug.

1.1.1 Current anti-obesity treatments

Lifestyle interventions are the cornerstone for the management of overweight/obesity and other NCDs, including T2D and cardiovascular disease. They aim to achieve an energy balance and a healthy body weight by dieting (in general, limiting the intake of fats, sugar and salt and increasing the consumption of healthy foods, such as vegetables and whole grains), and regular physical activity (World Health Organisation, 2004). However, patients have poor adherence to lifestyle changes (Dansinger *et al.*, 2005; Burgess, Hassmén & Pumpa, 2017) and, after weight loss, physiological factors (e.g., compensatory reductions in energy expenditure and changes in circulating appetite-regulatory hormones) can promote weight regain (Greenway, 2015).

1.1.2 Bariatric surgery

At present, the most effective and enduring anti-obesity treatment is bariatric surgery. It is a major gastrointestinal surgery usually only available for the most severe cases of obesity. Bariatric surgery is indicated for patients with BMI ≥ 40 kg/m^2 or a BMI between 35 and 40 kg/m^2 and an obesity-related condition (National Institute for Health and Care Excellence, 2014). In addition, these patients must have tried non-surgical treatment options that failed to achieve clinically beneficial weight loss. The Swedish Obese Subject trial (ClinicalTrials.gov., 2011) was the first long-term prospective study examining the effects of bariatric surgery (Sjöström, 2013). Bariatric surgery results in around 20-30% body weight loss and attenuates or reverses many obesity-associated diseases, including T2D, and reduces mortality. There are different bariatric surgical procedures available, of which the Roux-en-Y gastric bypass (RYGB) is the most popular. The RYGB surgery is based on creating a small stomach pouch whose outlet is a Y-shaped limb of the small intestine (Roux limb). Consequently, food does not pass through the stomach and the duodenum.

The mechanisms underlying the weight-loss achieved by RYGB have been studied in detail and are likely to be multifactorial. A widely accepted hypothesis suggests that a major element of the weight loss after RYGB is due to a reduced food intake caused by an increase release of anorexigenic gut hormones (see section 1.4.2), such as glucagon-like peptide 1 (GLP-1) and peptide YY (PYY) (Le Roux *et al.*, 2006; Pournaras *et al.*, 2010; Beckman *et al.*, 2011). On the other hand, it has also been suggested that the surgery could disrupt the vagus nerve, which is the main neural link between the gut and the brain, and which is involved in gut hormone action on the brain (Hao *et al.*, 2014).
In the near future, with the current obesity epidemic, an increasing number of surgeries will be needed. However, this is an irreversible procedure involving some risks and complications. Treatments that are as effective as bariatric surgery but less invasive are clearly needed.

1.1.3 Weight loss pharmacotherapy

Different drug-based weight-loss treatment strategies are under study and have been recently reviewed (Srivastava & Apovian, 2018). Various previously developed drugs had been removed due to low effectiveness and safety concerns. Rimonabant, an anti-obesity cannabinoid type-1 receptor (CB1) antagonist, caused psychiatric adverse effects and was worldwide withdrawn from the market in 2008. The centrally acting monoamine-reuptake inhibitor Sibutramine suppress appetite but also caused cardiovascular adverse events and was removed in most countries in 2010.

Currently, only two anti-obesity pharmacological treatments are available in the UK. Orlistat, licensed in 1998, is an inhibitor of gastric and pancreatic lipase (which hydrolyse dietary triglycerides in free fatty acids) that reduces fat absorption by approximately 30%. The gastrointestinal side effects (e.g., faecal incontinence, flatulence) and the modest weight loss achieved result in many patients stopping the treatment. Liraglutide (Saxenda), is a glucagon-like peptide 1 receptor (GLP-1R) agonist that was approved in Europe in 2015. Very recently, the latest generation of GLP-1R agonists have shown "game changing" weight loss benefits of up to 20 kg in some trials (Wilding *et al.*, 2021). In addition to its effects as an incretin (promoting glucose stimulated insulin secretion), GLP-1 is an anorectic gut hormone that also inhibits appetite via both vagal and central mechanisms (Turton *et al.*, 1996; Abbott *et al.*, 2005a; Secher *et al.*, 2014; Krieger *et al.*, 2016). This success shines a light on the utility of naturally derived appetite inhibitors for the safe treatment of obesity. New therapeutic approaches for obesity include exploiting combination gut hormones (see section 1.4.3).

In the US, additional central-acting anti-obesity treatments have been recently approved. In 2012, the United States Food and Drug Administration (FDA) approved Belviq XR (lorcaserin), an agonist of the 5-hydroxytryptamine (5-HT, also known as serotonin) receptor 2C, for weight loss. However, the FDA has recently requested the withdrawal of this drug due to an increased risk of cancer (U.S Food and Drug Administration, 2020). Also approved in 2012, Qsymia® is a combination treatment (phentermine/topiramate) the mechanism of which is not completely understood, but which has shown great weight loss efficacy. Contrave® (by Orexigen), a sustained release combination therapy of a dopamine and noradrenaline re-uptake inhibitor (bupropion) and a μ-opioid antagonist (naltrexone), was approved by the FDA in 2014. However, none of these drugs have been particularly well tolerated or effective in clinical practice and there remains a serious lack of safe, effective weight loss medications and none that can recreate the long-term weight loss and mortality reducing benefits of bariatric surgery.

1.2 Energy homeostasis regulation by the brain

In order to design safe and effective weight loss medications it is vital to understand in depth the complex neuroendocrinology of food intake and body weight regulation. Food intake and energy expenditure regulation are controlled by different circuits in the nervous system. Neural networks receive and process sensory information from external (e.g., taste, smell) and internal (e.g., meal-derived gastrointestinal signals, glucose levels) sources. The output, such as eating or neuroendocrine actions, is also influenced by behaviours (e.g., vigilance), circadian timing, and other sensory information (e.g., reward-aversion, memory).

The nervous system is divided into the central nervous system (CNS), which consists of the brain and the spinal cord, and the peripheral nervous system, which is formed by nerves that connect the CNS to the rest of the body. Within the CNS, autonomic circuits in the hypothalamus and the brainstem coordinate energy homeostasis by integrating peripheral signals and modulating other brain regions involved in non-homeostatic control of energy balance, such as motivation and reward (Berthoud, 2011; Gautron, Elmquist & Williams, 2015).

1.2.1 The role of the Hypothalamus in energy homeostasis

Energy homeostasis is controlled by subpopulations of neurones located in specific hypothalamic nuclei that can interact with other hypothalamic neuron subpopulations as well as with other extrahypothalamic sites. Discrete neuronal subpopulations in the arcuate nucleus (ARC) regulating energy homoeostasis have been of particular interest in recent years.

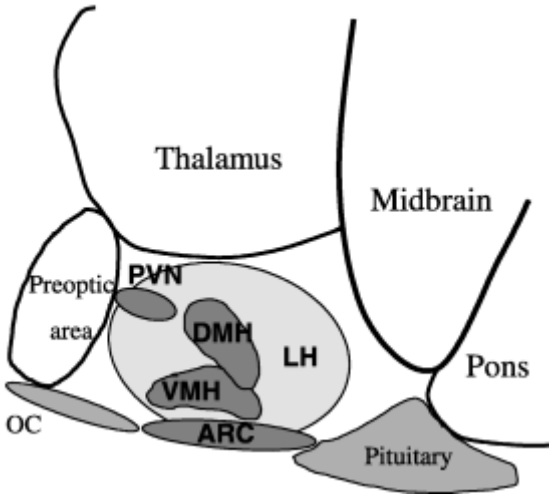

Figure 1.2.1.1. Schematic diagram of the hypothalamus (lateral view) and the nuclei important in energy homeostasis.

ARC, arcuate nucleus; DMH, dorsomedial nucleus of the hypothalamus; LH, lateral hypothalamic area; OC, optic chiasm; PVN, paraventricular nucleus; VMH, ventromedial nucleus of the hypothalamus; (adapted from (Neary, Goldstone & Bloom, 2004)).

1.2.1.1 The arcuate nucleus (ARC)

The hypothalamic ARC is ventrally situated on each side of the third ventricle, above the median eminence (ME). The ME is a circumventricular organ, which has an incomplete blood-brain barrier, so peripheral nutrients as well as hormones have easy access to the ARC.

There are two major ARC neuronal populations involved in the regulation of energy homeostasis. The first expresses agouti-related peptide (AgRP), neuropeptide Y (NPY) and γ-aminobutyric acid (GABA) (NPY/AGRP neurones) and increases food intake, and the second expresses proopiomelanocortin (POMC) and cocaine- and amphetamine-regulated transcript (CART) (POMC/CART neurones) and decreases food intake. Importantly, GABA tonically inhibits POMC/CART neurones (Cowley *et al.*, 2001) Initially, it was observed that adiposity signals such as leptin, activated anorectic POMC/CART neurones (Cowley *et al.*, 2001; Benoit *et al.*, 2002) and inhibited orexigenic NPY/AgRP neurones (Schwartz *et al.*, 1992, 1996), promoting negative energy balance via the melanocortin system. Importantly, other peripheral signals, such as gut hormones, can also modulate the activity of these ARC neuronal populations.

1.2.1.2 The central melanocortin system

Both POMC/CART and NPY/AGRP neurones interact with intrahypothalamic and extrahypothalamic sites to control feeding behaviour and energy homeostasis. These ARC neuronal populations, as well as other downstream target neurones, form the central melanocortin circuit.

The melanocortin system regulates endocrine and homeostatic processes, including feeding behaviour (Ellacott & Cone, 2006). Melanocortin peptides are derived from POMC precursor hormone, which undertakes different enzymatic steps to yield different peptides in a tissue-specific fashion. Melanocortin peptides exert their actions by binding to the melanocortin receptors (MC1-R to MC5-R). MC3-R and MC4-R are involved in energy balance regulation. MC3-R is mainly expressed in the hypothalamus and is the only MC-R found in POMC/CART and AgRP/NPY neurones. MC4-Rs are located in the other hypothalamic sites and in brainstem. MC4-Rs in the PVN and amygdala are involved in food intake suppression (Balthasar *et al.*, 2005). α-melanocyte-stimulating hormone (α-MSH) is the most potent endogenous MC4-R agonist, while AgRP acts as an endogenous antagonist for MC3-R and MC4-R. When POMC/CART neurones are activated by adiposity signals, α-MSH is released to act on downstream pathways. Evidence suggests that α-MSH tonic signalling restrains food intake, as having a dysfunctional or absent MC4-R results in obesity in rodents and humans (Huszar *et al.*, 1997; Vaisse *et al.*, 1998; Yeo *et al.*, 1998). When adiposity and nutritional signals are low, NPY/AgRP activation results in the release of AgRP, which inhibits melanocortin signals, increasing appetite.

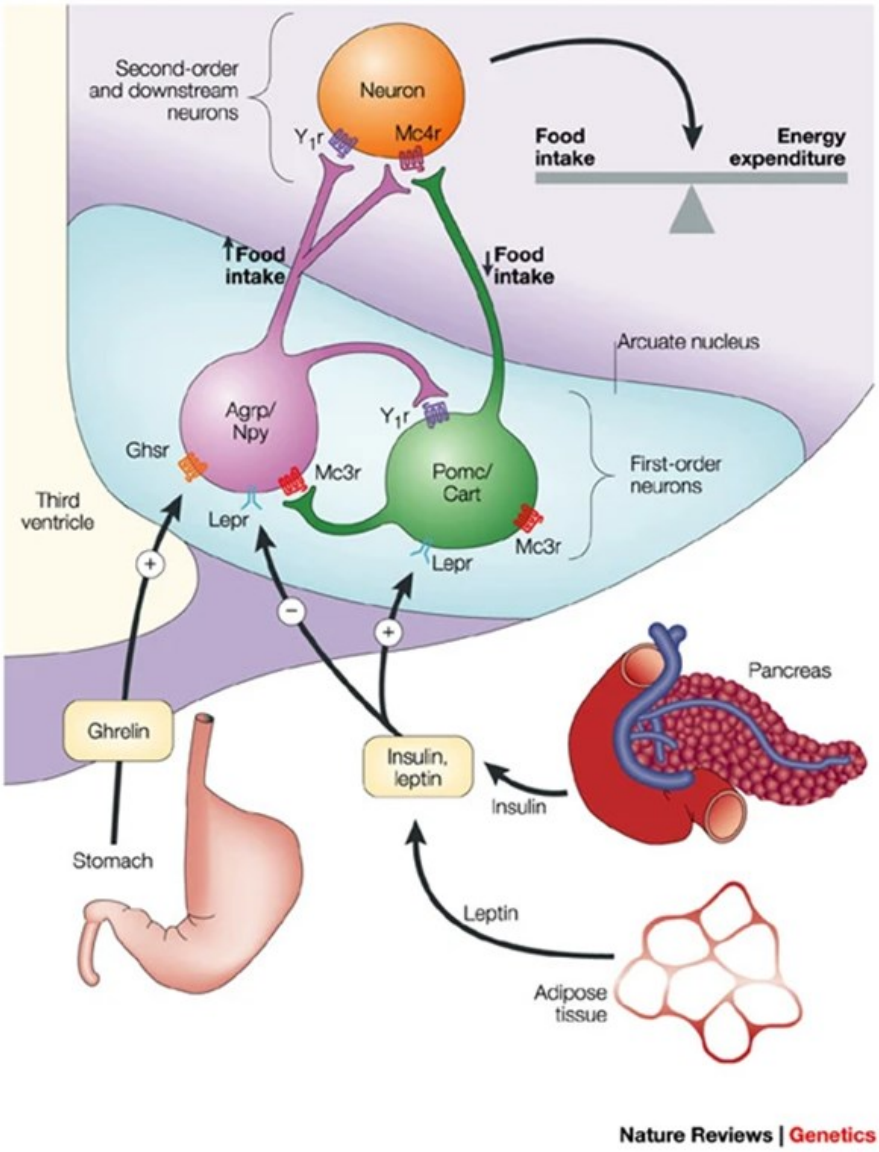

Figure 1.2.1.2. Control of food intake by hormones.

Two sets of neurones in the arcuate nucleus: AgRP/NPY and POMC/CART neurones. By communicating with second order neurones, AgRP/NPY and POMC/CART neurones promote or suppress food intake, respectively. They are regulated by circulating factors (e.g., ghrelin, insulin, leptin). AgRP, agouti-related protein; CART, cocaine- and amphetamine-regulated transcript; GHSR, growth hormone secretagogue receptor; LepR, leptin receptor; MC3/4R, melanocortin receptor 3/4; NPY, neuropeptide Y; POMC, proopiomelanocortin; Y1R, neuropeptide Y1 receptor. From (Barsh & Schwartz, 2002).

1.2.1.3 Other hypothalamic nuclei

The first-order POMC/CART (anorectic) and AgRP/NPY (orexigenic) neurones of the ARC innervate to similar locations in the forebrain. In these sites, they can activate or inhibit second-order neurones by the action of neuropeptides, including those of the melanocortin system (α-MSH and AgRP), GABA and NPY.

Within the hypothalamic nuclei receiving innervation from the ARC, some of the neuronal subpopulations involved in energy homeostasis regulation have been studied. Based on lesioning and stimulating studies (Tokunaga *et al.*, 1986), the paraventricular nucleus of the hypothalamus (PVN) was originally considered an anorectic nucleus, while the lateral hypothalamic area (LH) was considered an orexigenic site. While this model has been superseded by one which recognises that different neuronal circuits within a nucleus can have contrasting effects on energy homeostasis, it nevertheless remains the case that the PVN mediates important anorectic signalling pathways, and the LH contains circuits involved in increasing food intake.

Second-order neurones of the PVN involved in energy balance can express hormones, such as oxytocin, corticotropin-releasing hormone and thyrotropin-releasing hormone. These can be activated by leptin directly or indirectly via the ARC (Blevins, Schwartz & Baskin, 2004; Nillni, 2010).
The LH also receives innervation from the ARC. Here, orexin-and MCH-expressing neurones are located and believed to signal to promote food intake (Qu *et al.*, 1996; Sakurai *et al.*, 1998; Shimada *et al.*, 1998; Ludwig *et al.*, 2001).

Other nuclei innervated by the ARC involved in energy homeostasis include the ventromedial nucleus (VMH) and the dorsomedial hypothalamic nucleus (DMH). These nuclei also communicate with the brainstem.

1.2.2 The role of the Brainstem in energy homeostasis

Whereas the hypothalamus has been traditionally associated with the response to adiposity, the brainstem has been more associated with the response to acute food intake. Visceral sensory neurones carry gut feedback signals to the brainstem, which relays these signals to hypothalamic nuclei and the limbic system, which is involved in the motivation and reward aspects of feeding (see section 1.2.3). Within the brainstem, neuronal populations are heterogenous and express a range of appetite-regulating neuropeptides also expressed in the hypothalamus, including POMC, CART and NPY. Brainstem populations also express the enzymes required for the synthesis of GABA and dopamine (Schwartz, 2006). The melanocortin pathway is also present in the brainstem and can influence the processing of gut derived neural signals (Zheng *et al.*, 2005).

Within the caudal brainstem, the nucleus tractus solitarii (NTS) is key in transmitting information of energy-related signals from the periphery to the hypothalamus and other brain areas, but it also receives neuronal inputs from midbrain and forebrain areas (Schwartz, 2006).

1.2.2.1 The nucleus of the tractus solitarius (NTS)

The NTS is part of the dorsal vagal complex (DVC), which is formed by the nucleus of the solitary tract (NTS), the area postrema (AP) and the dorsal motor nucleus of the vagus nerve (DMX).
The DVC is directly exposed to circulatory satiety signals in response to meal intake via the AP, which is a circumventricular organ with an incomplete blood brain barrier, like the ME in the ARC. The afferent neurones of the vagus nerve (see section 1.3.1 and 2.1) carry mechanical and chemical information from the gastrointestinal tract to the NTS. In contrast, the neurones within the DMX are parasympathetic motor neurones projecting to visceral organs (Schwartz, 2006).

The NTS is the primary site receiving sensory information from the gastrointestinal tract. It can integrate neural signals from the periphery and from other central regions, including the hypothalamus and limbic centres (van der Kooy *et al.*, 1984; Zhang, Fogel & Renehan, 1999; Zhang *et al.*, 2003). It is widely accepted that meal-related sensory feedback signals are transmitted via the afferent vagus nerve. These mechanosensory and chemosensory vagal afferent neurones, communicating information such as gastric load and cholecystokinin (CCK), can activate NTS neurones and reduce meal size. The NTS is organized so that neuron subpopulations of different subnuclei respond differently to vagal neural signals from the gastric and duodenal compartments (Zhang, Fogel & Renehan, 1995).

The NTS can also integrate circulating signals. For example, leptin increases the excitatory response of gut-connected NTS neurones in response to gastric load (Schwartz & Moran, 2002). MC4-Rs expressed in NTS seem to be involved in mediating the anorexigenic effect of CCK and leptin (Fan *et al.*, 2004; Zheng *et al.*, 2010).

1.2.2.2 The dorsal raphe nucleus

The dorsal raphe nucleus (DRN) is a brainstem nucleus located in the dorsal midbrain and it is involved in reward processing (Liu *et al.*, 2014b) and food intake (Nonogaki *et al.*, 1998) via the serotonin system. A recent study identified two distinct DRN neuron populations that respond to the energy status and regulate food intake, potentially via a local circuit (Nectow *et al.*, 2017). DRN neurones expressing the vesicular GABA transporter Vgat increase feeding and can inhibit DRN neurones

expressing the vesicular glutamate transporter VGLUT3, which suppress food intake (Nectow *et al.*, 2017).

1.2.2.3 The parabrachial nuclei

The parabrachial nuclei (PBN) are located in the rostral brainstem, in the pons. The PBN receives innervation from the NTS, the spinal cord and the forebrain, and sends projections to other forebrain regions, including inhibitory input to the hypothalamus (Palmiter, 2018). PBN neuron populations express different neuropeptides of which calcitonin gene-related peptide (CGRP) has received special attention for its role in feeding regulation (Carter *et al.*, 2013; Campos *et al.*, 2016). Parabrachial CGRP neurones can be activated postprandially and by peripheral gut peptides, such as CCK and GLP-1, and its activation suppresses food intake by promoting meal termination (Carter *et al.*, 2013; Campos *et al.*, 2016). In addition, activation of these CGRP neurones was sufficient to promote conditioned taste aversion, a form of learning in which a novel food is paired with a toxic visceral stimulus, usually lithium chloride (Carter, Han & Palmiter, 2015). Parabrachial CGRP neurones receive inhibitory input from AgRP neurones (Campos *et al.*, 2016) and send projections to the central nucleus of the amygdala that mediate food intake suppresion (Carter *et al.*, 2013)

1.2.3 Reward pathways

Apart from homeostatic-regulated systems, mainly controlled by the hypothalamus and brainstem, non-homeostatic processes are also involved in energy balance regulation (Berthoud, Lenard & Shin, 2011). Non-homeostatic or hedonic eating is controlled by cognitive, emotions and reward factors. Homeostatic and non-homeostatic signals can modulate and override each other to generate a coordinated response (Berthoud, 2011).

Before eating, reward expectancy is determining for the outcome of eating. This involves motivation and the appetitive phase (involving visual and smell cues). During the consummatory phase, direct pleasure from smell and taste drives consumption until satiation. After the first bout during meal intake, other reward signals occur independently of taste receptors and might be mediated by calorie-rich nutrients (de Araujo *et al.*, 2008).

Cortico-limbic reward centres involved in appetite include hippocampus, nucleus accumbens, basal ganglia and amygdala. Within the brain mesolimbic system, dopamine signalling from the ventral tegmental area is involved in encoding the rewarding aspects of food. These dopamine neurones project to other areas, such as the nucleus accumbens, the central amygdala and the prefrontal cortex. Dopamine signalling in the nucleus accumbens is important in both the appetitive phase but also

during the consummatory phase (Hernandez & Hoebel, 1988; Hajnal, Smith & Norgren, 2004; Berthoud, Lenard & Shin, 2011).

The nucleus accumbens, ventral tegmental area and LH form a circuit in which activation of orexin neurones of the LH is linked to consummatory rewards, including food (Harris, Wimmer & Aston-Jones, 2005). Metabolic signals can also modulate food-related reward. Leptin has been shown to modulate dopamine neurones directly as well as indirectly via LH neurones (Leinninger *et al.*, 2009). Gut hormones have also been shown to modulate activity in reward centres using functional magnetic resonance imaging (fMRI) in humans (Batterham *et al.*, 2007; Malik *et al.*, 2008; De Silva *et al.*, 2011).

The vagus nerve also plays a role in gut-derived reward signals (Shechter & Schwartz, 2018). Using optogenetic-mediated activation of vagal sensory neurones and viral tracing, Han and colleagues reported that the sensory neurones of the right NG innervating the upper gut excite brain dopamine cells in the substantia nigra (a structure in the basal ganglia), via the PBN (Han *et al.*, 2018). More recent studies have suggested a role of the vagus nerve in food seeking. A vagal-brainstem circuit has been shown to be critical to develop sugar preference (Tan *et al.*, 2020). Post-ingestive sucrose can support food seeking by modulation of dopamine neurones of the ventral tegmental area, and this effect depended on the vagus nerve (Fernandes *et al.*, 2020).

1.3 Energy homeostasis regulation by the peripheral nervous system

The gut-brain axis is crucial for the control of food intake and regulation of energy balance. The peripheral nervous system connects the CNS with the rest of the body via different nerves. Within the peripheral nervous system, the autonomic nervous system controls involuntary physiological actions, such as digestion, and maintains homeostasis. Autonomic neurones can carry information from the periphery to the CNS (afferent neurones) or vice versa (efferent neurones).

The autonomic nervous system has been classically divided in the sympathetic nervous system, the parasympathetic nervous system and the enteric nervous system. Both the sympathetic and the parasympathetic innervate many tissues where they have opposing effects. The sympathetic nervous system predominates during “fight-or-flight” situations and mainly has an inhibitory influence over the gastrointestinal tract. The parasympathetic nervous system predominates during “rest-and-digest” conditions, promoting homeostatic processes such as digestion and salivation.

The parasympathetic nervous system originates in the brainstem and sacral plexus, and its preganglionic fibres, which have long processes, typically synapse on postganglionic fibres, which are short, in a ganglion near the target organ. The connection between the preganglionic fibre and the postganglionic fibre as well as between the postganglionic fibre and the effector organ is typically cholinergic. Preganglionic neurones from the brainstem leave the brain through specific cranial nerves.

1.3.1 The vagus nerve

The tenth (X) cranial nerve, usually referred as the vagus nerve (see section 2.1), is the largest cranial nerve. It is involved in the bi-directional transmission of information between the brain and visceral organs, including the gastrointestinal tract and pancreas. Afferent (sensory) neurones carry mechanical or chemical information from the gastrointestinal tract to the NTS. The role of the vagus nerve in appetite regulation within the gut-brain axis has been of great interest in recent years. Satiety signals, such as leptin and some gut hormones, can signal to the vagus nerve, which can ultimately mediate appetite suppression via central mechanisms. In addition, the sensitivity of the vagus to these signals is reported to be influenced by nutritional and metabolic status.

1.3.2 The enteric nervous system

The enteric nervous system (ENS), also referred as the “second brain”, is a network of neural and support cells located along the digestive tract that locally regulates gastrointestinal tract functions, such as secretion, gut motility and barrier function. They are formed by enteric neurones, enteric glial cells and interstitial cells of Cajal that are organised into two ganglionated plexuses, the submucosal plexus and the myenteric plexus. Enteric afferent neurones can detect mechanical and chemical stimuli that modulate CNS activity (Knauf *et al.*, 2020). The CNS can also signal via sympathetic and parasympathetic efferent neurones to alter ENS responses (Furness, 2012). A recently characterized microbially-responsive subset of enteric neurones have been reported to modulate blood glucose independently of the CNS (Muller *et al.*, 2020a), suggesting that ENS might act autonomously to regulate processes beyond gastrointestinal motility or secretion.

1.4 Energy homeostasis regulation by metabolic hormones

Peripheral factors, such as nutrients, hormones and cytokines, can directly interact with the brain at sites like circumventricular organs or by interacting with afferent neurones.

1.4.1 Adiposity signals

Adiposity signals are factors that circulate in proportion to body fat mass and that can tonically signal to the CNS. Leptin and insulin are well established adiposity signals that work as long-term homeostatic signals of energy homeostasis.

1.4.1.1 Leptin

Leptin is encoded by the *ob* gene and secreted from white adipocytes into the circulation proportionally to fat mass (Zhang Y *et al.*, 1994). Mice with mutations in the *ob* gene (*ob/ob* mice) are obese, hyperphagic, diabetic and show reduced energy expenditure; administration of exogenous leptin can reverse this phenotype (Halaas *et al.*, 1995; Campfield *et al.*, 1996; Pelleymounter *et al.*, 1995; Halaas *et al.*, 1997). Mutations in the long leptin receptor isoform LeprB in mice (*db/db*) show a phenotype similar to that of *ob/ob* mice.

Leptin is a peripheral signal of energy storage that can cross the blood-brain barrier and modulate neuronal function via LeprB, which is expressed in POMC/CART and NPY/AGRP neurones of the ARC, as well as in other neuronal populations and hypothalamic nuclei, such as the PVN (Schwartz *et al.*, 1996; Cheung, Clifton & Steiner, 1997). Leptin can alter POMC mRNA levels and can also alter the firing rate of POMC/CART and AgRP/NPY neurones (Schwartz *et al.*, 1997; Cowley *et al.*, 2001; Takahashi & Cone, 2005). Leptin suppresses food intake and increases energy expenditure (Weigle *et al.*, 1995).
Plasma leptin is significantly higher in obese humans and animals (Maffei *et al.*, 1995; Considine *et al.*, 1996), which become insensitive to leptin action. This leptin resistance limits the utility of leptin as an anti-obesity agent. Lartigue and colleagues suggested that leptin signalling disruption in the vagus nerve is involved in the initiation of obesity (de Lartigue, Ronveaux & Raybould, 2014).

In contrast to the classical long-term signalling of energy storage, leptin can regulate energy homeostasis in the short-term. Leptin can activate neurones of the NTS involved in gastric distension (Huo *et al.*, 2007). Leptin may also regulate short-term energy intake by potentiating the effects of CCK (Barrachina *et al.*, 1997) at the level of the afferent vagus (de Lartigue *et al.*, 2012).
Leptin is constitutively expressed by adipose tissue but it can also be secreted from endocrine cells of the gastric mucosa after food intake (Cammisotto & Bendayan, 2012).

1.4.1.2 Insulin

Insulin is a hormone secreted from pancreatic β-cells of the islet of Langerhans that has been classically associated with glucose metabolism. Insulin reduces blood glucose levels by stimulating

glucose uptake in liver, muscle and adipose tissue. In addition, insulin also has an anorectic effect. Chronic central administration of exogenous insulin in baboons (Woods, McKay & Stein, 1980) and rats (Mcgowan *et al.*, 1993) decreases food intake, and effect also observed after peripheral insulin administration (Woods *et al.*, 1984). Insulin can act on POMC/CART and NPY/AGRP neurones of the ARC, where it alters the expression of NPY and POMC to promote an anorexigenic response (Schwartz *et al.*, 1992; Benoit *et al.*, 2002). Neuron-specific disruption of the insulin receptor increased food intake and body weight in mice (Bruning *et al.*, 2000).

1.4.2 Enteroendocrine cells and gut hormones

The gastrointestinal tract is key in nutrient sensing, digestion and absorption and is comprised of the stomach, small intestine (formed by duodenum, jejunum and ileum) and large intestine. Enteroendocrine cells (EECs) of the gut secrete hormones that coordinate the response to food intake, insulin secretion and regulate metabolism. Gut hormone release is modulated by molecular mechanisms that are influenced by factors, such as nutritional status and intestinal microbiota (Gribble & Reimann, 2019). Many gut hormones can also act as neuropeptides or neuromodulators in the CNS and peripheral nervous system.

1.4.2.1 L-cells

EECs are dispersed along the epithelial layer of the gastrointestinal tract. While they comprise only 0.1-1% of the gut epithelium, they play crucial roles in the regulation of metabolism. EECs, like other intestinal epithelial cells, originate from local LGR5+ stem cell division cycles in the crypts. They differentiate from different progenitors moving towards the villus and turn over every few days (Cheng & Leblond, 1974; Gribble & Reimann, 2016). They have been traditionally classified according to the hormones they produce (Sjölund *et al.*, 1983). For example, X/A cells of the stomach produce ghrelin, and L-cells produce GLP-1 and PYY, which are discussed in greater detail below. However, EECs can produce combinations of hormones which do not map precisely to the traditional EEC classifications (Habib *et al.*, 2012).

L-cells have an apical membrane which faces the gut lumen, and a basolateral membrane which faces the interstitial space. The products of food digestion stimulate L-cells by acting on a range of receptors or transporters. Stimulation of L-cells by ingested nutrients, which is linked to the local rate of nutrient absorption, triggers the secretion of gut hormones (GLP-1 and PYY) (Gribble & Reimann, 2019). L-cells are distributed with low frequency in the duodenum and higher number in jejunum, ileum and colon (Sjölund *et al.*, 1983). Most of food absorption occurs in the proximal small intestine so it is accepted that EECs of the upper gut dominate the increase in plasma levels of gut hormones that contribute to

the early postprandial control of appetite. Only long after a meal, ingested nutrients reach the colon so it is unlikely that colonic L-cells are involved in appetite control after a meal. However, colonic L-cells contain an important proportion of endogenous GLP-1 and PYY reserves. Therefore, role of distal L-cells is not well understood. Selective chemogenetic-mediated stimulation of distal colonic L-cells improved glucose tolerance and reduced food consumption via the GLP-1R and the Y2R (the receptor of PYY_{3-36}), respectively (Lewis *et al.*, 2020), suggesting that these cells play a role in energy and glucose homeostasis and could be targeted for treating obesity and diabetes.

EECs express a range of receptors, channels and transporters that can sense small molecules in the gut lumen produced after food ingestion as well as gut microbiota-derived metabolites (Gribble & Reimann, 2016). The sodium-coupled glucose transporter 1 (SGLT-1) depolarises L-cells in response to glucose and tightly controls incretin secretion (Gribble *et al.*, 2003). G protein-coupled receptors (GPCRs), the largest family of transmembrane receptors, are common sensors of digested nutrients (Figure 1.4.2.1.1). Some of these nutrient sensing GPCRs have been linked to gut hormone secretion upon binding of molecules, such as amino-acids (e.g., calcium sensing receptor (CasR) (Mace, Schindler & Patel, 2012)) or free fatty acids (FFA) (e.g., GPR40/FFA1R (Edfalk, Steneberg & Edlund, 2008)).

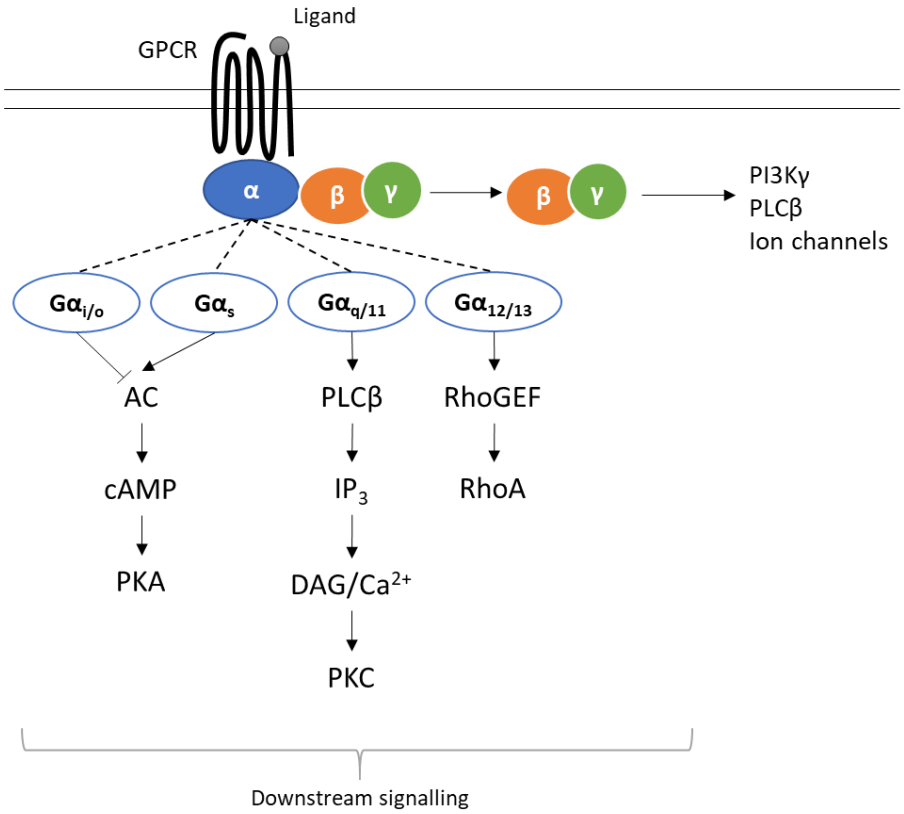

Figure 1.4.2.1.1. Overview of GPCR signalling through heterotrimeric G proteins.

GPCRs have a common structure based on 7 transmembrane helical regions, with an extracellular N-terminal and an intracellular C-terminal. Heterotrimeric G proteins are composed of α, β and δ subunits. Upon binding of the extracellular ligand, conformational changes result in the activation of G proteins and dissociation of the Gα subunit. Activated Gα and Gβγ activate downstream intracellular responses. GPCRs are classified based on the α subunit type. AC, adenylate cyclase; Ca^{2+}, calcium; cAMP, cyclic adenosine monophosphate; DAG, diacylglycerol; IP_3, inositol triphosphate; PI3Kγ, phosphoinositide 3-kinase γ; PLC, phospholipase C; PKA, protein kinase A; PKC, protein kinase C; Rho, Ras homolog family; RhoGEF, Rho guanine nucleotide exchange factor.

In recent years, the microbiota-gut-brain axis has proved of increasing interest to researchers (Holzer & Farzi, 2014; Bonaz, Bazin & Pellissier, 2018). Short chain-fatty acids (SCFA) are produced by the microbial fermentation of fibre in the colon, and can be detected by L-cells. Chambers and colleagues demonstrated that increasing propionate in the human colon stimulated PYY and GLP-1 release and prevented weight gain in overweight humans (Chambers *et al.*, 2015).

In contrast to the classical endocrine and paracrine action of gut hormones, some studies have suggested that EECs can also secrete neurotransmitters to rapidly communicate with the brain and this can be modulated by gut hormones. More recently, the Bohorquez group has shown that some

EECs have structures, termed neuropods, that can interact directly via synapse-like structures with enteric neuronal terminals by secreting glutamate to directly activate them (Bohórquez *et al.*, 2015; Kaelberer *et al.*, 2018, 2020). In addition, ATP is co-secreted with GLP-1 from EECs and can act to modulate vagal afferent signalling (Lu *et al.*, 2019).

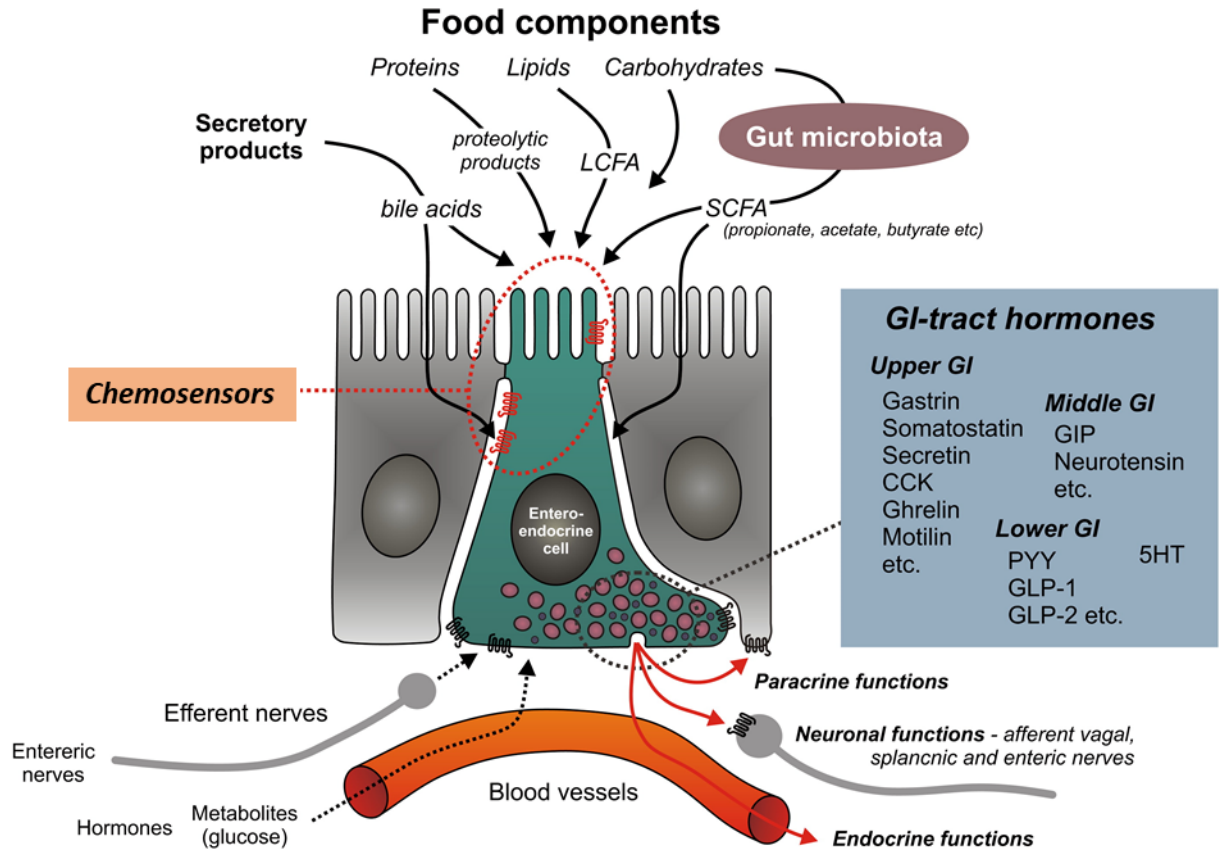

Figure 1.4.2.2. Overview of sensory and secretory functions of EECs.

5-HT, 5-hydroxtryptamine(serotonin); CCK, cholecystokinin; GI, gastrointestinal; GIP, gastric inhibitory peptide; GLP, glucagon-like peptide; LCFA, long-chain fatty acid; SCFA, short-chain fatty acid. Adapted from (Engelstoft *et al.*, 2008).

1.4.2.2 GLP-1

In pancreatic alpha cells the proglucagon prohormone is processed to generate bioactive glucagon, the classical counter regulatory hormone to insulin which, in the fasted state, promotes hepatic gluconeogenesis. However, in the gut and the NTS, proglucagon is differentially cleaved to form the peptide hormone GLP-1. There are two active forms: GLP-1 (7-36 amide) and GLP-1 (7-37) (Holst, 2007).

Circulating GLP-1, which is mostly GLP-1 (7-37), is mainly secreted from L-cells postprandially, along with PYY and oxyntomodulin (OXM). The main GLP-1 secretion stimuli are macronutrients (carbohydrates, fat and protein) and bile acids (Gribble & Reimann, 2021). GLP-1 binds to the GLP-1R, to exert its actions (Thorens, 1992). GLP-1R is a GPCR acting via the stimulatory Gs signalling pathway. Using Glp1r-Cre mice crossed with reporter strains, *Glp1r* has been found in metabolically relevant tissues including pancreatic β and δ cells, the brain (importantly, in the AP and the hypothalamus) and the afferent vagus nerve, as well as in other tissues, such as cardiomyocytes (Richards *et al.*, 2014).

GLP-1 stimulates cAMP-dependent insulin secretion from pancreatic β-cells (Gromada, Holst & Rorsman, 1998). It acts to potentiate glucose-stimulated insulin release, an effect known as the incretin effect. Glucose-dependent insulinotropic peptide (GIP), secreted from K cells in the duodenum, also contributes to this incretin effect (Gasbjerg *et al.*, 2019). At the level of the pancreas, GLP-1 also inhibits glucagon secretion from α cells (Nauck *et al.*, 1993) via an indirect, somatostatin-mediated mechanism (de Heer *et al.*, 2008).

In the gut, GLP-1 along with PYY contributes to the 'ileal brake'. The ileal brake is a process by which the presence of food in the ileum, as a result of fast nutrient flow and incomplete absorption in the upper gut, leads to ileal L-cells releasing more GLP-1 and PYY, which slows gastric emptying.
GLP-1-based treatments are already available for the treatment of obesity and T2D (see section 1.4.3). Exogenous GLP-1 can suppress appetite in animals and humans (Turton *et al.*, 1996; Verdich *et al.*, 2001; Chelikani, Haver & Reidelberger, 2005; De Silva *et al.*, 2011) and this effect is thought to be mediated by central GLP-1R. However, whether physiological levels of GLP-1 reach the hypothalamus or brainstem to regulate food intake is still unclear.

In mice, preproglucagon neurones of the NTS are the main source of GLP-1 within the CNS (Llewellyn-Smith *et al.*, 2011). These neurones do not respond to physiological food ingestion but respond to large meal ingestion, CCK and leptin (Cork *et al.*, 2015), and are thought to mediate stress-induced hypophagia (Holt *et al.*, 2019). Several studies have suggested that the vagus nerve could mediate the anorectic effect of GLP-1 (see section 3.1.2.2).

1.4.2.3 Oxyntomodulin

Oxyntomodulin (OXM) is a 37-amino-acid peptide also derived from preproglucagon. Like GLP-1 and PYY, OXM is secreted from L-cells postprandially proportionally to the caloric intake (Le Quellec *et al.*, 1992). Circulating levels peak at 30 min and remain elevated for several hours. While it has been

suggested that there is a as yet uncharacterised OXM specific receptor, current evidence suggests that it mediates its biological effects via the GLP-1R, for which it has a moderate affinity, and the glucagon receptor for which it has a low affinity (GCGR) (Kerr, Flatt & Gault, 2010).

OXM can reduce food intake following peripheral administration in animals and humans (Cohen *et al.*, 2003; Baggio *et al.*, 2004; Dakin *et al.*, 2004; Wynne *et al.*, 2005), and can also increase energy expenditure, an effect thought to be mediated by the GCGR (Wynne *et al.*, 2006; Tan *et al.*, 2013). OXM is thought to reduce food intake via the GLP-1R (Baggio *et al.*, 2004) and has a more potent anorectic effect than GLP-1; this may reflect its longer persistence in circulation overcoming its ostensibly lower affinity for the GLP-1R (Dakin *et al.*, 2004). In addition, OXM treatment results in a lower incidence of nausea than GLP-1 administration (Cohen *et al.*, 2003). OXM reverses obesity in mice and is more effective than GLP-1 monotherapy (Pocai *et al.*, 2009). Therefore, OXM is an interesting target for obesity treatment.

1.4.2.4 Cholecystokinin (CCK)

Cholecystokinin (CCK) is a peptide hormone expressed in I cells in the proximal small intestine, which like L cells are exposed to the luminal content. CCK is also widely distributed in the brain (Moran & Kinzig, 2004). First recognised for its effects on pancreatic exocrine secretion, CCK has subsequently been shown to have multiple roles. In the gut, its secretion is stimulated by protein and fat (Pilichiewicz *et al.*, 2007). The pre-pro-CCK molecule is the precursor of the multiple bioactive forms of CCK (Moran & Schwartz, 1994). Like other gut peptides, CCK exerts its effects by binding to Gq-coupled GPCRs. Two CCK receptors have been identified, CCK-RA and CCK-RB, which are located principally in the periphery and in the brain, respectively (Moran & Kinzig, 2004).

Acute administration of CCK in lean and obese subjects (Pi-Sunyer *et al.*, 1982) as well as in rats (Gibbs, Young & Smith, 1973) reduces food intake. In rats, CCK triggers early meal termination but chronically this is compensated by an increase in meal frequency (West, Fey & Woods, 1984). This anorectic effect is mediated by local actions via CCK-RA expressed in vagal afferents (Smith *et al.*, 1981a; Garlicki *et al.*, 1990). CCK can activate both mechanosensitive and chemosensitive fibres. CCK has other functions in the gastrointestinal tract, including inhibition of gastric emptying (Moran & McHugh, 1982; Moran & Kinzig, 2004).

Importantly, there is a synergistic interaction between CCK and leptin in food intake inhibition (Barrachina *et al.*, 1997). The anorectic effect of Leptin-CCK treatment was abolished by a CCK-A

antagonist or by sensory afferent ablation (Barrachina *et al.*, 1997). Leptin is thus thought to increase the sensitivity of vagal afferents to CCK (de Lartigue *et al.*, 2012).

1.4.2.5 Ghrelin

Most of the gut hormones are anorexigenic, but the gastric hormone ghrelin and the more recently discovered insulin-like 5 peptide (INS5L) are gut peptides known to have orexigenic effects. Ghrelin is a 28-amino-acide peptide mainly secreted from X/A cells in the stomach. These cells are not in contact with gastric content, suggesting they do not directly sense the presence of nutrients in the stomach lumen (Gribble & Reimann, 2019). Ghrelin is synthetised as a pro-ghrelin peptide that is cleaved and acylated to generate the bioactive peptide.

In contrast, with anorectic peptides, plasma ghrelin levels increase pre-prandially, and are thought to play a role in triggering meal initiation (Cummings *et al.*, 2001), although the mechanisms underlying this have not been fully elucidated. After food ingestion, ghrelin levels decrease; it has been suggested that this is regulated by nutrient absorption (Williams *et al.*, 2003a). In obese individuals, ghrelin levels are lower (Tschöp *et al.*, 2001), while diet-induced body weight loss increases ghrelin levels, which may contribute to the lack of success of dieting in most individuals. Exogenous ghrelin increases food intake in rats and humans (Wren *et al.*, 2001a, 2001b) and chronic treatment causes body weight gain in rats (Wren *et al.*, 2001b). The ghrelin receptor (growth hormone secretagogue receptor, GHSR) is a Gq-coupled GPCR that is found in several locations, including ARC, brainstem, pituitary, gastrointestinal tract and the afferent vagus nerve (Zigman *et al.*, 2006).

The feeding effects of ghrelin are mediated by ARC NPY/AgRP neurones (Kamegai *et al.*, 2001); mice lacking these peptides or these neurones do not increase their food intake in response to ghrelin (Chen *et al.*, 2004). Vagotomy and vagal-selective GHSR silencing also block the orexigenic effects of ghrelin, suggesting the vagus nerve plays a role in mediating these effects (Williams *et al.*, 2003b; Davis *et al.*, 2020). This is further discussed in section 3.1.2.4.

1.4.2.6 PP family

The PP family members are peptides that share a similar tertiary structure of an alpha helix and polyproline helix connected by a beta-turn known as a PP-fold (Holzer, Reichmann & Farzi, 2012). The family is comprised of neuropeptide Y (NPY), pancreatic polypeptide (PP) and peptide YY (PYY). While NPY and PP are expressed in neurones and endocrine cells respectively, PYY is expressed by both cell types. These peptides of the PP-fold family exert their actions via a family of GPCRs named NPY

receptors (YRs). Five different YRs (Y1R, Y2R, Y4R, Y5R and Y6R) have been characterized and classified according to their affinity to NPY, PP and PYY (Cabrele & Beck-Sickinger, 2000). The YRs differ in function and distribution but they are all assumed to belong to the inhibitory Gi/o family of GPCRs.

All these peptides inhibit gastrointestinal motility and secretion and are involved in regulating food intake and energy homeostasis (Holzer, Reichmann & Farzi, 2012). Synthetic analogues of these neuropeptides are under investigation for obesity therapy, such as the dual Y2R/Y4R agonist TM-30338/Obininepitide (7TM Pharmaceuticals).

NPY is the most abundant neuropeptide in the brain and is expressed by several neuronal populations in different regions. Centrally, NPY has a strong orexigenic effect, which is believed to be mainly mediated by Y1R and Y5R (Mullins *et al.*, 2001). In the ARC, NPY/AgRP neurones can suppress POMC/CART neurones via GABA and NPY, which binds to Y1R (Roseberry *et al.*, 2004). In the gut, NPY is mainly secreted from ENS and postganglionic sympathetic neurones (Cox, 2007).

PP is mainly secreted from pancreatic islet PP cells post-prandially under vagal control, and suppresses food intake via selective binding to the Y4R (Sainsbury *et al.*, 2010). Exogenous PP also suppresses food intake and increases energy expenditure (Batterham *et al.*, 2003b; Jesudason *et al.*, 2007) but its action is limited by its short half-life. PP is believed to act via the hypothalamus, brainstem and/or the vagus nerve (Asakawa *et al.*, 2003; Dumont *et al.*, 2007). It was shown that PP binds to Y6R, whose expression is critical for regulation of body composition and energy homeostasis (Yulyaningsih *et al.*, 2014).

PYY is mainly co-secreted from L-cells along with GLP-1 and OXM after meal intake. The truncated form PYY_{3-36}, further discussed in section 1.5, potently reduces appetite and is a focus of research into anti-obesity treatments.

1.4.3 Gut hormone-based therapies

Gut hormones are hormones produced by the enteroendocrine system in response to changes in the content of the gut and absorbed nutrients and metabolites. They regulate a range of functions, including gastrointestinal motility, gastric acid secretion and pancreatic exocrine secretion, and they are also involved in the regulation of food intake and glucose homeostasis. A number of them are anorectic (appetite-suppressing), and therefore have potential as anti-obesity drug targets.

The gut hormone GLP-1 and its receptor provide the basis of a number of drugs to treat type 2 diabetes, and more recently, obesity. The first GLP-1R agonist, exenatide (based on exendin-4), was approved in 2005, and other agonists such as Liraglutide have subsequently been approved as treatments for T2D and obesity. Liraglutide (Victoza) has been available as a T2D treatment since 2009. The most common side effects of Liraglutide are gastrointestinal, and include nausea or diarrhoea. Liraglutide (Saxenda) at 3.0 mg (once daily) was more effective for weight loss than orlistat (Astrup *et al.*, 2009). Liraglutide's success has demonstrated the potential of gut hormone-based drugs as weight loss treatment. However, GLP-1 analogues achieve only modest weight loss (around 8% (Pi-Sunyer *et al.*, 2015)) compared to RYGB. One of the main limitations are the gastrointestinal side effects, particularly nausea, which may reflect the extreme of the spectrum of GLP-1 anorectic action.

The data from the latest semaglutide studies point to the potential for clinically significant weight loss with a single gut hormone agent, yet the real-world data still does not quite match that achieved with bariatric surgery. OXM also has potential as an anti-obesity agent as it binds to both GLP-1R and GCGR to supress appetite and increase energy expenditure, respectively. The circulating half-life of OXM is still too low for the endogenous molecule to be of practical use as a drug, due to the breakdown by dipeptidyl peptidase-IV (DPP-IV). Longer acting analogues are currently being studied, such as TKS1225 (Druce *et al.*, 2009).

PYY is another gut hormone under investigation as an anti-obesity agent. Batterham and colleagues showed that PYY reduces appetite in lean and obese subjects and that lower PYY levels are found in the obese state (Batterham *et al.*, 2002, 2003a). Long-acting analogues are currently being studied for their utility on obesity (ClinicalTrials.gov, 2012; Rangwala *et al.*, 2020).

The main limitations of using gut hormones are the side effects, mainly nausea, and the short half-life due to peptidase-mediated degradation, such as DPP-IV. Oral administration is now possible with the advent of oral semaglutide (Wilding *et al.*, 2021), although they require much higher doses to overcome gastric breakdown and are not as potent as their parenterally administered alternatives. Different strategies have facilitated the design of gut-hormone based treatments with increased stability in blood and that achieve sustained elevated plasma levels without causing nausea. These include polyethylene glycol (PEG)ylated conjugates, albumin-bound analogues (like Liraglutide (Victoza)), slow-dissolving microspheres of exenatide and a long-acting antibody-bound PYY (Rangwala *et al.*, 2020). Another limitation of gut hormone-based treatment is tachyphylaxis, i.e., acute reduction in the response to a drug after an initial dose or serial doses.

After RYGB, there is an increase in postprandial GLP-1, OXM and PYY, and these changes are thought at least partly responsible for the weight loss and improved glycemia observed post-surgery. Therefore, treatments based in gut hormone combinations could mimic the physiological effects of bariatric surgery (McGavigan & Murphy, 2012; Alexiadou, Anyiam & Tan, 2019) and feasibly achieve better results than the modest weight loss observed with single gut hormone therapies. The most promising combinations are GLP-1 with PYY (Neary *et al.*, 2005), and GLP-1 with glucagon (Cegla *et al.*, 2014). A combination of GLP-1, OXM and PYY has been shown to be effective in reducing energy intake and improving glycaemia in obese subjects (Tan *et al.*, 2017; Behary *et al.*, 2019). In contrast to long-acting agonist, a continuous subcutaneous infusion of these three hormones allows better regulation of tolerability.

1.5 Peptide YY (PYY)

Peptide PYY is a 36-amino-acid peptide hormone discovered in the 80s that was originally named in allusion to the two tyrosine (Y) residues at its terminals (Tatemoto, 1982). It belongs to the PP family of peptides (section 1.4.2.6). Two forms of PYY can be found in circulation (Eberlein *et al.*, 1989): the full-length peptide, PYY_{1-36}, and the truncated form, PYY_{3-36}. PYY_{1-36} and PYY_{3-36} have high affinity to different NPY receptors and, consequently, they drive different effects on appetite and glucose homeostasis. PYY_{3-36} exerts its action by specifically binding with higher affinity to Y2R (with low affinity for Y1R and Y5R) while PYY_{1-36} is an agonist of Y1R, Y2R and Y5R (Cabrele & Beck-Sickinger, 2000).

1.5.1 Expression of PYY

PYY is mainly secreted from enteroendocrine L-cells after meal ingestion, along with GLP-1 (Habib *et al.*, 2012). Although the highest levels are found in L cells of the distal gastrointestinal tract (rectum, colon and ileum) (Adrian *et al.*, 1985; Ekblad & Sundler, 2002), it is also expressed at lower levels in the human duodenum (Kim *et al.*, 2005).

Circulating PYY levels are low during fasting and increase within 15 minutes of ingesting food, peak at 1-2 hours post-ingestion and remain elevated for up to 6 hours (Adrian *et al.*, 1985). PYY levels are influenced by caloric intake, macronutrient composition and meal consistency but it is still unclear if the most potent macronutrient stimulus of PYY release is protein (Batterham *et al.*, 2006) or fat (Adrian *et al.*, 1985). PYY levels then progressively decrease in the fasted state. Plasma PYY increases

before nutrients reach the distal gastrointestinal tract suggesting that PYY release is initially triggered by a neural reflex (Fu-Cheng *et al.*, 1997).

The full-length peptide, PYY_{1-36}, is cleaved by DPP-IV at the last two N-terminal amino-acids resulting the truncated form PYY_{3-36} (Mentlein, Gallwitz & Schmidt, 1993). PYY_{3-36} is the main circulating form in fed humans and animals (Grandt *et al.*, 1994; Batterham *et al.*, 2006). It is important to consider that PYY research has been limited by the ability to specifically detect PYY_{3-36} instead of total PYY (Manning & Batterham, 2014). In addition, PYY levels are higher in the hepatoportal circulation and might be more relevant than systemic PYY levels in energy homeostasis (Chandarana *et al.*, 2013), if interactions with vagal afferents in the portal vein (a blood vessel transporting blood from the gastrointestinal tract to the liver) are an important signalling conduit. This also raises the broader question of whether drug therapies that are delivered orally versus subcutaneously, matched for potency, have variable effects due to the preferential activation of alternative signalling pathways. PYY is also expressed in neurones of the CNS (Ekblad & Sundler, 2002), in enteric neurones of the stomach (Böttcher *et al.*, 1993) and in pancreatic cells (Upchurch, Aponte & Leiter, 1994).

1.5.2 Function of PYY

PYY_{1-36} and PYY_{3-36} exert their actions via different NPY receptors, which have different distributions, so they have different functions. It is widely accepted that peripheral PYY_{3-36}, the main circulating PYY form, signals to suppress appetite in animals and humans (Karra, Chandarana & Batterham, 2009; Manning & Batterham, 2014). There is little evidence to suggest a role of peripheral PYY_{1-36} in food intake (Chelikani, Haver & Reidelberger, 2004; Unniappan *et al.*, 2006; Sloth *et al.*, 2007).

Central administration of PYY_{1-36} has orexigenic effects (Karra, Chandarana & Batterham, 2009). Intracerebroventricular injection of PYY_{3-36} also showed orexigenic effect (Corp *et al.*, 2001) but this was abolished in Y1R and Y5R KO mice (Kanatani *et al.*, 2000). Since PYY_{3-36} has some affinity for these receptors, this might be a pharmacological effect and, at physiological doses, PYY_{3-36} might not have access to this region. In support of this, direct injection of PYY_{3-36} into the ARC of the hypothalamus, where its receptor Y2R is expressed, had an anorectic effect (Batterham *et al.*, 2002).
Plasma PYY levels are lower in the obese state (Batterham *et al.*, 2003a), though it is unclear whether PYY is involved in the pathogenesis of obesity. Postprandial circulating PYY levels increase after bariatric surgery (Pournaras *et al.*, 2010).

PYY may also be involved in glucose homoeostasis and this is discussed in Chapter 4. In the lower small intestine, PYY_{3-36} contributes to the 'ileal brake' (Pappas *et al.*, 1986).. Ileal infusion of lipids results in

delay of gastric emptying and this is related to PYY levels (Pironi *et al.*, 1993). Immunoneutralization of PYY in dogs showed that ileal brake depends on PYY (Lin *et al.*, 1996). Exogenous PYY inhibits gastric emptying in healthy subjects (Savage *et al.*, 1987).

PYY might have a role in other physiological processes. Apart from feeding, PYY_{3-36} is involved in modulating multiple behaviours (Stadlbauer *et al.*, 2015). It was recently suggested that PYY is involved in the pathogenesis of bone loss (Leitch *et al.*, 2019). NPY-Y2R signalling was suggested to play a pathogenic role in kidney disease in a mouse model (Lay *et al.*, 2020). Further research would be required to clarify if these would limit the usefulness of PYY based treatments. It is possible that the PYY dose that would alter weight or appetite does not alter bone and kidney health. It is also possible that long-term treatment with PYY-based agents require monitorisation of bone or kidney health and that is not suitable for specific vulnerable patients. Combination of PYY with other gut hormone analogues could also promote weight loss while avoiding the potential side effects of PYY.

1.5.3 Exogenous PYY_{3-36} in appetite regulation

Peripheral administration of PYY_{3-36} acutely inhibits food intake in mice and rats (Batterham *et al.*, 2002; Challis *et al.*, 2003; Halatchev *et al.*, 2004; Abbott *et al.*, 2005b; Chelikani, Haver & Reidelberger, 2006; Koda *et al.*, 2005; Talsania *et al.*, 2005; Scott *et al.*, 2005; Unniappan *et al.*, 2006; Unniappan & Kieffer, 2008), including in obese-diabetic rodents (Pittner *et al.*, 2004; Vrang *et al.*, 2006). Initially conflicting results in the anorectic ability of exogenous PYY_{3-36} (Tschöp *et al.*, 2004) were thought to be caused by the stress caused by handling and injections, so acclimatisation of animals is critical for reproducing these studies (Halatchev *et al.*, 2004). Intrameal acute administration of PYY_{3-36} in the hepatic portal vein also reduced meal size and duration (Stadlbauer *et al.*, 2013).

Chronic treatment with peripheral PYY_{3-36} also reduced food intake and body weight in rats (Batterham *et al.*, 2002; Unniappan *et al.*, 2006; Vrang *et al.*, 2006; Unniappan & Kieffer, 2008) but this was not observed in chow-fed mice (Challis *et al.*, 2004). In high-fat diet (HFD)-fed mice, no differences were observed in body weight or food intake with chronic treatment of PYY_{3-36} (Talsania *et al.*, 2005) but other group did observe an effect in body weight (Vrang *et al.*, 2006).

In humans, infusion of physiological levels of PYY_{3-36} to lean subjects reduces food intake (Batterham *et al.*, 2002, 2003a; le Roux *et al.*, 2006; Batterham *et al.*, 2007; Sloth *et al.*, 2007). This anorectic effect was preserved in obese subjects despite their lower postprandial PYY levels (Batterham *et al.*, 2003a). Therefore, in contrast to leptin, sensitivity to PYY appears not to be reduced in the obese state, which suggests the PYY system may have potential for weight loss therapy. Other studies have shown that

exogenous PYY_{3-36} can inhibit food intake additively with GLP-1 (Neary *et al.*, 2005; Talsania *et al.*, 2005; De Silva *et al.*, 2011; Schmidt *et al.*, 2014), leptin (Unniappan & Kieffer, 2008) and in combination with GLP-1 and OXM (Tan *et al.*, 2017).

Acute PYY_{3-36} administration also inhibits gastric emptying in rodents (Chelikani, Haver & Reidelberger, 2004; Talsania *et al.*, 2005). In addition, conditioned taste aversion has been observed after PYY_{3-36} injection in a dose-dependent manner (Halatchev & Cone, 2005; Chelikani *et al.*, 2006). The contribution of these effects to PYY_{3-36}'s anorectic effect is unclear.

1.5.4 Endogenous PYY_{3-36} in appetite regulation

Most of the studies that have revealed an anorectic effect of PYY_{3-36} are based on exogenous administration of PYY. These studies have revealed the pharmacological action of PYY_{3-36} but it is possible that endogenous PYY acts on different sites to regulate energy homeostasis. This is also influenced by the short half-life of endogenous PYY (Nonaka *et al.*, 2003; Torång *et al.*, 2016).

Regarding endogenous PYY, an attenuation in postprandial PYY release in obese subjects was associated with reduced satiety (le Roux *et al.*, 2006). A positive correlation between PYY and satiety was also reported (Guo *et al.*, 2006).

Transgenic mice have been used to study the role of endogenous PYY-Y2R signalling. PYY KO mice showed increased body weight and adiposity (Boey *et al.*, 2006b). PYY KO mice also showed increased food intake after fast-refeeding compared to controls (Batterham *et al.*, 2006). Y2R KO mice showed increased body weight but no differences in food intake (Naveilhan *et al.*, 1999). In contrast, conditional KO of hypothalamic Y2R showed temporal changes in food intake and body weight (Sainsbury *et al.*, 2002). More recently, Boland and colleagues reported that there were no differences in daily food intake nor in body weight in HFD-fed or chow-fed Y2R KO mice compared to controls. RYGB had similar effects in both groups (Boland *et al.*, 2019).

The main limitation of germline knockout (KO) approaches is the potential for compensatory changes during early development, as shown for Y2R (Sainsbury *et al.*, 2002), and this might contribute to the discrepancies in the resultant phenotypes. In addition, sex differences have been reported in PYY-Y2R signalling in energy homeostasis (Sainsbury *et al.*, 2002; Boey *et al.*, 2006b; Edelsbrunner *et al.*, 2009).

1.5.5 PYY_{3-36} in energy expenditure

Few studies have investigated the role of PYY on energy expenditure (EE). Observational studies in humans revealed that fasting PYY levels are negatively correlated with resting metabolic rate (Guo *et al.*, 2006). In healthy women, circulating postprandial PYY levels correlated with postprandial EE and

with the thermic effect of food (postprandial EE minus resting EE) (Doucet *et al.*, 2008). Infusion of PYY_{3-36} may have increased EE, though this effect did not achieve statistical significance, and caused significantly greater fat oxidation as indicated by the respiratory quotient (Sloth *et al.*, 2007).

Mice overexpressing PYY were protected against diet-induced obesity and showed increased thermogenesis (Boey *et al.*, 2008). Other studies in mice also observed effects in substrate partitioning after PYY_{3-36} treatment in lean (van den Hoek *et al.*, 2007) and obese mice (Van Den Hoek *et al.*, 2004; Adams *et al.*, 2006). Peripheral exogenous PYY_{3-36} increased locomotor activity in rats (Vrang *et al.*, 2006). More recently, using mice congenitally deficient in PYY and/or NPY, it was suggested that PYY could play a role in locomotor-associated EE, though this effect was sex-dependent (Edelsbrunner *et al.*, 2009).

1.5.6 Y2 receptor

PYY_{3-36} exerts its actions by specifically binding with high affinity to Y2R (with low affinity for Y1R and Y5R) (Wahlestedt, Yanaihara & Håkanson, 1986; Dumont *et al.*, 1995; Michel *et al.*, 1998). The NPY Y2R receptor is a 381-amino-acide protein that is mainly found in presynaptic neurones (Stanić *et al.*, 2006). Y2R protein expression has been found in many brain regions in mouse, including ARC and NTS (Stanić *et al.*, 2006). Importantly, 80% of ARC NPY neurones co-express the Y2R (Broberger *et al.*, 1997). In the periphery, Y2R has been found in the intestine (Goumain *et al.*, 1998), the vagus nerve (Zhang *et al.*, 1997; Abbott *et al.*, 2005a) and within the ENS (Wang *et al.*, 2010).

All YRs, including Y2R, are Gi/o-coupled GPCRs (Fig. 1.4.2.1.1). This signalling pathway results in the inhibition of adenylate cyclase and inhibition of cAMP accumulation. It was suggested that Y2R could couple to Gq proteins, which activate the PLC/IP3/Ca^{2+} pathway, in smooth muscle cells (Misra *et al.*, 2004).

Batterham and colleagues identified that Y2R mediates the anorectic effect of PYY_{3-36}. Exogenous peripheral and intra-ARC PYY_{3-36} induced a reduction in food intake in rodents but the anorectic effect of peripheral exogenous PYY_{3-36} was abrogated in global Y2R KO mice (Batterham *et al.*, 2002). In addition, other studies showed that the Y2R antagonist BIIE0246 administered in the ARC or i.v. abolished PYY_{3-36}-mediated appetite suppression (Abbott *et al.*, 2005b; Scott *et al.*, 2005; Talsania *et al.*, 2005).

1.5.7 Mechanism of PYY_{3-36} in appetite signalling

The mechanism by which PYY_{3-36} inhibits appetite has not been fully elucidated. It is widely accepted that Y2R mediates the effects of PYY_{3-36}. However, the site or sites of action mediating the anorectic effects of PYY_{3-36} are not fully understood. The most accepted mechanism was proposed by Batterham and colleagues (Batterham *et al.*, 2002). Peripheral PYY_{3-36} injection increased expression of cFos, an early gene used as neuronal activation marker, in POMC neurones in the ARC. This cFos induction by PYY_{3-36} has also been reported by others (Koda *et al.*, 2005; Abbott *et al.*, 2005a; Blevins *et al.*, 2008; Stadlbauer *et al.*, 2013). Electrophysiological studies in POMC-GFP neurones showed that PYY_{3-36} increased the firing rate and reduced the frequency of GABA release. NPY neurones tonically inhibit POMC neurones via GABA and express the Y2R, which is an auto-inhibitory presynaptic receptor (Broberger *et al.*, 1997; Cowley *et al.*, 2001). It was therefore suggested that PYY_{3-36} acts by inhibiting NPY neurones and, consequently, disinhibiting POMC neurones. Therefore, circulating PYY_{3-36}, which can cross the blood-brain barrier (Nonaka *et al.*, 2003), might access central Y2R through the median eminence, and act in food intake via the melanocortin system. Other electrophysiological studies reported that PYY_{3-36} inhibited both POMC and NPY neurones (Acuna-Goycolea *et al.*, 2005).

However, the anorectic effects of peripheral exogenous PYY_{3-36} are preserved in POMC KO (Challis *et al.*, 2004), MC4R KO (Halatchev *et al.*, 2004) and Agouti KO mice (Martin *et al.*, 2004). Therefore, peripheral PYY_{3-36} do not require the melanocortin system for its anorectic effects, though it does seem likely that PYY_{3-36} can regulate the melanocortin system, as shown by its effects on POMC and NPY mRNA expression (Sainsbury *et al.*, 2002; Challis *et al.*, 2003; Boey *et al.*, 2006b).

Although there are some discrepancies, exogenous PYY_{3-36} might activate limbic structures (Blevins *et al.*, 2008; Baraboi *et al.*, 2010; Stadlbauer *et al.*, 2013). In humans, peripheral PYY_{3-36} modulates activity of neurones within the homeostatic centres but also in reward centres, such as the ventral tegmental area, amygdala and orbitofrontal cortex (Batterham *et al.*, 2007; De Silva *et al.*, 2011). Batterham and colleagues postulated that PYY_{3-36} switches food intake regulation from the hypothalamus to the orbitofrontal cortex (Batterham *et al.*, 2007). Therefore, the actions of PYY_{3-36} on hedonic eating might also contribute to its anorectic effect.

An albumin-conjugated PYY (PYY_{3-36}-HSA), which cannot cross the blood-brain barrier and has a longer half-life than PYY_{3-36}, was used to better understand the mechanisms underpinning the anorectic effects of PYY_{3-36} (Baraboi *et al.*, 2010). Peripheral injection of PYY_{3-36}-HSA acutely reduced food intake for up to 24 h, when body weight was also reduced. It also increased cFos expression in limbic

structures, the medial NTS, PBN, AP as well as in the subfornical organ, which is a circumventricular organ in the third ventricle and is considered a thirst-regulating structure. However, combined lesions of the AP and subfornical organ or subdiaphragmatic vagotomy attenuated or abolished this neuronal activation and transiently inhibited the anorectic effect.

Like the ARC, the NTS of the brainstem is also exposed to peripheral signals via a circumventricular organ, the AP. Indeed, Y2R is also expressed in the NTS (Stanić *et al.*, 2006) and PYY_{3-36} could act here to regulate appetite as shown by the increased NTS cfos expression (Abbott *et al.*, 2005a; Halatchev & Cone, 2005; Blevins *et al.*, 2008; Stadlbauer *et al.*, 2013). In rats, Stadlbauer and colleagues did not observe cFos increase in the AP upon administration of PYY_{3-36} in the hepatic portal vein (Stadlbauer *et al.*, 2013). However, there are discrepancies with other study after i.v. PYY_{3-36} in rats (Blevins *et al.*, 2008). Lesion of the vagus nerve but not of the AP abolished the anorectic effect of PYY_{3-36}-HSA (Baraboi *et al.*, 2010). Therefore, PYY_{3-36} might act on the brainstem via the vagus nerve, which also expresses the Y2R (this is discussed in section 3.1.4).

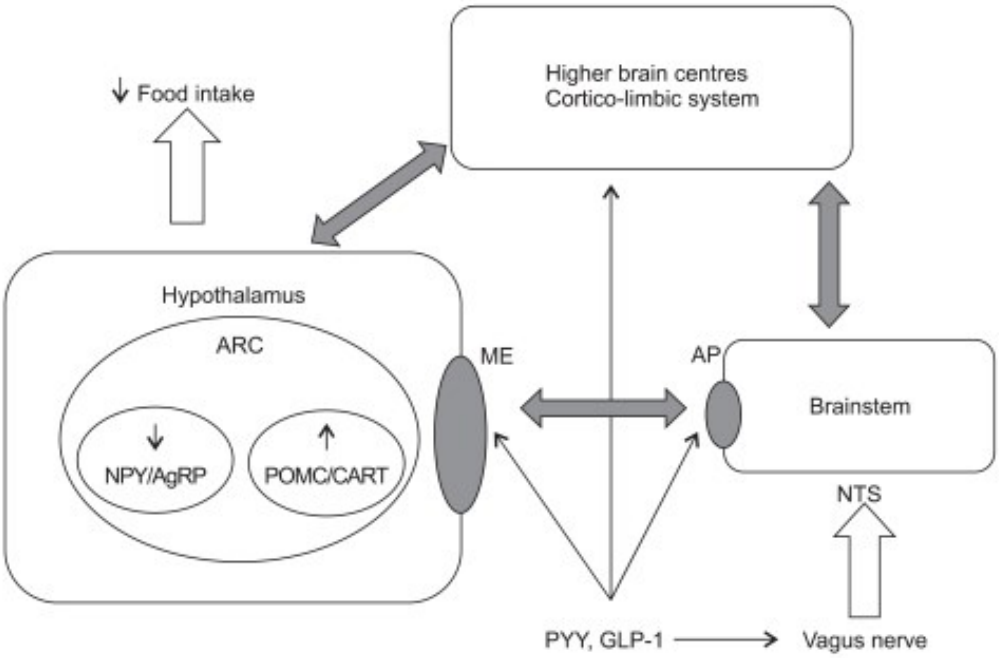

Figure 1.5.7.1. The role of PYY and GLP-1 in appetite control.

AgRP, agouti-related peptide; AP, area postrema; ARC, arcuate nucleus; CART, cocaine-and amphetamine-regulated transcript; GLP-1, glucagon-like peptide 1; ME, median eminence; NPY, neuropeptide Y; NTS, nucleus of the tractus solitarii; POMC, pro-opiomelanocortin; PYY, peptide YY. From (De Silva & Bloom, 2012).

.

1.6 Overview

This chapter introduces the current literature in energy homeostasis and appetite regulation by the gut-brain axis and the gut hormone PYY_{3-36}. In Chapter 2, we aimed to elucidate the effect of PYY_{3-36} in vagal afferent neurones activity as well as the effect of afferent vagus activation in feeding, glucose tolerance and gut immune homeostasis. Chapter 3 aims to elucidate the role of the vagus nerve in mediating PYY_{3-36} anorectic effect as well as its role in regulating feeding by means of disrupting Y2R expression in vagal afferents in different animal models. Chapter 4 focuses on investigating the effects of a long-acting PYY_{3-36} analogue on the body regulation, glucose homeostasis and islet function of a diet-induced obese mouse model.

1.6.1 Hypotheses and aims

The aims and related hypotheses of this thesis were:

1. To investigate the effect of global activation of vagal afferents on feeding, glucose tolerance and gut immunity. To achieve that, we optimised a surgical technique for the delivery of virus driving the expression of an activatory chemogenetic receptors in the nodose ganglia in order to modify vagal afferent neuron activity. We hypothesized that activation of vagal afferents using a selective chemogenetic system would mask the physiological effects of PYY_{3-36} (since the normal pathway would have been hijacked) and would have additional effects on the composition of immune cells in the gut wall.
2. To develop a mouse model of super selective vagal deafferentation of PYY_{3-36} signalling by knocking-down the Y2R in the afferent vagus using the Cre-loxP system and the delivery of virus in the vagal afferents. We hypothesized that loss of vagal PYY_{3-36} signalling would affect the physiological modulation of food intake but that pharmacological doses of PYY would bypass this.
3. Finally, we investigated the effects of a long-acting PYY_{3-36} agonist on body weight regulation and pancreatic islet activity using a directly observed model of pancreatic islet function in diet-induced obese mice. We hypothesized that PYY would not worsen islet secretory function.

Chapter 2: Effect of chemogenetic-mediated activation of the afferent vagus nerve on appetite, glucose homeostasis and gut immunity

2.1 Introduction

2.1.1 The vagus nerve

The vagus nerve is the longest cranial nerve and transmits bidirectional information between the brain and the viscera. The vagus nerve provides parasympathetic innervation to most visceral organs. It is the main neuroanatomical link between the gut and the brain and plays an important role in the gut-brain axis.

2.1.1.1 Anatomy of the vagus nerve

The vagus nerve is a mixed sensory-motor cranial nerve. Vagal afferent neurones are pseudounipolar and transmit sensory information from the viscera to the CNS, while vagal efferent neurones integrate information from the vagus nerve and from other brain nuclei and carry motor information from the brain to the periphery. At the cervical and abdominal level, most vagal neurones are afferents (around 80%) while the rest are efferents (Prechtl & Powley, 1990).

The vagus nerve originates in the medulla oblongata and leaves the cranium through the jugular foramen (Fig. 2.1.1.1.1). The efferent fibres innervating the gastrointestinal tract from the stomach to the descending colon originate from the DMX (Berthoud, Carlson & Powley, 1991). The cell bodies of vagal afferents innervating the gut are located in a paired extracranial structure named the nodose ganglia (NG), which are distal to the jugular ganglia at the level of the jugular foramen. In the mouse, the NG contains around 2300 neurones (Fox *et al.*, 2001). The cervical vagus nerve continues in parallel with the carotid arteries and separates into many branches that innervate different organs as it travels from the brainstem to the abdomen. In contrast with other neurones, there are no specific markers for vagal afferents that can be used in immunohistochemistry. Neuronal tracing has allowed the specific labelling of vagal afferents innervating the viscera (Berthoud, Carlson & Powley, 1991; Berthoud & Neuhuber, 2000). In the abdomen, the branching pattern of the vagus nerve was first characterized in rats (Prechtl & Powley, 1985) and is similar in other species. The left and right vagus nerve enter the abdomen along with esophagus and divide in primary branches asymmetrically (Berthoud & Neuhuber, 2000). Most of the dorsal or posterior trunk (from the right vagus) divides into the celiac branch. The ventral or anterior trunk (from the left vagus) divides into the common hepatic, anterior gastric and celiac branches, and innervates the liver, pylorus, antrum, pancreas and proximal duodenum. Vagal afferent innervation density is higher in the stomach and upper gastrointestinal tract, decreasing distally (Berthoud, Carlson & Powley, 1991).

The NG mainly contains C-type neurones, which have small-diameter unmyelinated axons and transmit sustained signals at low speed. The NG contains a lower proportion of A-type fibres which have myelinated axons that rapidly transmit short-lived potentials. At the abdominal level, afferent fibers are mostly C-type (Agostoni *et al.*, 1957). However, new technical approaches have allowed a better understanding of vagal afferent subpopulations (Wang, de Lartigue & Page, 2020). In recent years, vagal afferent subtypes have been classified and studied based on the expression of specific genes (Egerod *et al.*, 2018; Kupari *et al.*, 2019; Bai *et al.*, 2019) or the identification of specific circuits (Williams *et al.*, 2016; Han *et al.*, 2018; Kaelberer *et al.*, 2018).

In the brain, the vagal afferents synapse on second order neurones of the brainstem NTS, principally using glutamate as neurotransmitter (Andresen & Yang, 1990). The NTS sends axonal projections to third order neurones in local sites, such as the DMX, as well to the forebrain, including hypothalamic nuclei. The NTS also receives inputs from other brainstem areas and higher CNS centres. Therefore, metabolic signals generated in the vagal afferents can have multiple effects and they are integrated within the NTS to generate a response. However, the course of the vagal afferents in the brain has not been fully elucidated. Neural tracing allows mapping the distribution of vagal afferent terminals. Anterograde tracers are injected in the cell nuclei (e.g., the nodose ganglia) where is taken up and transported to terminal processes, while retrograde tracers are injected in the terminals (e.g., vagal afferent terminals in the gut) and transported back to the cell body. Biochemical-based tracers (e.g., fluorogold or dextran amines) can be used to visualise vagal-gut-brain circuit. Recently developed viral approaches enables studying the communication of brain centres with vagal afferents subtypes as well as mapping neuronal circuits in specific pathways receiving vagal input (see section 2.1.1.3).

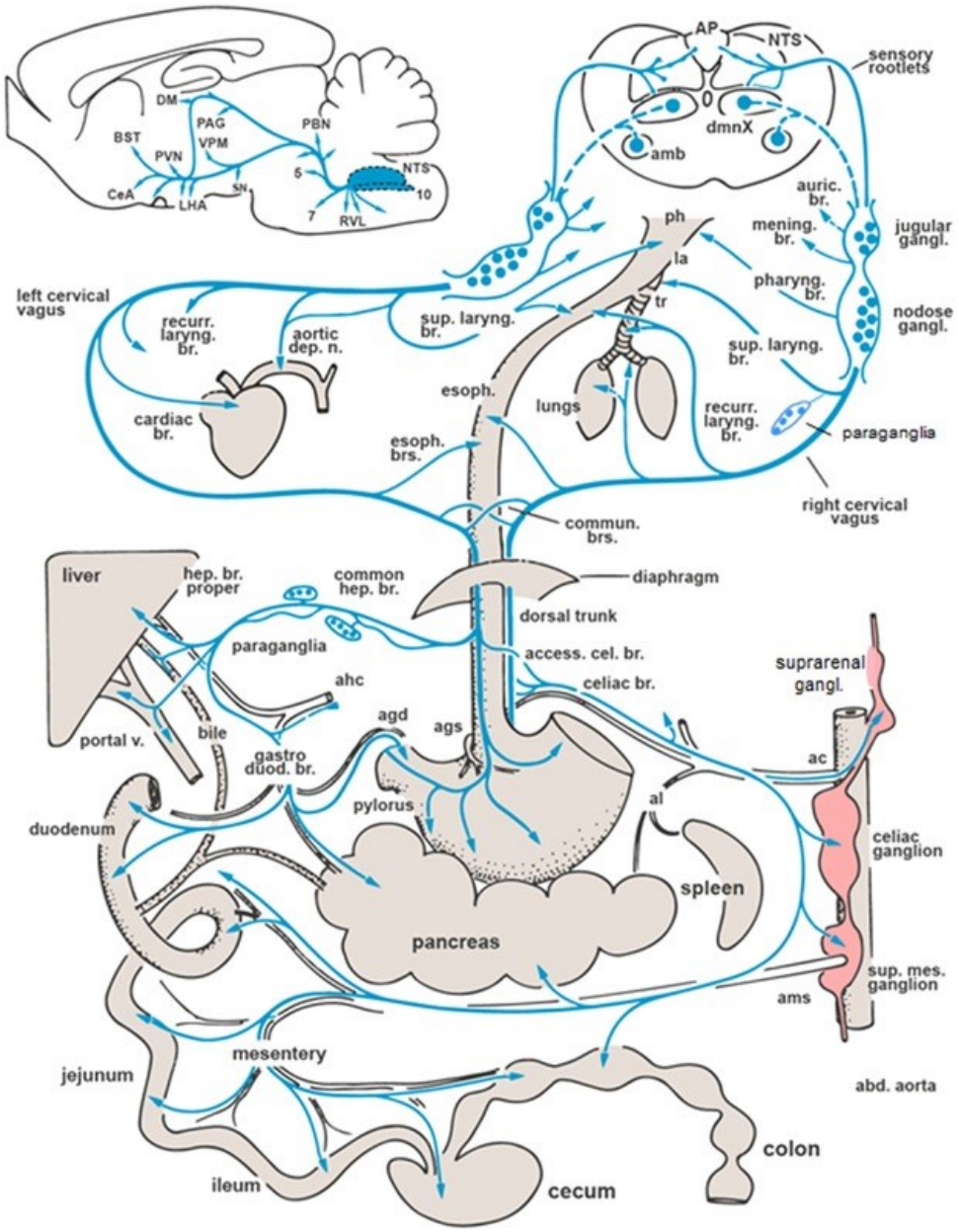

Figure 2.1.1.1. Vagus nerve anatomy.

From (Berthoud & Neuhuber, 2019).

2.1.1.2 Vagus nerve innervation in the gut wall

The afferent vagus nerve can send mechano- and chemo-sensory information from the gastrointestinal tract to the brain via afferent terminals that detect sensory stimuli (Page, Martin & Blackshaw, 2002; Berthoud *et al.*, 2004). Vagal afferent terminals are characterised by their distribution and their complex terminal structures.

Vagal terminals have been typically classified into three categories. The most abundant vagal afferent terminals are the intraganglionic laminar endings (IGLEs) that form a flattened plate-like structure and are associated with ENS neurones of the myenteric plexus (Berthoud *et al.*, 1997). IGLEs are abundant in the upper and lower gastrointestinal tract and contain tension receptors that detect nutrient volume and respond to changes in the length of the gut wall (stretch) as well as gut wall tension. Intramuscular arrays (IMAs) are mainly located in the upper gastrointestinal tract and are found within the circular or longitudinal muscle layers where they detect gut stretch-related signals (Berthoud, Kressel & Neuhuber, 1992; Berthoud & Neuhuber, 2000).

Vagal mucosal afferents terminate close to the gut epithelium, within the lamina propria, where they can respond to different stimuli. Mucosal endings are frequently found in the stomach and proximal small intestine, but they are less abundant in the distal small intestine (Bai *et al.*, 2019). Their mechanoreceptors are thought to detect mucosal stroking and distension (Page, Martin & Blackshaw, 2002).

2.1.1.3 Current approaches to study vagal afferents

Neurotropic viral vectors have enabled neural tracing of vagal afferent and dissecting vagal afferent subtypes and their function. Adeno-associated virus (AAV) is a favourite tool for a wide variety of applications studying the vagal afferent circuitry. AAV are widely used for gene delivery *in vivo* because of its low immunogenicity, it is non-pathogenic and they remain episomal (without integrating into the genome). Episomal stability is a key advantage of AAV since it enables long term transgene expression in non-dividing cells.

Wild type AAV is a non-enveloped single-stranded DNA virus isolated from adenovirus. AAV genome consists of two open reading frames, Rep (which is translated to proteins required for the AAV life cycle), Cap (which is translated to capsid proteins) flanked by two inverted terminal repeats (ITRs). In research applications (recombinant AAV), the transgene is between the ITRs and Rep/Cap genes are supplied 'in trans'. In addition, a helper plasmid containing genes from adenovirus (involved in AAV replication) is supplied. A limiting factor in recombinant AAV transduction efficiency is the fact that the virus relies on the host cell machinery to synthetise the complementary strand and transgene expression may be delayed. Another key limitation of AAV for gene delivery is the low cargo capacity (~4.7 kb).

Several AAV serotypes have been identified and they differ in the type of cell they infect. Most of native AAV serotypes have tropism towards neurons with variable degrees. By mixing the capsid and genome from different AAV serotypes (pseudotyping) tropism and transduction efficiency can be optimised. Apart from the serotype, a widely used approach to drive gene expression in specific cells or tissues is combining recombinant AAV with Cre/loxP technology (see below). Other neurotropic viral vectors used in neural tracing are rabies virus and herpes virus (suitable for retrograde tracing).

Using these approaches, fluorescent viruses retrogradely transported from the gut vagal terminals allow to trace ascending vagal fibres from the NG. Vagal afferent terminals from specific organs innervate distinct regions within the DVC, with gut-innervating afferents innervating the ventromedial NTS. The gut-innervating neurons of the right NG innervates the NTS but the ones of the left NG mainly innervates the AP (Han *et al.*, 2018).
In order to visualise genetically defined vagal afferents, Chang and colleagues generated knock-in mouse lines in which Cre-recombinase is co-transcribed with a neuropeptide receptor gene (e.g., Npy2r) (Chang *et al.*, 2015). To visualise the peripheral projections of the specific Cre-expressing subtype, AAV containing a Cre-dependent fluorescent marker was injected into the nodose ganglia (Chang *et al.*, 2015) .

AAV is commonly used in optogenetics and chemogenetics. These techniques allow the modulation of neural activity through polarization or depolarization of the neuron membrane, and are now used to assess vagal afferent function. Optogenetics is a technique that uses light to control the activity of cells in which the expression of a light-sensitive depolarizing channel (e.g., channelrhodopsin) has been induced, and behaviour can be studied in vivo. Williams and colleagues activated specific vagal neurons (e.g., GLP1-R-expressing neurons) to study their role in physiology (Williams *et al.*, 2016). In order to map vagal afferents circuit in the gut-brain axis and in reward pathways, Han and colleagues used a combinatorial viral approach and optogenetics (Han *et al.*, 2018). They combined a virus carrying the Cre-recombinase that is transported retrogradely from specific areas of the gut with a light-sensitive depolarizing channel expressed in a Cre-dependent manner in the NG. Upper gut-innervating vagal afferents induced reward related behaviour and dopamine release in the substantia nigra (Han *et al.*, 2018). Han and colleagues aimed to map the circuit connecting the NG with nigral dopamine neurons using an anterograde transsynaptic viral tracer. This tracer is taken up by the cell nuclei at the NG and can spread to the post-synaptic neuron depending on Cre recombinase for replication and transcription of a red reporter. It was reported that the dorsolateral PBN links

the right NG with the substantia nigra (Han *et al.*, 2018). Using retrograde and anterograde tracers and optogenetics, this study revealed a PBN-substantia nigra-dorsal striatum pathway and revealed a novel role in reward of the right NG.

The most popular chemogenetic technique is based on Designer Receptor Exclusively Activated by Designer Drugs (DREADD). The DREADD system artificially induces expression of a genetically engineered GPCR (see section 1.4.2.1) on target cells and in the administration of a receptor-specific synthetic ligand. DREADDs are commonly based on the human muscarinic acetylcholine receptor family and, depending on the coupled signalling pathway, activation of these receptors can result in different physiological outcomes. Activation of Gq-DREADDs excite the neuron while Gi-DREADDs activation has an inhibitory effect. These mutant receptors are insensitive to endogenous acetylcholine and have no detectable constitutive activity in the target cell. Therefore, cellular signalling and activity of DREADD-expressing cells is modulated remotely by administration of a synthetic ligand, which is physiologically-inert. Bai and colleagues used chemogenetics to selectively activate vagal afferent subtypes and study their function (Bai *et al.*, 2019).

Using the powerful Cre/LoxP technology, genetic modifications can be highly tissue-specific and precise. The Cre recombinase recognized loxP sites and rearranges the genetic material. Depending on the location and orientation of the loxP sites, genetic material can be inverted, deleted or translocated. Some common ways to control Cre expression are Cre induction by a ligand (e.g., tamoxifen) and expression of Cre under a promoter. Cre-driver and Cre-dependent transgenic models have been developed to study vagal afferent and its subtypes. Some limitations of this approach are the potential non-specific gene expression and toxicity of Cre. One of the most common Cre-driver line used to study vagal afferent function in the gut-brain axis and in food intake regulation is Nav1.8-Cre. Stirling and colleagues generated the Nav1.8-Cre mouse model in which Cre recombinase expression is directed by the Nav1.8 promoter (Stirling *et al.*, 2005). Nav1.8 is a tetrodotoxin resistant voltage-gated sodium channel especially found in peripheral sensory neurons, including spinal and vagal afferents. Regarding the vagus nerve, Nav1.8 is expressed in over 75% of vagal afferents in mice (Stirling *et al.*, 2005). Gautron and colleagues investigated the innervation of Nav1.8-expressing vagal afferents in the viscera as well as the anatomical interaction of these afferents with enteroendocrine cells using Nav1.8-Cre-tdTomato, in which vagal afferents are fluorescently labelled (Gautron *et al.*, 2011). The NG contained the largest number of tdTomato-positive neurons and fibers originating from the NG were observed in the vagus nerve and in brainstem (NTS, AP). Within the gastrointestinal tract,

Nav1.8-expressing vagal afferents innervated the mucosa and myenteric plexus in stomach and small intestine, and a small subset were IGLEs (Gautron *et al.*, 2011). Nav1.8-Cre line has been used to selectively knockout the leptin receptor in Nav1.8 neurons (de Lartigue, Ronveaux & Raybould, 2014).

2.1.2 Vagus nerve activity in feeding and physiology

The afferent vagus nerve is the main neuroanatomical link transmitting satiety signals, both hormonal and mechanical, from the gut to the brain. Vagus nerve activity is increased with gastric distension (Schwartz, McHugh & Moran, 1993; Schwartz & Moran, 1994). In addition, some anorectic hormones have been shown to activate the vagus nerve, such as CCK (Schwartz, McHugh & Moran, 1993; Schwartz & Moran, 1994) and PYY_{3-36} in rats (Koda *et al.*, 2005). .

Therefore, regulation of the vagus nerve signalling or activity could have potential as a target for anti-obesity therapy, for example, vagus nerve stimulation (VNS) (see below). However, gross activation or disruption of the vagus nerve has yielded inconclusive results in terms of food intake and body weight effects (Berthoud, 2008a).

After gastric surgery and vagotomy, humans lose weight and exhibit reduced food intake at a buffet meal (Le Roux *et al.*, 2005). Most specific vagal afferent lesioning can alter the feeding response to exogenous gut hormones (see section 3.1.2), although previous studies show that vagal lesioning in rodents does not alter total food intake or body weight but rather alters meal pattern (Schwartz *et al.*, 1999; Powley *et al.*, 2005). Bilateral vagotomised mice ate smaller and more frequent meals (Powley *et al.*, 2005) while subdiaphragmatic vagal deafferentiation in rats caused larger and less frequent meals (Schwartz *et al.*, 1999). The afferent vagus nerve is formed by mechanosensitive and chemosensitive neurons that receive gut-derived anorexigenic and orexigenic signals and this are integrated and transmitted to the central nervous system to regulate metabolism. The vagus nerve also express neuropeptides that modulate vagal afferent signalling (de Lartigue, 2014). Disruption of the vagal expression of hormone receptors and neuropeptides alters metabolism (see 3.1.2 and 3.1.3). Gut hormones can also modulate mechanical signals. For example, ghrelin reduces the mechanosensitivity of vagal afferent neurons (Page *et al.*, 2007). In addition, gut hormones might also interact with each other at the afferent vagus level to regulate feeding (De Lartigue *et al.*, 2010). Thus, it seems likely that the complex interplay of numerous neuroendocrine factors add together in a way that remains to be fully elucidated. In Chapter 3, the effect of disrupting the vagal signalling of a single gut hormone (i.e., PYY_{3-36}) is explored.

The pancreas is innervated by parasympathetic, sympathetic and sensory nerves that regulate pancreatic functions. Vagal and spinal afferents transmit sensory information from the pancreas to the brain but the role of sensory neurons innervating the pancreas is not understood (Babic & Travagli, 2016). Mice treated with capsaicin, a drug that causes deafferentiation of small unmyelinated C-fibres (most of vagal afferents are capsaicin-sensitive), showed an increased glucose tolerance due to an early glucose-stimulated insulin secretion (Karlsson *et al.*, 1994). Capsaicin-treated rats also showed increased insulin sensitivity (Koopmans, Leighton & DeFronzo, 1998). On the other hand, electrical activation of the vagus nerve stimulates insulin secretion and lowers blood glucose (Ahrén, 2000). However, there are conflicting results regarding the effects of vagus nerve lesioning and stimulation in pancreatic function, for example it is particularly difficult to disentangle the direct effects of VNS on insulin secretion from indirect actions on gut hormone secretion. Vagal afferents could be involved in a neural circuit activated by glucose in which peripheral adrenergic nerves are also involved (Karlsson *et al.*, 1994). This puts in focus the importance of understanding the various elements of vagal signalling in order to design better targeted interventions.

VNS requires the implantation of electrodes on the cervical vagus and applying electric pulses to generate a firing potential. Several parameters of VNS can be modulated, such as intensity, pulse frequency or duration of the stimulation period. However, the precise signalling profile associated with satiety remains to be fully understood and hence current vagus stimulation devices are not highly tuned or specific. For this reason, they are not yet licensed to treat obesity although VNS is approved to treat epilepsy and depression. In a retrospective study of patients treated for refractory epilepsy, the potential anti-obesity application of VNS was revealed (Burneo *et al.*, 2002). However, in another retrospective study in patients treated for epilepsy, VNS did not affect body weight (Koren & Holmes, 2006). In an initial study, stimulation of the vagus nerve at the thoracic level in dogs reduced body weight (Roslin & Kurian, 2001). In lean rats, unilateral and subdiaphragmatic VNS reduced food intake and body weight (Krolczyk *et al.*, 2001; Laskiewicz & Sobocki, 2003). In a more recent study, a VNS device controlled by stomach peristalsis showed to be a highly effective body weight control approach in rats (Yao *et al.*, 2018). In obese mini-pigs, VNS prevented weight gain and reduced intake of fat-rich and carbohydrate-rich food (Val-Laillet *et al.*, 2010). In obese rats, VNS caused a reduced food intake and body weight as well as delayed gastric emptying and increased plasma levels of anorectic gut hormones (Dai, Yin & Chen, 2020). Despite these studies suggesting that VNS could be beneficial for weight loss, the mechanism is not well understood (de Lartigue, 2016).

Another method for neuromodulation is vagal blockade therapy (vBloc), which is based on implanting electrodes closed to the oesophago-gastric junction and in applying kilohertz frequency alternating current to block electrical conduction. Vagal blockade has been approved by the FDA for the treatment of obesity although the mechanism remains unknown (Shikora *et al.*, 2015; de Lartigue, 2016), and real-world clinical results are disappointing. The classical methods used for studying vagus nerve function, vagotomy and VNS, do not specifically target the role of vagal afferents. In contrast, chemogenetic and optogenetic technologies allow the manipulation of neuronal activity non-invasively in order to remotely and reversibly study the effect of vagal activity in physiology. This can be used to specifically study vagal afferents as well as genetically-defined populations by means of Cre-loxP technologies. These technologies have been used in recent studies to evaluate the activity of vagal afferents in autonomic reflexes (Chang *et al.*, 2015; Williams *et al.*, 2016) and feeding behavior (Bai *et al.*, 2019). The results of studies using this technology suggested that food intake is more sensitive to mechanical signals than to nutrient-activated mucosal afferents in mice (Bai *et al.*, 2019). Thus, animal studies that investigate the relative contribution of different fibres within the vagus towards satiety, alongside a deeper understanding of their firing patterns using electrophysiology, could inform the development of precision VNS devices that could induce clinically really meaningful weight loss benefits.

2.1.3 Neuro-immune crosstalk in the gut

It is important to remember that a device developed to activate the vagus for therapeutic benefit could have off target effects that need to be considered. For example, the vagus nerve not only controls feeding and digestion but also has other roles in physiology, such as immunoregulation in mucosal barrier function.

The gastrointestinal mucosa is continuously exposed to environmental agents, such as nutrients, commensal microbiota, pollutants, and pathogens. Therefore, maintaining the balance between tolerance to non-pathogenic microbes and the immune response to insults is key for homeostasis. An unbalanced immune modulation can lead to conditions such as inflammatory bowel disease (IBD) and food allergy. It has also been implicated itself in obesity (Shoelson, Herrero & Naaz, 2007).

Most of these immune processes occur in the gut mucosa (comprised of the epithelium, lamina propria and muscularis mucosa). The ENS is largely organized into two major plexuses, the myenteric plexus and the submucosal plexus but the immune cell population is less diverse in these locations compared to the other layers (Veiga-Fernandes & Mucida, 2016). While intra-

epithelial immune cells play critical roles in immune responses, most of enteric immune cells are actually concentrated in the lamina propria, where they potentially interact with nerve endings. The concept of neural modulation of immune responses is a rapidly growing field of immunology. Since the ENS and gut-associated immune system are so vast, it stands to reason that the neuronal regulation of gut immunity is likely to be a hugely important area of research. Enteric associated neurones include the ENS itself and the extrinsic sympathetic and parasympathetic neurones of the autonomic nervous system. Extrinsic and intrinsic neuronal terminals are found in all the layers of the gut wall.

Apart from the close location of immune cells and neuronal terminals, the intestinal immune cells express receptors for neurotransmitters and neuropeptides. In addition, enteric neurones express cytokine receptors so they can respond to immune signals. This co-localisation and functional crosstalk between neurones and immune cells have led to individual functional units of this crosstalk being defined as 'neuro-immune cell units' (Godinho-Silva, Cardoso & Veiga-Fernandes, 2019; Jakob, Murugan & Klose, 2020).

2.1.3.1 Immunity in the gastrointestinal tract

In the gastrointestinal tract, intestinal epithelial cells are a key part of the barrier function and innate immunity (Peterson & Artis, 2014). Firstly, the intestinal epithelium acts as a physical barrier as a result of the tight junctions between epithelial cells as well as mucins, which form a viscous mucus layer. In addition, specific types of epithelial cells, such as Goblet cells and Paneth cells, secrete anti-bacterial peptides that create a chemical barrier. The intestinal epithelium strategically expresses a range of receptors that recognize pathogens and danger-associated molecular patterns, but that also limit inflammatory responses to commensal bacteria and innocuous antigens. Intestinal epithelial cells release cytokines that modulate different immune cells in order to promote a tolerogenic environment. Importantly, the microbial recognition by pattern recognition receptors contributes to intestinal homeostasis and repair (Rakoff-Nahoum *et al.*, 2004) a process to which neurones contributes actively (Jarret *et al.*, 2020).

In response to bacterial entry, epithelial cells secrete factors that recruit other immune cells, such as phagocytic cells (macrophages and neutrophils), eosinophils or T cells. Intestinal macrophages are mostly derived from blood monocytes that enter the gut in steady state conditions and then differentiate and mature (Bain *et al.*, 2013). The monocyte pool is heterogenous and different subsets have been defined in mice and humans. Macrophages are mainly found in the lamina propria and their main functions are phagocytic and bactericidal but,

importantly, they do not promote pro-inflammatory responses as much as other tissue macrophages (Bain *et al.*, 2013; Bain & Mowat, 2014). Eosinophils express granules containing enzymes that are released upon activation. They are associated with the responses to helminths and contribute to the pathology of allergic disease, but are also present in normal intestinal mucosa suggesting a physiological role that is still not understood (Bain *et al.*, 2013; Fulkerson & Rothenberg, 2008). Mast cells have been classically involved in allergic responses by secreting histamine but they also have regulatory functions and interact with local neurones (Bischoff, 2009; Stakenborg, Viola & Boeckxstaens, 2020).

Innate lymphoid cells (ILC) were discovered more recently and are of great interest in barrier immunity. Among ILCs, cytotoxic (conventional natural killer cells) and helper ILCs have been defined. Helper ILCs are involved in the defense against infectious pathogens, in tissue remodeling and they also regulate adaptive immunity (Sonnenberg & Hepworth, 2019). They share transcriptional and functional features with their counterpart lymphocytes of the adaptive immune system. Importantly, they can secrete cytokines in response to signals such as neuronal mediators, microbial products or diet. In contrast to adaptive lymphocytes, ILCs do not have genetically encoded unique antigen-specific receptors and reside mostly in peripheral tissue and mucosal barriers. This strategic location allows them to respond early upon an immune challenge, whereas adaptive lymphocytes require expansion, differentiation and migration to the tissue (Klose & Artis, 2016). Helper ILCs are divided into three groups characterized by the expression of transcription factors and the cytokines they secrete. The most abundant ILC type in the intestine is type 3 ILC (ILC3s, typically characterized by the expression of the retinoic-acid receptor-related orphan receptor-γt (RORγt) and production of interleukin (IL)-17A and IL-22). ILC3s defend against bacteria but also stimulate mucus production and enhance epithelial junctions and repair. Type 2 ILC (ILC2s, which express the transcription factor GATA-binding 3 (GATA3) and produce several cytokines, including IL-4, IL-5 and IL-13) are also present in the intestine and they respond to large extracellular parasites and allergens. Type 1 ILC (ILC1s, characterized by expression of the transcription factor Tbet and large productions of interferon γ (IFN-γ) are less abundant in the intestine but they can represent key agents against viral infections.

In contrast to the innate immune system, the adaptive immune system is activated in response to infection, targeting antigens specific for each pathogen, and displays what is called immunological memory (i.e., it is able to react faster and more efficiently to a secondary infection by the same pathogen). The adaptive immune system is composed of lymphocytes (B

and T cells) and their secreted molecules. The main lymphoid tissues in the gut are Peyer's patches and mesenteric lymph nodes. In these sites, dendritic cells (DCs) are important sensors of pathogens and can influence the adaptive immune response. DCs present antigens to naïve lymphocytes that then differentiate into effector T cells, regulatory T cells or B cells (mainly immunoglobulin A (IgA)-producing plasma cells). Antigens are delivered to DCs via epithelial microfold cells (M cells) as well as goblet cells (McDole *et al.*, 2012), or are directly sampled by DCs from the intestinal lumen. After presentation, effector lymphocytes enter the circulation and return to the lamina propria due to the expression of gut-specific adhesion molecules and chemokine receptors. In the gastrointestinal tract, the major form of adaptive immunity is humoral immunity mediated by IgA antibodies secreted from B cells or plasma cells of the lamina propria. T cells expressing the cluster of differentiation 4 (CD4) can differentiate into distinct helper T (T_H) lineages associated with the expression of specific transcription factors and cytokines, similar to their ILC counterparts. Under steady state conditions, the most abundant T_H types are T_H17 (mainly characterized by the expression of transcription factor RORγt and secretion of IL-17 family cytokines) and T_H1 (mainly characterized by the expression of T-bet and secretion of IFN-γ and tumor necrosis factor (TNF)). These cells infiltrate the gut mucosa under healthy steady-state conditions, they do not promote inflammation unless prompted by intracellular (T_H1) or extracellular (T_H17) pathogens or tissue insults (Belkaid, Bouladoux & Hand, 2013). Mirroring ILC2s, T_H2 cells can be identified by GATA3 expression, and production of IL-4, IL5 and IL-13 during parasitic infections (Walker & McKenzie, 2018). $CD4^+$ $FoxP3^+$ regulatory T cells (T_{reg}) are key in maintaining immune homeostasis and tolerance by expressing, amongst others, the immunosuppressive cytokine IL-10. In addition, there are differences in immune function between the anatomical regions of the gastrointestinal tract, and these are influenced by factors such as the secondary lymphoid organ draining that segment or luminal content (Mowat & Agace, 2014). The segregation of gut-draining lymph nodes also allows the wider orchestration of tolerogenic and inflammatory responses (Esterházy *et al.*, 2019).

2.1.4 Vagus nerve and intestinal immune homeostasis

In a key experiment, it was showed that vagus nerve stimulation lowered the production of pro-inflammatory cytokines in a model of sepsis (Borovikova *et al.*, 2000) and introduced the concept of the 'cholinergic anti-inflammatory pathway' (CAIP). In CAIP, afferent neurones are activated by inflammatory mediators during local tissue inflammation and carry this information to the CNS, where it is integrated and, consequently, efferent neurones modulate cytokine secretion and inflammation (Tracey, 2002).

The proinflammatory cytokine IL-1β can activate vagal afferents after intraportal administration and, consequently activate vagal efferents (Niijima, 1996). In rats, intraperitoneal IL-1β results in c-fos induction in vagal afferents (Goehler *et al.*, 1998). The IL-1β receptor is expressed in vagal afferents and paraganglionic cells (Goehler *et al.*, 1997; Ek *et al.*, 1998; Goehler *et al.*, 2000). It has been suggested that low doses of IL-1β act on the vagus nerve but that higher doses can act centrally (Hansen *et al.*, 2001; Pavlov & Tracey, 2012). In addition, vagal afferents express the pattern recognition receptor toll-like receptor-4 (TLR4) and can, therefore, respond to the microbial product lipopolysaccharide (LPS) (Hosoi *et al.*, 2005; de Lartigue *et al.*, 2012). LPS is increased after meal intake and the vagus nerve has been involved in suppressing postprandial inflammation (Pavlov & Tracey, 2012).

After central integration of these signals, vagal efferents release neuromediators to modulate local immune cells. In a later study, it was shown that the inflammatory reflex was mediated by the link of acetylcholine (ACh) secreted from vagal efferents acting on the α7 subtype of the nicotinic ACh receptor (α7nAchR) expressed in macrophages (Wang *et al.*, 2003). Apart from CAIP, the vagus nerve could systemically suppress inflammation via regulation of hypothalamic-pituitary-adrenal (HPA) axis by vagal afferents or by stimulating the splenic sympathetic nerve via vagal efferents (Bonaz, Sinniger & Pellissier, 2016). The latter pathway proposes that vagal efferents activate sympathetic neurones in the mesenteric ganglion that consequently release noradrenaline. Noradrenaline activates T cells in the spleen, which release ACh that inhibit α7nAchR-expressing splenic macrophages (Rosas-Ballina *et al.*, 2008, 2011).

However, inflammation is usually local and, in the case of local intestinal inflammation, other neuro-immune circuits have been proposed (Goverse, Stakenborg & Matteoli, 2016; Veiga-Fernandes & Mucida, 2016). Vagal efferents are confined in the myenteric plexus and interact with gut macrophages indirectly via other enteric neurones, rather than directly (Cailotto *et al.*, 2014). In the muscular layer and myenteric plexus, a population of muscularis macrophages (MM) are located close to enteric neurones and can express the α7nAchR (Cailotto *et al.*, 2014). MMs were shown to regulate the activity of enteric neurones as well as intestinal peristalsis, and this crosstalk was dependent on the microbiota (Muller *et al.*, 2014). MMs have a tissue-protective phenotype and, in response to infection, prevent excessive neuronal damage which involves β_2-adrenergic signalling (Muller *et al.*, 2014; Gabanyi *et al.*, 2016; Matheis *et al.*, 2020). On the other hand, lamina propria macrophages have a pro-inflammatory profile (Gabanyi *et al.*, 2016).

Pulling all of this together, vagal afferent activity has been shown to influence gut sympathetic activity and its effects on macrophage function. Importantly, vagotomised mice are more susceptible to colitis and had fewer T_{reg} in the lamina propia and in lymphatic tissue, suggesting a role for vagal nerve tone in immune tolerance at the lamina propria (Ghia *et al.*, 2006; Di Giovangiulio *et al.*, 2016). Therapeutically, VNS targets α7nAchR-expressing MMs which does not involve the spleen or T cells (Matteoli *et al.*, 2014). Apart from pre-clinical data, clinical pilot studies have suggested that targeting the vagus nerve is a promising therapeutic approach for the treatment of Crohn's disease, a type of IBD in which parts of the digestive tract are chronically inflamed and mixed with healthy areas (Bonaz *et al.*, 2016; Bonaz, 2018).

ILCs are also regulated by the nervous system and potentially by the vagus nerve (Klose & Artis, 2019). Peritoneal ILC3s with a similar phenotype to intestinal ILC3s are located close to choline acetyltransferase-expressing cells, express cholinergic receptors and are responsive to vagus nerve regulation (Dalli *et al.*, 2017). Vagotomy reduced peritoneal ILC3s, delayed the resolution of *Escherichia coli* infection, and this effect was rescued by administration of ILC3 cells (Dalli *et al.*, 2017). ILC2s are located adjacent to cholinergic neurones in the small intestine lamina propria and respond to neuropeptides (Cardoso *et al.*, 2017; Klose *et al.*, 2017; Klose & Artis, 2019). ILC2 cells also express ACh receptors (Galle-Treger *et al.*, 2016; Chu *et al.*, 2021) and an α7nAchR agonist was shown to dampen ILC2 activity in a model of allergy (Galle-Treger *et al.*, 2016). In contrast, ACh was shown to activate ILC2 activity and to defend against helminth infection, suggesting that ACh can act on different receptors and that the outcome depends on the context (Chu *et al.*, 2021; Roberts *et al.*, 2021). More recently, it has been shown that ILC2s can also synthetize ACh to promote ILC2 population expansion and barrier immunity to helminths (Roberts *et al.*, 2021). Although vagal terminals are located in the gut wall, the interaction between vagal terminals, ENS and immune cells is remain poorly characterized, though several circuits have been proposed (Veiga-Fernandes & Mucida, 2016).

In summary, the neuro-immunology of the gut is an extremely complex and poorly understood system. In particular, evidence points to an important interaction between ILC populations and the vagus in terms of the regulation of inflammatory responses. Inflammation is usually a temporary event but chronic inflammation is part of the pathogenesis of a range of syndromes, including obesity. Vagus nerve stimulation has already shown promise in other gut syndromes with chronic inflammation, such IBD. The anti-inflammatory reflex of the vagus nerve could be a therapeutic tool to treat obesity (Pavlov & Tracey, 2012). A deeper understanding of the

effects of vagal stimulation on gut immunity may therefore aid the development of non-pharmacological interventions to treat obesity.

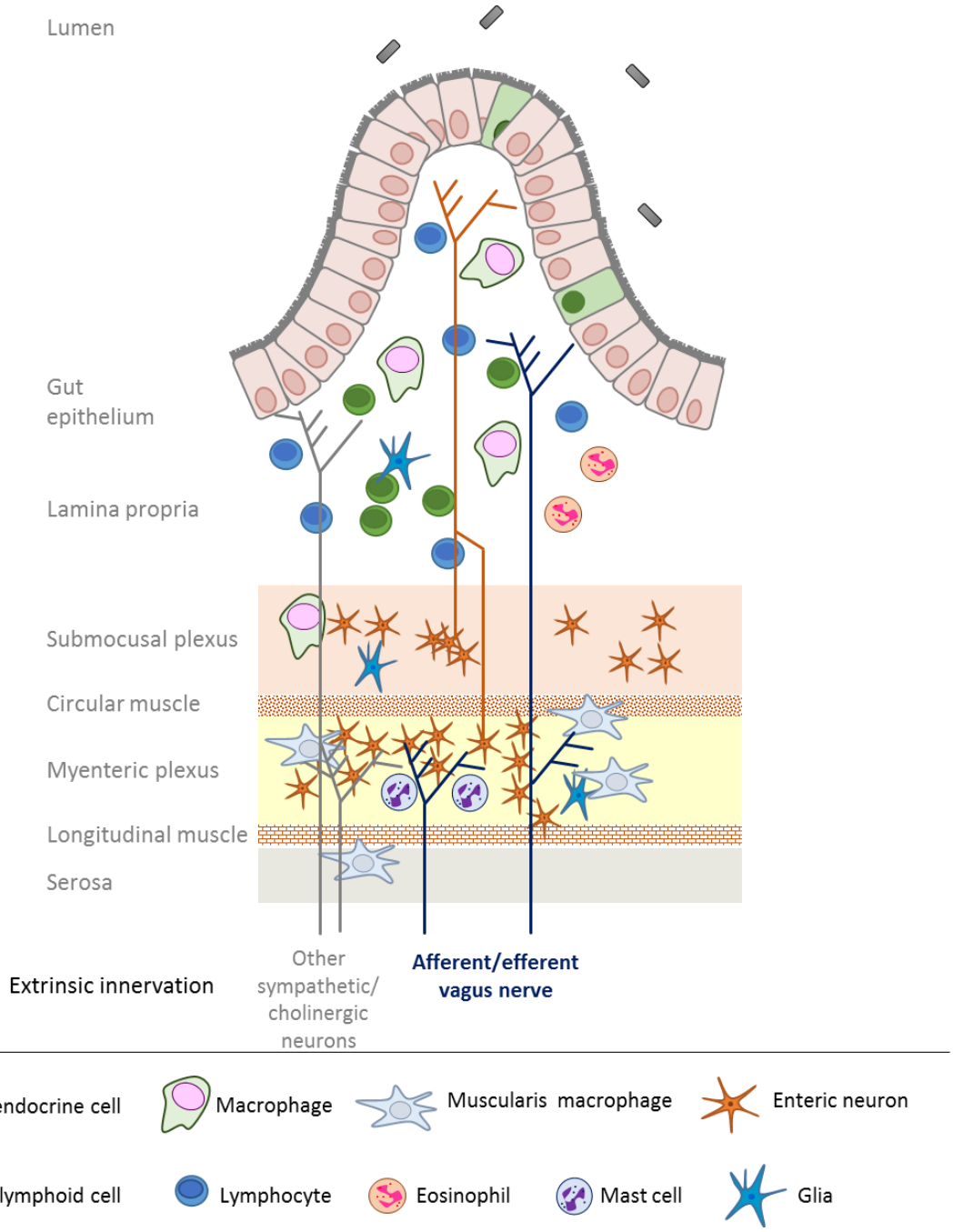

Figure 2.1.4.1. Neuro-immune crosstalk in the intestine.

2.2 Hypotheses and aims

The aims of the experiments described in this chapter were to:

- Assess the effect of chemogenetic activation of vagal afferents on feeding and glucose tolerance.
- Investigate the effect of PYY_{3-36} on vagal afferent activity.
- Assess the effect of chemogenetic activation on immune homeostasis in the intestinal mucosa.

The hypotheses were that:

- Chemogenetic activation of the afferent vagus can modulate feeding and glucose tolerance.
- The gut hormone PYY_{3-36} activates the vagus nerve.
- Chronic activation of the afferents promotes an anti-inflammatory phenotype in the intestinal mucosa.

2.3 Materials and methods

2.3.1 Animals

Mice were housed in ventilated cages under controlled conditions (21-23°C, 45-56% humidity) in a 12 h light/dark cycle (lights on at around 7 am). For the chemogenetic study, female C57Bl6/J mice (8 weeks old) were provided by Charles River. They were maintained in groups (6 animals/cage) except when specified. They had *ad libitum* access to water and chow (RM1). This work was conducted under the project licence PD75F462C (PPL holder Prof KG Murphy) and all procedures adhered to the UK Home Office Animals (Scientific Procedures) Act 1986.

2.3.2 Surgery

Mice were anaesthetised with 5% isoflurane (IsoFlo®, Zoetis, London, UK) and 1L/min oxygen in an anaesthetic chamber. Mice were weighed, shaved from the chin to the thorax, placed on a heated pad (37°C) in a supine position and anaesthesia was maintained by mask inhalation of isoflurane adjusted accordingly to maintain surgical-plane anaesthesia. Mice received subcutaneous (s.c.) injections of 2 mg/kg atropine sulfate (Hameln Pharmaceuticals, Gloucester, UK) and 5 mg/kg analgesic carprofen (Rimadyl®, Zoetis) at the onset of surgery. A midline neck incision was performed using toothed forceps and scissors, and the salivary glands were retracted. Neck muscles were gently retracted to expose the carotid artery, which was separated

from the adjacent vagus nerve. The vagus nerve was caudally dissected (with a minimum touch technique) and separated from the hypoglossal nerve, until the NG (just below the jugular foramen) was visualised and accessible for injection. A 0.58 mm-diameter glass capillary (World Precision Instruments, Hertfordshire, UK) containing the virus was attached to a micromanipulator and the NG was injected with a PV820 Pneumatic Picopump (World Precision Instruments). Salivary glands and the skin were closed with sterile Coated VICRYL® (polyglactin 910) suture (Ethicon, Livingston, UK). While recovering from anaesthesia, mice received a s.c. injection of 0.05 mg/kg buprenorphine hydrochloride (Vetergesic, Ceva Animal Health, Buckinghamshire, UK). Mice were allowed to recover in a ventilated heating chamber (37°C) and then they were returned to their home cage and received mash (powdered chow mixed with water). Animals body weight and state was recorded daily until body weight values reached pre-surgery levels. Animals were group housed pre- and post-surgery as a refinement to improve surgical recovery. Animals recovered for 3 weeks to allow expression of the viral constructs before studies were conducted.

For bilateral injections, the above-described protocol was first performed on one NG side. After a recovery week, the same surgery was performed on the left NG. This was because bilateral surgery in the same day results in massive vagal activity alteration and high mortality.

For the chemogenetic experiment, ready-to-use viral particles of pAAV5-hSyn-hM3D(Gq)-mCherry ($3x10^{12}$ vg/ml) were delivered in the NG of female mice. This virus was supplied by Addgene (deposited by the University of North Carolina at Chapel Hill). The DREADD hM3D(Gq) or hM3Dq is a genetically engineered human M3 muscarinic receptor with two-point mutations. The expression of this modified $G_{q/11}$-coupled GPCR is induced on target cells and administration of a receptor-specific synthetic ligand induces an increase in intracellular calcium levels that causes second messenger signalling and results in neuronal firing.

2.3.3 DREADD ligand administration

The DREADD ligand Compound 21 dihydrochloride (water soluble; Hello Bio, UK) was used as a ligand for hM3Dq activation. Compound 21 was allowed to equilibrate to RT, diluted in 0.9% NaCl (saline) and aliquots were stored at -20°C (at 0.6 µg/µL). Compound 21 was diluted in saline before injection so that animals received i.p. injection at 3 mg/kg (in a volume around 100 µL). The ligand was once daily-administered before dark phase (around 7 pm), except on the day of the terminal experiment (in which they received the treatment earlier in the light

phase), for a total of 10 days. Control animals received vehicle (saline) in parallel. For habituation, mice were i.p. injected for 3-5 days before drug administration.

2.3.4 Feeding studies

Before the start of feeding studies, animals were individually housed for 4 days. Using a crossover design, animals received each treatment (PYY_{3-36} or saline) in a random order. The daily treatment with Compound 21 or vehicle started the day before the first feeding test.
On the day of the feeding test, animals were weighed, and chow (RM1, SDS Diets) was removed around 2 h before the start of the study. Animals had *ad libitum* access to water during all the study.
For the study, chow was pre-weighed using a PLJ 420-3F (Kern & Sohn GmbH, Germany) precision balance (0.001 g readability). PYY_{3-36} was prepared on the experimental day just before the i.p. injection by adding saline to pre-prepared freeze-dried vials or directly to the lyophilized form. The volume of i.p. was around 100 µL (for an average size 25 g mouse).

Mice expressing the hM3Dq in the NG received Compound 21 or vehicle at t = -30 min. At t = 0 (dark phase onset), animals received PYY_{3-36} (Tocris Biosciences, Abingdon, UK) at 3 µg/kg or saline and pre-weighed chow was placed in the hopper. Food weight was recorded at t= 0.5, 1, 2 and 3 h post-injection of PYY_{3-36}/saline.

In the case of feeding studies to test the effect of the DREADD ligand in acute food intake of non-hM3Dq expressing control mice, Compound 21 (3 mg/kg) or vehicle was administered at t = 0 min and food weight was recorded at t= 0.5, 1 and 2 h post-injection of DREADD ligand.

2.3.5 Intraperitoneal glucose tolerance test (IPGTT)

Food was removed 5 h prior to the start of the IPGTT and animals received Compound 21 or saline at 30 min before the start of the tolerance test. Topical anaesthesia (lidocaine/prilocaine, EMLA™, Aspen, UK) was applied in the mice tail before tail venepuncture. Baseline blood glucose measurement was recorded using a glucometer (GlucoRX Nexus, GlucoRX, UK) and then i.p. injection of 20% w/v glucose (Baxter) was administered (2 g/kg). Subsequent blood glucose measurements were recorded at 15, 30, 45, 60, 90, 120, 150 and 180 min post-injection. After the study, mice were returned to their cages with *ad libitum* access to food and water.

2.3.6 Terminal experiment

A final experiment was performed at day 8 of chronic treatment with Compound 21/vehicle. Animals were fasted for around 4 h (with ad libitum access to water) and they received i.p. injection of Compound 21 or saline at the usual dose. After 90 min, tissue was harvested.

2.3.7 Lamina propria isolation

This was performed in collaboration with Dr Noe Rodriguez-Rodriguez (Andrew McKenzie's lab, MRC Laboratory of Molecular Biology, Cambridge, UK), who also kindly shared this protocol and provided the reagents.

Small intestine was dissected and placed in 10 mM HEPES (Gibco) in 1X PBS (Sigma) (PBS/HEPES) on ice. Intestinal contents were removed by gently applying pressure along the length of the intestine. Intestines were opened longitudinally, cut in 3 cm long pieces and washed by vortexing in the PBS/HEPES for 10-20 sec. The tissue was then transferred to a fresh tube with PBS/HEPES and washed again.

To remove the epithelial cells, tissue was incubated with Roswell Park Memorial Institute Medium (RPMI; Gibco) supplemented with 10 mM HEPES, 2% FCS (Gibco), 1 mM dithiothreitol (VWR Life Sciences) and 5 mM EDTA (Sigma) for 35 min at 37°C with shaking (200 rpm) at a 35-degree angle. The supernatant was strained through a 50 µm cell strainer (Celltrics), and remaining intestinal tissue fragments were incubated again with the supplemented RPMI for 20 min. Supernatant was strained again and the intestinal pieces were incubated with RPMI containing 2% FCS, 0.125 KU/mL DNaseI (Sigma-Aldrich) and 62.5 µg/mL Liberase TL (Roche/Sigma-Aldrich) at 37°C with shaking as previously for 40-45 min until digestion is complete.

The digested tissue was passed through a 70 µm strainer (Greiner Bio-One) using a syringe to push it through the strainer. The remaining digested tissue was washed with 3% FCS in 1X PBS (PBS/FCS) and strained again. The resulting strained single cell suspension was centrifuged at 400 *xg* for 5min at 10°C and the resultant pellet was separated over a 40% - 80% gradient of Percoll (GE HealthCare/Cytiva). For that, the pellet was resuspended in 5 mL Percoll at 40%, transferred to a 15 mL falcon tube, underlayed with 3 mL of 80% Percoll and spun at 600 x*g* for 20 min (without brakes). The lymphocytes of the lamina propia were isolated from the interface

and PBS/FCS was added. The lymphocytes were used for in vitro stimulation or directly for flow cytometry.

2.3.8 Flow cytometry

Flow cytometry is a laser-based technology widely used for analyzing the expression of extracellular or intracellular cell-associated molecules (markers). It allows the identification of cell types and subpopulations in a heterogenous cell population and it can also be used to sort specific cell types to obtain an enriched population (cell sorting). Briefly, this method involves staining a single-cell suspension so that cell molecules (markers) are specifically bound to fluorochrome-labeled antibodies (directly or indirectly) or fluorescent ligands. In the flow cytometer, cells in sheath fluid pass through a beam or a laser in a single-file stream of cells. The light scattered by the cell is measured as forward scatter (FSC), which is proportional to the cell size, and side scatter (SSC), which is proportional to the cell granularity. Fluorochromes (bound to the marker-specific antibodies) are excited by lasers of specific wavelengths and they emit a fluorescent signal that is collected by sensors. Each sensor detects fluorescence at a specific wavelength and converts it into a voltage pulse (event).

Dr Noe Rodriguez-Rodriguez advised on panel design and kindly donated the reagents. Lymphocytes were distributed in round bottom 96-well plates and pelleted (400 x*g*, 5 min). In a 100 µL volume, cells were stained with PBS/FCS fluorochrome- or biotin-conjugated antibodies (see Table 2.3.8.1) and incubated in the fridge/on ice for 40 min protected from light. Cells were washed with 150-200 µL of PBS/FCS per well and centrifuged at 400 x*g* for 5 min. After repeating the wash, cells previously incubated with biotin-conjugated antibodies were incubated with fluorochrome-conjugated streptavidin for 30-40 min in the fridge/on ice protected from light. After performing 2 washing steps (as before), cells were fixed/permeabilised with 100 µL of fixing solution (eBioscience™ Foxp3 / Transcription Factor Staining Buffer Set) for 30-60 min in the fridge/on ice following manufacturer's instructions. To wash, 150-200 µL of eBioscience permeabilization buffer (prepared following manufacturer's instructions) was added per well and cells were centrifuged at 400 x g for 5 min. After repeating the washing step with the permeabilization buffer, cells that did not require intracellular cytokine staining (ICS) were resuspended in 200-400 µL of PBS/FCS and stored at 4°C until analysis by flow cytometry. A non-ICS control was included.

For the in vitro stimulation conditions to analyze cytokine production (e.g., IL-17A) by lamina propria-resident lymphocytes, single cell suspensions were plated in a flat-bottom 96 well plate,

in 300 µL of complete RPMI (10% FCS, 10mM HEPES, 100 µM β-mercaptoethanol, Penicillin/Streptomicin) in the presence of 1x eBioscience™ Cell Stimulation Cocktail (plus protein transport inhibitors) and incubated overnight (10-12 h) at 37°C at 5% CO_2. Cells were transferred to a round-bottom 96 well plate and washed once before proceeding with fluorescence-activated cell sorting (FACS) staining.

For ICS, cells were stained with the mix of ICS antibodies (panel 1) in 100 µL of eBioscience permeabilization and incubated overnight in the fridge/on ice or at RT for 30-60 min protected from light. To wash, 150-200 µL of eBioscience permeabilization buffer was added per well and cells were centrifuged at 400 x g for 5 min. Cells were resuspended in 200-400 µL of PBS/FCS and stored at 4°C until analysis by flow cytometry. Cells were analysed in a customized BD LSRFortessa™ (5 laser) flow cytometer (LMB, Cambridge UK) by Dr N Rodriguez-Rodriguez as soon as possible. Precision Count beads™ (Biolegend) were used for counting the absolute number of cells (44.31 beads/µL). Data was analyzed in FlowJo (Ashland, OR).

Data is presented as percentage of cells in a subpopulation. This was supplemented with the total number of cells within each population. Total number of cells is calculated using the counting beads, which can be easily distinguished from the cells. By counting the number of beads, the volume of sample analysed is calculated and, therefore, the absolute count of cells within a subpopulation can be calculated.

Table 2.3.8.1. Antibodies and dyes used for flow cytometry.

List of the targets of antibodies are shown in alphabetical order. The dilution and the panels in which antibodies were used are indicated. AF, Alexa Fluor™; APC, allophycocyanin; Arg1, arginase 1; BUV, Brilliant Ultraviolet™; BV, Brilliant Violet™; CD, cluster of differentiation; CX3CR1, CX3C chemokine receptor 1; Cy, cyanine; FcεRI, Fc fragment of immunoglobulin E receptor; FITC, fluorescein isothiocyanate; FoxP3, forkhead box P3; GATA3, GATA binding protein 3; MHC, major histocompatibility complex; PE, phycoerythrin; PerCP, peridinin chlorophyll; RORγt, RAR (retinoic acid receptor)-related orphan receptor γ; TCRβ, T-cell receptor β chain.

Target	ID	Supplier	Expression system	Label	Dilution	Panel
Arg1	48-3697-82	eBioscience	Rat / IgG2a, κ	eFluor450	1:300	3
B220	56-0452-82	eBioscience	Rat / IgG2a, κ	AF700	1:300	1, 2, 3
CD103	121423	Biolegend	Armenian hamster / IgG	BV510	1:200	3

Target	ID	Supplier	Expression system	Label	Dilution	Panel
CD11b	101257	Biolegend	Rat / IgG2b, κ	BV605	1:300	2
CD11b	612800	BD Biosciences	Rat / IgG2b, κ	BUV737	1:300	3
CD11c	17-0114-82	eBioscience	Armenian hamster / IgG	APC	1:300	3
CD19	115528	Biolegend	Rat / IgG2a, κ	AF700	1:300	1, 2, 3
CD24	101827	Biolegend	Rat / IgG2b, κ	BV605	1:300	3
CD25	102042	Biolegend	Rat / IgG1, λ	BV510	1:300	1
CD3	100216	Biolegend	Rat / IgG2b, κ	AF700	1:300	1, 2, 3
CD4	56-0041-82	eBioscience	Rat / IgG2b, κ	AF700	1:300	1, 2
CD4	100451	Biolegend	Rat / IgG2b, κ	BV605	1:300	1
CD45	103138	Biolegend	Rat / IgG2b, κ	BV510	1:200	2
CD45	564279	BD Biosciences	Rat / IgG2b, κ	BUV395	1:200	1, 3
CD64	139307	Biolegend	Mouse / IgG1, κ	PerCP-Cy5.5	1:200	2, 3
CD8α	100730	Biolegend	Rat / IgG2a, κ	AF700	1:300	1, 2
cKit	135138	Biolegend	Rat / IgG2b, κ	BV785	1:300	2
CX3CR1	149006	Biolegend	Mouse / IgG2a, κ	PE	1:200	3
F4/80	123141	Biolegend	Rat / IgG2a, κ	BV785	1:300	3
FcεRI	48-5898-82	eBioscience	Armenian hamster / IgG	eFluor450	1:200	2
FcγRIII / FcγRII (Fc block)	BE0307	BioXcell	Rat / IgG2b, κ	BE0307	1:200	1, 2, 3
Fixable Viability Dye	65-0865-14	eBioscience	-	eFluor™ 780	1:300	1, 2, 3
FoxP3	25-5773-82	eBioscience	Rat / IgG2a, κ	PECy7	1:300	1
GATA3	46-9966-42	eBioscience	Rat / IgG2b, κ	PerCP-eFluor710	1:300	1
I-A/I-E (MHC class II)	107641	Biolegend	Rat / IgG2b, κ	BV650	1:300	3
IFN-γ	505838	Biolegend	Rat / IgG1, κ	BV785	1:300	1
IL-13	53-7133-82	eBioscience	Rat / IgG1, κ	AF488	1:300	1
IL-17A	506930	Biolegend	Rat / IgG1, κ	BV650	1:300	1
IL-7Rα	121104	Biolegend	Rat / IgG2b, κ	Biotin	1:300	1
Ki67	25-5698-82	eBioscience	Rat / IgG2a, κ	PECy7	1:300	3
Ly6C	128005	Biolegend	Rat / IgG2c, κ	FITC	1:300	3
Ly6G	127618	Biolegend	Rat / IgG2a, κ	PECy7	1:200	2

Target	ID	Supplier	Expression system	Label	Dilution	Panel
SiglecF	552126	BD Biosciences	Rat / IgG2a, κ	PE	1:300	2
RORγt	12-6988-82	eBioscience	Rat / IgG2a, κ	PE	1:300	1
Streptavidin	612775	BD Biosciences	-	BUV737	1:300	1
Tbet	50-5825-82	eBioscience	Mouse / IgG1, κ	eFluor660	1:300	1
TCRβ	48-5961-82	eBioscience	Armenian hamster / IgG	eFluor450	1:200	1

2.3.9 NG culture

Following overdose with pentobarbital, NG were extracted and added to a 1.5 mL Eppendorf tube containing 22 µL of Liberase™ Dispase High (Roche,UK) in 500 mL of HKRB buffer (see Appendix I). For digestion, NG cells were incubated at 37°C in a heat block for 45 min (inverting every 15 min). Supernatant was removed and cells were washed 2 times with 1 mL warmed sterile PBS. Cells were resuspended in Advanced Dulbecco's Modified Eagle medium (DMEM) (Gibco-Thermo Fisher) containing 1% penicillin/streptomicin (P/S; Gibco), 10% fetal bovine serum (FBS) (Gibco) and 1:1000 nerve growth factor (Sigma-Aldrich). Tissue was triturated by pipetting up and down and filtered through a 70 µm filter to another tube, rinsing well with the media.

Cells were transferred to a µ-Slide VI 0.4 (Ibidi, UK) previously coated with poly-D-lysine (Sigma-Aldrich). For the coating, wells (including both reservoirs and channels) were incubated with 100 µL of poly-D-lysine (0.1 mg/mL in PBS) for 30 min at 37°C, washed twice with PBS 1X and allowed to air-dry. Cells (~60 µL/well) were incubated at 37°C (5% CO_2) for 1 h before adding 100 µL of conditioned media and incubated overnight.

2.3.10 Calcium imaging of NG neurones in the presence of PYY_{3-36}

Imaging of NG neurones was performed using Fluo-4, which is a fluorescent calcium indicator that allows in-cell measurement of calcium signalling upon GPCR ligand binding. The 2X Fluo-4 Direct™ Calcium reagent loading solution (Thermo Fisher Scientific) was pre-made following the supplier instructions. Probenecid reduces background fluorescence by preventing the efflux of intracellular dyes. The Fluo-4 Direct™ Calcium Assay kit formulation also includes a suppression dye to minimize growth medium-derived background signal.

The 2X Fluo-4 Direct™ reagent loading solution was defrosted and diluted to 1X with HKRB buffer. After removing 50 µL of media per well, 50 µL of the dye was added and cells were incubated during 30 min at 37°C followed by a 30 min incubation at RT (in the dark). Before starting imaging, wells were washed twice with HKRB.

Imaging was performed in an Eclipse Ti2 inverted microscope (Nikon) with an ORCA-Flash 4.0LT+ digital camera (Hamamatsu) using Micro-Manager software. Cells were imaged in a 100 µL volume at x10 magnification, 0.5 s intervals and 2x2 binning in the FITC channel (100 ms exposure). For baseline recording, wells were imaged containing 100 µL HKRB. PYY_{3-36} was added to achieve the desired final concentration in the 100 µL volume. Then, 50 mM potassium chloride (KCl) was added to cells (100 µL/well) (see Appendix I).

For analysis, macros developed by the Facility for Imaging by Light Microscopy (Imperial College London) for Fiji software were used. If required, time frames were manually aligned using a region of interest (ROI) as a reference. Then, ROIs were generated in each cell making sure that the ROIs covered the cell area in all the time frames and intensity was measured. Intensity signal was normalized to the average intensity of the first 30 s of the baseline period. Blurry frames, cells not responsive to KCl and outliers were discarded from the analysis.

2.3.11 Statistical analysis

All data is presented as mean ± SEM. Data was analysed by two-way ANOVA followed by Dunnett's or Bonferroni's multiple comparison test. In other cases, one-way ANOVA followed by Tukey's multiple comparisons test was performed. For non-parametric analysis, Kruskal-Wallis test or Mann-Whitney test were performed. Statistical analyses were performed using Prism 8.0 software (GraphPad, La Jolla, CA).

2.3.12 Experimental design

C57Bl6/J females were acclimatised for a week upon arrival. Mice received AAV expressing the hM3Dq bilaterally in the NG, where the cell nuclei of vagal afferents are located (section 2.3.2). Approximately three weeks after surgery, animals were randomised and received daily injections of the DREADD ligand (Compound 21) or vehicle (saline). Compound 21 would activate the vagal afferent neurons expressing the DREADD. On the second and third day of receiving the DREADD ligand (or vehicle), feeding studies (crossover) were performed in response to PYY_{3-36} or control vehicle (saline). Glucose tolerance was assessed on the fourth day of treatment.
The effect of PYY_{3-36} on the activity of vagal afferent neurons was further investigated by calcium imaging of neurons from nodose ganglia of littermate control mice.

After eight days of chronic treatment with DREADD ligand (or vehicle), lamina propria was collected in a terminal experiment and immunophenotyped by flow cytometry.

2.4 Results

2.4.1 The effect of chemogenetic activation of the afferent vagus nerve in body weight

In order to study the effect of bulk vagal afferent activation by chemogenetics, females received bilaterally in the NG a neuron-specific AAV driving the expression of the DREADD hM3Dq. In order to study the effect of chronic activation of the vagal afferents on body weight, animals were weighed before and after daily treatment with the DREADD ligand (or vehicle) started (Fig. 2.4.1.1, A). Body weight change was similar between groups before start of the treatment. After the first injection of Compound 21 (between day 19-20 post-surgery), a reduction in body weight was observed in the first couple of days (Fig. 2.4.1.1, B). There was a significant interaction of time x treatment in body weight gain (two-way ANOVA: $p = 0.0002$, $F(4, 100) = 6.036$).

Animals were grouped house and allocated into groups so that animals of both groups co-existed in cages. Therefore, daily food intake could not be compared between saline and Compound 21. Due to time constraint, energy expenditure and activity were not measured.

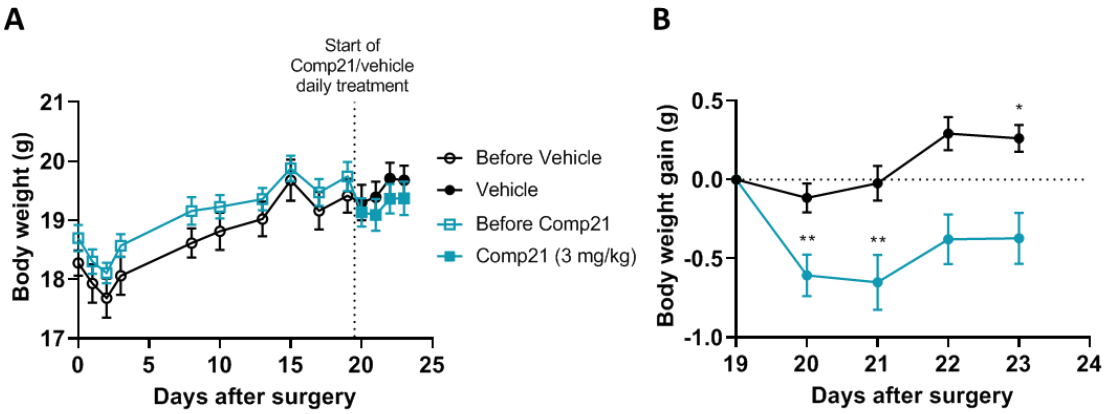

Figure 2.4.1.1. Body weight in mice expressing hM3dq in vagal afferents before and during chronic treatment with the DREADD ligand.

Body weight post-surgery (A) and body weight gain (B) after start of daily i.p. injection of the DREADD ligand Compound 21 (Comp21) (n = 13-14/group). Daily treatment started between day 19 and day 20 post-surgery. B: Two-way ANOVA followed by Dunnett's multiple comparison test compared to day 19 (*$p < 0.05$, **$p < 0.01$).

2.4.2 The effect of chemogenetic activation of the afferent vagus nerve in glucose homeostasis

To investigate if chemogenetic activation of specifically vagal afferents has an effect in glucose homeostasis, an IPGTT was performed after DREADD ligand administration (on the 4th day of daily DREADD administration). Compound 21 did not affect glucose tolerance compared to control (Fig. 2.4.2.1).

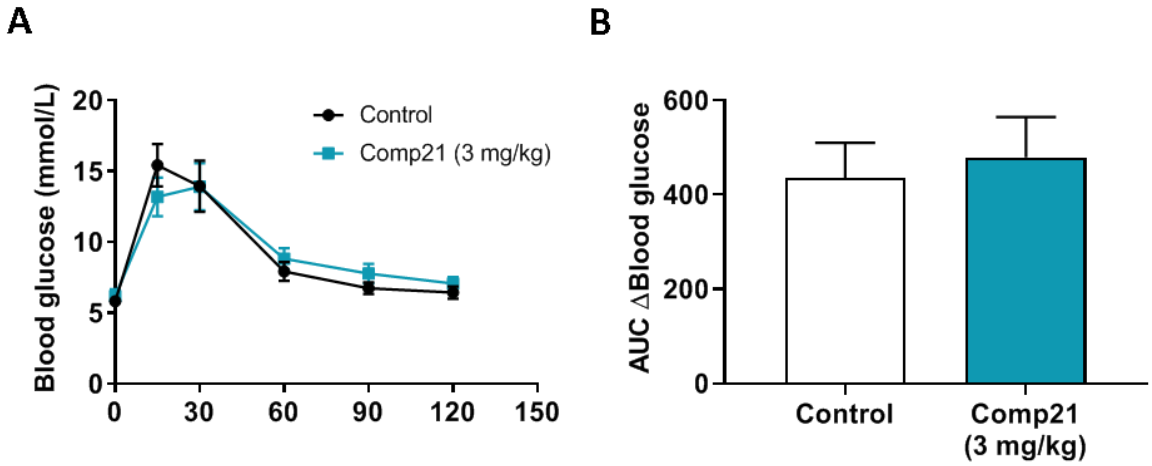

Figure 2.4.2.1. Glucose tolerance in mice expressing hM3dq in vagal afferents after treatment with DREADD ligand.

Blood glucose (mmol/L) during an IPGTT (A) and AUC of the blood glucose increase (from t =0) (B) in 5 h-fasted NG-hM3dq mice (n = 12/group) on the fourth day of daily i.p. injection with the DREADD ligand Compound 21 (Comp21) or vehicle (saline). Compound21/vehicle was injected 30 min before the start of the test.

2.4.3 The effect of chemogenetic activation of the afferent vagus nerve in the food intake response to PYY_{3-36}

PYY_{3-36} has been shown to increase gastric vagal afferent firing in rats (Koda *et al.*, 2005). In addition, the Y2R is expressed in vagal afferents. However, as previously described, Y2R is considered an auto-inhibitory presynaptic inhibitory receptor (coupled to Gi/o). To further study the effect of PYY_{3-36} on the vagus nerve activity, we assessed acute food intake after exogenous PYY_{3-36} administration in mice in which the afferent vagus nerve has been activated. We aimed to observe the effect of PYY_{3-36} on afferent vagus activity (if any). It is possible that gross activation by chemogenetics override the effect of PYY_{3-36} on vagal activity and, therefore, on food intake.

Thirty minutes after receiving Compound 21 or control, PYY_{3-36} at low dose (3 µg/kg) or saline were injected to perform acute feeding studies (crossover study on the 2nd and 3rd day of daily DREADD administration) (Fig. 2.4.3.1). Compound 21-treated mice (receiving vehicle instead of PYY_{3-36}) showed an acute decrease in food intake compared to the control group (not receiving DREADD ligand) as revealed by three-way ANOVA (group x treatment: $p = 0.045$, $F(1, 70) = 4.167$), which also revealed significant interaction between time and group ($p < 0.0001$, $F(4, 70) = 9.660$) (Fig. 2.4.3.1, A).

A trend towards reduced food intake was observed in the first hour after PYY_{3-36} injection in control mice but this did not reach significance (at 30min: $p = 0.071$; at 1h: $p = 0.059$) (Fig. 2.4.3.1, B,C). No differences in food intake after administration of Compound 21 alone and in combination with PYY_{3-36} were observed. Two-way ANOVA did not reveal significant interaction between group and treatment at 30 min or 1h post-injection.

Previous studies have shown that Compound 21 at this dose does not affect feeding behaviour in control animals that do not express the DREADD receptor (Thompson *et al.*, 2018). In a separated feeding study, we investigated if the strong anorectic effect after Compound 21 treatment was due just to the hM3dq-mediated activation of the afferent vagus nerve or if Compound 21 at this dose had an anorectic effect in our experimental setting (Fig. 2.4.3.1, D). Wildtype male mice (not injected in the NG and not expressing hM3Dq) showed a reduction in food intake in response to Compound 21 injection (two-way ANOVA; time x treatment: $p<0.0001$; $F(3, 45) = 9.648$). However, the degree of this Compound 21-mediated reduction in food intake was lower in non-hM3dq controls (e.g., 26% food suppression at 1 h post-injection) compared to NG-hM3dq mice (e.g., 80% food suppression at 1 h post-injection).

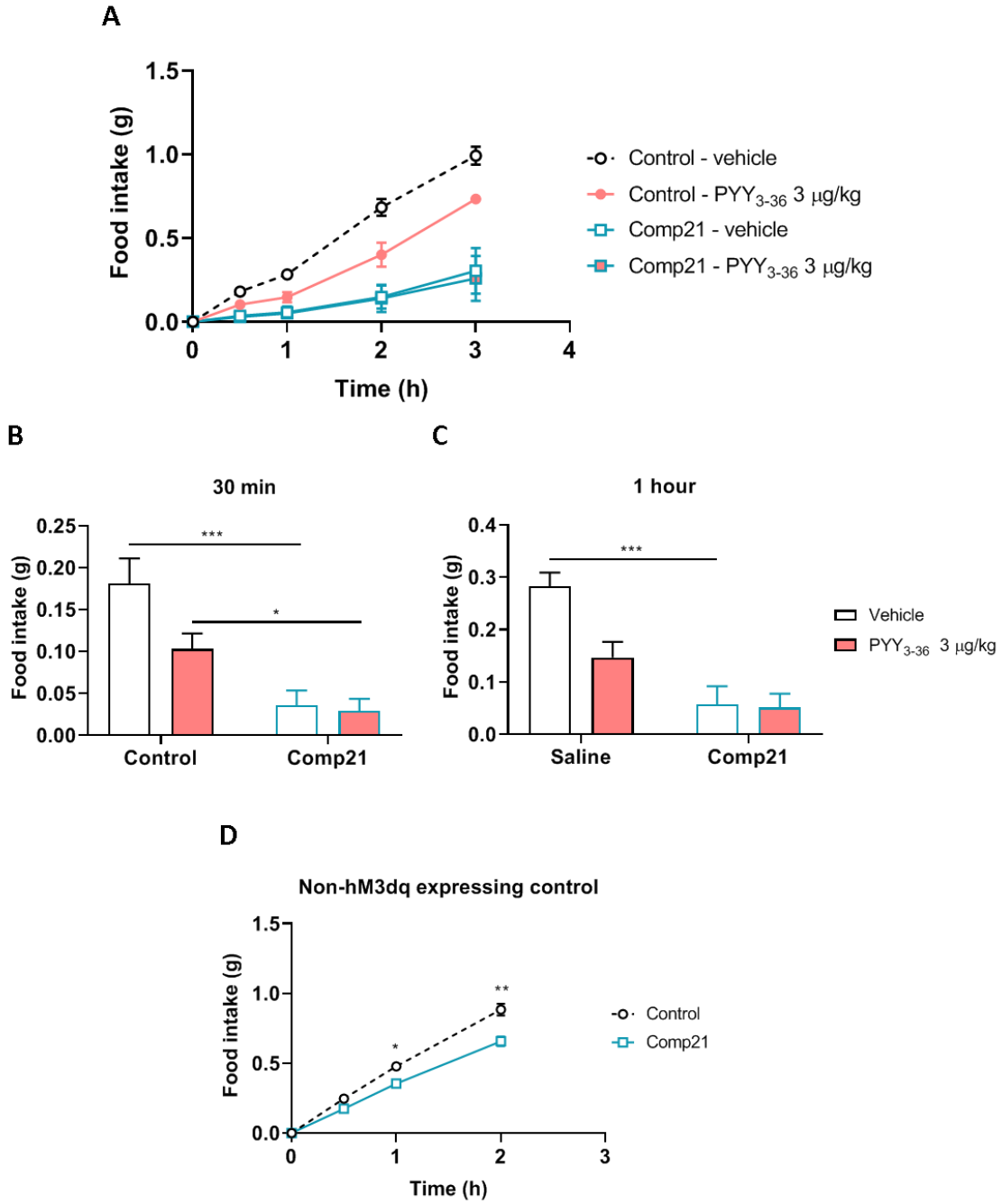

Figure 2.4.3.1. Cumulative food intake after i.p. injection of PYY_{3-36} in mice expressing hM3dq in vagal afferents after treatment with DREADD ligand.

Food intake overtime after i.p. injection of PYY_{3-36} at 3 µg/kg or vehicle (saline) in NG-hM3dq mice previously (t = -30 min) treated with Compound 21 (Comp21; n = 6) or control (n = 3) (A). Food intake is shown at 30 min (B) and at 1 h (C). Food intake overtime after i.p. injection of Compound 21 (n = 11) or control (n = 6) in wildtype males (not expressing hM3dq in the NG) (D). B,C,D: Two-way ANOVA followed by Bonferroni's multiple t test (*$p < 0.05$, **$p < 0.01$, ***$p < 0.001$).

2.4.4 Calcium activity of NG cultured neurones in response to PYY_{3-36}

The receptor of the anorectic gut hormone PYY_{3-36}, the Y2R, is a putative inhibitory pre-synaptic receptor (Broberger *et al.*, 1997; Batterham *et al.*, 2002). Electrophysiological studies revealed that PYY_{3-36} activated gastric vagal afferents in rats (Koda *et al.*, 2005). In order to explore the activity of mouse vagal afferents in response to PYY_{3-36}, calcium imaging was performed in cultured NG neurones (example image in Fig. 2.4.4.1, A). KCl is widely used as positive control as it reliably depolarizes neurons (calcium influx). Functional neurons were considered as respondent to KCl. Fluorescence signal (F) of each cell was normalised to its own baseline signal (average of first 30 frames) and maximum F/ΔF values during the stimulation period with PYY_{3-36} or vehicle were compared (Fig. 2.4.4.1, B), revealing significant differences between the studied stimuli (one-way ANOVA: $p = 0.026$, $F(2, 87) = 3.828$). Maximum values were significantly higher during 1000 nM PYY_{3-36} compared to saline ($p = 0.0196$). No significant differences in maximum fluorescence values between vehicle and 500 nM were observed. Of note, 1000 nM PYY_{3-36} was tested in three different wells while 500 nM was tested in one well so it is possible that by increasing n number, we could observe more differences between saline and 500 nM PYY_{3-36}. After a period of time in the presence of PYY_{3-36} or saline, cells were treated with KCl (Fig. 2.4.4.1, C and D).

Not all vagal afferents express the Y2R so it is expected that not all cells will respond to PYY_{3-36}. Based on previous methods used in the team, we define PYY_{3-36}-respondent cells as those with maximum F/ΔF values higher than 2 times the standard deviation from the mean of maximum F/ΔF values at saline condition. In the 1000 nM PYY_{3-36} condition, 38.3 ± 12% of cells (3 wells) were responding to PYY_{3-36}.

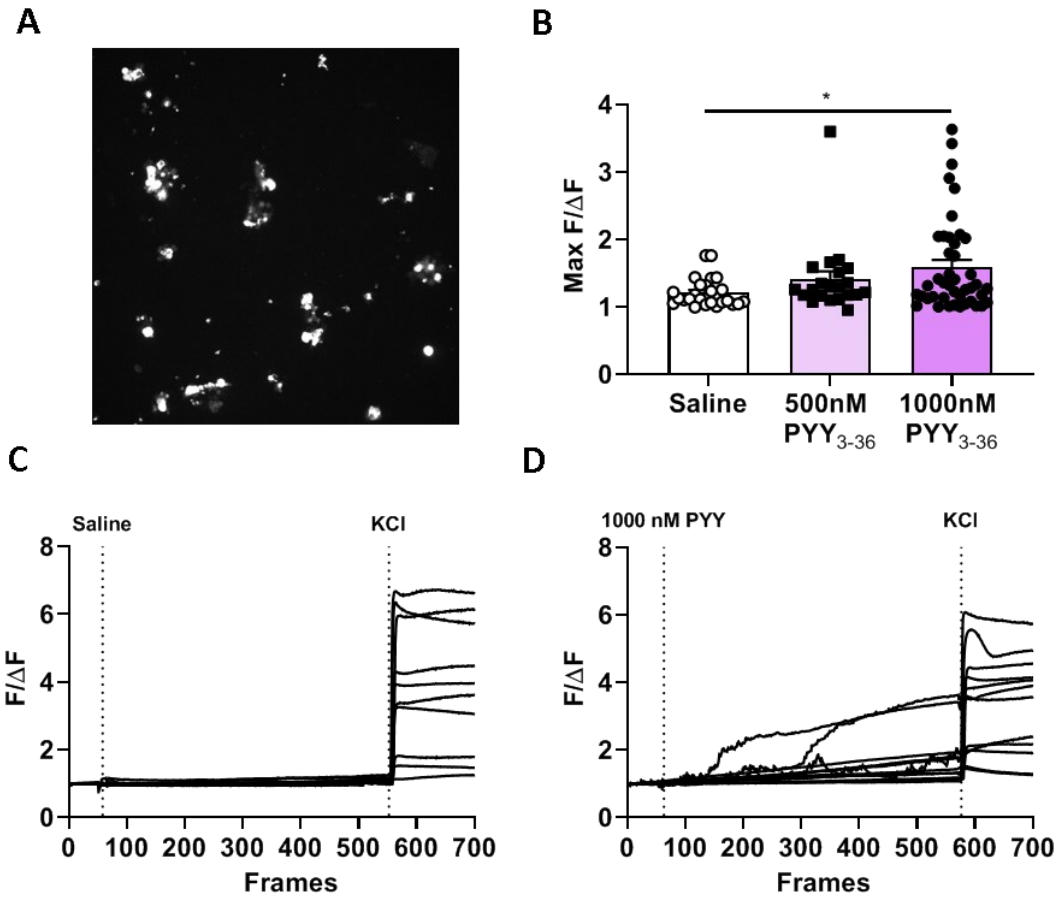

Figure 2.4.4.1. Calcium signal in cultured NG neurones in response to PYY_{3-36}.

NG cultured neurones from littermate controls were plated in wells and, using the calcium indicator Fluo-4, calcium signal was recorded in response to PYY_{3-36} (or vehicle) and KCl as positive control. Example of imaged NG neurons after stimulation with 1000 nM PYY_{3-36} (A). Fluorescent signal was normalised to the first 30 frames of baseline signal (F/ΔF) and maximum F/ΔF during PYY_{3-36} stimulation (500 nM PYY_{3-36}, n = 21 cells; 1000 nM PYY_{3-36}, n = 43) or vehicle (n = 26) was compared. Examples of F/ΔF from NG neurons in wells where saline (C) or 1000 nM PYY_{3-36} (D) were added followed by KCl. The times (frames) at which these stimuli were added in the wells are indicated. B: One-way ANOVA followed by Tukey's multiple comparisons test (*$p < 0.05$).

2.4.5 The effect of chemogenetic activation of the afferent vagus nerve in gut ILC and T cell population

In order to assess the effect of vagal afferent activation in ILCs and T cells, a panel of 13 colours and a viability dye was used to identify and quantify these populations' subsets. The gating strategy (Fig. 2.4.5.1) was as follows. Firstly, lymphocytes were identified based on size (forward scatter or FSC) and granularity (side scatter or SSC), and doublets and cell clumps were excluded

by FSC-H (height) vs FSC-A (area) followed by SSC-H vs SSC-A. The viability dye allowed the exclusion of dead cells from the analysis and CD45 was used as a marker of hematopoietic cells.

To analyse ILCs, cells expressing the lineage markers CD3 (T cells), B220 (B cells, subsets of T and NK cells), CD19 (B cells and some DCs), CD4 (thymocytes) and CD8α (cytotoxic T cells) were excluded (Lineage-negative, Lin- gate). Within the ILC gate (Lin- IL-7Rα$^+$ cells), ILC1 was defined as GATA3$^-$, RORγt$^-$ and Tbet$^+$. ILC2 and ILC3 were defined as GATA3$^+$ and RORγt$^+$ cells, respectively. In stimulated cells, IFN-γ$^+$, IL-13$^+$, IL-17A$^+$ cells were detected in the ILC1, ILC2 and ILC3 gates, respectively.

In order to analyse T cell populations, Lin$^+$ cells expressing the T cell antigen receptor β chain (TCRβ) were selected followed by gating CD4$^+$ T cells (cytotoxic CD8$^+$ T cells were not analysed with this approach). T_{reg} cells were defined as FoxP3$^+$. CD25 could not be used for defining T_{reg} cells due to low signal. T_H cells were defined as FoxP3$^-$ cells. Within the T_H gate, T_H2 and T_H17 were defined as GATA3$^+$ RORγt$^-$ and GATA3$^-$ RORγt$^+$ cells, respectively. Within GATA3$^-$ RORγt$^-$ gate, T_H1 cells were defined as Tbet$^+$. In stimulated cells, expression of cytokines IFN-γ$^+$, IL-13$^+$, and IL-17A$^+$ from T_H gate were analysed.

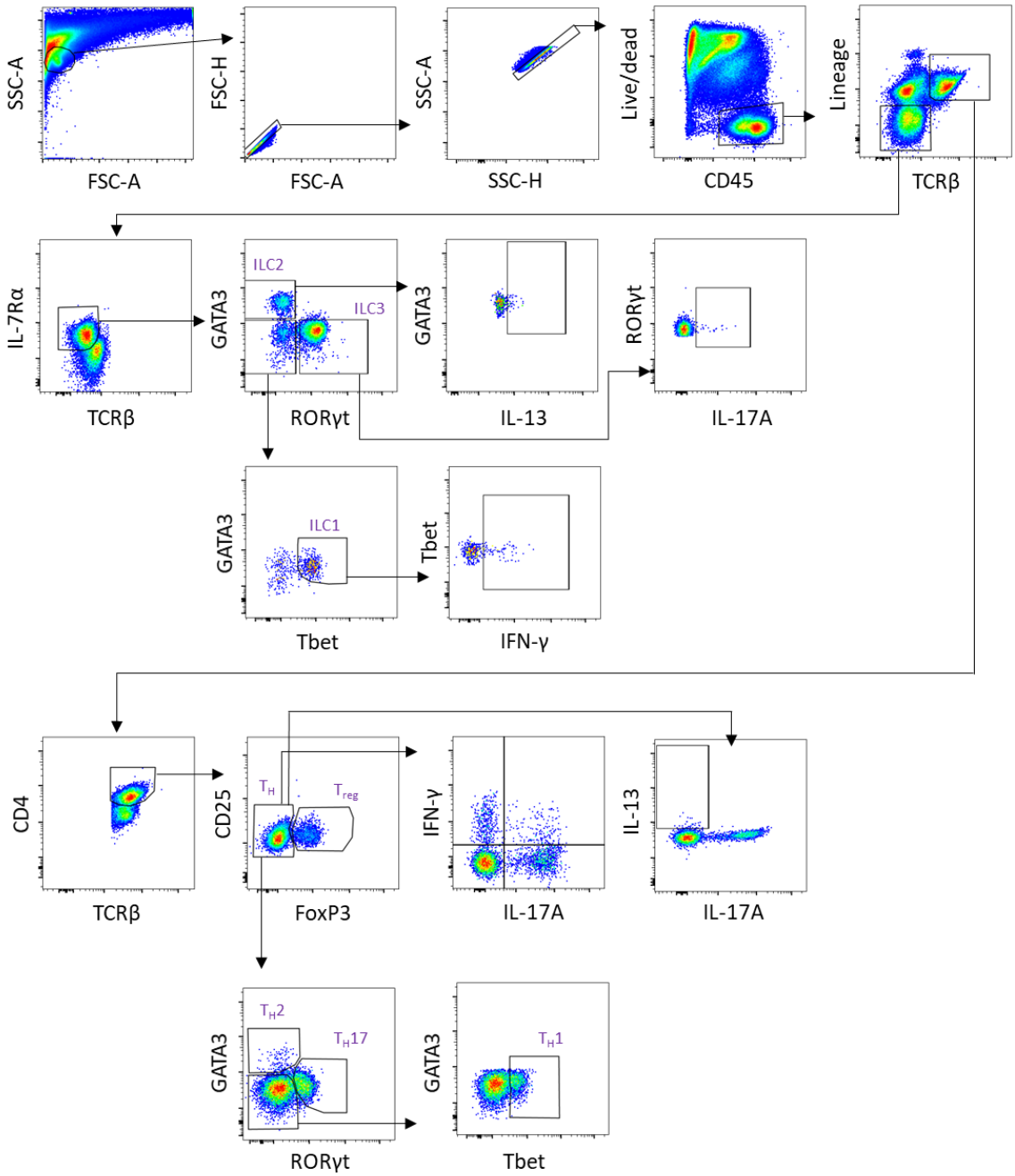

Figure 2.4.5.1. Example of contour plots and gating strategy for identification and quantification of ILCs and T cells as well as cytokine expression in mouse lamina propria.

Lineage markers are CD3, B220, CD19, CD4 and CD8α. SSC-A, side scatter (area); FSC-A, forward scatter (area); SSC-H, side scatter (height); FSC-H, forward scatter (height); CD, cluster of differentiation; TCRβ, T-cell receptor β chain; IL, interleukin; IL-7Rα, IL-7 receptor subunit α; GATA3, GATA-binding 3; RORγt, RAR (retinoic acid receptor)-related orphan receptor γ; IFN-γ, interferon γ; FoxP3, forkhead box P3; ILC, innate lymphoid cell; T_H, Helper T cell.

Due to the long processing time and the waiting time between tissue harvesting and tissue processing, more than the normal (≥20%) proportion of lamina propria sample preparations failed, decreasing the available sample size. Out of a total of 12 mice, the lamina propria preparation was only successful in 7 animals (2 controls and 5 Compound 21-treated animals). Since n = 2 in the control group, the non-parametric Mann-Whitney test was used for comparisons. Data is shown as total number of cells and as percentage (or frequency) of subpopulations. Total cell counts indicate cell infiltration while percentage or frequency is also influenced by the contraction or expansion of another subset.

Frequency and absolute counts of ILC, T cells and its subtypes were analysed in non-stimulated cells (Fig. 2.4.5.2) while cytokine expression was analyzed in stimulated cells (Fig. 2.4.5.3). The percentage of ILC subsets was higher in the control group compared to Compound 21-treated group albeit not significant ($p = 0.095$) (Fig. 2.4.5.2, B). As expected, ILC3 population was more frequent than ILC1 and ILC2 in both groups. Absolute counts seemed higher in ILC subsets, but no differences in frequency of ILC subsets between treatment groups were observed (Fig. 2.4.5.2, C-E). It remains to be elucidated if the difference in total number of cells is functionally meaningful (e.g., reduced inflammation, altered homeostatic control).

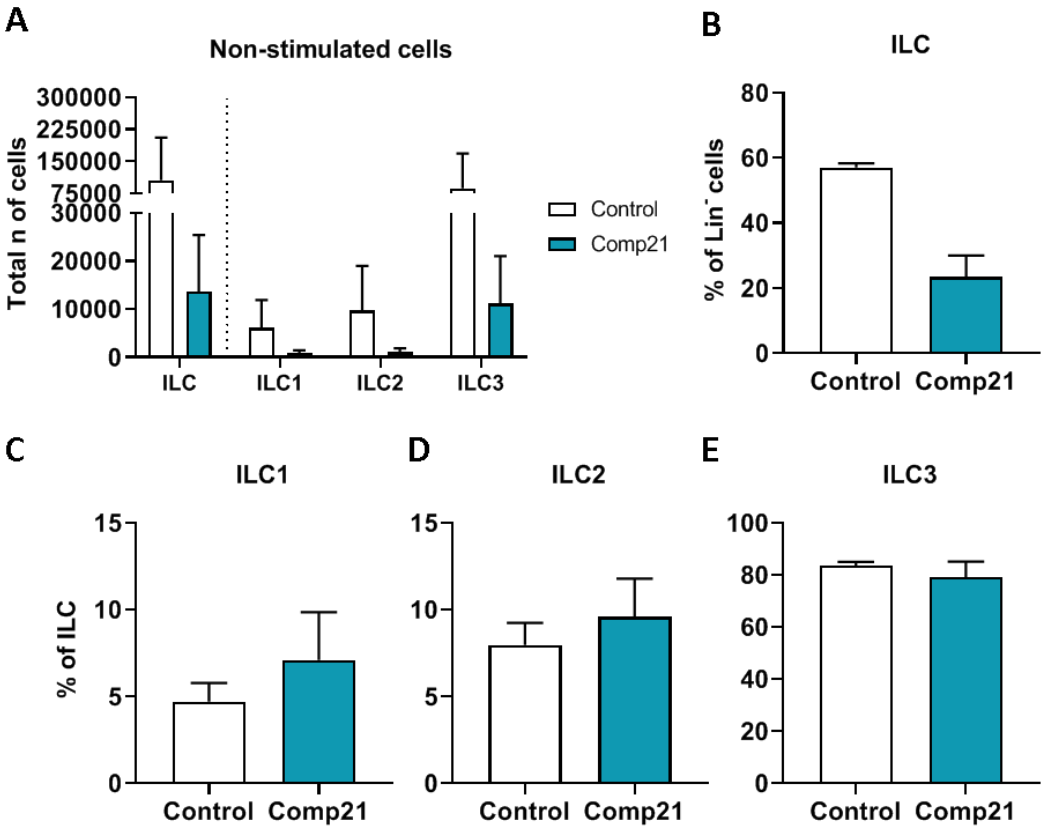

Figure 2.4.5.2. Total number and frequency of non-stimulated cells ILC subtypes in mice expressing hM3dq in vagal afferents chronically treated with DREADD ligand.

Number of non-stimulated cells in ILC and ILC subtype gates (A) and frequency (%) of parent population of ILC (B) and ILC subtypes (C-E) in lamina propria of Compound 21 (Comp21; n = 5) and control (n = 2) groups. ILC, innate lymphoid cell; Lin, lineage.

Number of stimulated cells of lamina propria in ILC and in each ILC subset is shown (Fig. 2.4.5.3, A). Stimulation induces cell death in some cells (compared to non-stimulated cells, Fig. 2.4.5.2, A). No significant differences in cytokine expression were observed between treatment groups (Fig. 2.4.5.3, B-D). Compared to ILC1 and ILC2, the frequency of ILC3-secreting (IL-17A) cells was lower in both treatment groups. Median of the proportion of secretory ILC3 cells was higher in Compound 21-treated groups (0.7, n = 4) compared to control (0.3100, n = 2) but this difference did not reach significance.

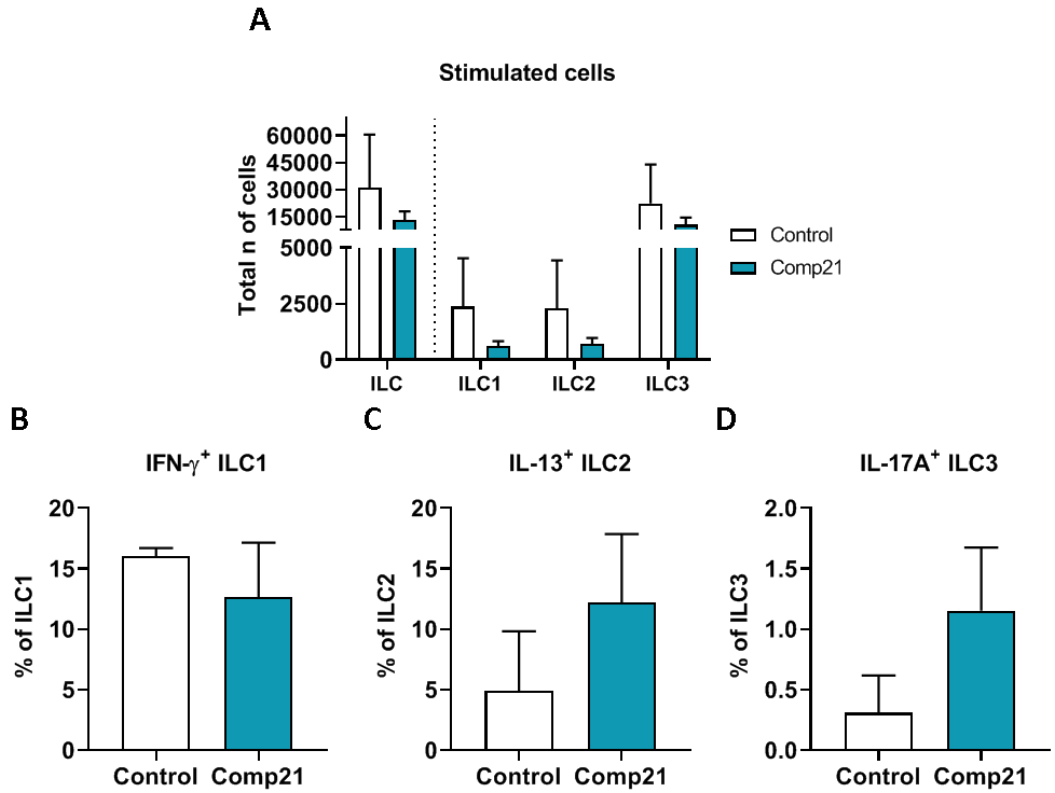

Figure 2.4.5.3. Total number and frequency of stimulated cells ILC subtypes in mice expressing hM3dq in vagal afferents chronically treated with DREADD ligand.

Number of stimulated cells in ILC and ILC subtype gates (A) and frequency (%) of parent of cytokine-expressing ILC subtypes (B-D) in lamina propria of Compound 21 (Comp21; n = 4) and control (n = 2) groups. IFN-γ, interferon γ; IL, interleukin; ILC, innate lymphoid cell.

In the case of T cells, the number of cells per group is shown (Fig. 2.4.5.4, A). Absolute counts of T cell subsets seemed higher, albeit not significant (p = 0.191, Kruskal-Wallis test) but this was not reflected in the percentage of the T cell subtypes since there was no significant differences between Compound 21-treated and control mice (Fig. 2.4.5.4, B-F). Of note, there was a trend towards a reduction in the percentage of T_{reg} cells in Compound 21-treated mice (p = 0.095, Mann-Whitney test). As expected, T_H17 and T_H1 populations were more frequent than T_H2 in both groups.

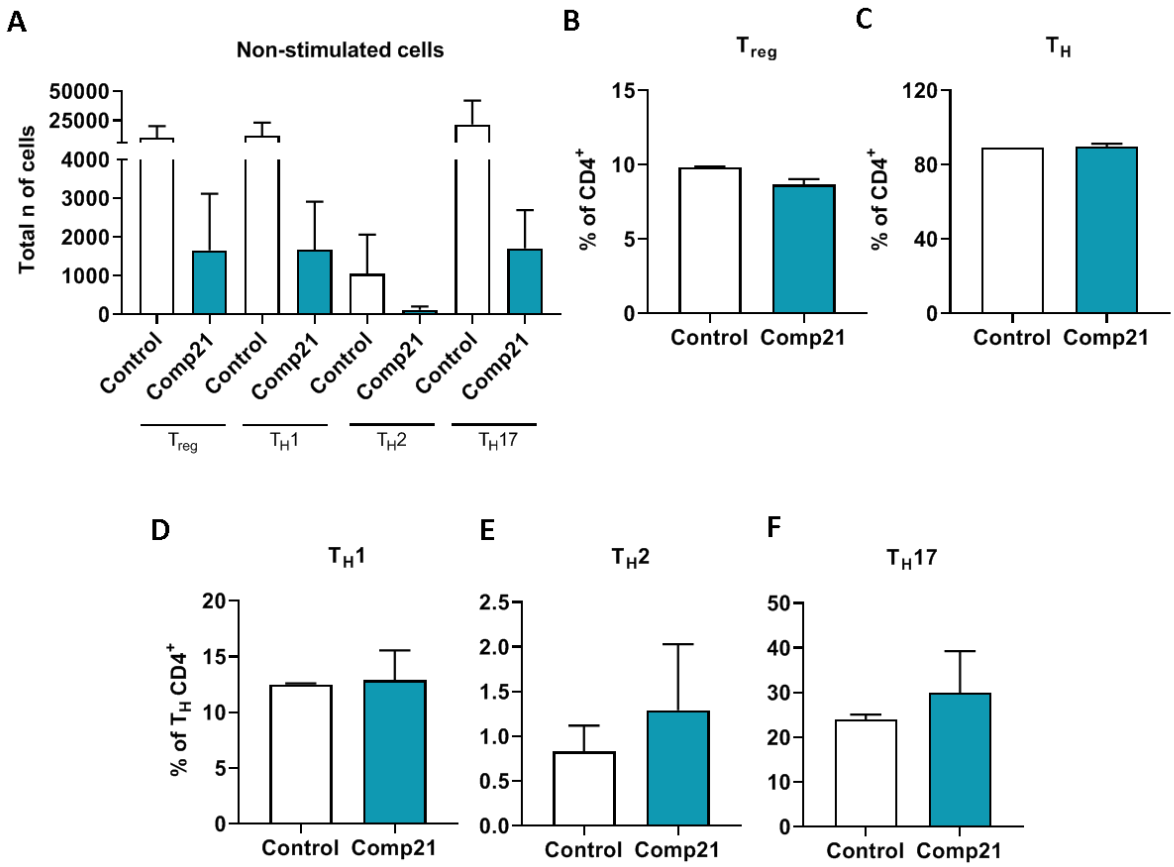

Figure 2.4.5.4. Total number and frequency of non-stimulated CD4$^+$ T cell subtypes in mice expressing hM3dq in vagal afferents chronically treated with DREADD ligand.

Number of non-stimulated T cell subtypes (A) and frequency (%) of parent of T_{reg} (B), T_H (C) T_H1 (D), T_H2 (E) and T_H17 (F) in lamina propria of Compound 21 (Comp21; n = 5) and control (n = 2) groups. CD, cluster of differentiation; T_H, Helper T cell.

Cytokine secretion was measured in stimulated T cells (Fig. 2.4.5.5). Within the T_H gate, IL-13 expression showed a trend towards increased expression in lamina propria cells from Compound 21-treated mice ($p = 0.133$) (Fig. 2.4.5.5, B). Most of the T_H cells did not secrete cytokines (Fig. 2.4.5.5, C) and a lower proportion expressed IFN-γ, IL-17A or both (Fig. 2.4.5.5, D-F).

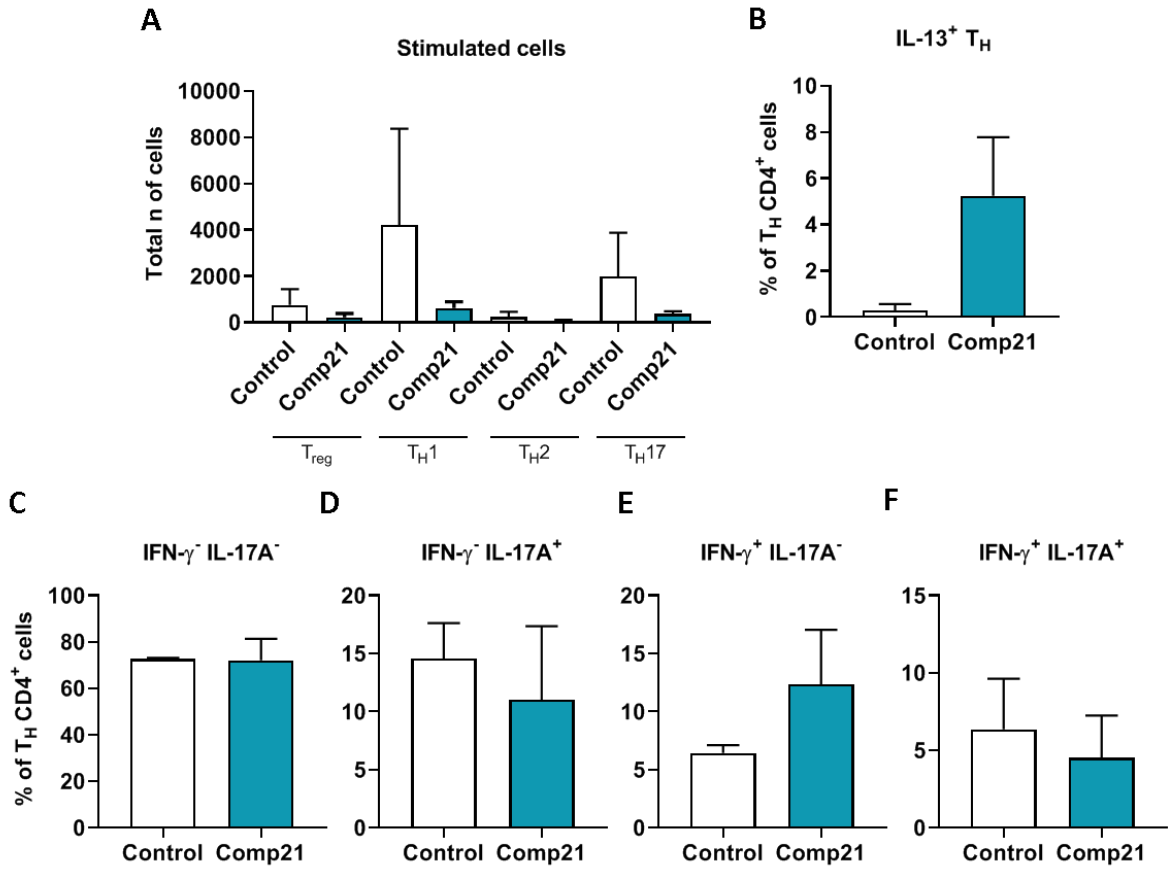

Figure 2.4.5.5. Total number and frequency of stimulated CD4+ T cell subtypes in mice expressing hM3dq in vagal afferents chronically treated with DREADD ligand.

Number of stimulated T cell subtypes (A) and frequency (%) of T_H expressing IL-13 (B), IFN-γ and IL-17A (C-F) in lamina propria of Compound 21 (Comp21; n = 4) and control (n = 2) groups. CD, cluster of differentiation; IFN-γ, interferon γ; IL, interleukin; T_H, Helper T cell.

2.4.6 The effect of chemogenetic activation of the afferent vagus nerve in granulocytes, DCs and macrophages

The effect of vagal afferent activation was also assessed in other immune cells. A panel of 8 colours and a viability dye was used to identify and quantify granulocytes. The gating strategy (Fig. 2.4.6.1) identifies leukocytes based on size and granularity, select singlet cells and exclude dead cells. From live $CD45^+$ gate, cells expressing lineage markers CD3, B220, CD19, CD4 and CD8α were excluded. Eosinophils were defined as $CD11b^+$ $SiglecF^+$ and basophils were defined as $CD11b^-$ $Fc\varepsilon RI\alpha^+$. Neutrophils ($Cd11b^+$ $Ly6G^+$) and mast cells ($CD11b^-$ $Fc\varepsilon RI\alpha^+$ $cKit^+$) were not observed in any sample so the gate is not shown.

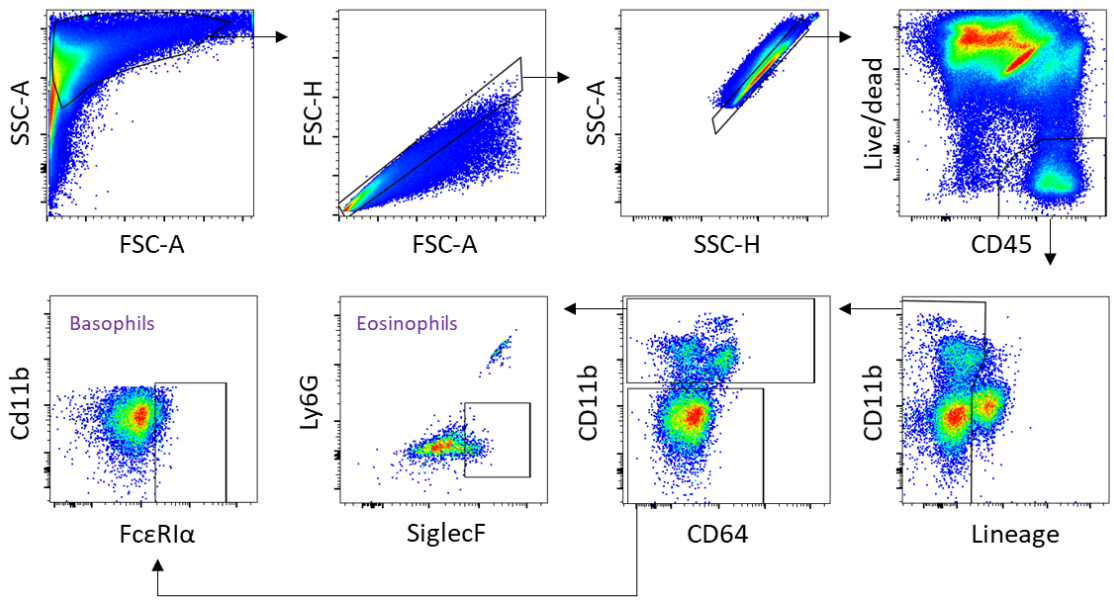

Figure 2.4.6.1. Example of contour plots and gating strategy for identification and quantification of granulocytes in mouse lamina propria.

Lineage markers are CD3, B220, CD19, CD4, CD8α. SSC-A, side scatter (area); FSC-A, forward scatter (area); SSC-H, side scatter (height); FSC-H, forward scatter (height); CD, cluster of differentiation; FcεRI, Fc fragment of immunoglobulin E receptor.

Since sample size was very low in the control group (n = 1), no statistical analysis could be performed and we were unable to draw any firm conclusions. Total number of eosinophils and basophils are shown (Fig. 2.4.6.2, A) as well as the frequency of these granulocytes in the parent group (Fig. 2.4.6.2, B,C).

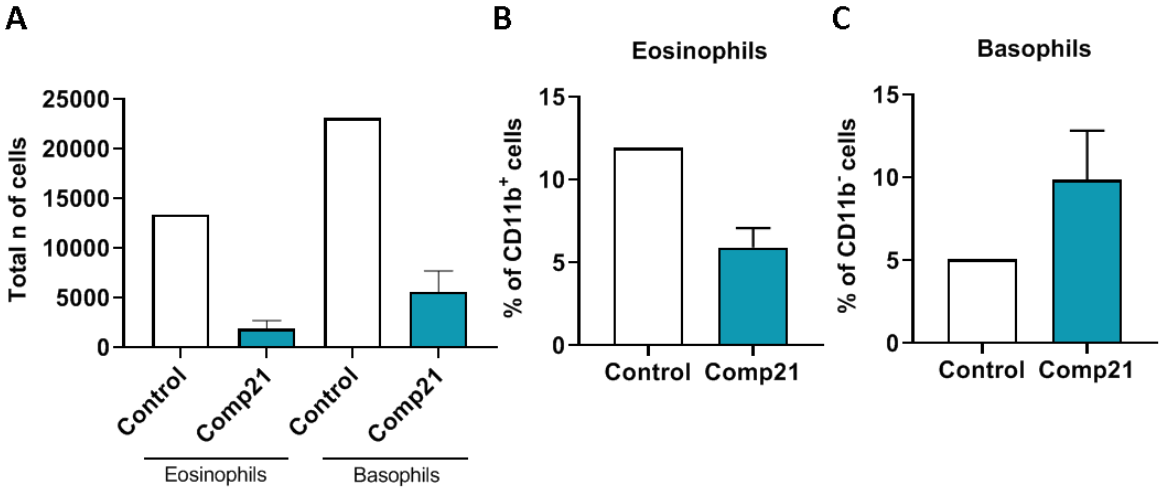

Figure 2.4.6.2. Total number and frequency of eosinophils and basophils in mice expressing hM3dq in vagal afferents chronically treated with DREADD ligand.

Number of eosinophils and basophils (A) and frequency (%) of parent of eosinophils (B) and basophils (C) in lamina propria of Compound 21 (Comp21; n = 4) and control (n = 1). CD, cluster of differentiation.

In order to identify and quantify DCs, macrophages and monocytes, a panel of 13 (plus viability dye) was used. The gating strategy (Fig. 2.4.6.3) selects single myeloid cells by size-granularity and includes single live $CD45^+$ cells similar to the above strategies. From $CD11c^+$ $MHCII^+$, Ki67 expression was used to quantify proliferation of DCs. $CD103^+$ DCs expressing or not $CD11b^+$ were identified. CD64 and CD24 expression allow distinguishing macrophages from DCs but CD64 staining was not conclusive and this marker was not considered.

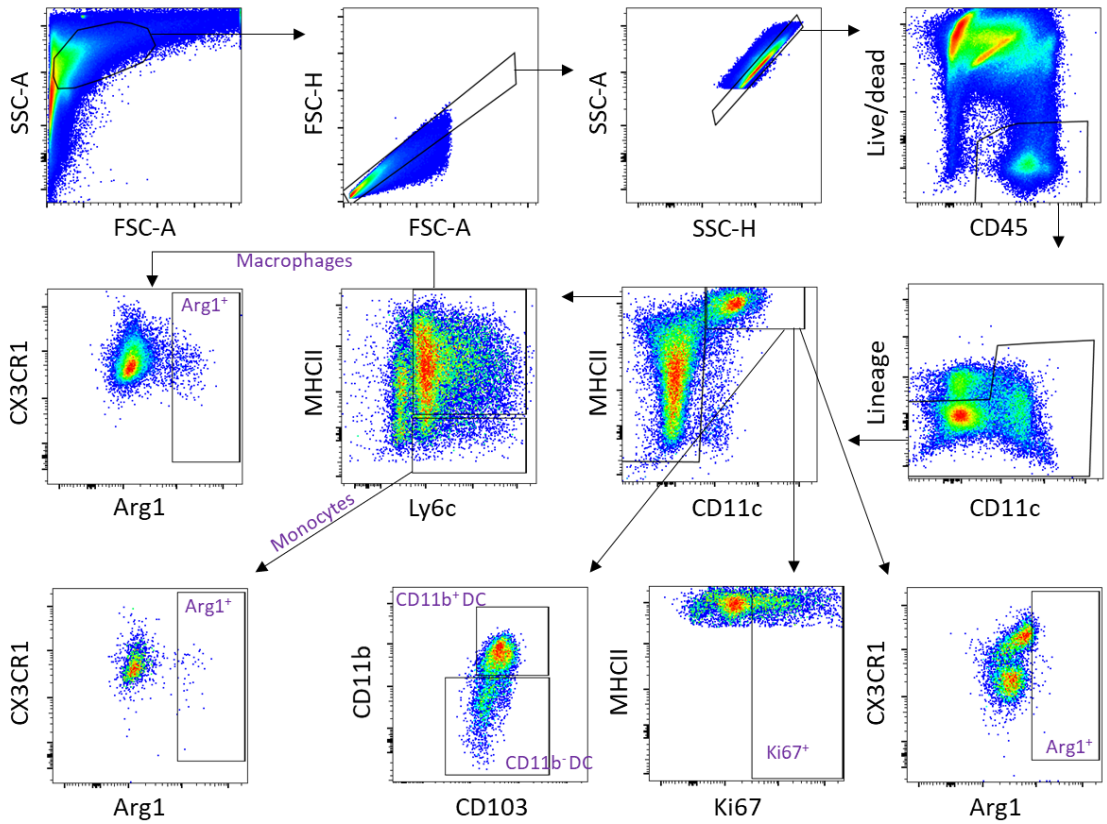

Figure 2.4.6.3. Example of contour plots and gating strategy for identification and quantification of DC, monocytes and macrophages in mouse lamina propria.

Lineage markers are CD3, B220 and CD19. SSC-A, side scatter (area); FSC-A, forward scatter (area); SSC-H, side scatter (height); FSC-H, forward scatter (height); CD, cluster of differentiation; MHC, major histocompatibility complex; CX3CR1, CX3C chemokine receptor 1; Arg1, arginase 1; DC, dendritic cell.

As in the previous panel, the low number of subjects in the control group made it difficult to draw conclusions and statistical tests could not be performed. Number of DCs, monocytes and macrophages analysed from Compound 21-treated and control group are shown (Fig. 2.4.6.4, A). No differences in frequency of DC subsets were observed between treatment groups (Fig. 2.4.6.4, B-D). Arg1 is expressed in DCs and monocytes/macrophages, and is a marker of M2 anti-inflammatory macrophages (in contrast to classically activated pro-inflammatory M1 macrophages). Frequency of Arg1-expressing DCs was lower in lamina propria of Compound 21-treated mice (1.41 %) compared to control mice (3.59 %) (Fig. 2.4.6.4, E). No differences between the means of frequencies in monocytes and macrophages were observed between groups (Fig. 2.4.6.4, F-I).

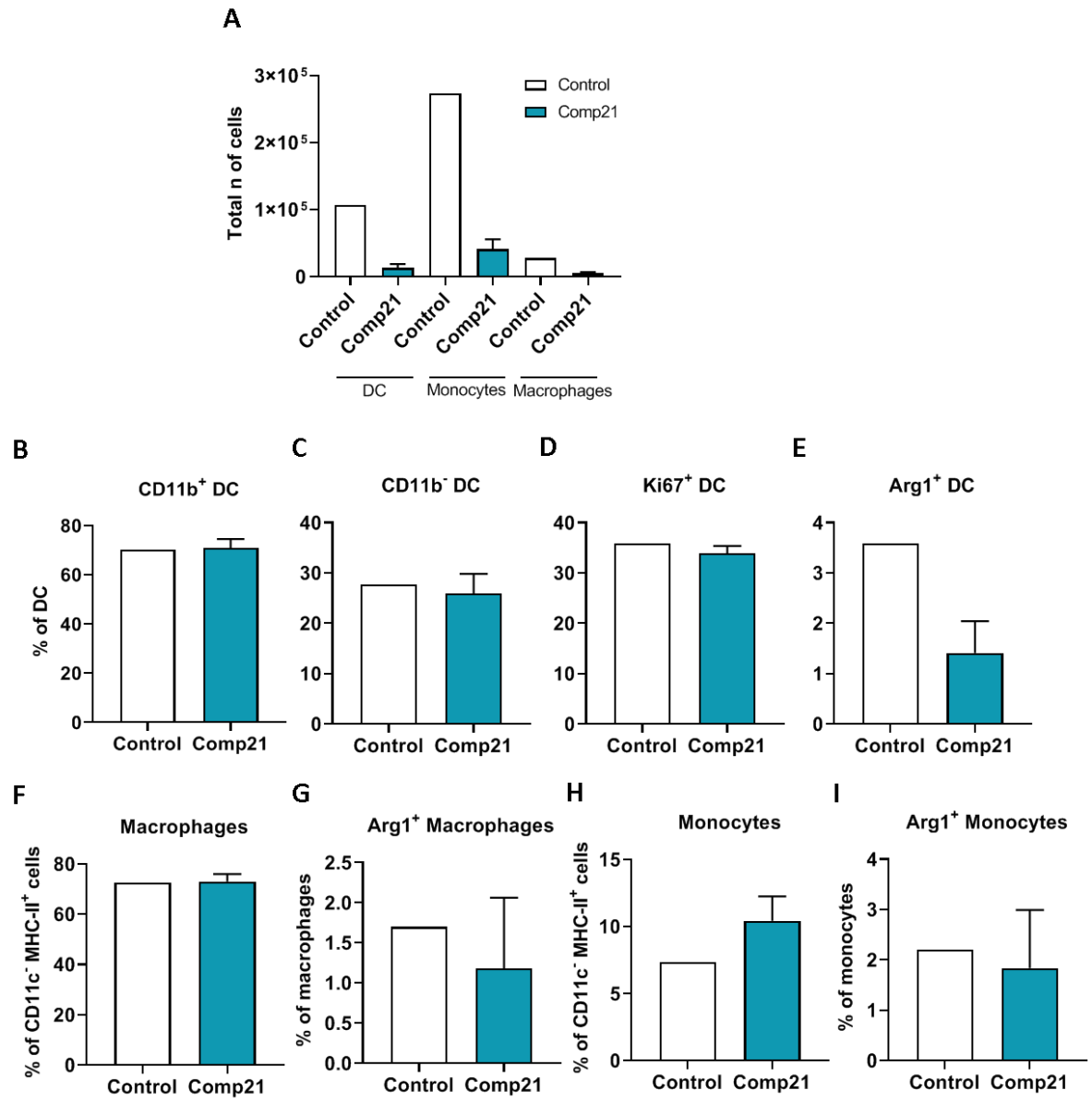

Figure 2.4.6.4. Total number and frequency of DCs, monocytes and macrophages in mice expressing hM3dq in vagal afferents chronically treated with DREADD ligand.

Number of DCs, monocytes and macrophages (A) in lamina propria of Compound 21 (Comp21; n = 4) and control (n = 1) groups. Frequency (%) of parent of DC expressing or not CD11b (B-C), the proliferation marker Ki67 (D) and Arg1 (E). Frequency of parent of macrophages (F) and Arg1-expressing macrophages. Frequency of parent of monocytes (H) and Arg1-expressing monocytes (I). Arg1, arginase 1; CD, cluster of differentiation; DC, dendritic cell; MHC, major histocompatibility complex.

2.5 Discussion

The novelty of this work relies on the induction of chronic whole afferent vagus activation by delivering a neuron-specific AAV expressing the activatory DREADD hM3Dq to study food intake and glucose homeostasis. In accordance with our hypothesis, treatment with the DREADD ligand in mice expressing hM3dq in the vagal afferents caused a reduction in body weight as well as in acute food intake. However, chemogenetic activation of the afferent vagus did not alter glucose tolerance. PYY_{3-36}, which activates calcium cultured vagal afferents as measured by calcium imaging, suppressed appetite. The effect of the DREADD ligand was in the same direction, although the magnitude of the anorectic effect was different. This suggests that vagal Y2R may act to activate neurones in the vagus nerve. However, it is also possible that whole vagus stimulation is overriding other more specific signalling pathways and that stimulation of several different neuronal pathways results in food intake suppression. This approach does not allow to dissect the role of Y2R expressed in the afferent vagus in feeding. To achieve this, in Chapter 3 we generate mouse model to specifically target vagal Y2R signalling.

To my knowledge, this is also the first work using chemogenetic activation of vagal afferents by injection into the NG in order to study the immune cell landscape in the intestinal lamina propria. Although this work does not allow us to draw conclusions about intestinal vagal-immune communication due to the low sample size, activation of vagal afferents might reduce immune cell numbers in the lamina propria. However, it might favour a more proinflammatory environment, based on a trend towards enhanced production by innate and adaptive lymphocytes of cytokines that are linked with gut inflammation (i.e., IL-13 and IL-17A).

2.5.1 Effect of activation of vagal afferents in body weight and glucose tolerance

In order to understand the effect of vagal afferent activation in body weight and food intake as well as in PYY_{3-36} anorectic ability, a chemogenetic approach was used. Chemogenetics provides the ability to study the role of both right and left NG (Han *et al.*, 2018). Clozapine-N-oxide (CNO) is the prototypical ligand of muscarinic receptor-based DREADDs. However, in *in vivo* studies, CNO might not cross the blood-brain barrier and might convert to clozapine, which has high DREADD affinity and potency and can also act at endogenous receptors (Gomez *et al.*, 2017; Mahler & Aston-Jones, 2018). The alternative ligand used in this study, Compound 21 (11-(1-piperazinyl)-5H-dibenzo[b,e][1,4]diazepine); (Chen *et al.*, 2015)), does not back-convert to clozapine and it might be more suitable for *in vivo* studies (Thompson *et al.*, 2018).

Chemogenetic activation of the vagus nerve caused a reduction in body weight and this was maintained in the following days in which daily DREADD ligand administration was continued. These results agree with the observations in body weight changes from unilateral and bilateral subdiaphragmatic VNS in lean rats (Krolczyk *et al.*, 2001; Laskiewicz & Sobocki, 2003).

A previous report has shown that Compound 21 at 3 mg/kg have the same effect in food intake as vehicle control (Thompson *et al.*, 2018). Animals expressing the hM3dq in the NG showed a large reduction in food intake after acute DREADD ligand treatment compared to saline. Importantly, non-DREADD expressing wildtype mice also showed a reduction in food intake in response to the DREADD ligand but to a much lesser extent. Although Compound 21 might be favourable to CNO, Compound 21 can bind to other receptors and therefore could potentially have off-target effects (Jendryka *et al.*, 2019). However, previous studies have shown that Compound 21 (also at 3mg/kg) do not cause changes in behaviour (i.e., attention and impulsivity) (Jendryka *et al.*, 2019). Further evaluation of feeding behaviour during chronic DREADD ligand treatment and a non-DREADD control are required to investigate if the off-target effects of Compound 21 contribute to the reduction in body weight observed in vagal hM3dq-expressing mice.

The action of afferent vagal activation in this experiment might be due to a combination of different mechanisms. Previous reports have observed that general optogenetic activation of vagal afferents slowed gastric motility (Chang *et al.*, 2015). VNS also slowed gastric emptying in rats (Dai, Yin & Chen, 2020). Therefore, it is possible that exogenous activation is reducing gastric motility and consequently reducing caloric intake and body weight. Future studies should explore this in a gastric emptying assay. Bai and colleagues reported that chemogenetic and optogenetic activation of gastrointestinal mechanoreceptors, but not chemoreceptors, reduced food intake (Bai *et al.*, 2019). Therefore, the observed effects might be mostly mediated by mechanoreceptors. Chemogenetic activation of vagal cholinergic motor neurones in the DMV also caused a reduction in body weight (NamKoong *et al.*, 2019). In addition, it was suggested that energy expenditure contributed to the reduction in body weight observed in VNS-treated rats by reducing mesenteric fat independently of food intake (Banni *et al.*, 2012). Peptides involved in metabolism might also be altered upon vagal afferent activation. In obese rats, VNS caused an increase in plasma levels of the anorectic hormones GLP-1 and PYY without altering ghrelin levels (Dai, Yin & Chen, 2020). Hypothalamic brain-derived neurotrophic factor, a growth factor involved in energy homeostasis, is increased after VNS and it has been suggested that contribute to the effects of VNS in body weight (Banni *et al.*, 2012). The plasma levels of gut

hormones or other factors involved in energy homeostasis have not been investigated in this study. In addition, it is possible that chemogenetic activation alters expression of receptors in the vagus nerve or neuropeptide secretion from the vagus nerve. Future studies should explore if chemogenetic activation prevents obesity, as observed in VNS-treated rats (Bugajski *et al.*, 2007).

The role of vagal afferents in pancreatic function is not well understood. Activation of the afferent vagus did not alter basal glucose levels or glucose tolerance in an IPGTT. In contrast, chemogenetic activation of vagal motor neurones in mice has been shown by others to improve glucose tolerance (NamKoong *et al.*, 2019). Cervical VNS showed impaired glucose tolerance and reduced glucose-induced insulin levels in rats (Stauss *et al.*, 2018). Previous studies showed that afferent-selective VNS increases blood glucose and might be responsible for the impaired glucose tolerance but these studies are limited by the effect of anesthesia (Meyers *et al.*, 2016; Payne *et al.*, 2020). VNS could alter the secretion of glucagon and GLP-1 (Dai, Yin & Chen, 2020; Payne *et al.*, 2020). Therefore, there is controversy regarding the effect and mechanism of vagal afferent versus efferent activation in glucose tolerance as well as different methods of vagal activation.

The receptor of PYY_{3-36}, Y2R, was suggested to inhibit feeding by acting as an auto-inhibitory pre-synaptic receptor in the hypothalamic ARC (Batterham *et al.*, 2002). PYY_{3-36} activated cultured NG neurones as revealed by increased intracellular calcium mobilization. The concentration used to stimulate NG neurons is likely higher than the concentrations of PYY_{3-36} reaching the NG or the vagal afferent terminals within gastrointestinal tract. Future experiments should assess the PYY_{3-36} levels achieved in plasma and in the hepatoportal vein after injection of the low dose exogenous PYY_{3-36}.

As did vagal chemogenetic activation, PYY_{3-36} reduced food intake. Overall, these suggest that binding of PYY_{3-36} to Y2R activates the vagal afferents, which is in agreement with a previous *in vivo* electrophysiological study in which peripheral PYY_{3-36} increased vagal afferent activity (Koda *et al.*, 2005). The contribution to food intake suppression of PYY_{3-36} in the mice treated with DREADD ligand plus PYY_{3-36} could not be observed due to the strong anorectic effect of gross vagal activation. A lower DREADD ligand concentration might allow to unmask the effect of PYY_{3-36} in this treatment condition. As mentioned above, it is possible that chemogenetic activation of the afferent vagus caused an increase in circulatory anorectic gut hormones and, therefore, exogenous PYY_{3-36} treatment is redundant.

2.5.2 Afferent vagus nerve activation and gut immunity

Mucosal barriers, including airways and gastrointestinal lumen, are exposed to external agents. Immune cells and neurones coordinate with one another to maintain immune homoeostasis and to respond to immune challenges. The exact mechanisms by which sensory neurones and immune cells communicate are unknown.

Mice expressing the activating DREADD hM3Dq in vagal afferents were immunophenotyped after chronic treatment with DREADD ligand Compound 21. The results from this work suggest that counts of different immune cell types, such as ILC subtypes, T_{reg} cells or DCs, may be reduced when vagal afferents are exogenously activated. This is in contrast with previous reports that show that activation of sensory neurones by capsaicin increased lung airway leukocytes, including eosinophils and T cells, and that this response was increased in allergic mice (Talbot *et al.*, 2015). Silencing of sensory neurones only decreased immune cell counts in allergy (Talbot *et al.*, 2015). However, the interrelations between the nervous system, in this case the vagus nerve, and the immune system are critically dependent on environmental conditions and challenges. For example, contrary to the observations in the context of allergy, silencing of lung vagal afferents promoted increased infiltration of some immune cell subsets in the inflamed lung, which is in line with our observations (Baral *et al.*, 2018).

ILCs are innate cells important for the maintenance of barrier integrity. Recent studies have suggested the interaction of ILCs, mainly ILC2, with sensory neurones (Klose & Artis, 2019). The crosstalk between ILC3, which is the most abundant ILC type in the gut, and neurones remain undetermined. This work suggests that frequency of ILC subtypes and total number of ILC3 are potentially reduced by an activated afferent vagus nerve. Although it is possible that a higher proportion of ILC3s have a secretory phenotype when vagal afferents are activated, the study was not sufficiently powered to conclude this. In addition, while we were only able to measure IL-13 and IL-17A in this pilot experiment, gut ILC2 and ILC3 are major producers of IL-5 and IL-22, respectively. Future work should include the study of these cytokines. These results are in contrast with a previous report showing that vagotomy reduces a population of peritoneum resident ILC3s (with a similar phenotype to ILC3s of the small intestine lamina propria) (Dalli *et al.*, 2017). No differences in frequency of ILC3 (within ILC population) were observed in activated versus non-activated vagal afferent conditions. Although sensory neurones interact with ILC subtypes in other tissues, it is possible that sensory neurones in the gut do not have a key role

in modulating specifically the ILC3 population. Indeed, enteric glial cells have shown to regulate ILC3 via glia cell-derived neurotrophic factor (GDNF) (Ibiza *et al.*, 2016).

In the intestinal barrier, ILC2 cells are less abundant than ILC3 and this is supported by this work. ILC2 can respond to a range of neuropeptides (Quatrini, Vivier & Ugolini, 2018). ILC2 are close to cholinergic enteric neurones in the submucosa that express the neuropeptide neuromedin U (NMU), which activate intestinal ILC2 (Cardoso *et al.*, 2017; Klose *et al.*, 2017). NMU is a neuropeptide highly expressed along the gut-brain axis. In this context, NMU has been involved in food intake inhibition, energy balance regulation and increased smooth muscle contraction (also in the gastrointestinal tract) with most studies focused on central NMU signalling (Martinez & O'Driscoll, 2015). ILC2s also respond to vasoactive intestinal peptide (VIP), which promotes IL-5 secretion, according to feeding status and circadian rhythm (Nussbaum *et al.*, 2013). In this experiment, intestinal ILC2 frequency and total cell count did not seem to be influenced by vagal afferent activation and therefore it is unlikely that gastrointestinal NMU or VIP action has been enhanced. Future research should study if the communication of ILC2 with other peptides in the gut is functionally related with the effects of this peptides in feeding or metabolism. NMU is not expressed in nodose/jugular ganglia (Wallrapp *et al.*, 2017) but VIP is secreted by $Nav1.8^{+}$ neurones upon activation with IL-5 (Talbot *et al.*, 2015). This results in activation of ILC2 and T helper cells in airway inflammation (Talbot *et al.*, 2015). Therefore, intestinal ILC2 communication with vagal afferents might be context dependent.

Regarding adaptive immunity, vagal afferent activation did not significantly alter the proportion of T cell subtypes, only frequency of T_{reg} showed a trend towards reduction when activating the vagus. A trend towards an increased proportion of T cells expressing IFN-γ and IL-13 was also observed. This could indicate that activation of vagal afferents promotes inflammatory responses. In support of this, silencing of nociceptor neurones reduced expression of T_H2 in allergy (Talbot *et al.*, 2015). This work does not allow us to draw conclusions regarding DCs. It is possible that the lower number of mucosal DCs observed when activating afferents influence the number of T_H subtypes.

Another aspect to consider is the fact that this approach activates different types of neurones whose soma resides in the NG. From this diverse group of neurones, some may produce stimulating factors for ILC and T cells, while others may secrete inhibitory modulators (Klose *et al.*, 2017; Nagashima *et al.*, 2019). However, if the results here presented indicate an actual trend of lymphocytes behaviour, stimulation of vagal afferents will result in a net reduction of

immune cells, either by increasing tissue egress, immune cell apoptosis or decreasing proliferation, while slightly promoting cytokine secretion.

With the limited amount of data available, it is impossible to further characterize the immune composition of the lamina propria and the effect that vagal stimulation has on the immune cell populations analysed. Cell count and activation profile of monocyte/macrophages and granulocytes could confirm if more eosinophils and macrophages are recruited and activated. Vagus nerve stimulation can limit allergic responses and this was suggested to be mediated by inhibition of mast cell expansion (Bosmans *et al.*, 2019). In this work we could not detect mast cells, likely because of degranulation or cell death during tissue processing. It would be of great interest to investigate the effect of vagus nerve modulation on mast cell number and activation status in homeostasis as well as in inflammatory conditions.

2.5.3 Limitations of this study and future work

The main limitation of this work is the lack of confirmation of viral infection in afferent neurones. Therefore, the next step is to assess by immunofluorescence the viral fluorescent marker (cherry) as well as of the neuronal activation marker c-fos in the NG.

The metabolic phenotyping was performed just after 3 weeks from viral administration completion and, therefore, it is possible that virus infection was not optimum. Although a control of Compound 21 was included, the study should evaluate the effect in body weight (in addition to food intake, as we have shown) in controls which do not express DREADD. Non-DREADD expressing control mice showed that Compound 21 at the dose used has off-target effects in food intake. Of note, the non-DREADD wildtype control mice are males whereas the vagal hM3dq-expressing mice were females. In addition, the non-DREADD wildtype did not undergo surgery and a control receiving a control virus would me more suitable. The level of the DREADD ligand upon administration of different DREADD ligand doses should be assessed in plasma, brain and hepatoportal vein. In addition, its effect on feeding behaviour should be further explored. Vagal activation did not have an effect in glucose tolerance but future studies should measure glucose-induced insulin levels and fasting insulin levels.

This work aimed to activate all vagal afferents but NG injection of Cre-expressing viruses in the adult mouse with a floxed gene of interest would allow the study of individual populations. Although feeding behaviour after activation of specific genetically-defined vagal afferent populations has been reported, the Y2R-expressing population has not been studied (Bai *et al.*,

2019). It would be of interest to determine if the Y2R vagal afferent population is chemosensing or mechanosensing. This work suggests that PYY_{3-36} activates some vagal afferents and, therefore, that Y2R acts to activate neurones in the NG. This could be further confirmed by electrophysiological studies to determine if PYY_{3-36} activates gastric vagal afferents in mice, as observed in rats (Koda *et al.*, 2005) or by calcium imaging of NG in the presence of a Y2R antagonist or a high-affinity Y2R-specific PYY_{3-36} analogue. A calcium indicator of the GCamP family could be driven using a Cre-expressing line that targets Y2R-expressing sensory neurons (i.e., Npy2r-ires-Cre) and a Cre-dependent reporter allele (e.g., lox-GCamP3). Ires-Cre lines drives expression of GCamP in areas other than the nodose. To overcome this, AAV driving Cre-dependent GCamP expression (AAV-flex-GCamP) could be instead injected in the nodose ganglia of Npy2r-ires-Cre to achieve more specificity (Chang *et al.*, 2015). The Npy2r-GCamP neurons could be isolated for imaging in response to PYY_{3-36} (as performed in this work). A more physiologically relevant experiment would involve the surgical exposure of the NG of Npy2r-GCamP mice for *in vivo* imaging in response to intravenous PYY_{3-36} or duodenal nutrient administration (Williams *et al.*, 2016).

This study has used a chemogenetic approach to explore the effect of chronic vagus nerve stimulation in lamina propria immune homeostasis. This pilot experiment was designed to maximize the output of experimental readings/measurements. However, as demonstrated by the low rate of success in the preparation of single cell suspensions from lamina propria, future experiments should have a more tailored and focused approach to reduce the time between tissue harvesting and tissue processing. This way, future experiments should ensure that lamina propria tissue processing yields a reliable and consistent number of samples, thus providing more conclusive results. In addition, experiments investigating changes to the intestinal immunophenotype following DREADD-mediated vagal afferent inhibition would also be useful.
This work has focused on the vagal-immune interaction in the lamina propria. However, the vagus nerve is important in interacting with ENS and tissue-protecting MMs (Muller *et al.*, 2020b; Matheis *et al.*, 2020). In addition, VNS increased mast cell number in the muscularis (Gil *et al.*, 2009). Future work should assess the effect of afferent vagus activity in the count and activity of MMs.

Vagal afferents might modulate gut sympathetic neurones in a microbiota dependent-manner (Muller *et al.*, 2020b). Therefore, it would be interesting to study the effect of vagal activity modulation in intestinal microbiota signalling. In addition, the complex interconnections between different immunological sites (e.g., lung and gut mucosa, mucosa and secondary

lymphoid organs) that are simultaneously innervated by the vagus nerve adds an extra layer of complexity to the interpretation of results. For example, upon inflammation, lymphocytes can migrate from the lamina propria into the lung. Since the activation of the vagus nerve would affect both intestinal and lung afferents (amongst others), the possible decrease observed in immune cell numbers in lamina propria could be due to migration of these cells to other tissues. Vagal afferents transmit information from the gut to the brain depending on the expression and activation of a range of receptors. Transcriptional profiling of Nav1.8-expressing neurones showed that they expressed a range of cytokine receptors (Talbot *et al.*, 2015). Future experiments should investigate if the expression of cytokine receptors and pattern recognition receptor, such as TLR4, in afferent terminals depend on vagal activity, inflammatory or nutritional status. Level of cytokines and neuropeptides in intestinal mucosal samples following the activation or inhibition of vagal afferents should also be measured.

Future work is needed to characterize how specific vagal neurones crosstalk with ENS and immune cells during homeostasis and in pathological conditions, such as food allergy or IBD. However, this pilot experiment suggests that the approach proposed here can be useful in investigating these systems. As explained above, using Cre/loXP and viral strategies to alter the activity of specific vagal afferent subpopulations could help dissecting this crosstalk.

Taking into account the relevance of inflammation in obesity, further research should explore the effects of bariatric surgery in intestinal immunity as well as the role of the vagus nerve, which is partly altered during metabolic surgery (Berthoud, 2008a). The vagus nerve is of great interest in the neuro-immune crosstalk as well as its role in inflammation, as occurs postprandially and in the obese state. Vagal plasticity is altered in obesity (section 3.1.3) and future studies should explore if other signaling pathways, such as neuro-immune communication, are also altered.

Chapter 3: Investigating the role of vagal Y2R in feeding behaviour and glucose homeostasis

3.1 Introduction

3.1.1 Vagus nerve in the gut-brain axis

In recent years, the role of the vagus nerve has been of much interest in energy homeostasis, especially its role in the homeostatic control of food intake in the short-term. Anterograde tracing studies indicated that the stomach afferent terminals induce meal termination in response to mechanical stimuli while the terminals innervating the small intestine are chemosensitive (Berthoud, 2008b).

As food enters the gastrointestinal tract, the mechanosensitive afferent terminals within the stomach can sense a change in tension. As observed in electrophysiological studies in rats, gastric load activates vagal afferents in a volume-dependent manner (Schwartz, McHugh & Moran, 1991). This gastric distension induces the activation of NTS neurones (Willing & Berthoud, 1997) in a volume-dependent manner and suppresses food intake due to the volume rather than nutrient content (Phillips & Powley, 1996). In contrast to tension receptors, mucosal endings can respond to stroking (Page, Martin & Blackshaw, 2002) and gastric acid (Michl *et al.*, 2001) and, therefore, to the presence of food. Vagal afferent terminals are close to the basolateral surface of the epithelium and they can sense the gastric hormones ghrelin and leptin. However, mechanosensitivity is dependent on the feeding status, with fasting associated with lower sensitivity to stretch compared with the fed state (Kentish *et al.*, 2012; Kentish & Page, 2014).

The epithelium can sense the nutrients via a range of receptors and transporters. Here, mucosal endings are more abundant in the proximal duodenum than distally (Berthoud, 2008b). Most of the nutrient-sensing receptors are found in the EECs (see section 1.4.2.1), which only represent ~0.1-1% of the gut epithelial cell population. Mucosal endings are not exposed to the luminal content but are close to EECs (Berthoud *et al.*, 1995). These different types of EECs can secrete a range of gut hormones depending on the nutritional status and these hormones can act on vagal afferent terminals resulting in different responses. Recently, gut hormones signalling in the vagus nerve have been of much interest. Gut hormones can also enter the bloodstream, from where they could activate vagal afferents in a non-paracrine fashion, as well as directly act on central areas, such as the brainstem and the hypothalamus. In addition, vagal afferents express nutrient receptors (de Lartigue, 2016; Egerod *et al.*, 2018) and nutrients could directly activate hepatic vagal afferents thanks to their strategic location at the portal vein.

It is assumed that afferent terminals largely sense nutrients indirectly via the secretion of hormones from the EECs. However, in contrast to the indirect action of EEC on neuronal terminals, some epithelial cells, named neuropods, could directly synapse with the afferent vagus nerve, using glutamate to signal across the synapse and transmitting information faster to the brainstem (Bohórquez *et al.*, 2015; Kaelberer *et al.*, 2018). Recent research has found that EECs can transduce glucose stimuli to vagal afferents via glutamate and CCK (Kaelberer *et al.*, 2018). A recent report observed that intragastric infused fat did not inhibit NPY/AgRP neurones in the ARC of vagotomised mice, suggesting a role of the vagus nerve in transmitting fat-mediated satiety (Goldstein *et al.*, 2021). These studies suggest that vagal afferent signalling also depends on the specific macronutrients ingested.

After the afferent vagus carry information from the gut to the brain, different physiological responses are modulated to regulate metabolism, such as gut motility. The NTS integrates the visceral information from vagal afferents (or from circulating hormones with access to circumventricular organs at the brainstem) and communicates with higher brain centres and other brain centres in the brainstem. The brainstem nuclei DMV is involved in gut motility control especially in the upper gastrointestinal tract. DMV neuron firing regulate the vagal efferent output. Gastric vagal efferents communicate with postganglionic myenteric neurons that control gastric smooth muscle contraction and ultimately motility (Travagli & Anselmi, 2016). Gastric emptying rate measures the speed at which the stomach content is delivered into the duodenum and is key for the subsequent digestion and absorption. Gastric emptying is dependent on the properties of food (physical and chemical) and is regulated by complex neuro-hormonal mechanisms (Goyal, Guo & Mashimo, 2019). Gut hormones can also influence gastric emptying via the vagus nerve. For example, studies using capsaicin treatment showed that CCK acts on the afferent vagus to delay gastric emptying (Raybould & Tache, 1988; Forster *et al.*, 1990).

3.1.2 Gut hormones and the vagus nerve

Gut hormones released from EECs are considered key messengers between the gut epithelium and vagal afferents. The most traditional approach to study the role of vagal afferents in the gut-brain axis is vagotomy, a surgical approach that interrupts bidirectional vagal communication, and capsaicin, which has a long-term toxic effect in NG. In recent years, new approaches have allowed more nuanced dissection of the role of the afferent vagus in gut hormone signalling.

3.1.2.1 CCK

CCK is the best-known gut hormone that mediates satiety via the vagus nerve. CCK inhibits food intake by binding to CCK-RA, which is found in the periphery, mainly in the gastrointestinal tract, and in some areas of the central and peripheral nervous system (vagus nerve (Moran *et al.*, 1987)). CCK-RA is highly selective for sulfated analogues of CCK. Tother receptor, CCK-RB, which is found principally in the brain, has high affinity for both sulfated and nonsulfated peptide analogues. CCK-RB regulates dopamine release and anxiety (Wank 1995) . CCK triggers vagal afferent discharge (Schwartz, McHugh & Moran, 1991) and increases intracellular calcium in vagal neurones (Peters *et al.*, 2004). The actions of CCK on vagal afferents regulate several processes, including inhibition of gastric emptying and food intake (Dockray, 2009). After vagotomy or capsaicin treatment, the anorectic effect of exogenous CCK is abolished (Smith *et al.*, 1981b; MacLean, 1985). Blocking the CCK-RA also abolishes this effect (Garlicki *et al.*, 1990). More recently, Han and colleagues suggested a reward-related neural pathway for the appetite-suppressing effect of CCK (Han *et al.*, 2018). In addition, CCK acts a gatekeeper of the phenotype of the vagus nerve (see section 3.1.3).

3.1.2.2 GLP-1

As for CCK, the anorectic effect of exogenous GLP-1 is abolished after vagotomy in humans and rats (Abbott *et al.*, 2005a; Rüttimann *et al.*, 2009; Plamboeck *et al.*, 2013) and in capsaicin-treated mice (Talsania *et al.*, 2005), albeit these results could depend on the route of administration (Rüttimann *et al.*, 2009). The interaction of the anorectic gut hormone GLP-1 and the vagus nerve has been studied more recently using molecular approaches. Vagal-specific GLP-1R knockdown using virus-delivered silencing RNA in rats resulted in an increase in meal size and duration while reducing the number of meals, and also increased gastric emptying without affecting long-term energy homeostasis (Krieger *et al.*, 2016). *Glp1r*-expressing vagal afferents do not densely innervate the intestine but they mostly terminate in the stomach as IGLEs (Williams *et al.*, 2016; Bai *et al.*, 2019). Most of these GLP-1R positive neurones responded to gastric distension (Williams *et al.*, 2016). Moreover, optogenetics revealed that specific activation of *Glp1*r positive neurones resulted in a reduction in food intake, which was more acute than that observed following the stimulation of other mucosal ending subtypes (Bai *et al.*, 2019). It has been suggested that GLP-1 acts on the vagus by lowering the threshold at which distension activates vagal afferents (Cork, 2018). This could be additive to the effect of GLP-1 in the GLP-1R-expressing chemosensitive afferents.

PYY is co-secreted with GLP-1 post-prandially, and also has an anorectic action. Since nutrient absorption occurs in the proximal small intestine, L-cells of the upper gut are widely accepted to be

the main source of the increase in plasma GLP-1 and PYY levels and, therefore, to regulate incretin effect and appetite control after meal intake. Only late after meal intake nutrients reach the colonic L-cells, which contain a large proportion of endogenous PYY and GLP-1. A recent study aimed to study the effect of selective stimulation of colonic L-cells (expressing the insulin-like peptide 5) by chemogenetics (an approach that employs selective compounds that target genetically engineered receptors expressed in the cell of interest in order to remotely control the activity of that cell) (Lewis *et al.*, 2020). Stimulation of the distal L-cells improved glucose tolerance and reduced food intake and body weight, and these effects were maintained after exposure to high-fat diet. By blocking Y2R or GLP-1R, this study demonstrated that PYY, and not GLP-1, from colonic EECs is responsible for the appetite suppression observed following the activation of these cells. In contrast, the improved glucose tolerance observed after colonic L-cell stimulation depended on GLP-1R and the authors suggested an endocrine GLP-1 signalling from the gut to the pancreas underlies this effect.

3.1.2.3 Leptin

Leptin activates gastric and duodenal neurones (Peters, Ritter & Simasko, 2006) and, in addition, the LepRb is expressed in the human and rat NG (Burdyga *et al.*, 2002). Leptin can modulate sensitivity of the afferent vagus nerve according to nutritional status in order to promote or inhibit satiety (Kentish *et al.*, 2013). While leptin potentiates the sensitivity of mucosal receptors (which detect presence of food) in the fed state (promoting satiety), it reduces the sensitivity of tension receptors (which detect amount of food) in the fasted state (Kentish *et al.*, 2013). Exogenous leptin administration in the celiac artery (in the upper gastrointestinal tract) suppressed sucrose intake but this effect was not observed in vagotomised or capsaicin-treated rats (Peters *et al.*, 2005). Leptin and CCK can activate the same vagal neurones synergistically (Peters *et al.*, 2004; Peters, Ritter & Simasko, 2006) and it was shown that leptin can prolong CCK-induced anorexia (De Lartigue *et al.*, 2010). Using transgenic animals, it has been shown that semi-specific vagal LepRb knockdown in vagal afferents promotes obesity (de Lartigue, Ronveaux & Raybould, 2014).

3.1.2.4 Ghrelin

The orexigenic effects of ghrelin are abolished in truncal vagotomised humans (Le Roux *et al.*, 2005) and in subdiaphragmatic vagotomised rodents (Date *et al.*, 2002; Davis *et al.*, 2020). Importantly, the ghrelin receptor, GHSR, is expressed in the vagus nerve (Burdyga *et al.*, 2006). Exogenous ghrelin reduces vagal afferent sensitivity to gastric tension (Page *et al.*, 2007). This has no effect on mucosal receptors (which is the opposite effect to that of leptin in the fed state) (Kentish *et al.*, 2012). In the fasted state, ghrelin inhibits mucosal receptors and its inhibitory effect on vagal mechanosensitive neurons is augmented (Kentish *et al.*, 2012). Ghrelin has been shown to both activate (Murray *et al.*,

2006; Davis *et al.*, 2020) and inhibit vagal firing (Asakawa *et al.*, 2001) and this might be dependent on the location of the terminals. Importantly, like CCK, ghrelin has a regulatory role in changing the vagus phenotype (Burdyga *et al.*, 2006). Knocking-down the vagal GHSR revealed a role of vagal ghrelin signalling in regulation of body weight regulation, meal patterning and gastric emptying, as well as a novel role in hippocampal-dependant contextual episodic memory (Davis *et al.*, 2020). More recently, an interaction between ghrelin and GLP-1 in vagal afferents has been suggested (Zhang *et al.*, 2020).

3.1.3 Vagus nerve plasticity

Studies in rats have revealed that the vagus nerve sensitivity to signalling molecules varies with nutritional status. This is achieved by changes in the expression level of receptors or peptides. Therefore, the afferent vagus nerve is not only a carrier of sensory information but also modulates the response to nutritional status. In the fed state, the afferent vagus nerve expresses receptors and peptides associated with reduced food intake, whereas in the fasting state, the expression of these receptors is reduced and orexigenic receptor expression is increased (Burdyga *et al.*, 2004, 2006, 2008; De Lartigue *et al.*, 2007, 2010).

Burdyga and colleagues observed that Y2R, the receptor for the gut hormone PYY_{3-36}, was expressed at a lower level in the NG under fasting conditions compared to the fed state, and this was rescued by CCK, and by re-feeding (which results in the endogenous release of CCK) but not if the CCK-RA was blocked (Burdyga *et al.*, 2008). There were similar effects on the expression of vagal CART (De Lartigue *et al.*, 2007), which mediates CCK-induced satiety in the vagus (Broberger *et al.*, 1999). CCK can also influence the expression of orexigenic receptors, such as the orexigenic CB1 and the melanin-concentrating hormone receptor-1 (MCHR1), in the opposite fashion (Burdyga *et al.*, 2004, 2006).

Ghrelin can counteract CCK modulation of the vagus nerve phenotype. CCK-induced vagal CART expression is inhibited by ghrelin (De Lartigue *et al.*, 2007). In addition, ghrelin blocked the decrease in vagal CB1 and MCHR1 in re-fed rats (Burdyga *et al.*, 2006). Importantly, the expression of CCK-RA (Burdyga *et al.*, 2004) and GHSR (Burdyga *et al.*, 2006) do not depend on the acute feeding status. Therefore, in the preprandrial state, when ghrelin levels are high and CCK levels are low, the vagus nerve is in a 'fasted phenotype' with low expression of anorectic pathways. After meal intake, when CCK is high, the vagus nerve switches to a 'fed phenotype', in which expression of anorectic signalling mediators is increased (Dockray, 2014). The intracellular mechanism of this interaction between CCK, leptin and ghrelin to modulate vagal afferent plasticity was revealed by Lartigue and colleagues (De Lartigue *et al.*, 2010). Leptin increases the expression of the transcription factor early growth response-1 (EGR-1) and, after food ingestion, CCK activates vagal afferents and induces the

translocation of EGR-1 to the nucleus. EGR-1 promotes the expression of CART (De Lartigue *et al.*, 2010) and presumably Y2R expression. Ghrelin inhibits the expression and translocation of EGR-1 (De Lartigue *et al.*, 2010).

Vagus nerve plasticity is altered in obesity: the afferent vagus nerve is fixed in the 'fasting phenotype' (de Lartigue, 2016). In obese rodents, afferent vagus nerve firing is impaired (Daly *et al.*, 2011) and vagal afferent sensitivity to distension is reduced (Kentish *et al.*, 2012). In obese rats, ghrelin's orexigenic effect is potentiated (Kentish *et al.*, 2012) while sensitivity to CCK is reduced (de Lartigue *et al.*, 2012). This prevents CCK-induced modulation of the vagal phenotype. On the other hand, leptin resistance in the vagus nerve in obesity impairs the sensitivity of vagal afferents to CCK, resulting in reduced satiety signalling (de Lartigue *et al.*, 2011, 2012). Similar to obese rats that develop leptin resistance, vagal-selective LepRb KO mice showed higher body weight and food intake in the dark phase compared to controls (de Lartigue, Ronveaux & Raybould, 2014). Disruption of vagal leptin signalling reduced sensitivity to CCK, which could mediate the hyperphagic response in diet-induced obesity. Interestingly, vagal-selective LepRb KO resisted body weight gain on a HFD, probably due to compensatory mechanisms (de Lartigue, Ronveaux & Raybould, 2014). The authors concluded that vagal leptin resistance is required for the development of obesity and that other mechanisms downstream of leptin resistance in the vagus also contribute to diet-induced weight gain. The reduced sensitivity to CCK results in loss of vagal plasticity so the expression of vagal neurotransmitters (e.g., CART) and receptors (e.g., Y2R) do not change. An altered vagal CART expression could be responsible for the reduced satiation and the resulting hyperphagia in vagal-selective LepRb KO mice. Lee and colleagues showed that a reduced vagal sensitivity to CCK blunted vagal CART expression in obese rats (Lee *et al.*, 2020). CART release from the vagus fails in the obese state but CART anorexigenic effect was retained by injecting CART in the NTS, suggesting that vagal CART is a potential target for anti-obesity treatments(Lee *et al.*, 2020). This putative role of the vagus nerve in obesity is not well understood and is under investigation. It is still unclear if the changes in vagus nerve sensitivity are the cause or a consequence of obesity.

3.1.4 The afferent vagus nerve in PYY_{3-36} signalling

As previously described (see section 1.5), PYY is secreted from L-type EECs postprandially, and the truncated form PYY_{3-36} reduces food intake. However, the site or sites of action responsible for this effect are not fully understood and still controversial. Batterham and colleagues suggested that PYY_{3-36} binds to Y2R in the ARC and supresses appetite via the NPY/AgRP – POMC/CART system (Batterham *et al.*, 2002).

However, as with other gut hormones, PYY_{3-36} could mediate its anorectic effect via the vagus nerve. The receptor for PYY_{3-36}, Y2R, is expressed in the vagus nerve in rodents (Zhang *et al.*, 1997; Koda *et al.*, 2005; Burdyga *et al.*, 2008; Chang *et al.*, 2015; Egerod *et al.*, 2018) and in humans (Burdyga *et al.*, 2008). Y2R expression level in the vagus nerve of rats depends on nutritional status, suggesting a role in feeding (Burdyga *et al.*, 2008).

In rats, Koda and colleagues observed that bilateral subdiaphragmatic vagotomy abolished the anorectic effect of PYY_{3-36}, as well as the PYY_{3-36}-induced activation of neurones in the ARC, as determined by c-fos detection. In addition, electrophysiological studies revealed that PYY_{3-36} induces gastric vagal afferent firing (Koda *et al.*, 2005). Another study also revealed that bilateral subdiaphragmatic vagotomy in rats abrogated the effect of PYY_{3-36} (as for GLP-1) (Abbott *et al.*, 2005a). Importantly, they observed the same in transectioned rats, indicating that projections from the brainstem into the hypothalamus are required for the anorectic effects of PYY_{3-36}. They also observed an ablation in ARC c-fos expression after PYY_{3-36} administration in vagotomised rats (Abbott *et al.*, 2005a).

In contrast, other studies have not found evidence of a role of the vagus nerve in mediating the anorectic effect of PYY_{3-36}. Capsaicin-mediated ablation of sensory neurones abrogated the anorectic effects of the GLP-1 agonist exendin-4 (Talsania *et al.*, 2005) (and CCK in mice (Barrachina *et al.*, 1997)), but not of PYY_{3-36} (Talsania *et al.*, 2005). Bilateral subdiaphragmatic vagotomy in mice did not alter the acute anorectic effect of exogenous PYY_{3-36} in the first hours post-PYY_{3-36} injection (Halatchev & Cone, 2005). Vagotomised mice showed more sensitivity to PYY_{3-36} than controls after 8h, which suggested some relationship between vagal tone and the anorectic effect of PYY_{3-36} (Halatchev & Cone, 2005). PYY_{3-36} was reported to induce neuronal activation in the NTS, the primary CNS site where vagal afferent signals are received (Halatchev & Cone, 2005), contrary to previous findings (Halatchev *et al.*, 2004).

The discrepancies between these studies might indicate that there are differences in PYY_{3-36} signalling between rats and mice. Y2R expression in the NG is higher in rats (Zhang *et al.*, 1997) than in mice (Koda *et al.*, 2005; Chang *et al.*, 2015). In addition, while Abbott and colleagues (Abbott *et al.*, 2005a) showed firing of the vagal afferents in response to PYY_{3-36}, a previous study showed an inhibitory effect in cultured rat NG by whole-cell patch clamp (Wiley, Gross & Macdonald, 1993). This Y2R inhibitory effect in brainstem-vagal circuits was also suggested in other electrophysiological studies (Schwartz & Moran, 2002; Browning & Travagli, 2003, 2009).

Several limitations might apply when studying PYY_{3-36} in the gut-brain axis. Capsaicin treatment and vagotomy alters all vagal signalling and leads to other off-target effects. Therefore, these models do not allow precise dissection of the PYY pathway or pathways of action. In addition, pharmacological doses of exogenous PYY_{3-36} might not act via the same pathways as endogenous PYY_{3-36} at physiological concentrations. Indeed, peripheral administration of PYY_{3-36} could suppress appetite by causing conditioned taste aversion depending on the dose (Halatchev & Cone, 2005). Depending on the administration route a central or a peripheral effect might be more favoured, as shown for GLP-1 (Rüttimann *et al.*, 2009).

In addition, it is still possible that PYY_{3-36} can act via both central and peripheral sites. PYY_{3-36} could access the Y2R in the NTS (Stanić *et al.*, 2006) by crossing the blood-brain barrier, as it has been suggested to act in the ARC, to regulate appetite. In contrast to the anorectic effect observed in ARC hypothalamus and in the periphery, intracerebroventricular injection of PYY_{3-36} has an orexigenic effect in rats (Corp *et al.*, 2001). Injection of PYY_{3-36} into the DVC of rats also had an orexigenic effect, and prevented exogenous CCK-induced anorexia (Huston *et al.*, 2019). However, the role of vagal efferents in this response, or whether this effect also occurs in mice, remains unknown.

In humans, fMRI revealed that PYY_{3-36} might act on homeostatic and hedonic centres (Batterham *et al.*, 2007; De Silva *et al.*, 2011) but it remains unclear if these effects are connected to vagal afferents, as has been shown for the effects of CCK in mice (Han *et al.*, 2018).

The interaction of anorectic gut hormones with vagal afferents results in inhibition of food intake but can also result in inhibition of gastric emptying, and together these effects limit nutrient delivery to the intestine (see section 3.1.2). PYY is believed to inhibit gastric emptying via the 'ileal brake' (Pappas *et al.*, 1986). Microinjection of low doses of PYY and Y2R agonists in the DVC of rats inhibited gastric motility induced by thyrotropin-releasing hormone (which activates gastric vagal efferents) (Chen & Rogers, 1995, 1997). This effect was blunted by vagal lesioning (Chen & Rogers, 1995). It was then suggested that PYY can access Y2R in the brainstem and directly inhibit DMV neurons to delay gastric motility (Chen & Rogers, 1997). However, other study suggested that PYY might interact with Y2R in the brainstem and decrease excitatory synaptic transmission between the NTS and DMV (Browning & Travagli, 2003). Apart from this endocrine action, gut hormones can also have a paracrine effect on gastric motility via vagal afferent fibres. For example, this might be the case for GLP-1 which, like PYY, is released from L-cells and is also a contributor to the 'ileal break'. Capsaicin-mediated vagal afferent denervation blunted the inhibitory effect on gastric emptying of both systemic and central administered GLP-1 (Imeryüz *et al.*, 1997). In addition, knockdown of the GLP-1R in vagal afferents accelerated gastric emptying, suggesting that GLP-1 acts on vagal afferents to modulate gastric

emptying (Krieger *et al.*, 2016). It remains to be elucidated if PYY follows a similar paracrine pathway to inhibit gastric emptying.

In order to study the role of vagal afferents in PYY_{3-36} signalling, we have generated different mouse models to disrupt vagal Y2R expression, and studied the resulting phenotype. Firstly, Nav1.8-Cre mice were crossed with Y2R-floxed mice. This approach has been used before to investigate vagal leptin signalling (de Lartigue, Ronveaux & Raybould, 2014). A more refined model was generated by inducing vagal afferent-specific Y2R knockdown in adult mice. This was achieved by bilaterally administering a neuron-specific Cre-expressing AAV into the NG (where the cell nuclei of vagal afferents are located) of Y2R-floxed mice.

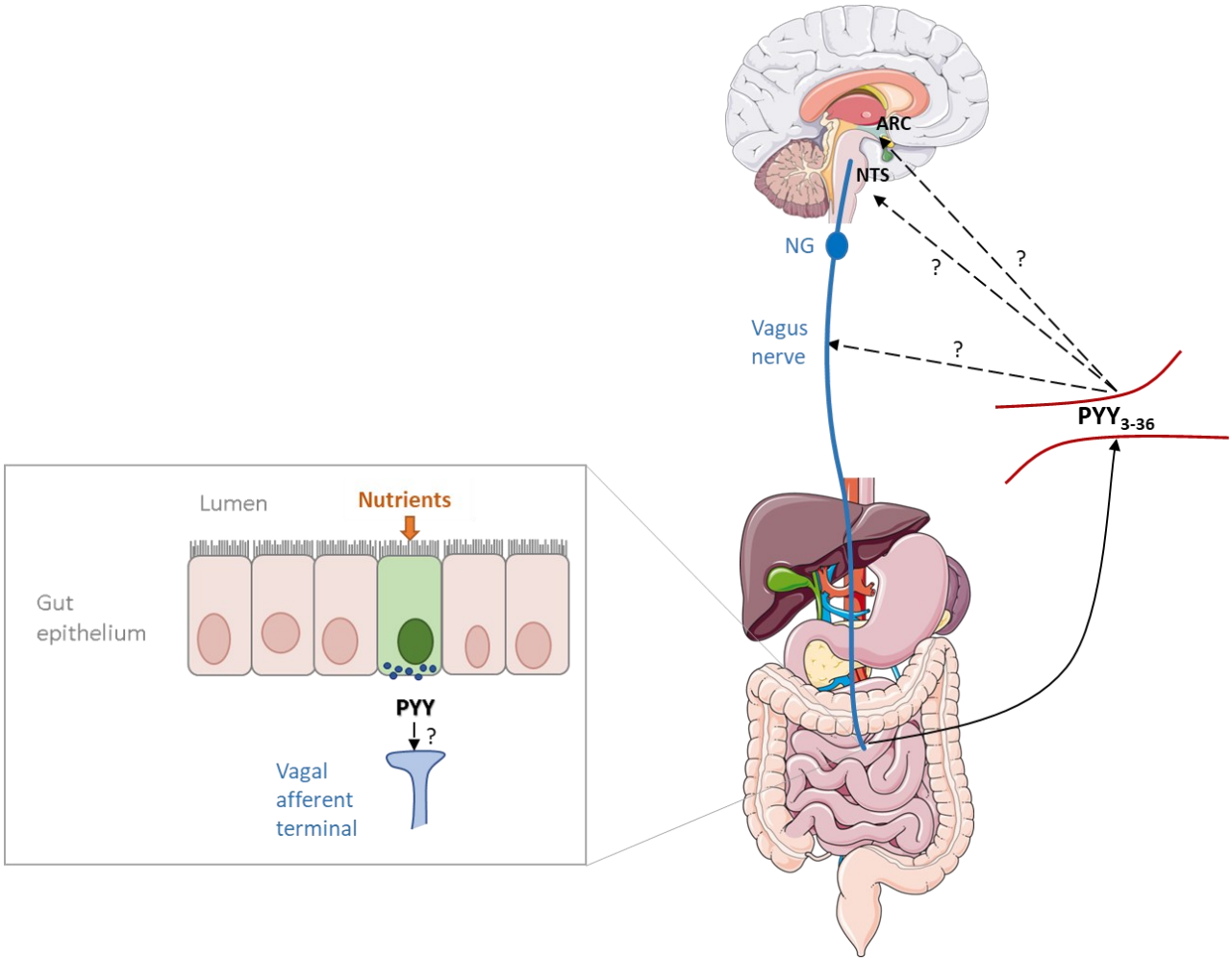

Figure 3.1.4.1. Potential sites where PYY_{3-36} may act to inhibit food intake.

After nutrient ingestion, PYY is released from L-cells and diffuse into the lamina propria where vagal afferent terminals are located. Vagal afferents express the receptor for PYY_{3-36}, the Y2R. PYY could also enter the circulation and act on vagal afferents or access appetite centres where Y2R is expressed. ARC, arcuate nucleus; NG, nodose ganglia; NTS, nucleus tractus solitarii; Peptide YY. Some of the images were obtained from Servier Medical Art.

3.2 Hypotheses and aims

The aims of the experiments described in this chapter were to:

- Assess the effect of vagal Y2R signalling disruption on the acute feeding response to exogenous PYY_{3-36}.
- Establish a surgical technique of bilateral injection into the NG of mice as a recovery procedure to achieve viral-mediated selective knockdown (KD) of the Y2R in vagal afferent neurones.
- Assess the effects of vagal Y2R signalling disruption on feeding behaviour.

The hypotheses were that:

- Peripheral PYY_{3-36} at physiological-like levels reduces food intake by activating Y2R in vagal afferents.
- Supraphysiological levels of PYY_{3-36} directly activate central appetite pathways and are therefore vagus independent.
- Vagal Y2R disruption alters satiety signalling.

3.3 Materials and methods

3.3.1 Animals

All animal procedures complied with the British Home Office Animals (Scientific Procedures) Act 1986 regulations and were performed under PPL PD75F462C (Prof Kevin Murphy, Imperial College London).

Mice were housed under controlled conditions (21-23°C, 45-56% humidity) and a 12h light/dark cycle schedule (lights on 7:00 to 19:00) with *ad libitum* access to water and food (RM1, SDS Diets, Witham, UK) unless otherwise specified. In case of early dark phase experiments, lights were on from 23:00 to 11:00.

To establish the $Y2R^{loxP/+}$ mice colony, an aliquot of sperm from $Y2R^{loxP/+}$ mice (donated by Prof Herbert Herzog, Garvan Institute of Medical Research, under a Material Transfer Agreement (MTA)) was used to fertilize C57BL/6J oocytes. In all studies, floxed-negative or $Y2R^{loxP/-}$ mice were used as controls.

Nav1.8 is a sodium channel isoform expressed in vagal afferents (over 75% of vagal afferents in mice) as well as in the spinal cord that have been used before to knockout LepRb in vagal afferents (de Lartigue, Ronveaux & Raybould, 2014). Sperm from Nav1.8-Cre mice was acquired from MRC Harwell under a MTA (Stirling *et al.*, 2005) and used to fertilize C57BL/6J oocytes. Nav1.8-Cre mice were crossed with Y2R-floxed mice to generate Nav1.8/Y2R KO.

For the conditioned taste aversion study (CTA), male C57Bl6/J mice (6 weeks old) were provided by Charles River. They were maintained in groups (6 animals/cage).

3.3.2 Tissue digestion

Ear notches were collected from 4-week-old mice using an ear puncher. For deoxyribonucleic acid (DNA) extraction, ear tissue was digested using KAPA Express Extract system (Sigma-Aldrich, Dorset, UK). Briefly, ear notches were transferred to 200 µL PCR tubes and 20 µL of a mix containing 1X KAPA Express Extract Buffer (stock 10X) and 0.02 U/µL KAPA Express Extract Enzyme (stock 1 U/µL) in molecular biology grade water (Ultrapure distilled water, Invitrogen, Paisley, UK) was added per tube. Lysis was performed in a thermocycler (Veriti™ 96-Well Thermal Cycler, Applied Biosystems, Warrington, UK) at 75°C for 10 min followed by a second step at 95°C for 5 min. DNA was diluted 1:10 with 10 mM Tris-HCl (pH 8.5) to dilute debris and digested proteins that might inhibit downstream steps. DNA extract was stored at -20°C.

3.3.3 Polymerase chain reaction

Primer sequences for genotyping Y2R-floxed and Nav1.8-Cre mice were provided by suppliers of the strains (Table 2.3.3.1). All primers used in genotyping were purchased from Sigma-Aldrich and were provided in dry form. They were re-suspended in molecular biology grade water and stored at 100 µM. A stock at 10 µM concentration was used for preparing the polymerase chain reaction (PCR) mix.

Table 3.3.3.1. Primers used for genotyping of mice

Name	Sequence (5' – 3')	Length	Tm (°C)	GC %
NHE-3A	TTAACATCAGCTGGCCTAGC	20	61.9	47.6
NHE-6	GGAAGTCACCAACTAGAATGG	21	60.0	50.0
Nav1.8Cre Forward	CAGTGGTCAGGCTGTCACCA	20	67.8	60
Nav1.8Cre Reverse	ACAGGCCTTCAAGTCCAACTG	21	65.4	52
Cre-seq	AAATGTTGCTGGATAGTTTTTACTGCC	27	72.4	37

For a 10 µL PCR reaction, 1 µL of DNA and 9 µL of the PCR mastermix were transferred to PCR tubes or plate. PCR mastermix was prepared by mixing KAPA2G Fast (HotStart) Genotyping Mix (Sigma-Aldrich), forward and reverse primers (at a final concentration of 0.5 µM) in PCR graded water. Reactions were mixed and PCR was run in the thermocycler (see Table 2.3.3.2). The KAPA genotyping mix used includes KAPA2G Fast DNA Polymerase, buffer, dNTPs (0.2 mM each at 1X), MgCl (1.5 mM at 1X) as well as inert dye, allowing direct analysis of PCR products by electrophoresis without adding loading solution.

Table 3.3.3.2. Thermal cycle profile PCR.

Step	Temperature (°C)	Time (sec)	Cycles
Initial denaturation	95	180	1
Denaturation	95	15	35
Annealing	60	15	
Extension	72	15	
Final extension	72	60	1

3.3.4 Agarose Gel Electrophoresis

A 2% agarose gel was prepared by mixing UltraPure™ agarose gel (Invitrogen) in 1X Tris-acetate-EDTA (TAE, see Appendix I). Agarose was dissolved by microwaving in pulses (swirling the flask occasionally). In order to visualize the DNA, 12 µL per 100 ml gel of 1% ethidium bromide (Merck, Hertfordshire, UK) was added. Agarose was poured into a gel tray (with the well comb) and the tray was incubated at room temperature (RT) until the agarose solidified. After removing the well comb, the gel was placed into the electrophoresis unit, which was filled with 1X TAE until the gel was covered. A molecular weight ladder (1 Kb Plus DNA Ladder, Invitrogen) and the samples were loaded into the lanes of the gel (5 µL/well). The gel was run at 100-150 V and stopped using the dye line as a guidance. The gel was visualised under ultraviolet light in a G:BOX imaging system (Syngene, Cambridge, UK).

In case of Y2R-floxed, band sizes were 340 bp for wild-type (WT) and 395 bp for Y2R-floxed homozygote; the presence of both bands indicated a heterozygote. In the case of Nav1.8-Cre, band sizes were 346 bp for Nav1.8-Cre and 258 bp for WT (see Appendix II).

3.3.5 RNA extraction

RNA was isolated using an acid guanidinium thiocyanate-phenol-chloroform method. Snap frozen tissue in 2 ml round-bottom tubes was homogenised in 500 µl of TRIsure™ (Bioline, London, UK) using the TissueLyser II. Lysate was mixed with 100 µl of chloroform, incubated for 15 min at RT and centrifuged for 15 min at 12000 x *g* at 4°C. RNA is precipitated by mixing the upper aqueous phase with 1 volume of isopropyl alcohol containing 1 µl/ml GlycoBlue™ Coprecipitant (Invitrogen) and incubated for 10 min at RT. After spinning the samples at 12000 x *g* for 8 min at 4°C, the pellet was re-suspended with 75% ethanol, spun at 12000 x *g* for 5 min at 4°C, and the resultant pellet air-dried at RT and then re-suspended in 10 µl of RNAse-free water. After incubating for 30 min at RT and for 20 min on ice, RNA was stored at -80°C. RNA concentration was measured using a NanoDrop™ Lite Spectrophotometer (Thermo Fisher Scientific, Hertfordshire, UK).

3.3.6 Complementary DNA preparation

DNA was digested using RQ1 RNAse-Free DNAse kit (Promega, Hampshire, UK). Briefly, RNA in a volume of 8 µL was prepared and mixed with 2 µL of DNAse mix (dilution 1:1 DNAse enzyme with DNAse buffer). After incubating for 30 min at 37°C, 1 µL of stop solution was added and samples were incubated at 65°C for 10 min.

For complementary DNA (cDNA) synthesis, High Capacity cDNA Reverse Transcription Kit (Thermo Fisher) was used. Reaction volume was 20 µl, consisting of 11 µl DNA-free RNA and 9 µl of the RT mastermix. The final reaction consisted of 1X RT Buffer, 1X dNTP mix, 1X RT Random Primers, and 1 µL MultiScribe™ Reverse Transcriptase with the RNA. cDNA was synthesised in a Veriti™ 96-Well Thermal Cycler (25°C for 10 min, 37°C for 120 min, 85°C for 5 min) and kept at 4°C until storage at -80°C.

3.3.7 Real-time quantitative polymerase chain reaction

For real-time quantitative polymerase chain reaction (RT-qPCR), 1 µL of cDNA was used in a 10 µL reaction volume containing 1X TaqMan™ Gene Expression Master Mix (which contains the *Taq* DNA polymerase, dNTPs and other components of the reaction) and 1X TaqMan Gene Expression Assay (containing target-specific primers and fluorogenic probes, see Table 2.3.8.1). Pre-designed TaqMan™ Gene Expression assays and master mix were purchased from Thermo Fisher. The 384 well-plate was run on the CFX384™ detection system (Bio-Rad, Hertfordshire, UK) at the conditions shown in Table 2.3.8.2. Reactions were performed in triplicate and relative levels of mRNA gene expression calculated using the $2^{-\Delta\Delta Ct}$ method.

Table 3.3.7.1. Thermal cycle profile for RT-qPCR

Gene symbol	Gene name	TaqMan assay ID
Npy2r	Neuropeptide Y receptor Y2	Mm01956783_s1
Ppil3	Peptidylprolyl isomerase (cyclophilin)-like 3	Mm00510343_m1

Table 3.3.7.2. Probes used for RT-qPCR

Step	Temperature (°C)	Time (min)	Cycles
Initial denaturation	50	2	1
Denaturation	95	10	60
Annealing	60	1	

3.3.8 Surgery

Adult mice (6-8 weeks old) were injected in the left and right NG with AAV following the method described in section 2.3.2. Ready-to-use viral particles of AAV were used: AAV9.hSyn.HI.eGFP.WPRE.bGH ($1.32x10^{14}$ genome copy (GC)/ml), AAV9.hSyn.HI.eGFP-Cre.WPRE.SV40 ($5.50x10^{13}$ GC/ml), AAV5.hSyn.Cre.hGH ($2.48x10^{13}$ GC/mL) or AAV5.hSyn.eGFP.WPRE.bGH ($2.22x10^{13}$ GC/mL). All viruses were provided by the Penn Vector Core, University of Pennsylvania Gene Therapy Program. Homozygous for Y2R-floxed ($Y2R^{loxP/+}$) received Cre-expressing AAV. Floxed-negative or $Y2R^{loxP/-}$ mice received control virus.

3.3.9 Feeding studies

Before the feeding studies, mice were singly caged at least for 5 days and accustomed to intraperitoneal (i.p.) injection (100 µL of saline) or oral gavage (300 µL water) in the early dark phase every other day during a week. Oral gavage was performed using a feeding needle attached to a 1 mL syringe.

Using a crossover design, animals received each treatment in a random order. In the case of studies following i.p. injection, the treatments used were PYY_{3-36} (Tocris Biosciences, Abingdon, UK) at different doses (3 to 30 µg/kg), 5 µg/kg sulphated cholecystokinin octapeptide (CCK-8;

Tocris Biosciences, Abingdon, UK) or saline (vehicle control). The volume of i.p. was around 100 µL (for an average size 25 g mouse). PYY_{3-36} and CCK-8 were prepared on the experimental day just before the i.p. injection by adding saline to pre-prepared freeze-dried vials or directly to the lyophilized form.

In the case of oral gavage studies, a nutrient bolus was tested. This bolus consisted in a mix 17% (w/v) of D(+)-Glucose (Sigma-Aldrich), 8.3% (w/v) of L-arginine (Sigma-Aldrich), 41.7% (v/v) of extra virgin olive oil (Sainsbury's Supermarkets Ltd) and 58.3% (v/v) of Ensure® Plus (Abbott, Maidenhead, UK). All the animals received 300 µL of the bolus (or water as vehicle control). Therefore, a 25 g mouse would receive 1 g/kg of L-arginine, 2 g/kg of glucose, 5 mL/kg of olive oil and 7 mL/kg of Ensure® Plus. The meal was prepared on the experimental day just before oral administration and was mixed using a stirrer until oral gavage was performed

Mice were fed *ad libitum* before and during the study. Just before the onset of the dark phase, animals and chow (RM1, SDS Diets) were weighed using a PLJ 420-3F (Kern & Sohn GmbH, Germany) precision balance (0.001 g readability). Any observable spilled food was removed from the cage. Mice received the treatment in the early dark phase (t = 0 h). Immediately thereafter, pre-weighed chow was placed on the hopper feeder and food intake measured as the difference between the chow weighed at t = 0 h and the weight of chow remaining at 1, 2, 4, 8 and 24 h post-injection. Treatments for an individual mouse were separated by 3-4 days wash-out period.

3.3.10 Conditioned taste aversion study

Male wildtype C57Bl/6J mice (6-week-old) were individually housed for 1 week with *ad libitum* access to food and water. Then, water was withdrawn (day 0) and mice were trained to consume daily water intake over 1 hour (light phase 11:00-12:00) for 6 consecutive days (day 1-6). To mimic the final experiment conditions and acclimate the mice, mice were weighed before giving them access to two water bottles (pre-weighed) during that hour. Immediately after the 1 h of water intake, water bottles were weighed. In addition, animals received i.p. injection with 100 µl of saline (on day 1,3,5).

On day 7, animals were randomly assigned to treatment groups using a strategy to minimise potential confounders (order of treatments, body weight and cage location). Instead of water, mice had access to a novel flavour (grape Kool-Aid) presented in two pre-weighed bottles. Immediately following the 1 h access to Kool-Aid, mice received i.p. injection of the treatment

and bottles were weighed. The treatments were vehicle (saline), 0.3M (1% BW) lithium chloride (LiCl, Sigma-Aldrich) and PYY_{3-36} at dose of 3 and 30 µg/kg.

On day 8 (test day), mice were given a free choice of water or grape Kool-Aid. They were presented with two pre-weighed bottles one containing water and the other grape Kool-Aid solution, alternating bottle position to minimise potential confounders (i.e., half of the mice within a treatment group was presented with the novel flavour on the right side of the cage, and the other half of the mice was presented with the novel flavour on the left-side of the cage). Immediately after, bottles were weighed. CTA data was represented as a ratio calculated by dividing weight of grape Kool-Aid bottle intake by the average of the weight of intake of grape Kool-Aid bottle intake in the control (saline) group.

3.3.11 Gastric emptying

Mice were fasted for 8 h in the light phase with *ad libitum* access to water and local anaesthetic cream was applied on the tail surface. Blood from the tail vein was collected (t = 0) and animals received an oral gavage of a bolus containing 1% paracetamol (100 mg/kg) 20% D(+)-glucose (Sigma-Aldrich). Blood from the tail vein was collected at 15, 30 and 60 min in Microvettes® CB 300 containing EDTA (Sarstedt Inc), spin at 3200xg for 15 min and plasma was stored at -80°C. The acetaminophen assay (Cambridge Life Sciences Ltd, Cambridgeshire, UK) was performed following a recommended reduced volume protocol from the kit supplier. Briefly, 5 µL of sample (neat plasma, diluted plasma in distilled water, paracetamol calibrator, diluted plasma in distilled water or distilled water (blank control)) were added to a clear 96-well microplate. Reconstituted enzyme reagent was added (50 µL/well), mixed and incubate at RT for 5 min. Then, 100 µL/well of Colour Reagent A and 100 µL/well of Colour Reagent B were added, mix and incubate for around 5 min. Absorbance was read at 620 nm.

3.3.12 Oral glucose tolerance test (OGTT)

Mice were fasted for 8 h with *ad libitum* access to water during the light phase. Local anaesthetic cream was applied on the tail of mice and the baseline blood glucose level was measured following venesection and sampling from the tail tip using a glucometer (GlucoRx) 15 min before glucose administration. Then, 2 g/kg of D(+)-glucose (20% w/v) was administered by oral gavage and blood glucose levels were measured at 15, 30, 60, 90 and 120 min.

3.3.13 Body composition

Body composition was measured in live non-anaesthetised mice using an EchoMRI™-100H analyser (Houston, Texas). Mice are placed in a holder to minimize its movements and the holder is inserted in the EchoMRI™-100H for scanning.

3.3.14 Metabolic assessment

Metabolic characterisation was performed during 10 days using an Oxymax-CLAMS system (Columbus Instruments Comprehensive Lab Animal Monitoring System, Columbus, OH, USA), a service provided by MRC London Institute of Medical Sciences (LMS). On the start of the experiment, body weight values of the animals were inputted into the system. Animals were previously accustomed to individual housing and were also accustomed to single housing in CLAMS cages for 10 days. The CLAMS cages were located in an environmental enclosure at 22°C and on a 12h light/dark cycle schedule provided by LED lighting (dark phase 8pm to 8am). Water and chow (RM1) were available *ad libitum*. The pelleted food was located in an overhead feeder under which crumbs accumulate in a surface that the animal could access so crumb weight was accounted for. A water bottle was suspended and its weight was constantly monitored.

Oxymax is an open-circuit indirect calorimeter that measures gas exchange by monitoring O_2 concentration. This system screens oxygen in each cage sequentially using a zirconia (ZrO_2) sensor so readings are obtained every 27 min. The O_2 consumption (VO_2) and CO_2 production (VCO_2) are the differences between O_2 fractions and CO_2 fractions, respectively, at the input and output ventilations. These are corrected for the nitrogen displaced in this gas exchange as well as normalised to the body weight of the animals. The input ventilation was set at around 0.50 L/min. The system also calculates the respiratory exchange ratio (RER, ratio between the VCO_2 and the VO_2) and the heat (kcal/h).

Activity monitoring was based on infrared photo beams arranged in a grid pattern in the X, Y and Z axis around the CLAMS cages. When the animal moved, the beams were interrupted so the position of the animal could be continuously recorded. Locomotor activity accounts for ambulatory activity (when consecutive adjacent beams are broken) plus repetitive movements (e.g., grooming). Rearing events are detected in the Z axis.

Food intake, water intake and activity are binned together in the same interval as the calorimeter readings and are also available as high-resolution data with shorter intervals. The web-based tool *CalR* was used to visualise the data (Mina *et al.*, 2018).

3.3.15 Endogenous PYY secretion induction with a nutritious bolus

Littermate controls (n = 13) were used to test the effect of a nutritious bolus (see section 3.3.9) on plasma PYY levels. This mix was prepared on the day of the study and 300 µL of this nutritious mix was administered by oral gavage. Blood was collected from 500 µL Microvette® tubes containing K3 EDTA (Sarsted) as well as 10 µL of the protease inhibitor Aprotinin (100,000 KIU/mL, Nordic Pharma Ltd). Blood samples were stored in ice until they were centrifuged at 1000-2000 x*g* for 15 min. Plasma was collected and stored at -80°C.

3.3.16 Radioimmunoassay of PYY

The radioimmunoassay was performed and analysed with the help of Prof KG Murphy and Dr G Franco-Becker. PYY-like immunoreactivity was measured using an established in-house radioimmunoassay (Adrian *et al.*, 1985). Plasma samples were run in singlets in parallel with several standard curves and other controls (in duplicate) were assayed in parallel. The standard curve was composed of 1, 2, 3, 5, 10, 15, 20, 30, 50 and 100 fmol/tube of synthetic unlabelled PYY. Tubes containing no sample/standard ('zero' controls) were at regular intervals throughout the assay. In addition, 'zero' controls containing half and double amount of label used in the standard/sample assays were used. To control for non-specific binding (NSB), tubes containing everything except standard/sample and antibody were run in parallel.

The assay was performed in 0.06 M phosphate buffer containing 9.8 mM EDTA and 0.05% sodium azide (pH 7.2) (see appendix I). On the day of the RIA, BSA (First Link UK Ltd) and Tween® 20 (Amresco) were added to this buffer at 1% and 0.02%, respectively. Firstly, buffer was added to all the tubes and 100 µl of 'zero plasma' was added to the tubes of the standard curve. 'Zero plasma' is a charcoal stripped fetal bovine serum that does not contain lipid-related components (e.g., hormones and cytokines) but does contain other materials of different molecular weights (e.g., salts, glucose, amino acids) so it acts as a control of the sample matrix effect. Plasma samples were vortexed and 100 µL was used per tube in singlet. Buffer was added to ^{125}I-PYY and radiation was monitored using the CAPRAC®-t system so the final level 20 counts per second (cps) per tube. Standard solution was added at different volumes to cover a range of concentrations. Plasma samples were vortexed and 100 µL was added per tube (singlet). The antibody Y21 (Bachem, UK) was used at a final dilution of 1:50,000. After vortexing the tubes, tubes were covered with foil and incubated for 3 days at 4°C. The Y21 antibody was raised in rabbits and is specific for the C-terminal of PYY. It fully reacts with both PYY_{1-36} and PYY_{3-36} and does not cross-react with PP, NPY or other known gut hormones.

The separation method was based on dextran-coated charcoal. The dextran coating allows only small molecules to absorb into the charcoal, while excluding larger complexes, i.e., antigen-antibody complexes. Charcoal was coated with dextran and mixed in phosphate buffer (used for running the RIA) with gelatine (VWR Chemicals). Charcoal was added (4 mg/tube) and tubes were centrifuged at 1500 x*g* for 30 minutes at 4°C. The fractions were separated and the supernatant was covered with hot wax. Both the pellet (bound PYY) and the supernatant (unbound PYY) were counted for 4 min in a γ counter (Multi Crystal LB2111, Berthold Technologies, Harpenden, UK). Peptide concentrations in the samples were calculated using a non-linear plot (Prism, GraphPad software). The intra-assay CV (calculated in duplicated standard curves) was 3.47%.

3.3.17 c-Fos induction

The early gene c-fos can be used as a marker of neuronal activation. C-fos protein expression was assessed at 90 min after treatment as that is when protein expression peaks (Morgan & Curran, 1991). On the experimental day, animals were randomised based by body weight (in the case of two treatments) and food was removed 4 h before experimental treatment to avoid food intake-mediated c-fos induction.

3.3.18 Mouse perfusion-fixation

Animals were anaesthetised with i.p. injection of pentobarbital and perfusion surgery was started once the animal was unresponsive to paw pinch. An incision was made below the diaphragm and the rib cage cut to expose the heart. A 15-gauge blunt needle (connected to the tube-syringe system) was inserted into the left ventricle and the right atrium cut to allow flow. Animals were perfused using a tube connected to a syringe that was previously primed to avoid bubbles. First, 30 mL of heparinized 0.01 M phosphate-buffered saline (PBS) was perfused, followed by 4% formaldehyde (FA) in 0.01 M PBS. The head was removed, the brain dissected and stored in 4% FA-PBS in 5 mL tubes overnight at 4°C. For cryoprotection, brains were stored in 30% sucrose (Sigma Aldrich), 0.02% sodium azide in 0.01 M PBS at 4°C until sectioning.

3.3.19 c-Fos immunohistochemistry

The brainstem was sliced using a sledge microtome (AS200, Shandon) connected to a solid-state freezer (Bright instruments). Serial sections (40 µm) were stored in 24-well plates in anti-freeze solution (see appendix I) at -20°C. Immunohistochemistry was performed in every fourth section of the brainstem (approximately every 120 µm of the tissue, around 30 sections/animal). In each

immunohistochemical assay, a few sections of brainstem from lithium chloride injected mice were used as a positive control of c-fos staining.

Free-floating sections were immunostained in Corning® 15 mm Netwell™ inserts with 74 µm polyester mesh (5 sections/well). Each tray contained sections from an experimental and a control group. Inserts containing the sections were placed on a Netwell holding tray using a well-holder. Sections were washed 3 times, 5 min each time in 0.01 M PBS at RT on the shaker. In order to block endogenous peroxidase activity, slices were incubated for 15 min at RT in 0.6% H_2O_2 (Sigma Aldrich) in methanol on the shaker. After repeating the washes in 0.01 M PBS, non-specific binding sites were blocked by incubating the sections for 2 h in 0.01 M PBS containing 3% normal goat serum (Gibco, UK) and 0.25% Triton X100 (VWR International, Leicestershire, UK) at RT. Anti-c-Fos antibody (ab190289, Abcam, Cambridge) was diluted 1:15,000 in the blocking solution. Inserts containing the sections were transferred to a 12-well plate and sections were incubated with the diluted antibody (3 mL/well) overnight at 4°C on the shaker.

Sections were washed 3 times, 5 min each time in 0.01 M PBS containing 0.05% Tween-20 (Amresco) (PBS-Tween) at RT on the shaker. The VECTASTAIN® Elite ABC kit (Vector Laboratories, Peterborough, UK) was used for immunoperoxidase detection. Firstly, biotinylated goat anti-Rabbit IgG (H + L) antibody was diluted 1:400 in 0.3% bovine serum albumin (BSA; Sigma-Aldrich) 0.25% Triton X100. In a 12-well plate, sections were incubated with the diluted antibody (3 mL/well) for 2 h at RT on the shaker. After repeating the PBS-Tween washes, slices were incubated in the avidin/biotin complex (ABC) solution for 1 h at RT on the shaker. The ABC solution contained both reagent A (avidin DH) and reagent B (biotinylated peroxidase) diluted 1:200 in 0.05M Tris·HCl, pH 7.6 (see appendix). Sections were washed 3 times with PBS-Tween and incubated in peroxidase substrate solution. Peroxidase substrate solution contained 1% of 50 mg/mL 3,3'-Diaminobenzidine tetrahydrochloride hydrate (DAB, Sigma-Aldrich) and 0.01% H_2O_2 in 0.01M PBS. When desired stain intensity was achieved (around 10-15 min), the reaction was stopped with 0.01M PBS. Sections were washed 3 times, 5 min each time in 0.01 M PBS at RT on the shaker and mounted on poly-lysine coated slides (VWR International) using a thin brush. When dry, slides were washed in 70% ethanol, 100% ethanol (twice) and xylene, sequentially (30 s each). The slides were then mounted in DPX and cover-slipped.

3.3.20 c-Fos quantification

Imaging was performed with an Eclipse Ti2 inverted microscope (Nikon) with an ORCA-Flash 4.0LT+ digital camera (Hamamatsu). All the sections were imaged in the brightfield channel (10

ms exposure) using 10X/0.3 NA (numerical aperture). For image acquisition, a grid was created using the *Multiple positions* mode using the edges of the brain sections as reference (overlap of 10%). Fiji software was used to stitch the images (order defined by image metadata) (Preibisch, Saalfeld & Tomancak, 2009).

For blind c-fos analysis, image files were renamed by a lab member (who saved the original and new code name). Each section was classified according to the mouse brain atlas (Bregma). Templates to define brainstem regions were created in PowerPoint (Microsoft) and c-fos-positive cells were manually counted. After counting was completed, the original names of the files, and therefore the identities (treatment, genotype) of the animals, were revealed.

3.3.21 Statistical analysis

Data is expressed as mean ± standard error of the mean (SEM). Statistical analyses were performed by two-tailed unpaired Student's t test or by one-way or two-way ANOVA. ANOVA where followed by multiple comparison tests. If there are missing values, mixed-effects model was used. Statistical analyses were performed using Prism 8.0 software (GraphPad, La Jolla, CA). In other cases, Kruskal-Wallis test, followed by Mann-Whitney test were used. Differences were considered significant if $p < 0.05$. Significant P values are shown as *.

High-resolution food intake data obtained from CLAMS cages was cleaned based on maximum cut-offs previously defined (Campos *et al.*, 2016); less than 0.1% of data points were lost. These cut-offs were 0.5 g as max meal size, 20 min as max meal duration and 80 min as max inter-meal duration. Probability distribution functions for meal patterning were produced using customised MatLab scripts. A probability distribution function shows the probabilities of a variable for all its possible values. These probabilities associated with specific values have to be between 0 (impossible event) to 1 (certain) and the sum of probabilities of the events is 1. Non-parametric kernel density estimation was used to estimate the probability distribution function. For *n* data on a given variable X, (x_1,x_2,...,x_n), the kernel-based estimate the density (*f*) of X at a generic point (Fig. 2.3.17.1). *K* is a kernel function that needs to satisfy certain properties and *h* is the bandwidth, a smoothing parameter that tends to zero while *n* tends to infinity. The bandwidth was chosen using *Silverman's rule of thumb*, which computes an optimal bandwidth by assuming the data is normally distributed (Silverman, 1986).

$$\hat{f}(x) = \frac{\sum_{i=1}^{n} K(\frac{x_i - x}{h})}{nh}$$

Figure 3.3.21.1. Function of kernel density estimation.

Because the data set is non-negative, the standard kernel function would have bias at boundaries (near 0). This was overcome by mirroring the data (Schuster, 1985) and by using an Epanechnikov kernel, which has a bounded support (Epanechnikov, 1969). The difference between comparator probability distribution functions was analysed using a Kolmogorov-Smirnov (K-S) test. This non-parametric test compares the empirical distribution of a given variable and hence focuses on cumulative distribution functions rather than densities. These analyses were performed by Dr V Salem and Prof W Distaso (Imperial College London).

3.3.22 Experimental design

Nav1.8-Cre mice were crossed with Y2R-floxed mice. Males Nav1.8/Y2R KO were subjected to body composition assessment and acute feeding studies in response to exogenous PYY_{3-36} at low and high doses. In a final experiment, animals received exogenous PYY_{3-36} or vehicle and c-Fos expression in brainstem was assessed and Y2R expression in the NG was assessed by qPCR.

The use of a low dose PYY_{3-36} aims to avoid the pharmacological effects of high doses PYY_{3-36} and, therefore, to study the action of PYY_{3-36} in a more physiological way. In an individual experiment in wildtype mice, we tested if the PYY_{3-36} doses used in this work caused aversion (3.3.10).

Nav1.8-Cre approach might alter Y2R expression in other locations and can develop compensatory mechanisms. To overcome this, we generated a vagus-specific knockdown model in the adult mouse by bilaterally administering a Cre-expressing AAV into the NG, where the cell nuclei of vagal afferents are located, of Y2R-floxed mice. This approach is similar to a previous approach in which a lentivirus delivering short-hairpin RNA (shRNA) construct was delivered in the NG of rats (Krieger *et al.*, 2016). Mice were subjected to body composition assessment. Acute feeding studies in response to low dose and high dose of PYY_{3-36} as well as CCK-8 (positive control of functional afferent vagus nerve) were performed. Acute feeding studies in response to a nutrient bolus were also performed. We confirmed in other littermate control animals that the nutrient bolus causes an increase in plasma PYY. In a final experiment, animals received this nutrient bolus to investigate c-Fos expression in brainstem, and Y2R expression in the NG was assessed by qPCR.

Gastric emptying (section 3.3.11) and glucose tolerance (3.3.12) was assessed in a different cohort. Another cohort was subjected to metabolic characterisation using a Comprehensive Lab Animal Monitoring System (CLAMS) (section 3.3.14). This system allowed to study meal patterning.

3.4 Results

3.4.1 Effect of fasting in vagal Y2R expression in mice

In order to test if nutritional status also alters Y2R expression in mice as shown in rats (Burdyga *et al.*, 2008), Y2R expression was quantified in single NG after a 24 h-fast in NG Y2R + control mice (Fig. 3.4.1.1). Two-way ANOVA revealed that Y2R expression was not altered by fasting and that there was no interaction between the feeding status and the NG side ($p = 0.5048$, $F(1, 12) = 0.4728$), but there was higher expression in the right NG ($p = 0.049$, $F(1, 12) = 4.778$).

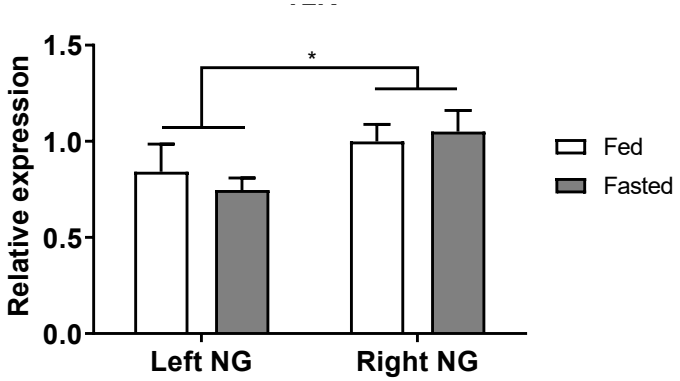

Figure 3.4.1.1. Relative expression of Y2R in left and right NG in fed and 24 h-fasted control mice.

Littermates of Y2R-floxed mice injected with control AAV9-GFP in the NG (n = 4 per group). Expression is relative to *Ppil3* and normalised to right NG Y2R expression in fed group.

3.4.2 Phenotype of Nav1.8/Y2R KO mice

In order to knockout the Y2R in vagal afferents, Y2R-floxed animals were crossed with Nav1.8-Cre mice (Stirling *et al.*, 2005). Littermate controls were a mix of $Nav1.8^{Cre/+}$ (homozygous), $Y2R^{loxP/+}$ and $Y2R^{loxP/-}$ (heterozygous). The Nav1.8/Y2R KO animals showed a significant reduction of around 60% in Y2R expression in both left and right NG compared to littermate controls (Fig. 3.4.2.1). There was no interaction between the expression and the NG side (two-way ANOVA: $p = 0.9863$, $F(1, 12) = 0.0003$). Although not a complete knockout, these mice will be hereby referred to as Nav1.8/Y2R KO.

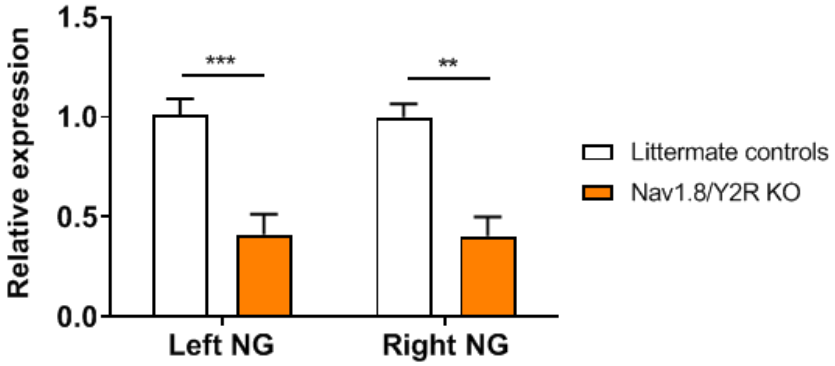

Figure 3.4.2.1. Relative expression of Y2R mRNA in left and right NG in Nav1.8/Y2R KO mice.

Expression is relative to *Ppil3* (normalised Y2R expression in right NG of control group). Animals were sacrificed at 16-30 weeks of age (n = 3-5 per group). Two-way ANOVA followed by Bonferroni's multiple comparisons test (** $p < 0.01$, ***$p < 0.001$).

No differences in body weight were observed between age-matched Nav1.8/Y2R KO and controls (mixed effect analysis: time x genotype: $p = 0.1123$, $F (19, 178) = 1.442$) (Fig. 3.4.2.2, A). No differences in body composition were observed between age-matched Nav1.8/Y2R KO and controls (Fig. 3.4.2.2, B,C).

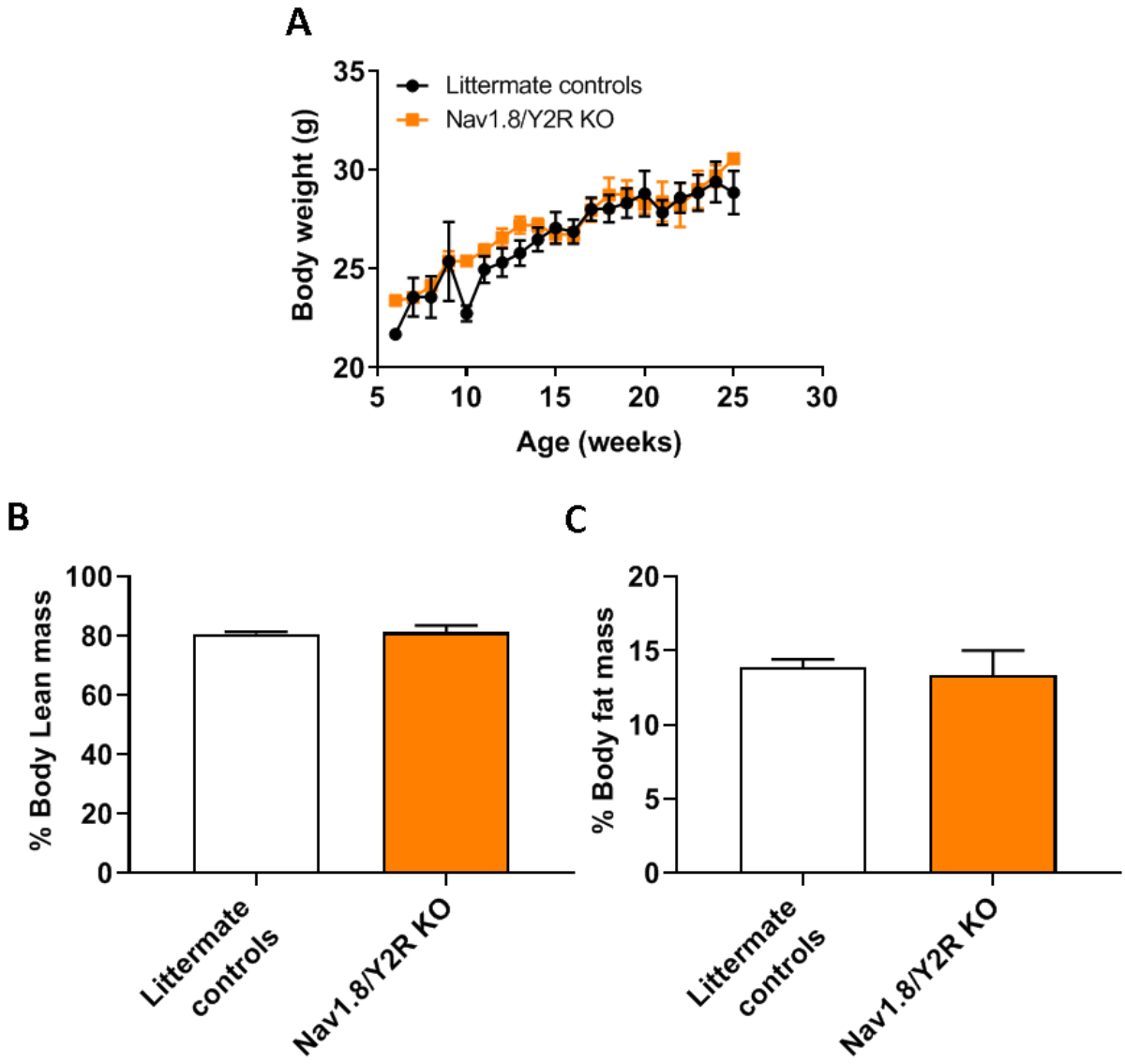

Figure 3.4.2.2. Body weight and body composition of Nav1.8/Y2R KO mice.

Age-matched body weight (g) of Nav1.8/Y2R KO and controls over time (A). Lean mass (B) and fat mass (C) as % of body weight in Nav1.8/Y2R KO (n = 6) and in littermate controls (n = 12) at age 6-12 weeks.

3.4.3 Acute effects of exogenous PYY_{3-36} in food intake of Nav1.8/Y2R KO mice

In order to study the feeding response to PYY_{3-36} in Nav1.8-specific Y2R KO, fed mice were injected with PYY_{3-36} at doses previously studied in rodents (Batterham *et al.*, 2002; Halatchev *et al.*, 2004) in the early dark phase. No significant interaction was observed between treatment and genotype (two-way ANOVA: p =0.1486, F (2, 48) = 1.984) at 1hr; p = 0.4305, F (2, 48) = 0.8577 at 2h) (Fig. 3.4.3.1).

In control mice, a reduction in food intake was observed after low dose (p = 0.0016 at 1 h; p = 0.0465 at 2 h) and high dose PYY_{3-36} in a dose-dependent manner (p = <0.0001 at 1 h and 2 h). However, the anorectic effect of the low dose of PYY_{3-36} was abrogated in Nav1.8/Y2R KO mice (p >0.9999 at 1 h and 2 h).

Of note, no significant differences were observed between Nav1.8/Y2R KO and controls at low dose PYY_{3-36} (p = 0.189 at 1h; p = 0.470 at 2 h). This is likely due to the small magnitude of PYY_{3-36} effect in food intake at this dose (around 20-30% reduction in FI in control).

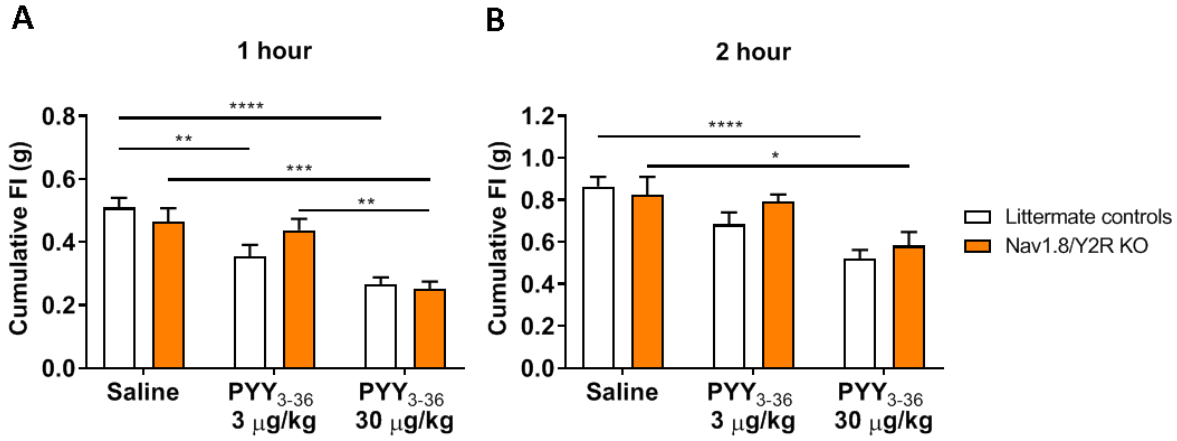

Figure 3.4.3.1. Cumulative food intake after i.p. injection of PYY_{3-36} in Nav1.8-Y2R KO mice.

Food intake (FI) at 1 h (A) and 2 h (B) after PYY_{3-36} was injected at different doses or saline in 14 weeks-old Nav1.8/Y2R KO (n = 7) or littermate controls (n = 11). Two-way ANOVA followed by Bonferroni's multiple comparisons test (*p < 0.05, **p < 0.01, ***p < 0.001, ****p < 0.0001).

3.4.4 Effect of exogenous PYY_{3-36} in brainstem neurone activation of Nav1.8/Y2R KO mice

In a final experiment, c-fos expression in the brainstem of Nav1.8/Y2R KO and controls was quantified after administration of vehicle or low dose PYY_{3-36} (Fig. 3.4.4.1). Kruskal-Wallis test did not reveal significant differences between groups (AP & NTS: 0.1329; NTS: p = 0.2309). A

trend towards an increased c-fos expression in the caudal NTS and AP was observed in littermate controls injected with PYY_{3-36} (p = 0.064, non-parametric Mann-Whitney test).

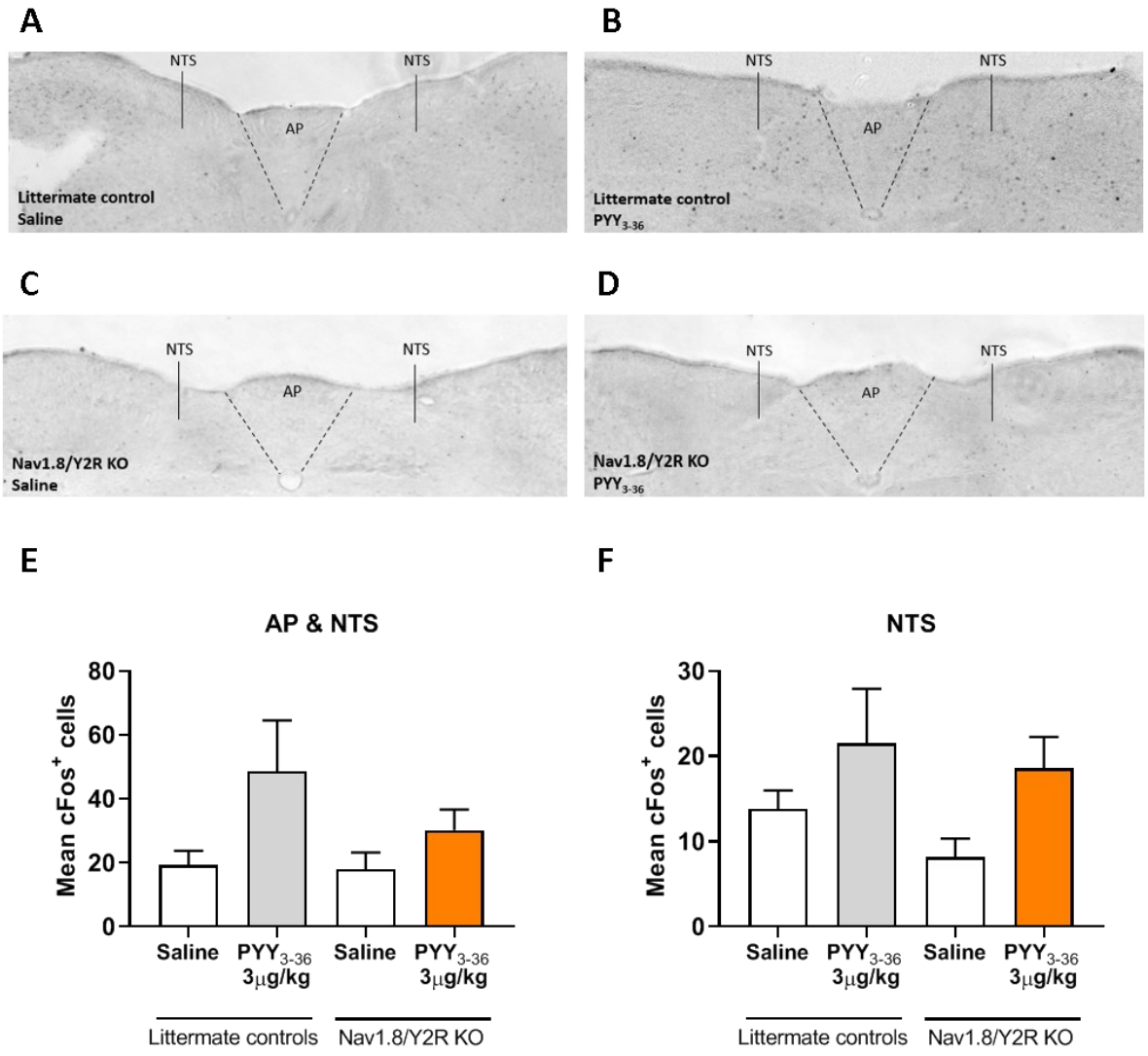

Figure 3.4.4.1. c-fos expression in brainstem of Nav1.8-Y2R KO after i.p. injection of PYY_{3-36}.

Representative images of brainstem in littermate controls (A,B) and Nav1.8/Y2R KO (C,D) approx. 90 min after i.p. injection of vehicle (A,C) or PYY_{3-36} at 3 µg/kg (B,D). Location of area postrema (AP) and nucleus tractus solitarius (NTS) are indicated. Mean of c-fos-positive neurones in AP and NTS of Nav1.8/Y2R KO (n = 2-3 per treatment group) or littermate controls (n = 4-5 per treatment group). In E, the number of c-fos-positive cells in 2 brain slices where the AP and caudal NTS are located (-7.48 to -7.32 Bregma (mm)) is shown. In F, the mean of the number of c-fos-positive cells in 3 to 6 slices between -6.24 to -7.48 Bregma (mm) in mouse brain atlas is shown. Mice were sacrificed at 16-30 weeks of age.

3.4.5 Condition aversion test in response to of exogenous PYY_{3-36}

Previous studies have shown that peripherally administered PYY_{3-36} causes conditioned taste aversion and suggested that this could contribute to the anorectic effect (Halatchev & Cone, 2005). Therefore, it was important to test if the i.p. injected PYY_{3-36} induced CTA in mice. We used a two-bottle, one-flavour CTA assay in male wild type mice to test the PYY_{3-36} doses used in the feeding studies. One-way ANOVA revealed significant differences ($p = 0.004$, $F(3, 28) = 5.544$). PYY_{3-36} did not reduce the intake of Kool-Aid compared to saline group at any tested dose (Fig. 3.4.5.1). The positive control LiCl caused a drastic reduction in the ratio compared to saline ($p = 0.029$), PYY_{3-36} 3 µg/kg ($p = 0.0107$) and PYY_{3-36} 30 µg/kg ($p = 0.0075$).

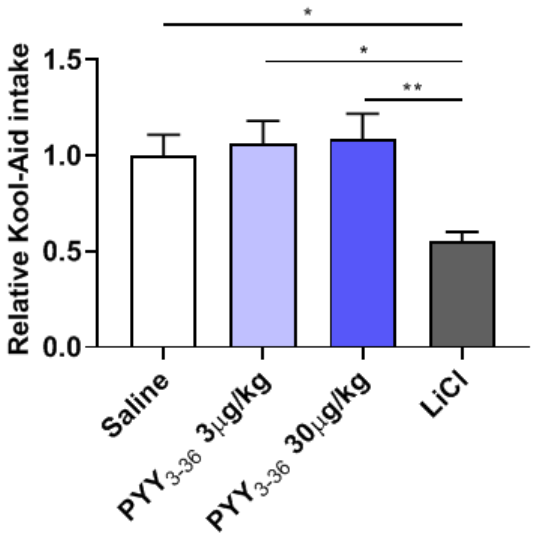

Figure 3.4.5.1. Conditioned taste aversion in lean wildtype mice trained to associate indicated treatments with grape Kool-Aid flavor.

Intake of Kool-aid is showed relative to the saline group. 0.3M LiCl is used as positive control (n=8/group). One-way ANOVA followed by Tukey's multiple comparisons test (*$p < 0.05$, **$p < 0.01$).

3.4.6 Characterisation of NG Y2R KD mice

Nav1.8 is expressed in vagal sensory neurones but also in other locations. In addition, germline mouse models can develop compensatory mechanisms. Since these factors can influence the resultant phenotype, we investigated the effect of a vagal-specific disruption of Y2R signaling in the adult mouse. In order to do that a Cre-expressing AAV was bilaterally injected in the NG of Y2R-floxed homozygous ($Y2R^{loxP/+}$) mice (Fig. 3.4.6.1, A). Control mice received a AAV control virus expressing GFP (Fig. 3.4.6.1, B). The expression of both this Cre-expressing AAV virus and

the AAV control (that does not express Cre recombinase) is neuron-specific due to the use of the human synapsin (hSyn) promoter.

After metabolic phenotyping, NG were individually collected for evaluation of Y2R expression. Control mice showed a higher Y2R expression in right NG compared to left NG ($p = 0.023$, unpaired Student's *t* test). There was no interaction between relative expression and NG side (two-way ANOVA: $p = 0.3629$; $F(1, 50) = 0.8430$). A reduction in Y2R mRNA was observed in left ($p = 0.0097$) and right NG ($p = 0.0002$) (Fig. 3.4.6.1, C).

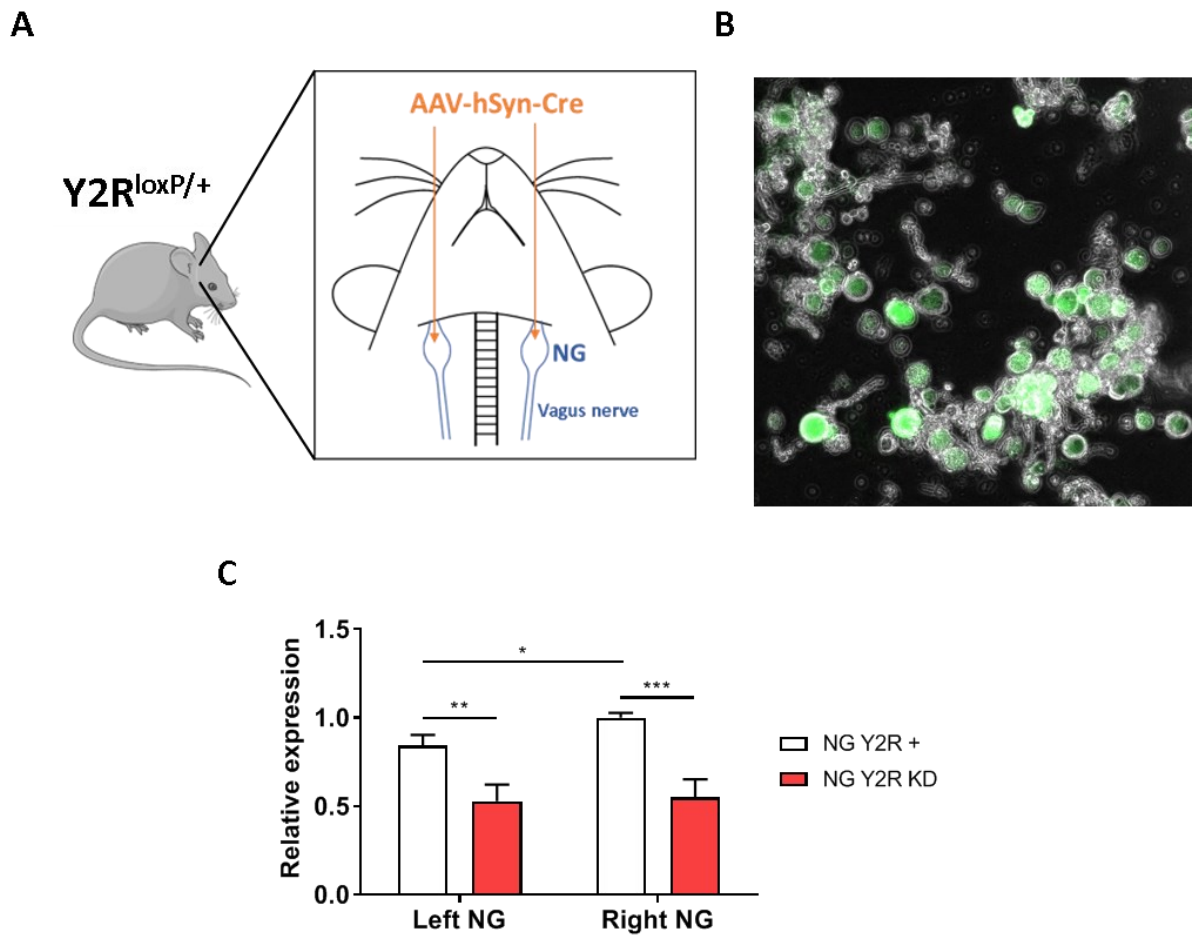

Figure 3.4.6.1. Vagal-specific Y2R knockdown in adult mice

Strategy by delivering neuron-specific adeno-associated virus (AAV) expressing Cre in the nodose ganglia (NG) of $Y2R^{loxP/+}$ (A). Representative image of NG in culture from control mice that received a GFP-expressing control virus in the NG (NG Y2R +) (B). Relative expression of Y2R mRNA in left and right NG to *Ppil3* (normalised Y2R expression in right NG of control group) in $Y2R^{loxP/+}$ mice injected with Cre-expressing AAV into the NG (NG Y2R KD) and of littermates injected with a control AAV (NG Y2R +) that were sacrificed at 17-21 weeks post-surgery (n = 13-14 mice). C: Two-way ANOVA followed by Bonferroni's test (**$p < 0.01$, ***$p < 0.001$). Unpaired two-tailed Student's *t* test (*$p < 0.05$).

Body weight was higher in the NG Y2R KD up to 6 weeks post-surgery but converged with that of controls by week 6 (two-way ANOVA: $p < 0.0001$; $F(12, 300) = 4.688$) (Fig. 3.4.6.2, A). No differences in cumulative food intake over a week were observed at week 7 (Figure 3.4.6.2, B). No differences in body composition were observed (Fig. 3.4.6.2, C-D).

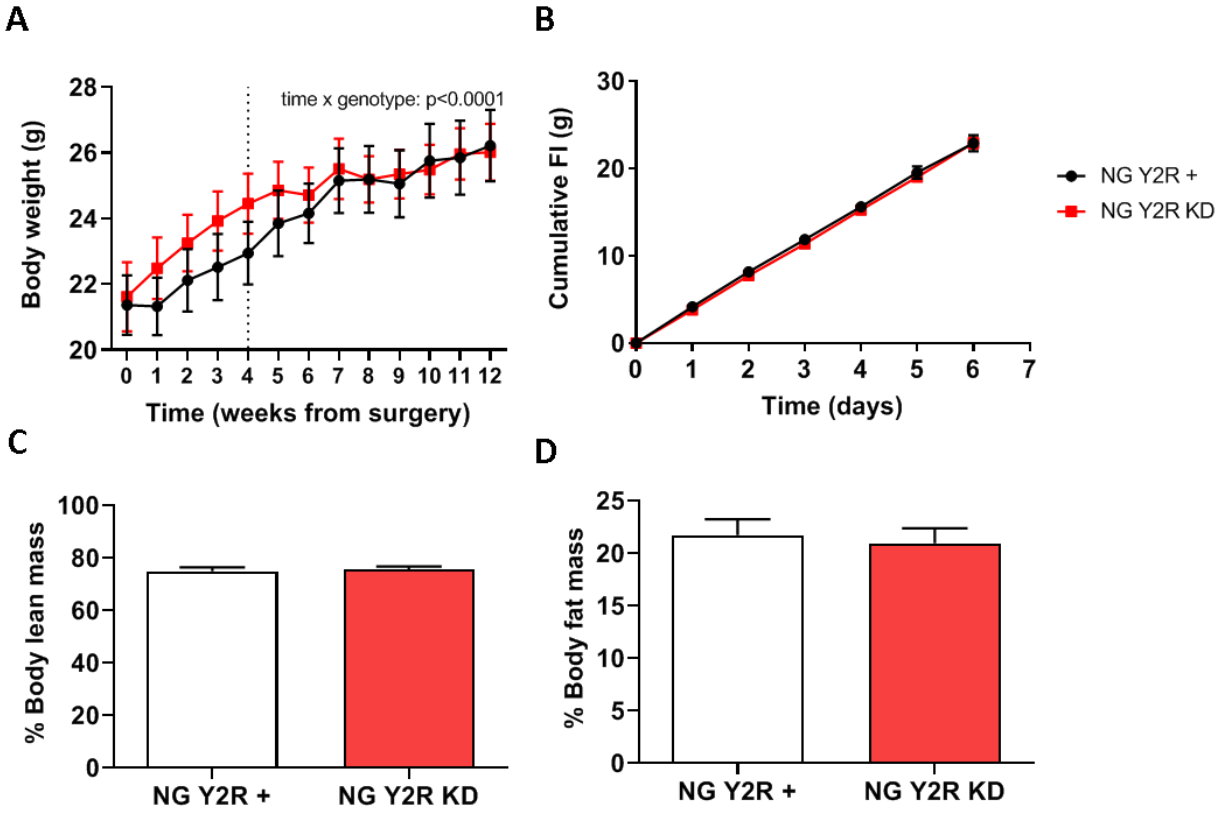

Figure 3.4.6.2. Body weight, food intake and body composition of NG Y2R KD mice.

Body weight post-surgery in NG Y2R KD (n = 15) and control mice (n =12) (A). Four weeks (dashed line) were allowed for virus expression after injection. Food intake in NG Y2R KD and controls over 6 days at week 7 post-surgery (n = 7 per group) (B). Lean mass (C) and fat mass (D) as % of body weight in NG Y2R KD (n = 7) and controls (n = 9) at 16 weeks post-injection. A: Two-way ANOVA.

3.4.7 Acute effects of exogenous PYY_{3-36} in food intake of NG Y2R KD mice

The response to a low and a high dose of PYY_{3-36} was assessed in feeding studies (Fig. 3.4.7.1, A-B). There was a tendency to interaction between treatment and genotype, albeit not significant, at 1 h (two-way ANOVA: $p = 0.098$, $F(2, 42) = 2.450$). In control animals, low-dose PYY_{3-36} showed a tendency to reduce food intake in the first hour post-injection compared to vehicle (p

= 0.059). This effect was abrogated in NG Y2R KD mice. High-dose PYY_{3-36} reduced food intake in both NG Y2R KD and control animals compared to vehicle although this did not reach significancy ($p = 0.058$ and $p = 0.089$, respectively).

After 2 h, there was no interaction between treatment and genotype ($p = 0.181$, $F(2, 42) = 1.781$). No differences in food intake between the first and second hour were observed between NG Y2R+ and NG Y2R KD (data not shown). Therefore, the changes observed at 2 h are caused by the effect of PYY_{3-36} in the first hour.

In order to confirm that vagal afferent signalling remained intact after injection, the response to CCK-8 was investigated. Both groups were respondent to CCK-8 and no differences were observed between them (Fig. 3.4.7.1, C). These data suggests that the anorectic effect of PYY_{336} at high dose is independent of vagal Y2R expression. Therefore, PYY_{3-36} is likely acting in Y2R located in other areas (e.g., hypothalamic ARC or brainstem).

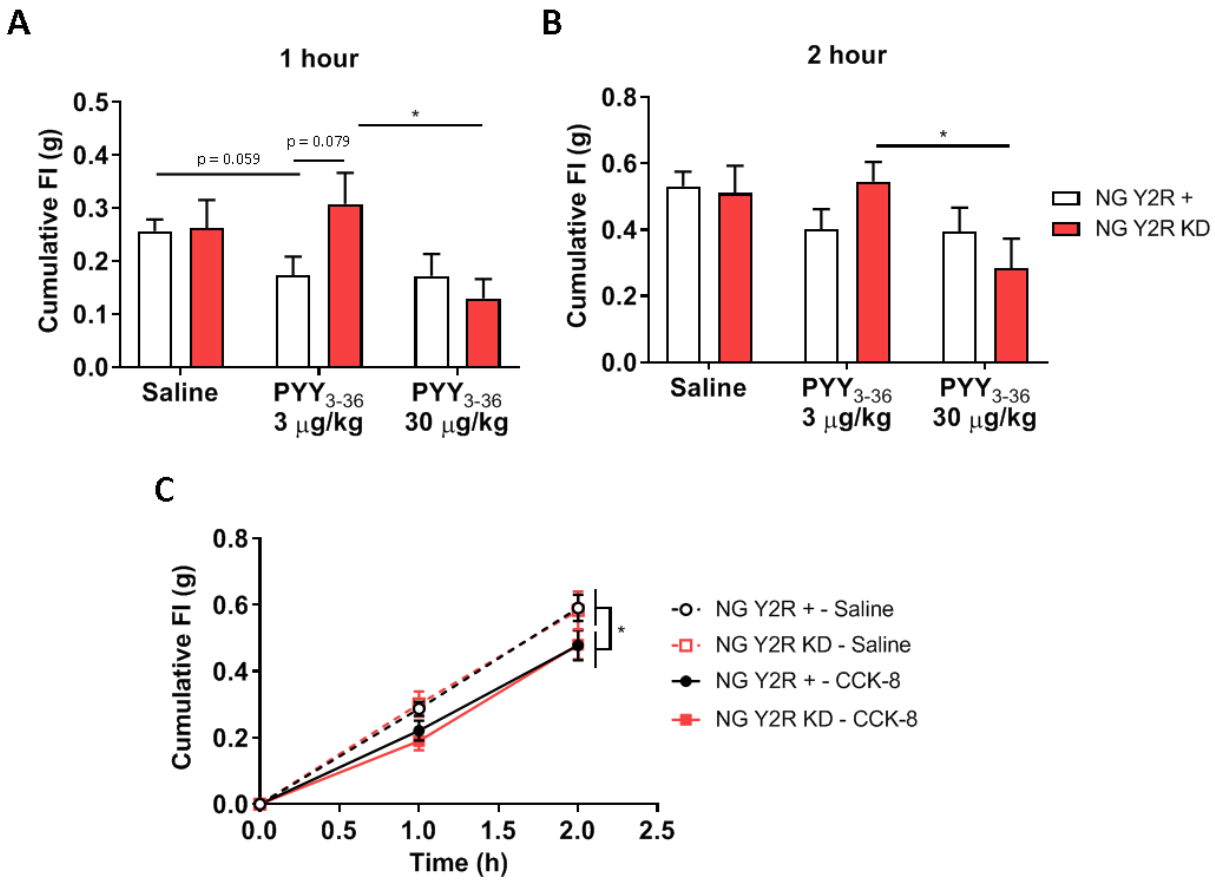

Figure 3.4.7.1. Cumulative food intake after i.p. injection of PYY_{3-36} and CCK-8 in NG Y2R KD mice.

Food intake (FI) at 1 h (A) and 2 h (B) post-i.p. injection of PYY_{3-36} at different doses or vehicle (saline) in the early dark phase in NG Y2R KD (n = 7) or controls (n = 9). Cumulative FI after CCK-8 or vehicle (saline) in the early dark phase in NG Y2R KD or controls (n = 13-14) (C). A, B: Two-way ANOVA followed by Bonferroni's test. C: Three-way ANOVA (time x treatment, *p < 0.05).

3.4.8 Effect of endogenous PYY in food intake of NG Y2R KD mice

In order to study the response to endogenously secreted PYY_{3-36}, a mix of Ensure, L-Arginine, glucose and olive oil was orally administered to 13 littermate control mice and the effect on plasma PYY levels investigated (Fig. 3.4.8.1). Blood was obtained before or after oral gavage of the bolus and PYY levels were detected by RIA. An increase in PYY was observed at 30 min post-oral gavage but this did not reach significance (p = 0.053).

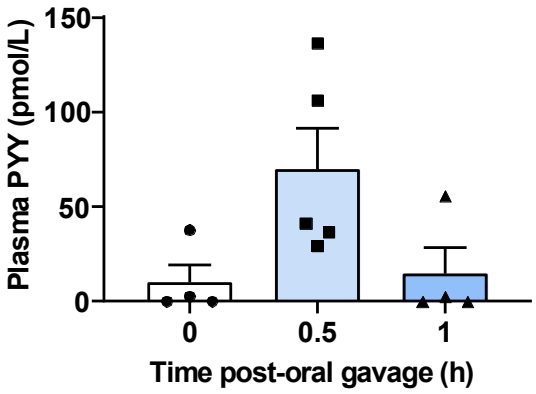

Figure 3.4.8.1. Plasma PYY levels after oral gavage of a nutritious bolus.

PYY levels were measured before oral gavage (n = 4), at 30 min (n = 5) and at 1h (n = 4) post-oral gavage of a nutritious bolus (300 µL).

Since the nutritious bolus caused an increase in plasma PYY, its acute effect in food intake was studied in NG Y2R KD animals (Fig. 3.4.8.2). The bolus caused a reduction in food intake in the first few hours after administration in both groups compared to vehicle (Fig. 3.4.8.2, A). When comparing NG Y2R + with NG Y2R KD, the effect of the bolus in feeding was attenuated in the NG Y2R KD group (Fig. 3.4.8.2, B). There was no time x treatment interaction (two-way ANOVA: $p = 0.206$, $F(2, 69) = 1.615$) (Fig. 3.4.8.2, B).

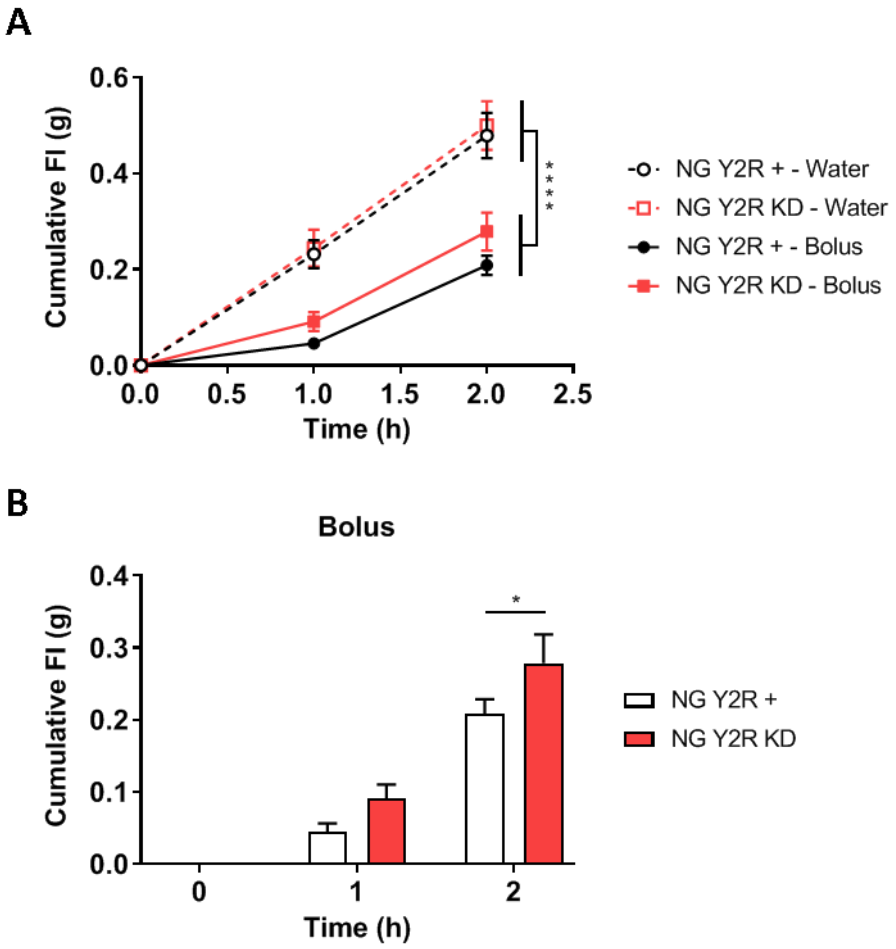

Figure 3.4.8.2. Cumulative food intake after oral gavage of a nutritious bolus in NG Y2R KD mice.

Food intake (FI) after oral gavage of a nutritious bolus (more detailed in B) or vehicle in NG Y2R KD (n = 12) or controls (n = 13) (A). A: Three-way ANOVA (time x treatment, ****p < 0.0001). B: Two-way ANOVA followed by Bonferroni's multiple comparisons test (*p < 0.05).

3.4.9 Effect of vagal Y2R KD in gastric emptying and glucose tolerance

It has been suggested that PYY_{3-36} inhibits gastric emptying (Chelikani, Haver & Reidelberger, 2004) but the mechanism is not well understood. We investigated if altered gastric emptying had a role in vagal Y2R-mediated feeding suppression in another cohort using an acetaminophen (paracetamol) absorption test. In this test, acetaminophen was administered with a glucose bolus and assumed to pass through the stomach at the same time as the nutrients. The acetaminophen would be rapidly absorbed in the small intestine and, therefore, the rate of appearance of this drug in plasma reflects the rate of gastric emptying. Higher circulating acetaminophen levels were observed after 15 min in NG Y2R KD group compared to controls (p = 0.031) (Fig. 3.4.9.1, A). There was a time x treatment interaction in the gastric emptying assay

(two-way ANOVA: p = 0.042, F (3, 24) = 3.179). In this same cohort, glucose tolerance was investigated in an OGTT (Fig. 3.4.9.1, B,C). No significant difference in AUC of glucose (p = 0.1275) was observed between NG Y2R KD group and control (Fig. 3.4.9.1, C).

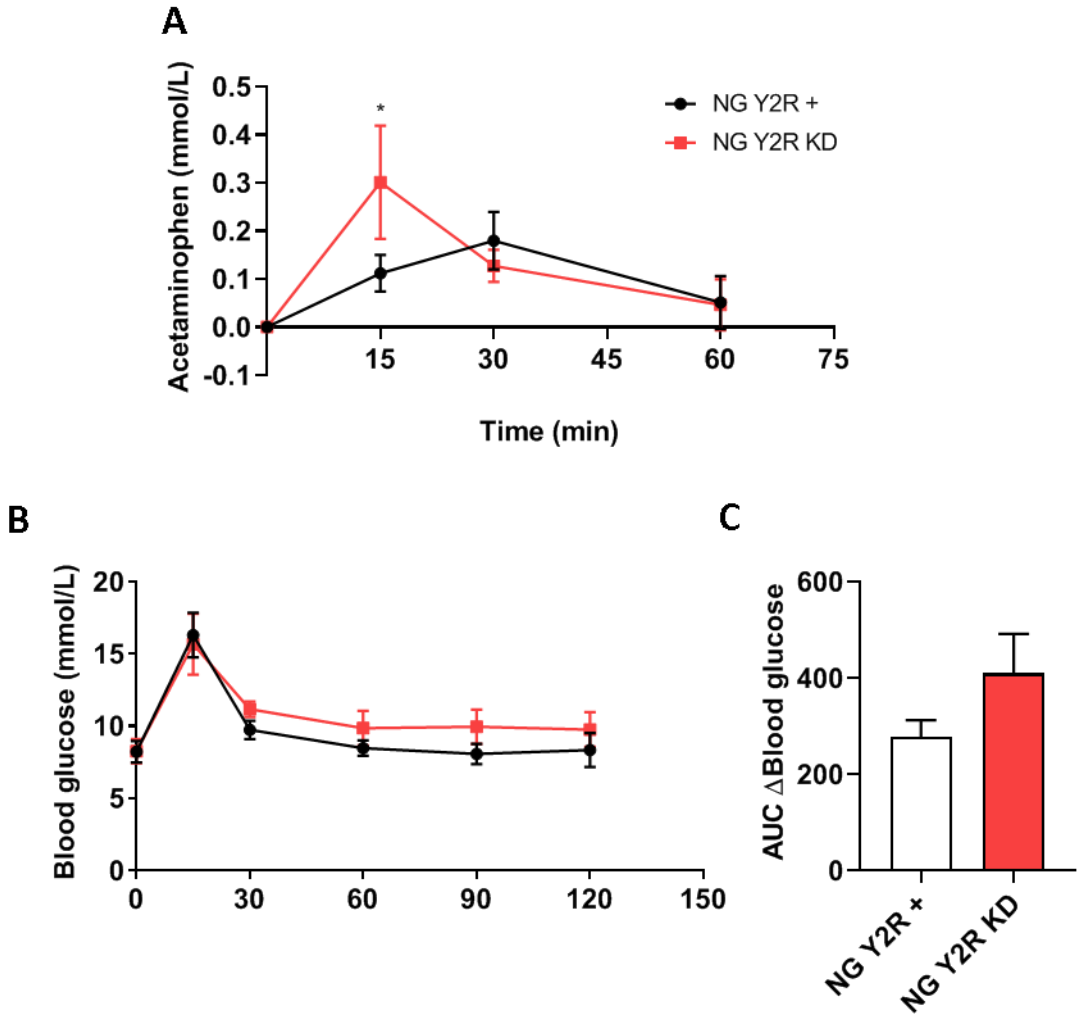

Figure 3.4.9.1. Gastric emptying and glucose tolerance in NG Y2R KD.

Plasma acetaminophen levels after oral gavage of a 20% glucose bolus containing 1% acetaminophen in 9 h-fasted NG Y2R KD (n = 3) and control animals (n = 7). Blood glucose (mmol/L) during an OGTT (B) and its AUC (C) in 4-h fasted NG Y2R KD (n = 5) and control animals (n = 7). A: Two-way ANOVA followed by Bonferroni's multiple comparisons test.

3.4.10 Effect of endogenous PYY in brainstem neuron activation of NG Y2R KD mice

We investigated the role of vagal Y2R in activating brainstem neurones upon endogenous PYY release in response to the nutritious bolus. No significant differences in c-fos-positive cells were observed between NG Y2R KD and controls (AP & NTS: p = 0.429; NTS: p = 0.429, Mann-Whitney test). (Fig. 3.4.10.1). Surprisingly, there was a tendency towards increase c-fos-positive cells in AP-NTS. This could be due to the small sample size in this experiment and the variability in the NG Y2R KD group.

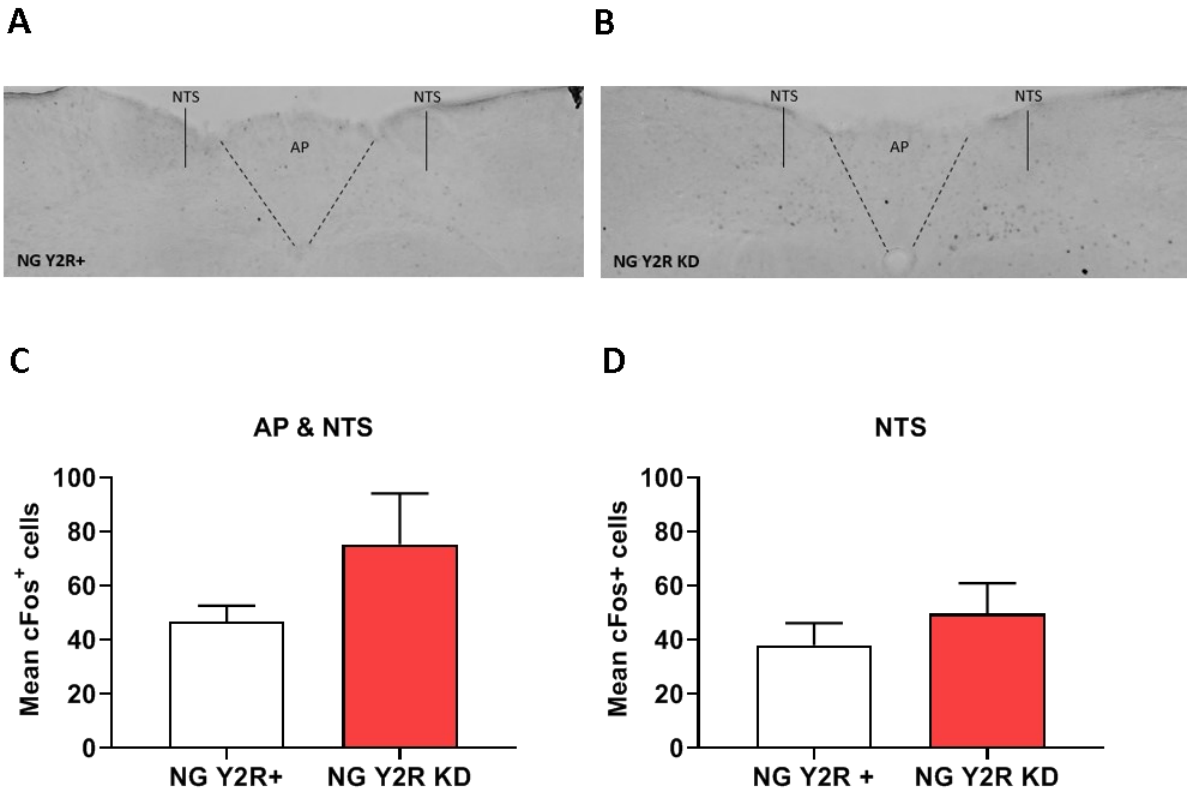

Figure 3.4.10.1. c-fos expression in brainstem of NG Y2R KD mice after oral gavage of a nutritious bolus.

Representative images of brainstem in NG Y2R+ (A) and NG Y2R KD (B) receiving a nutritious bolus approx. 90 min before. Location of area postrema (AP) and nucleus tractus solitarius (NTS) are indicated. Mean of c-fos-positive neurones in AP plus NTS (C) and in NTS (D) of NG Y2R KD (n = 6) or NG Y2R + (n = 5). In C, the mean of the number of c-fos-positive cells in 2 brain slices where the AP and NTS are located (-7.48 to -7.32 Bregma (mm)) is shown. In D, the mean of the number of c-fos-positive cells in 3 to 6 slices between -6.24 to -7.48 Bregma (mm) in mouse brain atlas is shown. Mice were sacrificed at 21 weeks post-surgery.

3.4.11 Meal patterning in NG Y2R KD

We investigated if vagal Y2R modulated meal patterning using metabolic cages for 7 days (following a three-day acclimatization period) 10-12 weeks post-injection. This system records food and water intake, physical activity as well as perform indirect calorimetry. No differences in EE, oxygen consumption and substrate utilization (data not shown) were observed in NG Y2R KD compared to NG Y2R + controls (Fig. 3.4.11.1, A, B). There was no significant difference in body weight between NG Y2R KD and NG Y2R + mice during this experiment.

Regarding ambulatory activity, there was a significant interaction in time x genotype (two-way ANOVA: $p = 0.001$, $F(23, 230) = 2.239$). Animals were more active in the dark phase as expected. A trend towards increased ambulatory activity was observed in the light phase and dark phase in NG Y2R KD ($p = 0.086$ and $p = 0.096$, respectively) (Fig. 3.4.11.1, C). These suggest that NG Y2R KD are more active than controls.

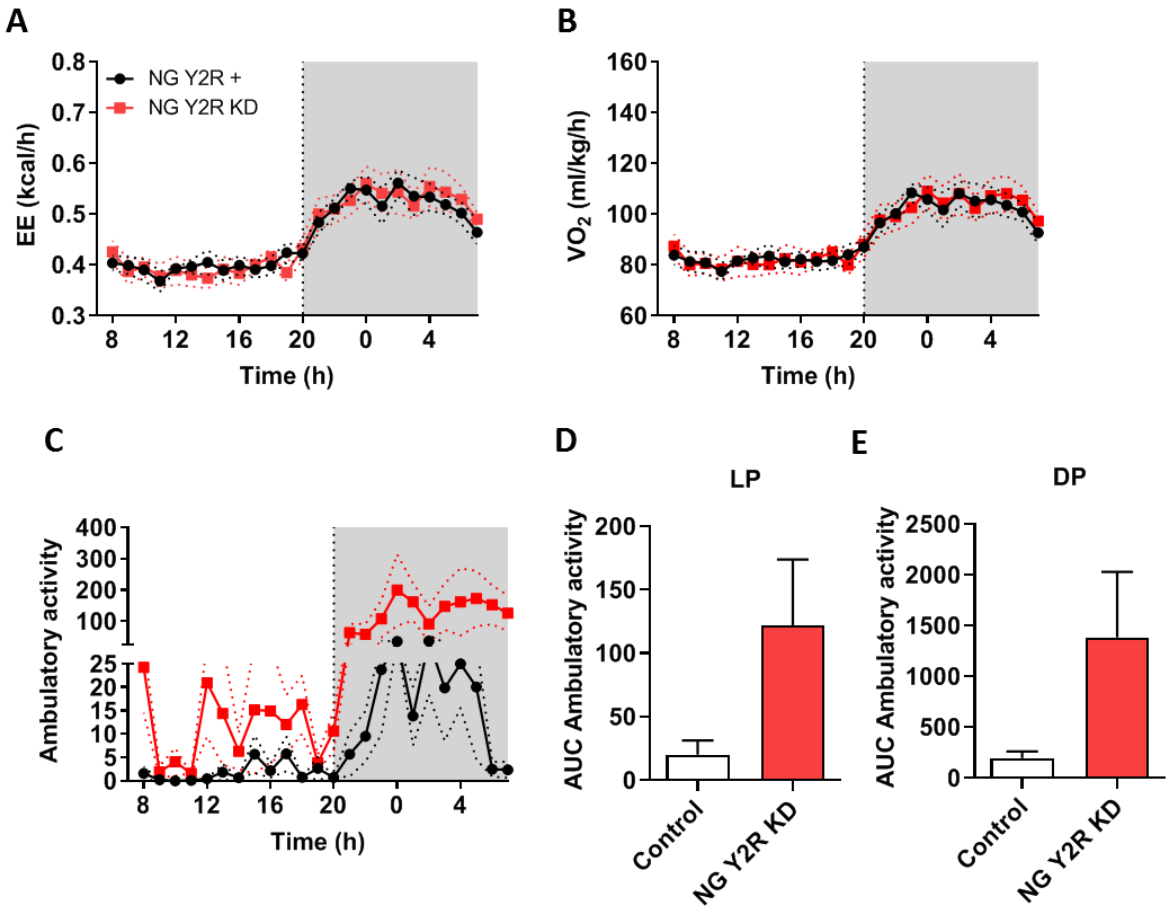

Figure 3.4.11.1. Metabolic assessment of NG Y2R KD.

Energy expenditure (A), oxygen (O_2) consumption (VO_2) (B) (n = 5-6 per group), and ambulatory activity (C) with its AUC (D,E) in the light phase (LP) and dark phase (DP) (n = 6 per group). Mean of 3 days (days 3, 6 and 9). DP is shown by the grey shading.

Although there were no differences in cumulative food intake, probability density functions for meal patterning readouts showed an increased probability of smaller and shorter meals in NG Y2R KD mice compared to NG Y2R + (Fig. 3.4.11.2). A non-significant tendency ($p = 0.09$) for more meals was observed in the NG Y2R KD mice over the duration of the CLAMS (data not shown).

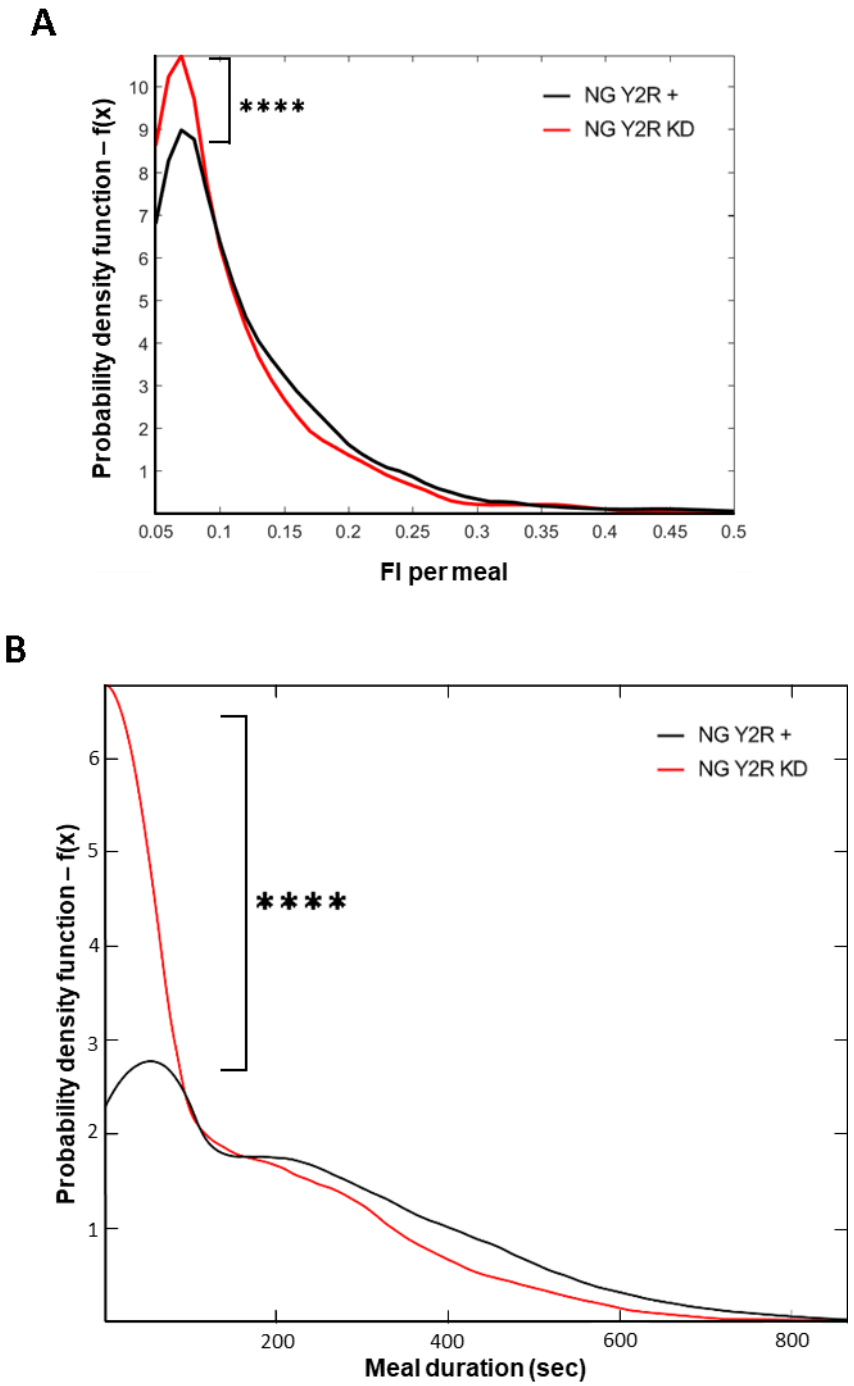

Figure 3.4.11.2. Meal patterning of NG Y2R KD mice.

Probability density function of food intake per meal (A) and of meal duration (i.e., time (s) taken for feeding bout) over 7 days in CLAMS system ((n = 6/group). A, B: Kolmogorov-Smirnov test (****p < 0.0001).

3.5 Discussion

PYY_{3-36} inhibits food intake via its specific receptor, Y2R, but the site of action is not well understood. The requirement of vagal signalling for the anorectic effect of peripheral PYY_{3-36} is still controversial. The experiments in this chapter aimed to study the role of the vagus in mediating the anorectic effects of PYY_{3-36} by disrupting only vagal afferent Y2R signalling and studying the resultant phenotype. In order to do that, two new models for targeting vagal Y2R target were used: a germline model of semi-specific vagal Y2R KO in Nav1.8-expressing neurones and a vagal afferent specific Y2R KD in the adult mouse.

We hypothesised that peripheral PYY_{3-36} at physiological-like levels reduces food intake by activating Y2R in vagal afferents but that pharmacological levels of PYY_{3-36} directly activate central appetite pathways. The results suggest that disruption of Y2R in the vagus abrogates the response to exogenous low-dose PYY_{3-36}, but does not alter the response to high-dose PYY_{3-36}. In the vagal Y2R KD model, an adult body weight phenotype was observed compared with controls but this was not observed in mice with loss of Y2R in Nav1.8-expressing vagal afferents. In accordance to the initial hypothesis, loss of vagal Y2R in the adult mouse also attenuated the anorectic effect to endogenously-released PYY, and altered meal patterning and gastric emptying.

3.5.1 Vagal Y2R disruption

Vagal afferent neurones innervate the gastrointestinal tract and express gut hormone receptors. However, the pathways by which these hormones signal appetite to the brain appetite centres and higher brain centres remain unknown. Two mechanisms could explain how vagal afferents transmit information of gut peptides to the brain. A neuro-paracrine model proposes that afferent endings close to basal EECs can rapidly respond to hormonal signals. In contrast with this, single cell profiling has suggested that vagal afferent mechanoreceptors might be more important that mucosal endings (Bai *et al.*, 2019). More recently, it has been revealed that some EECs can contact vagal afferent neurones via synapse-like structures (Bohórquez *et al.*, 2015; Kaelberer *et al.*, 2018).

There are discrepancies regarding the role of vagal Y2R in mediating the effect of the gut hormone PYY_{3-36} (Koda *et al.*, 2005; Abbott *et al.*, 2005a; Halatchev & Cone, 2005; Talsania *et al.*, 2005). These discrepancies could be due to differences between species. Y2R expression levels in the vagus are regulated by nutritional status as observed in 48 h-fasted rats (Burdyga *et al.*, 2008) but this was not observed in 24 h-fasted mice. Whether these different results are due to

the fasting time or to different neurochemical plasticity between species is unknown and requires further investigation.

Discrepancies in experiments investigating the role of the vagus could be due to the PYY_{3-36} dose used and the technical limitations since these studies exclusively employed vagal lesioning methods that have off-target effects. Subdiaphragmatic vagotomy lesions both afferents and efferent fibers innervating the intestine, stomach, pancreas and liver. Subdiaphragmatic vagal deafferentation (Norgren & Smith, 1994) was considered the gold standard since it has fewer side effects in the physiological food intake regulation but it still lesions half of the efferent vagus nerve, which could alter PYY secretion (Zhang *et al.*, 1993) and hedonic behaviour (Klarer *et al.*, 2019). Capsaicin ablates sensory neurones and is not specific for vagal afferents even if administered perivagally (Browning *et al.*, 2013). More recently a novel method for selectively ablating gastrointestinal vagal afferents by using saporin (a toxin that induces cell death) conjugated with CCK-8 was developed (Diepenbroek *et al.*, 2017). However, this still disrupts several afferent signaling pathways. In this work, we have used genetic non-lesioning approaches to specifically disrupt Y2R signalling in the vagus.

A germline model was generated by crossing Y2R-floxed mice with mice expressing Cre recombinase under the Nav1.8 promoter. Nav1.8 is involved in nociception and is mainly found in trigeminal ganglia (TG, a motor-sensory cranial nerve), dorsal root ganglia (DRG), the afferent neurones of which innervate the gut and synapse at the spinal cord to transmit information related with nociception and mechanoreception, and vagal sensory neurones (Stirling *et al.*, 2005). In this model, Y2R mRNA was significantly reduced, albeit there was not a complete KO. Y2R was expressed in 71% of vagal Nav1.8 neurones as assessed by in *situ* hybridization (Egerod *et al.*, 2018). Therefore, this partial reduction in Y2R expression may be due to incomplete co-expression of Nav1.8 and Y2R in vagal afferents and/or to not fully efficient Cre recombination. In this case we did not observe a difference between left and right Y2R mRNA level. This could be due to differences in transgenic mice or the sample size. Further research would be required to determine the functional relevance of left versus right vagal Y2R.

Nav1.8-Cre mice have been characterised in previous reports (Stirling *et al.*, 2005; Gautron *et al.*, 2011; Shields *et al.*, 2012) and have been successfully used to disrupt the expression of LepRb in vagal afferents (de Lartigue, Ronveaux & Raybould, 2014). Cre activity was not observed in peripheral tissues or the CNS in Nav1.8-Cre mice (Stirling *et al.*, 2005) and Cre was not expressed in the ARC or NTS of Nav1.8/LepR KO mice (de Lartigue, Ronveaux & Raybould, 2014). Some neurones in the superior cervical ganglion showed Cre expression in Nav1.8-Cre-tdTomato mice

and Y2R was detected in this region in rats (Zhang *et al.*, 1997). Y2R protein was also detected in the DRG and, less abundantly, in the TG of mice and rats (Zhang *et al.*, 1997; Brumovsky *et al.*, 2005). In this study, Y2R expression was not evaluated in these regions in the NaV1.8/Y2R KO model, so the influence of these potential Y2R deletions on the resultant phenotype is unknown. Other reports have used Phox2b-Cre to disrupt nutrient-sensing receptors but recombination also occurs in vagal efferents and other appetite centres (e.g., NTS) (Liu *et al.*, 2014a; Sisley *et al.*, 2014). Therefore, the limitations of these vagal germline models include the potential Cre activity in other regions and the only partial specificity for the vagal afferents.

In addition, germline KO models can develop compensatory mechanisms that would disturb the resultant phenotype, as has been suggested in previous reports of KO models of the NPY system (Sainsbury *et al.*, 2002, 2006; Shi *et al.*, 2012; Boland *et al.*, 2019). Anatomical proximity between Nav1.8-positive neurones and EECs might be different depending on the type of EEC. GLP-1-expressing cells of the duodenum were not observed close to mucosal afferents, in contrast to other EECs (Gautron *et al.*, 2011). Therefore, this model might not be suitable to study the role of vagal Y2R in response to gut-derived PYY.

We have overcome this using a vagus-specific knockdown model in the adult mouse generated by bilaterally administering a Cre-expressing AAV into the NG of Y2R-floxed mice. AAV is widely used for *in vivo* genetic modification, due to its stable long-term expression and the limited immune response to the virus. This approach is similar to a previous approach in which a lentivirus delivering short-hairpin RNA (shRNA) construct was delivered in the NG of rats (Krieger *et al.*, 2016). However, lentiviruses integrate into the genome and might alter the expression of other genes. In addition, this genetic alteration acted at the RNA level, whereas our approach acted at the DNA level.

In the vagal Y2R KD model, we observed a significant reduction in Y2R mRNA but it did not achieve a full knockdown. It remains unknown if this was because of the efficiency of the injection or because of the infection ability of the virus. Whereas the germline model of vagal Y2R disruption did not show a difference in body weight, a transiently higher body weight was observed in the vagal Y2R KD model after virus delivery. Food intake or feeding behaviours was not measured during this period since animals were recovering from surgery and housed in groups so it remains unknown if this was due to associated hyperphagia. This project prioritised the investigation of the vagal Y2R knockdown model, since we believed is superior to germline models, and meal patterning and daily food intake was not measured in the Nav1.8/Y2R KO model.

In a peripheral Y2R KD model, no differences in body weight, food intake or body composition compared to control were reported, similar to our observations (Shi *et al.*, 2012). However, in adenovirus-Cre mediated hypothalamic Y2R KD and germline Y2R KO, a reduced body weight was reported (Sainsbury *et al.*, 2002). However, as mentioned before, germline models can develop compensatory changes.

3.5.2 Vagal Y2R might be required to mediate the anorectic effect of endogenous PYY

We hypothesised that physiological levels of PYY would exert an anorectic effect via the vagus nerve, and would not directly interact with central appetite centres. On the other hand, PYY_{3-36} at pharmacological doses might directly interact with the hypothalamus or the brainstem. The low dose used (3 µg/kg) had previously been shown to suppress food intake (Batterham *et al.*, 2002; Halatchev *et al.*, 2004; Halatchev & Cone, 2005). This low dose was compared to a high dose (30 µg/kg) more likely to access centrally expressed Y2R (Halatchev *et al.*, 2004; Halatchev & Cone, 2005). The anorectic effect of acute peripheral administration of PYY_{3-36} at low dose was attenuated in the germline Y2R KO model and in the NG Y2R KD group compared to control animals. Despite differences between the Y2R KD model and control at low-dose PYY_{3-36}, the reduction in food intake did not reach significance in the control group. High dose PYY_{3-36} caused a reduction in food intake in most animals, independently of the level of vagal Y2R, but this did not reach significance in the NG Y2R KD cohort or its control group. These animals responded to CCK and, therefore, it is unlikely that this was due to a lesioned vagus nerve. However, it is possible that ambient stress as well as the fact that mice are non-fasted underlie this result.

In our approach, food intake is measured in *ad libitum*-fed in the early dark phase, when mice consume most of the daily food. An alternative approach would involve fasting the mice before the study. After fasting, mice could show high energy intake and this could mask PYY_{3-36} anorectic signalling. It has been shown that the reduced food intake (measured in the early dark phase) after exogenous PYY_{3-36} administration is exaggerated after 24 hour-fasting compared to non-fasted mice, and this could be due to other mechanisms that partially overule PYY_{3-36} anorectic effect (Challis *et al.*, 2003). Therefore, a more clear anorectic effect could be observed in fasted mice. However, 24 hour-fasting might cause drastic changes in energy homeostasis due to the nocturnal eating pattern of mice and therefore the experimental setting is not physiological. In addition, fasting has been shown to alter the neurochemical phenotype of vagal afferent and therefore the ability of the vagus to respond to other feeding-related signals, including the

expression of vagal Y2R (Burdyga *et al.*, 2008) although we did not observe a change in vagal Y2R mRNA in 24 h-fasted mice in our experimental setting. Future studies could explore the effect of exogenous PYY_{3-36} in different fasting conditions in this strain. Low dose PYY_{3-36} non-significantly increased neuron activation in the NTS in the germline Y2R KO model and controls, but there appeared to be an attenuation of neuronal activation in the caudal NTS and AP in the germline Y2R KO model. However, we cannot draw firm conclusions due to the small sample size. In general, c-fos induction experiments might not have enough resolution with the sample sizes used in this work and, therefore, they are underpowered.

Further studies are required to increase the statistical power and to determine if this is a true effect of the vagal Y2R knockdown. The oral gavage of the nutritious bolus also stimulates mechanoreceptors and the release of other gut hormones. Non-nutritive solutions with similar viscosity to the nutritious bolus should be used as controls. Correlation of these results with the level of other gut hormones in plasma and the portal vein post-oral administration of the nutritious bolus could also clarify as well as correlation with the level of expression of other vagal gut hormone receptors. If this is a true effect of vagal Y2R knockdown, it would be interesting to understand if this is a compensatory or indirect mechanism and to further identify the c-fos-positive cells (e.g., GLP-1 expressing cells of the brainstem).

In order to study the role of the vagal Y2R in response to physiological PYY_{3-36}, a mixed nutritious bolus was administered by oral gavage in NG Y2R KD. We confirmed that this bolus increased plasma PYY after oral gavage. Despite the high variability, we observed a clear an increase in plasma PYY 30 minutes after oral gavage of the mix. We expected an increase at this time point based on previous observations. The experiment was underpowered due to the small group size. In this setting, both gut mechanosensors and chemosensors are stimulated and other gut hormones may also be secreted, which could impact the results. It would have been beneficial to measure the plasma level of other gut hormones (e.g., GLP-1, ghrelin, CCK) but due to the limited sample volume and time available this was not possible. Despite this stimulation of gut sensors, differences were observed when reducing the expression of the vagal Y2R, which suggests an involvement of the vagus nerve in mediating PYY's anorectic effects. Although we have measured PYY after the nutritious bolus in plasma, it would be useful to measure levels in the hepatic portal vein (in close contact with the vagus). PYY infusion into the rat hepatic portal vein increases c-fos expression in the NTS and in the hypothalamus (Stadlbauer *et al.*, 2013). The neuronal activation in brainstem after administration of the nutritious bolus was no different

between Y2R KD mice and controls but it is difficult to draw conclusions due to the sample size and the lack of a vehicle control or a control of distension.

If one assumes that low dose exogenous PYY_{3-36} mirrors the effects of postprandial PYY, these results suggest that vagal Y2R contributes to the effects of endogenous PYY. In contrast, pharmacological doses of PYY_{3-36} might act centrally (Batterham *et al.*, 2002) and perhaps in part by causing aversion (Halatchev & Cone, 2005). However, in humans, PYY_{3-36} caused nausea without further reduction in food intake (Le Roux *et al.*, 2008).

3.5.3 Vagal Y2R modulates meal patterning

Indirect calorimetry did not reveal differences in EE, but an increased ambulatory activity was observed. In a peripheral Y2R KD model, increased ambulatory activity was also observed, along with reduced EE and altered RER (Shi *et al.*, 2012). However, we did not observe changed in RER or EE. The increased ambulatory activity was not accompanied by differences in body weight. Y2R KO does not alter EE or activity in two different models (Zhang *et al.*, 2010; Boland *et al.*, 2019).

We also investigated whether vagal Y2R modulates meal patterning. Despite no differences in total food intake, probability density functions for meal patterning readouts revealed highly significant differences in average meal size and duration. Meals were smaller and shorter in NG Y2R KD model, with shorter inter-meal durations. These data suggest a physiological role for vagal Y2R on meal patterning, even in the absence of an overall long-term effect on energy balance.

Shorter and smaller meals indicate that NG Y2R KD animals felt satiated faster. Smaller meals might reduce the amount of gut anorectic hormones that are subsequently released to regulate short-term food intake (e.g., CCK, GLP-1). The signalling of these gut hormones in the vagus nerve and in the brain should remain intact in these animals. It is also possible that the orexigenic hormone ghrelin is released earlier after a meal termination. Consequently, animals feel hungry faster leading to the reduced inter-meal duration and number of meals. In addition, the accelerated gastric emptying observed in vagal Y2R KD compared to controls after 15 min might underlie the increase in number of meals. Therefore, animals could feel hungry faster and eat again. Future studies should measure the levels of circulating ghrelin and CCK, the expression of other neuropeptides involved in satiety (e.g., CART) and the expression of gut hormone receptors in the afferent vagus nerve and in the brainstem. It is possible that compensatory changes in some of these gut-vagus-brain signalling caused this increased in satiety despite the

loss of the anorectic PYY. Although cumulative food intake and energy expenditure did not increase, animals are eating more frequently and moving more. It would be interesting to determine if the increase ambulatory activity correlates with the mouse accessing the food and if it underlies the hunger feeling. In addition, further analysis comparing meal patterning during light phase and dark phase would help clarifying the effect of vagal Y2R signalling (as has been shown for vagal LepR (de Lartigue, Ronveaux & Raybould, 2014)).

Similarly, vagal GLP-1R KD in rats using a viral approach altered gastric emptying, though it was sustained for a longer period (Krieger *et al.*, 2016). Global deficiency of Y2R, GLP-1R or both did not alter gastric emptying in mice (Boland *et al.*, 2019), which could be due to a compensatory mechanism. Vagal GLP-1R KD rats also showed no differences in energy expenditure and an altered meal patterning despite the fact that 24-h food intake was not affected (Krieger *et al.*, 2016). However, in contrast to what we observed in the vagal Y2R KD model, vagal GLP-1R disruption increased meal size and duration, and decreased in the number of meals (Krieger *et al.*, 2016). Since GLP-1R-expressing afferents are involved in mechanosensing these results might reflect a change in the sensitivity of vagal mechanoreceptors (Williams *et al.*, 2016; Bai *et al.*, 2019). Future studies should investigate the role in chemosensing and/or mechanosensng of the vagal Y2R-expressing afferents.

The contribution of gut hormones in the regulation of short-term food intake and longer-term energy homeostasis is well established. However, the pathways involved in gut hormone signalling, and the physiological effects of individual hormones are unclear. In particular, the complex role of the vagus nerve in the gut-brain axis is just beginning to be understood. Despite the residual Y2R signaling post-injection, we conclude that postprandial endogenous or low dose peripheral PYY_{3-36} requires intact vagal signalling in a novel model of vagal Y2R disruption. This is of interest in drug design since it is possible that by targeting the vagal Y2R we could overcome some limitations of PYY-based treatments, such as the administration route or dosage given in order to avoid the nauseating effect. This work adds to the body of literature suggesting that individual gut hormones can act, at least in part, through the vagus nerve to modulate feeding behaviours (de Lartigue, Ronveaux & Raybould, 2014; Krieger *et al.*, 2016; Davis *et al.*, 2020).

3.5.4 Limitations of this study and future work

Full Y2R disruption could not be achieved in any of the models and, therefore, vagal Y2R signalling was not completely absent. However, the incomplete knockdown achieved in both

models suggests that a more severe disruption of vagal Y2R might result in a more striking phenotype. If the expression or function of other feeding-related pathways was altered remains unknown. It would be of interest to assess postprandial levels of PYY, as well as the PYY_{3-36} form, in both models. In addition, PYY levels should be measured after low dose i.p. injection to confirm the validity of low dose PYY_{3-36} as a mimic of endogenous levels.

Despite trying to optimize immunostaining of Y2R in control NG and brain tissue, the result was negative with the antibody and conditions tested. Therefore, distribution of Y2R protein expression in the Nav1.8/Y2R KO and after viral-mediated knockdown could not be determined using this approach. Future studies should determine if Y2R was fully disrupted in specific neurones but not in others, or if a partial reduction in Y2R expression occurred in all the vagal afferents by using *in situ* hybridization and/or single nuclei RNA sequencing.

AAVs are widely used to modify gene expression *in vivo* as well as in anterograde tracing. AAV vectors are replication deficient, and so it is widely thought that they cannot spread to a subsequent cell, unlike rabies virus. However, a recent study showed that AAV9 can anterogradely spread to post-synaptic neurones in the brain, though AAV5 cannot (Zingg *et al.*, 2017). The mechanism of this trans-neuronal transport mechanism is unclear, and it is also unknown whether the virus causes transgene expression in the subsequent cell. The expression of the virus in the brain after delivery in the NG was not investigated.

In the germline Y2R KO model, c-fos expression after exogenous PYY_{3-36} was evaluated in animals with a wide age range. Therefore, the effect of age on the neuronal activity response is unknown. The next step is to assess c-fos expression after exogenous low-dose PYY_{3-36} in the vagal Y2R KD model. In addition, to confirm the functionality of this vagal Y2R KD, the activity of the vagus nerve should be assessed in response to low dose and high dose PYY_{3-36}. This could be done by examining c-fos expression in NG cells, taking electrophysiological recordings from vagal afferents, *in vivo* imaging of the NG calcium activity in response to PYY_{3-36}, or by assessing calcium activity in cultured NG neurones extracted from vagal Y2R KD mice.

In mice, CCK inhibits food intake via the right NG, but not the left NG, recruiting a reward circuit based on dopamine release in the dorsal striatum (Han *et al.*, 2018). In addition to the asymmetry in gastrointestinal innervation, left and right NG terminate in different regions of the brainstem (Han *et al.*, 2018), but the role of the left NG and its central circuitry are unknown. Future studies should investigate the role of left and right vagal Y2R as well as the central circuits involved. Although some vagal populations have been reported to be involved in

mechanosensing or chemosensing (Bai *et al.*, 2019), the role of the Y2R-expressing population remains unknown.

Chapter 4: Effect of the Long-Acting PYY analogue Y242 on obesity and glucose homeostasis

4.1 Introduction

4.1.1 Type 2 diabetes and obesity

Type 2 diabetes (T2D) is a chronic disease characterised by the inability of endogenous insulin to signal effectively within the body, resulting in an increase in blood glucose levels. T2D symptoms include thirst, tiredness, polyuria and blurred vision. T2D is the most common type of diabetes (National Institute of Diabetes and Digestive and Kidney Diseases, 2017; Diabetes UK, 2019), although the specific causes are still not fully elucidated. The main risk factors are obesity, age, ethnicity and having a relative with diabetes.

The link between obesity and T2D is well accepted. However, most obese individuals do not develop T2D. Insulin resistance is associated with obesity and is the driving factor for pre-diabetes and T2D. Insulin resistance is when muscles, fat and liver do not respond to insulin and therefore they take up less glucose from the bloodstream (National Institute of Diabetes and Digestive and Kidney Diseases, 2018). In response to insulin resistance, blood glucose levels are more likely to increase and the pancreatic β-cells keep producing more insulin so that the increased blood glucose enter the body's cells. The increased levels of insulin cause the liver and muscles to store blood sugar and eventually blood sugar is stored in adipocytes as fat. Abdominal fat is correlated with insulin resistance. Overtime, β-cell function is disrupted and the pancreas cannot cope with the insulin demand resulting in increased blood glucose levels. Pre-diabetes (when blood glucose levels are increased but not as high as in diabetes) affects 1 in 3 adults in the US (National Institute of Diabetes and Digestive and Kidney Diseases, 2018). Overtime, insulin resistance and prediabetes can develop into T2D.

The mechanism linking obesity, insulin resistance and T2D is not fully understood but several mechanisms have been proposed (Kahn, Hull & Utzschneider, 2006). Adipose tissue releases non-esterified fatty acids (NEFAs), hormones (e.g., leptin) and proinflammatory cytokines/adipokines, and its secretion is increased in obesity. Added to β-cell dysfunction, these can disrupt the insulin signalling leading to insulin resistance. Fat is an important energy source for skeletal muscle. A first study in humans linked insulin resistance with accumulation of intramuscular triglycerides and it is now accepted that accumulation of lipids within skeletal muscle is related to insulin resistance and T2D (Pan *et al.*, 1997; Corcoran, Lamon-Fava & Fielding, 2007). This is thought to be caused by an increased fatty acid accumulation within muscle in the obese state and diminished fatty acid oxidation due to mitochondrial abnormalities (Goodpaster *et al.*, 2000; Kelley *et al.*, 2002). A proposed mechanism suggests that fatty acids can alter insulin receptor 1 signalling in muscle and impaired activation of downstream signal transducers involved in glycogen synthesis and glucose transport (Corcoran,

Lamon-Fava & Fielding, 2007). More recent views suggest that specific lipids species, such as the fatty acid metabolite diacylglycerol, as well as the localization of lipids in the cell influence can influence insulin sensitivity (Bergman & Goodpaster, 2020).

Obesity is a major global health problem, and if the current trend continues, obesity-related diabetes will keep increasing. In the UK, it was predicted that 5 million people will be diagnosed with T2D by 2025 (Diabetes UK, 2019). T2D can cause other conditions, such as heart disease, blindness and kidney disease. In addition, T2D typically gets worse over time, and treatment needs to be adjusted or changed. Bariatric surgery is still the most effective procedure that achieves remission of T2D and metabolic syndrome. Safer and more effective treatments for obesity and T2D would reduce their economic and health burden. Treatments that enhance gut hormones action have shown promising results.

4.1.2 Glucose homeostasis and T2D

4.1.2.1 Pancreatic islets of Langerhans

The human pancreas is an organ located behind the stomach and it can be divided in head, body and tail, although some other parts have been suggested. In the mouse, the pancreas is less defined and can be macroscopically divided into the duodenal, splenic and gastric lobes (Dolenšek, Rupnik & Stožer, 2015). Although differences exist in the microscopic anatomy between humans and mouse, most of the pancreas consists of exocrine cells that secrete digestive enzymes. In contrast, the endocrine pancreas secretes hormones from endocrine cells into the blood stream. The endocrine cells are clustered together forming the islets of Langerhans, which are island-like structures within the exocrine tissue that account for 1-2% of the mass of the pancreas (Röder *et al.*, 2016). Within the islets of Langerhans, α-cells release glucagon, β-cells release insulin, amylin and C-peptide; γ-cells release PP, δ-cells release somatostatin, and ε-cells release ghrelin. α- and β-cells comprise most of the islet in both humans and rodents but the architecture differs. In human islets, α- and β-cells are interspersed, while in mice the β-cells are mostly located in the centre, with the other cell types distributed around the islet periphery (Brissova *et al.*, 2005; Dolenšek, Rupnik & Stožer, 2015). These pancreatic hormones have different functions and together regulate glucose homeostasis.

Glucose homeostasis is achieved by maintaining a balance between glucose production (mainly by the liver) and glucose consumption. When blood glucose is low, pancreatic glucagon is released to promote hepatic glycogenolysis, a catabolic process in which stored carbohydrate energy is transformed in glucose monomers that can be used by organs and to maintain fasting glucose levels.

When glycogen is depleted (for example, by prolonged fasting), glucagon promotes gluconeogenesis in liver and kidney, a process in which glucose is synthetised from precursors, such as lactate, pyruvate, glycerol and some amino acids (e.g., glutamine, alanine).

4.1.2.2 Insulin secretion and action

Circulating blood glucose is the main stimulus for insulin secretion. After a meal, glucose-stimulated insulin secretion (GSIS) from β-cells promotes glucose uptake into muscle and adipose tissue, and plasma (exogenous) glucose decreases. GSIS is in addition modulated by other nutrients, hormones and neural inputs (Komatsu *et al.*, 2013).

GSIS is based on adenosine triphosphate (ATP)-sensitive potassium (K_{ATP}) channels (Ashcroft, Harrison & Ashcroft, 1984; Cook & Hales, 1984). Glucose enters the β-cells via the glucose transporter GLUT-2/SLC2A2, is phosphorylated by glucokinase and enters the process of glycolysis. This process causes an increased ATP/ADP ratio that results in the closure of K_{ATP}-channels, depolarization of the membrane and the opening of voltage-dependent calcium channels (VDCC). This is followed by calcium influx and increased cytosolic free calcium levels. High intracellular calcium causes fusion of insulin granules with the membrane and insulin is released in a biphasic fashion (Grodsky, 1972). A glucose responsive insulin secretion mechanism independent of K_{ATP} was also reported (Curry, Bennett & Grodski, 1968; Komatsu *et al.*, 2001; Straub & Sharp, 2002). Both K_{ATP}-dependent and -independent mechanisms cause a pulsatile bi-phasic secretion of insulin. The first phase of insulin secretion, which is dependent on K_{ATP} signalling, lasts 3 to 10 min. This is followed by a second phase in which insulin release increase is gradually and that lasts at least 60 min. The second phase amplifies calcium-mediated exocytosis without an additional increase in intracellular calcium. The loss of first phase insulin secretion is an early feature of T2D. Importantly this second phase is less robust in isolated mouse islets (Nunemaker *et al.*, 2006).

β-cells can be primed by glucose so that exposure of these cells to high glucose increases insulin secretion in response to a subsequent stimulus (Grill, Adamson & Cerasi, 1978). Apart from glucose, other factors can potentiate insulin secretion, such as hormones, free fatty acids (FFA) and noradrenaline (Röder *et al.*, 2016). The incretins GLP-1 and GIP can bind Gs-coupled GPCRs on β-cells and cause an increase in intracellular cAMP, as well as in intracellular calcium. cAMP enhances GSIS via protein kinase A (PKA) and other mechanisms, such as the recently proposed exchange protein directly activated by cAMP 2 (Epac2) signalling cascade (Leech, Chepurny & Holz, 2010). In addition, the nervous system also influences glucose homeostasis (Ahrén, 2000; Faber *et al.*, 2020). Activation of the sympathetic efferents results in the release of noradrenaline that inhibits insulin secretion and

stimulates glucagon secretion. In contrast, activation of the parasympathetic efferents, results in a cholinergic-mediated increase in GSIS and glucagon secretion. The brain can also detect blood glucose by sensory afferents and via circumventricular organs. Several regions in the brain, including the brainstem and hypothalamus, integrate information on glucose handling and communicate with each other to regulate neural input into the pancreas and thus glucose homeostasis.

Insulin-mediated glucose transport into fat and muscle tissues is mediated by GLUT-4, which is localised in an intracellular compartment in the basal state. Insulin binding to the insulin receptor activates intracellular tyrosine kinase activity and results in the recruitment of PI3K to the membrane. A series of downstream reactions results in GLUT-4 translocation to the plasma membrane. Apart from the classical PI3K-dependent pathway, insulin can promote GLUT-4 translocation via other pathways (Khan & Pessin, 2002). In the liver and brain, glucose uptake is not directly mediated by insulin and other GLUT members (GLUT-1, -2 or -3), which are permanently located in the plasma membrane, transport glucose into cells. When cells of muscle, adipose tissue and liver do not respond well to insulin (that is, they show low insulin sensitivity), more insulin is secreted to promote glucose uptake under normal conditions. Hyperinsulinemia and β-cell expansion are followed by progressive deterioration of β-cell function and loss of β-cell mass. If β-cells are unable to compensate for the reduced insulin sensitivity, blood glucose increases (pre-diabetes) and T2D can develop.

4.1.3 Gut hormones as treatment of obesity and T2D

Incretin hormones (GLP-1 and GIP) postprandially stimulate insulin secretion and they have long been investigated as anti-diabetic treatments. Indeed, long-acting GLP-1 analogues are already approved treatments for obesity and diabetes. Another available class of anti-diabetic drugs that enhance gut hormone action is inhibitors of DPP-IV, the enzyme that degrades gut hormones GLP-1, GIP and PYY.
Bariatric surgery increases insulin sensitivity and secretion as well as glucagon secretion. After bariatric surgery in rodents, there is an increased number of β-cells per islet (Ramracheya *et al.*, 2016) and increased islet number (Zhang *et al.*, 2017). Several mechanisms by which bariatric surgery achieves T2D remission have been proposed (Holst *et al.*, 2018). One hypothesis suggests that increased secretion of GLP-1 post-surgery can drive improved β-cell function (Dirksen *et al.*, 2013; Jørgensen *et al.*, 2013; Holst *et al.*, 2018). Importantly, PYY levels are also increased after bariatric surgery (Le Roux *et al.*, 2006). The gut hormone PYY has been extensively investigated as a weight loss treatment. However, it may also have promise as an anti-diabetic therapy (Lafferty, Flatt & Irwin, 2018).

4.1.4 PYY in glucose homeostasis

PYY is mainly considered an anorectic hormone secreted from intestinal L-cells. However, early experiments observed that PYY is also expressed in the pancreas and that it might exert a paracrine effect (Bottcher *et al.*, 1989). PYY is co-expressed with glucagon in α-cells and to a lesser degree in δ and PP cells (Bottcher *et al.*, 1989; Upchurch, Aponte & Leiter, 1994). Although some differences exist between humans and rodents (Guida *et al.*, 2018), PYY is not observed in adult insulin-secretory cells (Bottcher *et al.*, 1989; Upchurch, Aponte & Leiter, 1994; Guida *et al.*, 2018). However, during early pancreatic development, α, β, δ and PP cells co-express PYY, suggesting a role of PYY in islet development (Upchurch, Aponte & Leiter, 1994).

In acute experiments, PYY_{1-36} intravenous (i.v.) injection in lean mice did not affect basal plasma levels of insulin, glucagon and glucose, but following glucose injection, PYY_{1-36} suppressed insulin and glucagon increase in a dose-dependent manner (Bottcher *et al.*, 1989). PYY_{1-36} (i.v.) also inhibited a glucose analogue-induced insulin release in dogs (Greeley *et al.*, 1988). PYY_{1-36} also inhibited insulin secretion in the presence of glucose in isolated islets (Nieuwenhuizen *et al.*, 1994) but this was not observed for PYY_{3-36} (Chandarana *et al.*, 2013).

Animal models have also revealed the importance of PYY in insulin secretion. PYY KO mice have significantly higher levels of basal and glucose-induced insulin with no differences in glucose tolerance to controls (Boey *et al.*, 2006b), and PYY KO islets also hypersecreted insulin in response to glucose (Boey *et al.*, 2006a). In contrast, another study observed that conditional ablation of pancreatic PYY-expressing cells in the adult mouse using a diphtheria toxin receptor-mediated knockout system reduced insulin secretion and triggered diabetes (Sam *et al.*, 2012).This was suggested to be caused by secondary β-cell death and a long-acting PYY analogue showed to rescue insulin decreased after PYY cell ablation and prevent streptozotocin-induced β-cell death (Sam *et al.*, 2012).This suggests a role of PYY in β-cell maintenance. *Ob/ob* mice overexpressing PYY showed lower insulin levels and were more glucose tolerant than *ob/ob* mice (Boey *et al.*, 2008).

Others have observed an insulinotropic effect of PYY (Sam *et al.*, 2012; Shi *et al.*, 2015; Ramracheya *et al.*, 2016), and increased GSIS was observed after mouse islets were exposed for 72h to PYY_{1-36} and PYY_{3-36} (Guida *et al.*, 2018). After gastric bypass, islets from diabetic rats had improved GSIS and improved glucagon response (Ramracheya *et al.*, 2016). Exposing islets to post-surgical serum or to chronic PYY reproduced the effects of surgery (Ramracheya *et al.*, 2016; Guida *et al.*, 2018, 2019). Interestingly, neutralization of PYY but not of GLP-1 reversed these effects (Ramracheya *et al.*, 2016;

Guida *et al.*, 2019). Indeed, the therapeutic benefits of DPP-IV inhibitors might be mediated by PYY rather than GLP-1 (Guida *et al.*, 2018). The discrepancies between studies might be due to the approach as well as the animal models and how obesity/diabetes was induced. Despite these discrepancies, these models suggest that PYY is relevant to β-cell function.

Several studies have shown that exogenous PYY_{3-36} also alters insulin secretion. Chronic continuous subcutaneous infusion (osmotic mini-pumps) with PYY_{3-36} improved glucose homeostasis in diabetic rats (Pittner *et al.*, 2004) and in diabetic obese mice (Moore *et al.*, 2002; van den Hoek *et al.*, 2007) although this was not observed in genetic models of obesity and diabetes (Pittner *et al.*, 2004). Chronic subcutaneous infusion of PYY_{3-36} in diabetic and/or obese rats also improved insulin sensitivity (Vrang *et al.*, 2006; Pittner *et al.*, 2004). PYY_{3-36} caused a reduction in body weight as well as adiposity, which would be expected to alter insulin sensitivity and secretion. Acute administration (i.v.) of PYY_{3-36} increased insulin sensitivity and glucose disposal in a hyperinsulinemic clamp (Van Den Hoek *et al.*, 2004). Later studies in diet-induced obese mice showed that chronic PYY_{3-36} also enhances insulin sensitivity and promote glucose disposal in adipose tissue and, to a lesser extent, in muscle (van den Hoek *et al.*, 2007). Importantly, this study showed that PYY_{3-36} metabolic effects were independent of PYY_{3-36} effects in food intake and body weight and lasted longer than the latter (van den Hoek *et al.*, 2007). Chandarana and colleagues reported that i.p. injection of PYY_{3-36} inhibited glucose-induced insulin secretion in the fed state but not in the fasted state supporting a nutrient-dependent effect of PYY_{3-36} in glucose homeostasis (Chandarana *et al.*, 2013). However, the postprandial levels of PYY_{3-36} in mouse are unknown and therefore these results do not confirm that physiologically occurring PYY_{3-36} modulates insulin action.

4.1.5 PYY and glucose homeostasis: evidence from humans

Circulating PYY levels are reduced in obese subjects (Batterham *et al.*, 2003a). Importantly, women who have a family history of T2D have low fasting PYY levels before T2D development (Boey *et al.*, 2006a). Moreover, fasting serum PYY levels were positively correlated with insulin sensitivity and negatively correlated with insulin secretion (Boey *et al.*, 2006a).

In humans, only a few studies have directly investigated PYY administration effects on glucose homeostasis. In the fasting state, acute intravenous PYY did not inhibit basal insulin secretion or have any effect in glucose or glucagon levels in healthy subjects (Adrian *et al.*, 1986). Similarly, infusion of PYY_{3-36} did not affect glucose or insulin levels in obese or lean subjects in the fasted state (Batterham *et al.*, 2002, 2003a). Although these results accord with the nutrient-dependent effect of PYY on insulin secretion, acute i.v. PYY_{1-36} or PYY_{3-36} did not alter i.v. glucose-induced insulin response in

healthy (Ahrén & Larsson, 1996) or overweight subjects (Tan *et al.*, 2014), respectively. In contrast, PYY_{1-36} and PYY_{3-36} infusion increased insulin secretion after an *ad libitum* meal, but this result is confounded by endogenous incretin secretion after food intake.

4.1.5.1 Mechanism of PYY action on glucose homeostasis

Although the purpose of this work is not to investigate the mechanism behind the effects of PYY on islet function or glucose homeostasis, a better understanding of this is key for the development of novel diabetes therapies. The mechanisms by which PYY regulates β-cell function as well as the receptors involved are still unknown. It is not understood if PYY's effects on glucose homeostasis are mediated by local action of islet-derived PYY (PYY_{1-36} or PYY_{3-36}) or if PYY in the general circulation is responsible.

PYY_{1-36} could have a more direct effect than PYY_{3-36} in insulin secretion because Y1R and Y4R expression has been detected in mouse pancreatic islets, whereas Y2R and Y5R expression were not (Burcelin *et al.*, 2001; Chandarana *et al.*, 2013; Guida *et al.*, 2018), and only one study has found Y2R mRNA in islets (Khan *et al.*, 2016). NPY has been shown to inhibit insulin secretion via the Y1R (Morgan *et al.*, 1998). Therefore, taking in account that most *in vitro* studies (Nieuwenhuizen *et al.*, 1994; Bottcher *et al.*, 1989; Chandarana *et al.*, 2013) and mouse models (Boey *et al.*, 2006b, 2008) support an insulinostatic role of PYY signalling, PYY_{1-36} could be released from α-cells and act in a paracrine fashion to inhibit insulin secretion from β-cells. In support of this, islets from Y1R KO mice hypersecrete insulin (Burcelin *et al.*, 2001), like PYY KO islets (Boey *et al.*, 2006a). Chandarana et al observed a direct effect of PYY_{1-36} to inhibit GSIS while PYY_{3-36} did not directly alter insulin secretion (Chandarana *et al.*, 2013). Other study has shown that PYY_{3-36} has insulinostatic effects, like PYY_{1-36}, and that these are mediated by both Y1R and Y2R in isolated islets (Khan *et al.*, 2016). They also showed a protective action of both PYY forms against streptozotocin-induced cytotoxicity (Khan *et al.*, 2016). In contrast, other studies in isolated islets have suggested that Y1R mediates the insulinotropic effects of PYY on islet function (Ramracheya *et al.*, 2016; Guida *et al.*, 2018, 2019).

In addition to a local intra-islet theory, PYY could indirectly influence glucose homeostasis peripherally or by acting centrally. PYY_{3-36} was shown to promote the incretin effect via stimulating GLP-1 secretion, and this effect to be mediated by the Y2R (Chandarana *et al.*, 2013). Y2R agonism was shown to partially inhibit cholinergic vagal efferent neurones of the DMX which might affect pancreas secretion (Chen & Rogers, 1997). It has recently been shown the important role of circulating factors, and specially PYY, preserved in serum after bariatric surgery and that can increase GSIS in isolated human islets (Guida *et al.*, 2019).

4.1.6 Islets in the anterior chamber of the eye

Islet function has been extensively studied in isolated islets and isolated pancreas slices but it is likely that islets behave differently *in vitro* compared to the physiological environment, in which they are vascularised and are abundantly innervated. *In vivo* imaging of islet can be performed in the exteriorised pancreas. However, this is an invasive procedure and islets are difficult to access for imaging.

Alternatively, islet function can be studied in islets engrafted into the anterior chamber of the eye (ACE) (Speier *et al.*, 2008a, 2008b). The anterior chamber of the eye is an immune-privileged area and the iris (which forms the base of the anterior chamber) contains blood vessels and autonomic nerves. After transplantation, islets are quickly vascularised and innervated (Adeghate, 2002), and are capable to maintain glucose homeostasis (Speier *et al.*, 2008a). This islet-in-eye platform is more accessible for imaging, maintains the pancreatic islet environment and can be combined with fluorescent indicators to study islet function (Speier *et al.*, 2008b).

The most studied signal in β-cell function is cytoplasmic free calcium concentration due to its role in insulin secretion. In this experiment, we have used islets from transgenic mice expressing genetically-encoded calcium indicators and monitoring its fluorescence in the eye of the recipient mice. This allows measurement of intracellular calcium oscillations in response to different physiological conditions (Chen *et al.*, 2016). Glucose increases ATP/ADP ratio resulting in closure of K_{ATP} channels. If glucose concentration is high enough, this results in β-cell membrane depolarization and opening of calcium channels. Then calcium influx into the β-cell causes an increase in cytoplasmic free calcium. Increased cytoplasmic calcium levels activate the signalling to promote fusion of insulin granules with the membrane and triggers insulin secretion. Calcium oscillations are synchronised via electrical coupling in all the β-cells. Intracellular calcium binds to the calcium indicator, which undergoes a conformational change and fluoresces. The intensity of the fluorescent signal increases according to the concentration and acts as a proxy of insulin secretion.

Major benefits of this platform are the possibility of performing repeated longitudinal measurements (Chen *et al.*, 2016) as well as the single cell resolution, which has allowed to study the connectivity between β-cells as well as to demonstrate the existence of leader β-cells (Salem *et al.*, 2019). These 'reporter islets' mirror the islet function in obesity as well as the plasticity of the endocrine pancreas as shown in leptin-deficient mice (Ilegems *et al.*, 2013) and in diet-induced obese mice (Chen *et al.*, 2016).

4.2 Aims and Hypotheses

The aims of the experiments described in this chapter were to:

- Establish a platform for longitudinal *in vivo* imaging of islets in the ACE as a direct readout for islet function and its evolution under different conditions.
- Assess the effects of high fat diet-induced obesity on islet function.
- Assess the effect of chronic treatment with a PYY analogue on glucose homeostasis.

The hypotheses were that:

- High fat diet would alter β-cell function and this could be longitudinally detected by *in vivo* imaging of islet in the ACE.
- Chronic administration of a long-acting analogue of PYY, Y242, would reduce body weight.
- Chronic Y242 administration would alter β-cell secretion in obese mice.

4.3 Materials and methods

4.3.1 Animals

This study was conducted under the project licence P0A6474AE (PPL holder Dr Bryn Owen) and all procedures were adhered under the UK Home Office Animals (Scientific Procedures) Act 1986. All animals were housed in ventilated cages under controlled conditions (21-23°C, 45-56% humidity) in a 12 h light/dark cycle (lights on at around 6 am).

4.3.1.1 Donor animals used in the chronic study

In a C57Bl/6J background, mice expressing GCaMP6f specifically in β-cells were generated using the Cre/LoxP system. GCaMP6f (fast) is a widely used genetically encoded calcium indicator that belongs to the green fluorescent protein (GFP)-based GCaMP sensor family.

Ins1-Cre mice (provided by Prof Jorge Ferrer, Imperial College London) were crossed with Cre-dependent GCaMP6f-expressing mice (stock n. 028865, The Jackson Laboratory). *Ins1* is the gene encoding preproinsulin-1 in β-cells of mice and rats. Therefore, GCaMP6f is specifically expressed in β-cells. Breeding was performed by Dr Yateen Suresh Patel (Imperial College London).

4.3.1.2 Animals used in the chronic study

Male C57Bl/6J mice (24 animals,~8 weeks-old, 25-30 g) were purchased from Charles River. Animals were initially housed in groups of 4 with *ad libitum* access to standard chow (RM1, Special Diet Services) and water. A 1-week acclimatisation was allowed before transplantation of syngeneic donor islets in the ACE. The donors of these islets express β-cell-specific GCaMP6f (see section 4.3.1.1).

4.3.2 Pancreatic islet isolation

Islets from Ins1/Gcamp6f donor mice were isolated in order to implant them in the ACE of the wild-type animals used in the chronic study. Collagenase (Universal Biologicals Ltd, UK) was diluted at 1mg/ml in RPMI 1640 medium (Sigma-Aldrich, UK) supplemented with 10% fetal bovine serum (FBS, Sigma-Aldrich), 1% penicillin-streptomycin (P/S, Thermo Fisher) and glutamate. This preparation was filtered and infused in mice through the bile duct using a 30G needle. The inflated pancreas was added to a 15 mL Falcon tube and incubated at 37°C for 10 min in a water bath for digestion of the exocrine pancreas and the connective tissue between pancreatic islets. For washing, the pancreas was centrifuged at 200 x g for 1 min, the supernatant was removed and 15 mL of non-supplemented RPMI (not containing FBS or P/S) was added. The pancreas was washed 3 times in total. Islets were separated in a Ficoll density gradient using 4 mL of Histopaque®-1119 and Histopaque®-1083 (both Sigma-Aldrich) in non-supplemented RPMI medium. After centrifugation for 20 min at 800 x*g* with a slow deceleration setting, the islets were collected from a layer between the second and third phase and were placed into a Petri dish. Islets were incubated in supplemented RPMI overnight (37°C; 5% CO_2). This was performed by Dr Kinga Suba (Imperial College London).

4.3.3 Pancreatic islet transplantation into the ACE

Mice were anaesthetised in an induction chamber using isofluorane at 5% (95% O_2,1.5 L/min). After confirming depth of anaesthesia (pedal reflex), animals were placed in a stereotaxic frame and isofluorane was adjusted so that breathing rate was 60-80 breaths/min. Under a microscope, a 25G needle was used to puncture the eye at the corneo-scleral junction, avoiding the iris. Donor islets from Ins1/GCaMP6f mice were preloaded in 20 µL of RPMI medium into a cannula that was attached to a 27G blunt needle and to a 100 µL gas tight Hamilton syringe. This system was manually operated to gradually inject the islets intro the ACE, allowing the islets to set on top of the iris. For recovery, carprofen was topically administered on the eye also 3 days post-surgery. For full implantation of the islets into the ACE, 4 weeks post-surgery were allowed. Animal surgeries were performed by Dr V. Salem.

4.3.4 Diet-induced obesity

After full islet implantation, animals were put on a high-fat diet (HFD, D14292, Research Diets, USA) *ad libitum* for 8 weeks to induce obesity. Glucose homeostasis (see section 4.3.8) and islet function (see section 4.3.9) were assessed before and after HFD. The study schematic is shown in Fig. 4.3.6.1.

4.3.5 Peptides

The PYY analogue Y242 was designed by Prof SR Bloom (Imperial College London) and custom made by Bachem (Merseyside, UK). It was synthesised using solid-phase synthesis and purified by reverse-phase high-performance liquid chromatography. Y242 showed 82% amino-acid sequence homology to the native peptide (Fig. 4.3.1.1) and binds to the Y2R with similar affinity (IC_{50} 0.28) to PYY_{3-36} (IC_{50} 0.21) (unpublished data). Previous studies (unpublished) showed that, after subcutaneous injection in rodents, Y242 acts for more than 72 h in rats and it was safe at doses that caused weight loss. Y242 is part of a confidential drug discovery line.

Peptide	Amino-acid sequence																																	
Y242	P	I	H	P	H	A	P	G	E	D	A	S	P	E	E	L	N	H	Y	Y	A	A	L	R	H	Y	L	N	H	V	T	R	Q	R	Y	NH_2
$hPYY_{3-36}$		I	K	P	E	A	P	G	E	D	A	S	P	E	E	L	N	R	Y	Y	A	S	L	R	H	Y	L	N	L	V	T	R	Q	R	Y	NH_2

Figure 4.3.5.1. Amino-acid sequences of Y242 and PYY_{3-36}.

Y242 was aliquoted and freeze-dried. On the day of the injection, Y242 aliquot was dissolved in sterile saline with zinc chloride (39059-100ML-F, Sigma Aldrich, UK) for a ratio 1:1 peptide to zinc). The addition of zinc enhances peptide depot formation and allows slow release into the circulation after subcutaneous (s.c.) injection.

4.3.6 Bioactivity of Y242

The bioactivity of Y242 was studied in an acute feeding study. Littermate controls with *ad libitum* access to chow and water received a subcutaneous injection of Y242 at 50 nmol/kg or vehicle in the light phase (mimicking the chronic treatment conditions). On one day all animals received Y242 and, 4 days later, all of them received saline. Food was pre-weighed (before injection) and food weight was recorded at different time points after injection and the difference in food weight before and after injection was calculated.

4.3.7 Chronic treatment with gut hormone analogues

Diet-induced obese (DIO) mice were singly housed and assigned to 2 different groups (Y242-treated group and vehicle control group) according to body weight. Animals received daily subcutaneous injection with saline or Y242. For the chronic study, a dose ramping protocol (Bloom Drug Discovery team) was used to start the chronic treatment. Mice were given 12.5% of maximum dose (25 nmol/kg) on the first day and 25% (50 nmol/kg daily) for the following two days. From day 4, a 50% of maximum dose (100 nmol/kg daily) was administered for a week, and subsequently the full dose (200 nmol/kg daily) was administered for the duration of the study. Treatments were administered at approximately

2 h before the start of the dark phase, unless otherwise stated. Body weight and food consumption were measured daily. After the treatment (6 weeks approx.), glucose homeostasis and islet function were evaluated. The study schematic is shown in Fig. 4.3.13.1.

4.3.8 Metabolic phenotyping

Intraperitoneal glucose tolerance tests (IPGTT) and insulin tolerance tests (IPITT) were performed on 4 occasions: i) before starting the HFD; ii) after 8 weeks in HFD; iii) 2.3 weeks (16 days) after the start of treatment with analogues; and iv) 6 weeks after chronic treatment with analogues.

Food was removed 5 h prior to the start of the test and the peptide treatment was administered 3 h prior to the start of the test. Topical anaesthesia (lidocaine/prilocaine, EMLA™, Aspen, UK) was applied to the mouse tail before tail venepuncture. Baseline blood glucose measurement was recorded using a glucometer (GlucoRX Nexus, GlucoRX, UK) and then IP injection was performed. In IPGTTs, D-(+)-glucose (Sigma Aldrich) was administered at 2g/kg. In IPITTs, insulin (Actrapid, Novo Nordisk, Denmark) was injected at 1U/kg. Subsequent blood glucose measurements were recorded at 15, 30, 45, 60, 90, 120, 150 and 180min post-injection. After the study, mice were returned to their cages with *ad libitum* access to food and water.

4.3.9 *In vivo* calcium imaging of islet in the ACE

Islet in the ACE were imaged on three occasions: i) after full implantation and before starting the HFD; ii) after 8 weeks in HFD; iii) 6 weeks after chronic treatment with analogues. All animals were imaged using a spinning disk confocal microscope (Yokogawa spinning disk, 20x water dipping 1.0NA objective, Cairn Instruments) and Metamorph software package (version 7.8.12.0). Animals were anaesthetised in an induction chamber and then placed in a stereotaxic head frame placed on a heated stage under the microscope objective. Islets expressing GCaMP6f were excited at 488 nm (exposure time of 300 msec) and images were acquired at 3 Hz acquisition rate. In each animal, a total of 401 frames were recorded per imaging session, which was conducted in the dark phase for maximum effect of the treatment. *In vivo* imaging was performed by Dr V. Salem and Dr K. Suba (Imperial College London).

4.3.10 Imaging processing

All images were processed and analysed using Fiji (ImageJ). A custom-made macro created by Mr Stephen Rothery (FILM facility, Imperial College London) was used. Briefly, images of the time series are manually aligned using a region of interest (ROI) as a reference. Frames with poor quality or showing different Z depth to the reference frame were removed preserving the temporal information of the time series. In the resultant corrected image sequence, a region of interest was placed around

the islet and the readouts of fluorescence intensity was measured. The calcium fluorescence signal (F) was normalised to the lowest intensity value (Fmin) for each individual islet image sequence. Calcium surges were identified as a normalised calcium fluorescence (F/Fmin) 20% above the baseline and by visual confirmation in the recorded images.

4.3.11 Calcium fluctuation analysis

Peaks were identified by their x/y values in the F/Fmin vs frame plot. The amplitude was calculated as the F/Fmin -1 (Fpeak). Calcium waves activity was quantified. The wavelength was calculated as the difference between the time point (frame) of two sequential peaks. Full width at half maximum (FWHM) was acquired by the difference between the frame number on the ascending limb at Fpeak/2 and the frame number of the descending limb of the peak at Fpeak/2.

A classification of islet-wide calcium activity was designed by Dr Salem's team (Fig. 4.3.11.1). Type 1 denoted quiescent islets with no discernible changes in calcium fluorescent activity. Type 2 activity was characterised by the calcium fluctuations in a cell or group of cells. In type 3 activity, a large area of calcium activity (20-50% of islet area) was detected but the whole islet does not propagate calcium oscillations. In type 4 activity, calcium waving is observed in the whole islet.

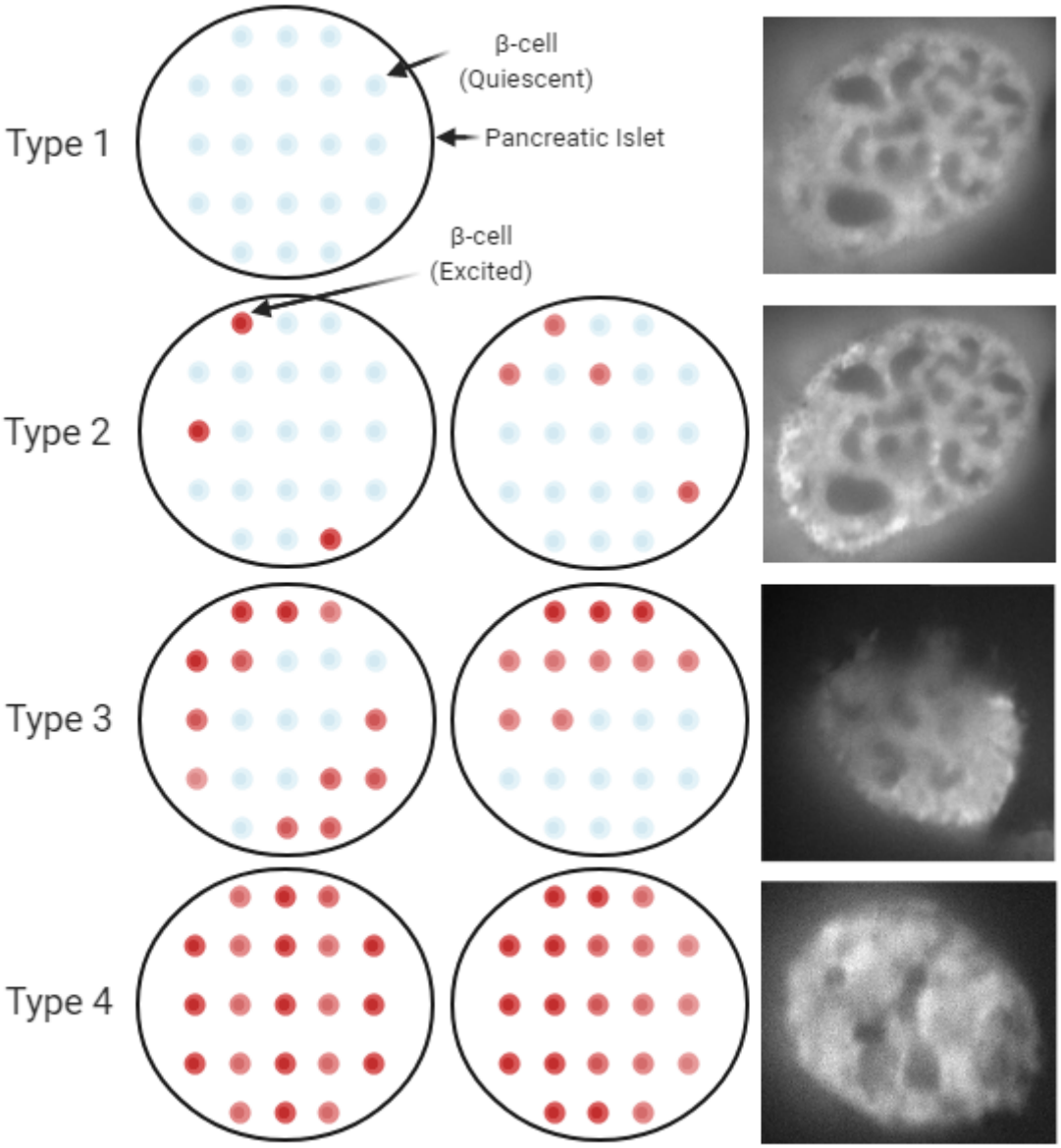

Figure 4.3.11.1. The islet "Wave Index" classification.

Semi-quantification of *in vivo* calcium imaging of pancreatic islets that contain GCaMP6f-expressing β-cells and that are implanted in the ACE. Image created by Dr Y Patel using Biorender.

4.3.12 Statistical analysis

All data is presented as mean ± SEM. Data was analysed by unpaired Student's *t* test or by two-way ANOVA followed by Bonferroni's multiple comparisons test.

4.3.13 Experimental design

C57Bl6/J mice were acclimatised for a week upon arrival. Mice received syngeneic transplant of islets expressing the calcium indicator GCaMP6f in β-cells in the eye (section 4.3.3). When transplanted islets were fully implanted (4 weeks post-surgery), baseline islet function (session 1) was assessed by *in vivo* calcium imaging (section 4.3.9). Baseline body weight and glucose metabolism was assessed (4.3.3). Until then, animals were lean and healthy.

In order to induce obesity, animals received high-fat diet. After 8 weeks, metabolism was assessed to confirm the obesity model. Then, we evaluated islet function by calcium imaging in the diet-induced obese state (session 2). Obese animals were randomised into groups so that one group would receive daily the long-acting PYY analogue (Y242) and another group would receive daily the vehicle. After 2 and 6 weeks of chronic treatment, glucose metabolism was assessed. After 6 weeks of treatment, transplanted islets were imaged again to assess their function.

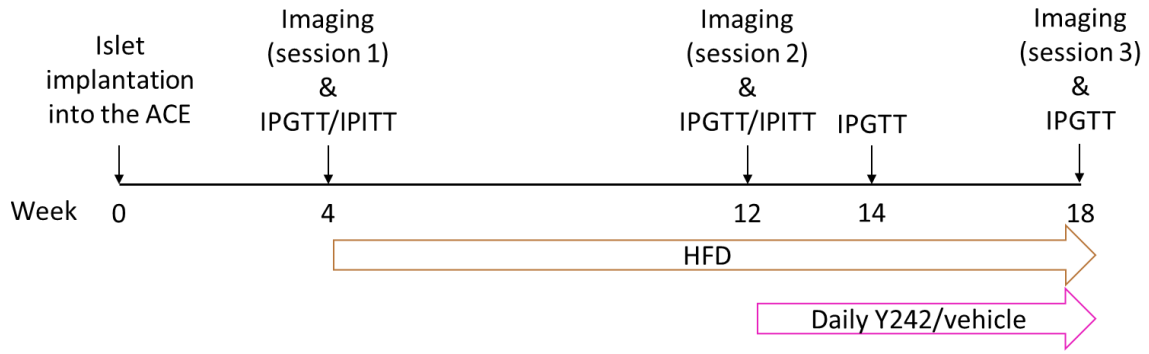

Figure 4.3.13.1. Study design.

ACE, anterior chamber of the eye; IPGTT, intraperitoneal glucose tolerance test; IPITT, intraperitoneal insulin tolerance test; HFD, high-fat diet.

4.4 Results

4.4.1 Effect of high-fat diet on the C57Bl6/J metabolic phenotype

Tolerance tests were performed when the mice cohort was chow-fed and after 8 weeks of HFD to assess the effect of diet-induced obesity (Fig. 4.4.1.1). Baseline blood glucose was lower than 10 mmol/L in lean and after HFD intervention. In lean mice given a glucose tolerance test, blood glucose peaked at 15 min and dropped at 30 min post-IP of glucose (Fig. 4.4.1.1, A). After 8 weeks of HFD, glucose tolerance was reduced, with the glucose peak observed at 30 min and blood glucose level decreasing only slowly over a 2 h-period (two-way ANOVA, time x treatment: $p<0.0001$, $F(7, 120) = 11.78$). The IPITT (Fig. 4.4.1.1, B) showed a rapid reduction in plasma glucose after 15 min of insulin administration with nadir at around 60 min post-injection. No significant differences were observed in insulin responsiveness between diets (two-way ANOVA: $p = 0.486$, $F(8, 240) = 0.9383$). Body weight significantly increased after HFD (Fig. 4.4.1.1, C).

Mice were treated equally and in parallel at this point. Prior to diet intervention and prior to the start of Y242 treatment, baseline glucose tolerance (Fig 4.4.1.2, A, B), insulin responsiveness (Fig 4.4.1.2, C, D) and body weight between the subsequent treatment groups were not different (Fig 4.4.1.2, E, F).

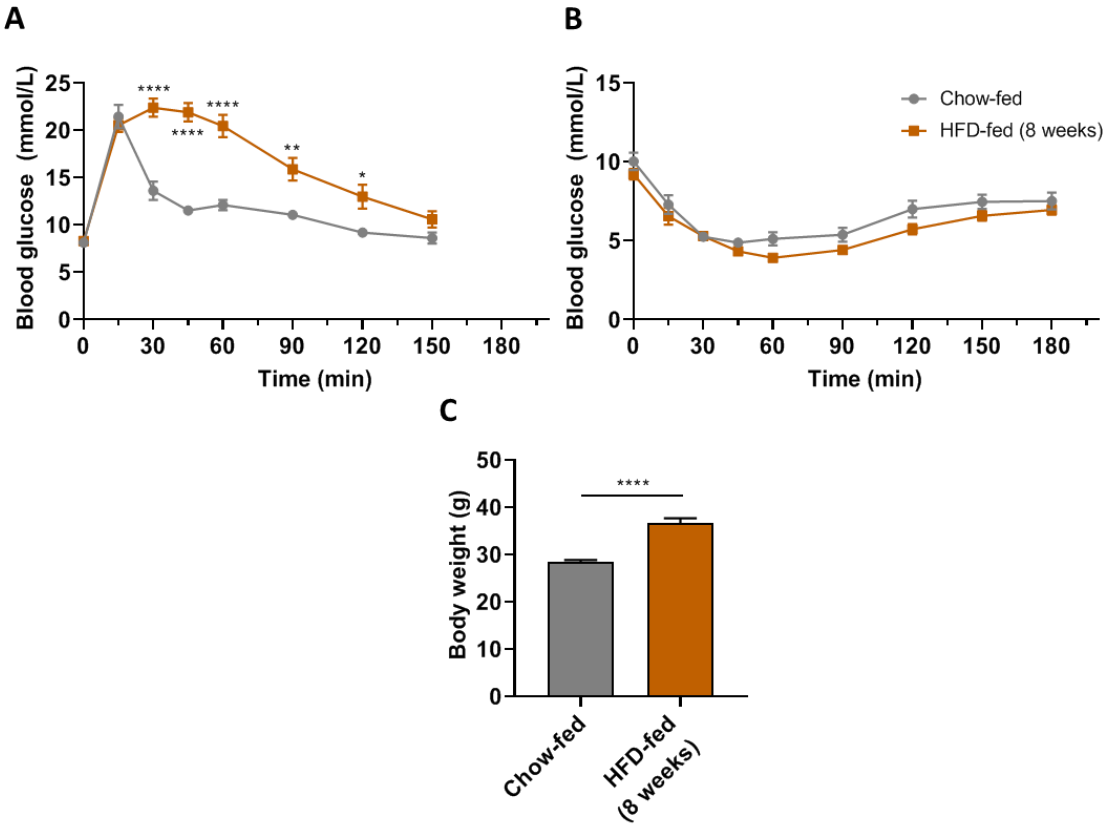

Figure 4.4.1.1. Glucose tolerance, insulin tolerance and body weight before and after HFD in wild-type mice.

Blood glucose (mmol/L) during an IPGTT (A) and an IPITT (B) in 5-h fasted chow-fed mice and after 8 weeks of HFD (n = 16/group). Body weight (g) on the day of the IPGTT when mice were chow-fed (E) and after 8 weeks of HFD (F). A: Two-way ANOVA (time x treatment: $p<0.0001$) followed by Bonferroni's multiple comparisons test. (*$p < 0.05$, **$p < 0.01$, ****$p < 0.0001$). C: Unpaired Student's *t* test (****$p < 0.0001$).

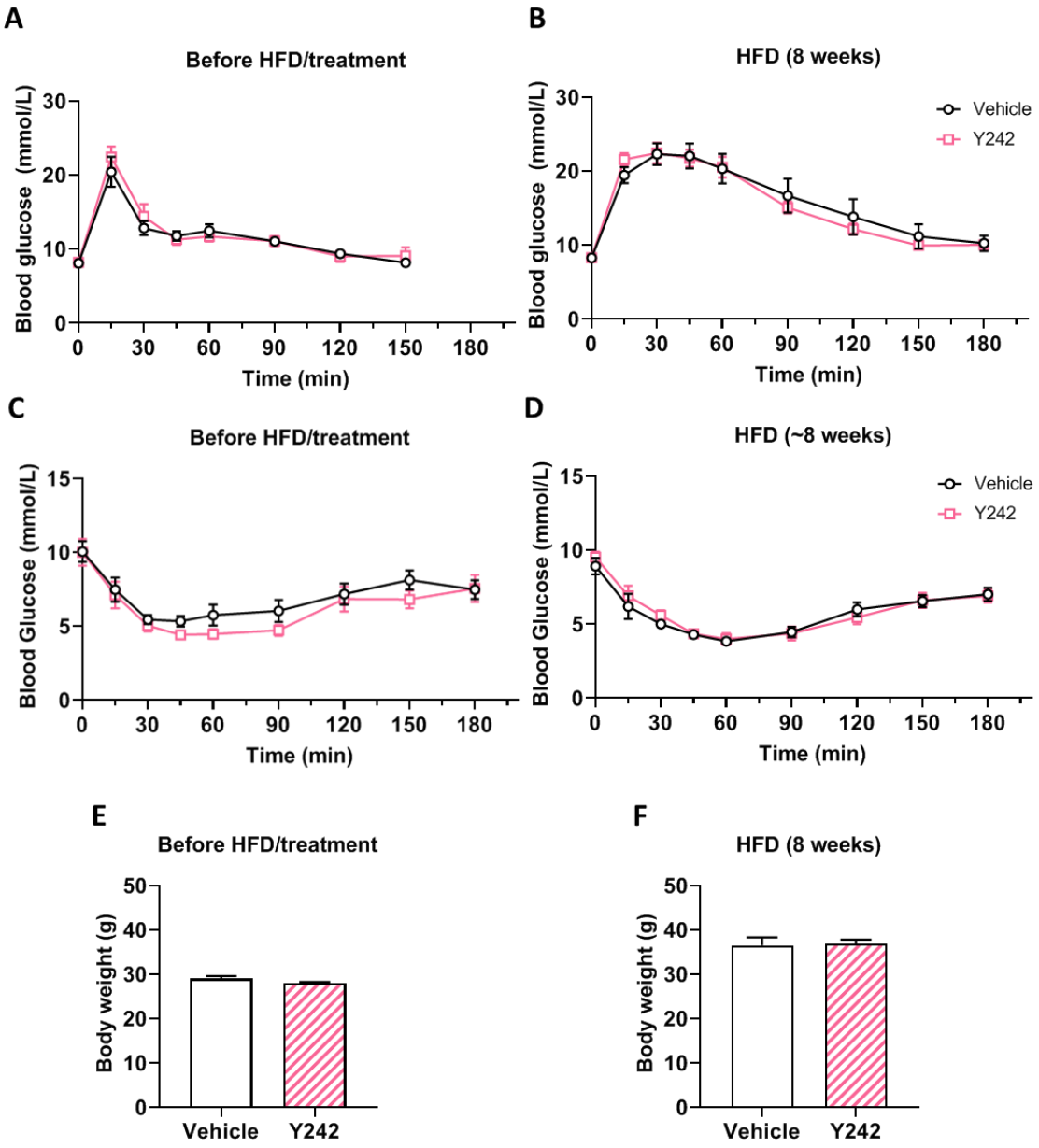

Figure 4.4.1.2. Glucose tolerance, insulin tolerance and body weight before and after HFD in wild-type mice showed according to subsequent treatment groups.

This figure shows the data from 4.4.1.1. grouped according to the treatment that mice subsequently received (chronic Y242 or vehicle). Blood glucose (mmol/L) during an IPGTT (A) in 5-h fasted chow-fed mice and after 8 weeks of HFD (B). Blood glucose (mmol/L) during an IPITT (C) in 5-h fasted chow-fed mice and after 8 weeks of HFD (C). Body weight (g) on the day of the IPGTT when mice were chow-fed (E) and after 8 weeks of HFD (F).

4.4.2 Acute effect of Y242 in food consumption

The bioactivity of Y242 was investigated in a feeding test after s.c. administration of 50 nmol/kg of Y242 in littermate control mice (Fig. 4.4.2.1). Y242 showed a strong anorectic activity overtime (time x treatment: $p < 0.0001$, $F(4, 50) = 32.96$) that lasted more than 8 h.

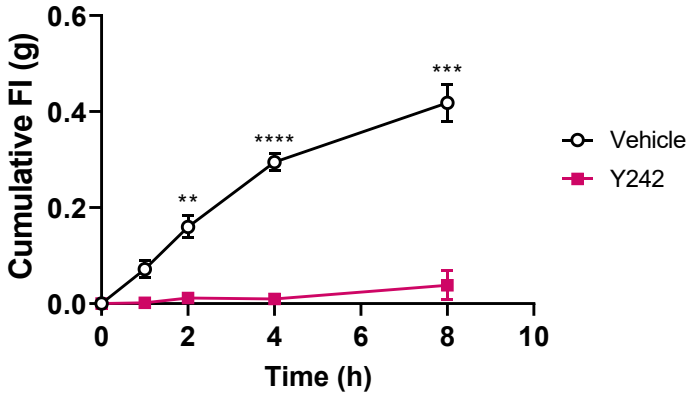

Figure 4.4.2.1. Food intake after Y242 administration.

Food intake (FI) of fed littermate control mice (6-week-old) after s.c. injection of vehicle or 50 nmol/kg of Y242 (n = 6/group) in the light phase (vehicle and Y242 were administered on different days). Two-way ANOVA (time x treatment: $p < 0.0001$) followed by Bonferroni's multiple comparisons test (**$p < 0.01$, ***$p < 0.001$, ****$p < 0.0001$).

4.4.3 Effect of chronic treatment with Y242 in body weight and food consumption in DIO mice

Body weight and food intake was recorded during the chronic treatment with Y242 (Fig. 4.4.3.1). The Y242 dose was established from previous murine food intake studies (unpublished) by the Bloom drug discovery programme as that producing acute 2-hour reduction of food intake of >80%. Two-way ANOVA revealed an effect of treatment ($p <0.0001$, $F(1, 308) = 18.25$) and time ($p <0.0001$, $F(43, 308) = 3.019$) but no interaction (Fig. 4.4.3.1, A). During the ramping of Y242 dose, a trend towards body weight reduction was observed (day 1: $p = 0.223$; day 2: $p = 0.063$; day 3: $p = 0.359$; day 4: $p = 0.082$; day 5: $p = 0.167$; by unpaired *t* test). At the end of the experiment, total body weight loss mean was non-significantly higher in Y242-treated animals than vehicle-treated mice ($p= 0.2463$) (Fig. 4.4.3.1, B). No differences in cumulative food intake were observed (Fig. 4.4.3.1, C).

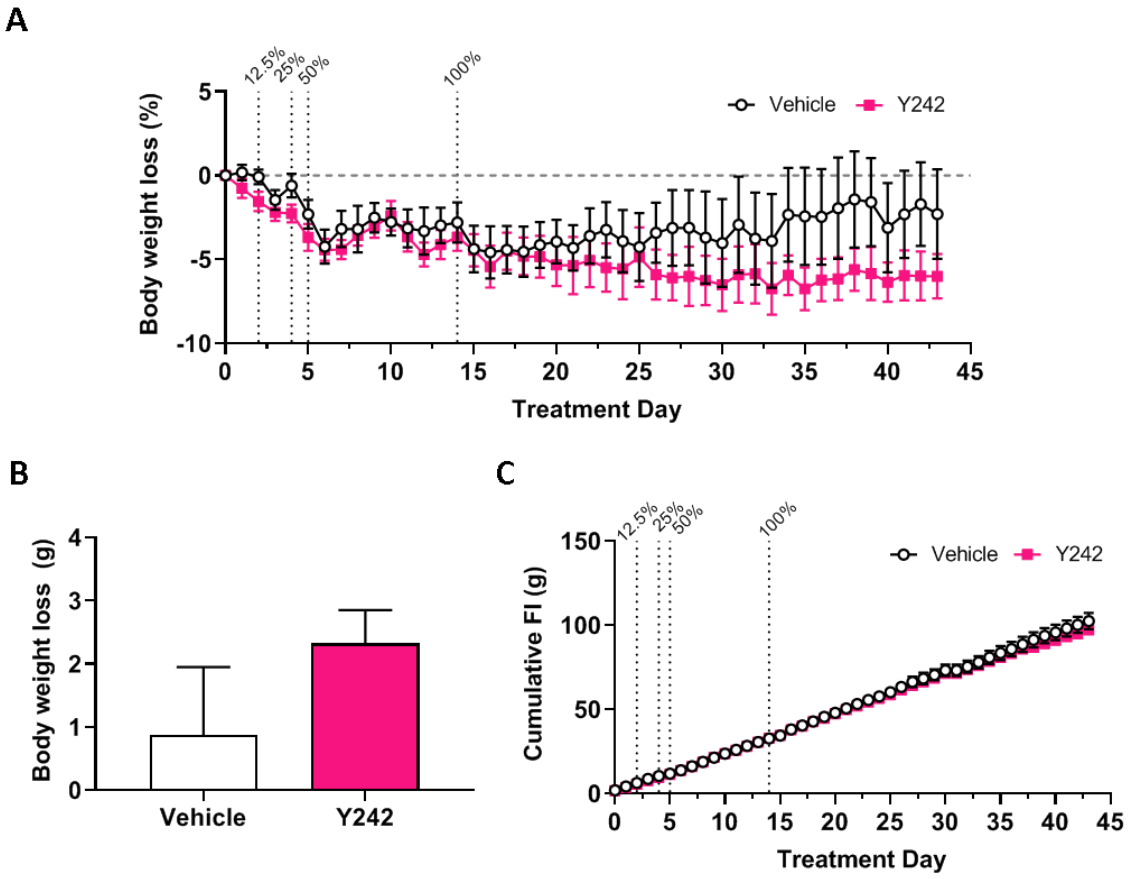

Figure 4.4.3.1. Body weight loss and food intake during chronic treatment with Y242 in DIO mice.

Body weight loss (as % of body weight before treatment) (A), total body weight loss (initial body weight minus final body weight) (B) and cumulative food consumption (C) in mice receiving daily s.c. Y242 or vehicle (n = 8/group). The % of maximum dose and when the treatment with these doses was started are shown in A and C.

4.4.4 Effect of Y242 in glucose homeostasis in DIO mice

Tolerance tests were performed at two different time points (around 2 weeks (16 days) and around 6 weeks (40 days)) after start of chronic treatment with Y242. No significant differences in glucose tolerance were observed between Y242-treated and vehicle-treated DIO mice after 16 days (two-way ANOVA: $p = 0.412$; $F(8, 112) = 1.038$) and 40 days (two-way ANOVA: $p = 0.091$; $F(8, 112) = 1.767$) of treatment (Fig. 4.4.4.1, A, B and E). Blood glucose curves in Y242-treated group showed a similar pattern to vehicle-treated group after 16 days and after 40 days of treatment (Fig. 4.4.4.1, A, B and E).

If comparing glucose AUC after 16 days and 40 days of treatment, no significant differences were observed during the IPGTT in the vehicle group (Fig. 4.4.4.1, C). No significant differences in glucose AUC between 16 and 40 days were observed in the vehicle group ($p = 0.1508$) (Fig. 4.4.4.1, E). Blood

glucose curves were similar after 16 and 40 days of Y242 treatment except at t = 60 min, in which blood glucose was significantly higher after 40 days of Y242 treatment ($p = 0.005$). This is reflected when analysing the glucose AUC since there was an interaction between treatment and treatment duration (two-way ANOVA: $p = 0.005$; $F(1, 14) = 11.37$) and significant differences were observed in glucose AUC between 16 and 40 days in the Y242 group (Bonferroni's multiple comparisons test: $p = 0.026$) (Fig. 4.4.4.1, E). Since vehicle and Y242 showed similar glucose tolerance at 16 and 40 days of treatment and there was variability in the vehicle group, the difference between 16 and 40 days with Y242 treatment might be an artifact.

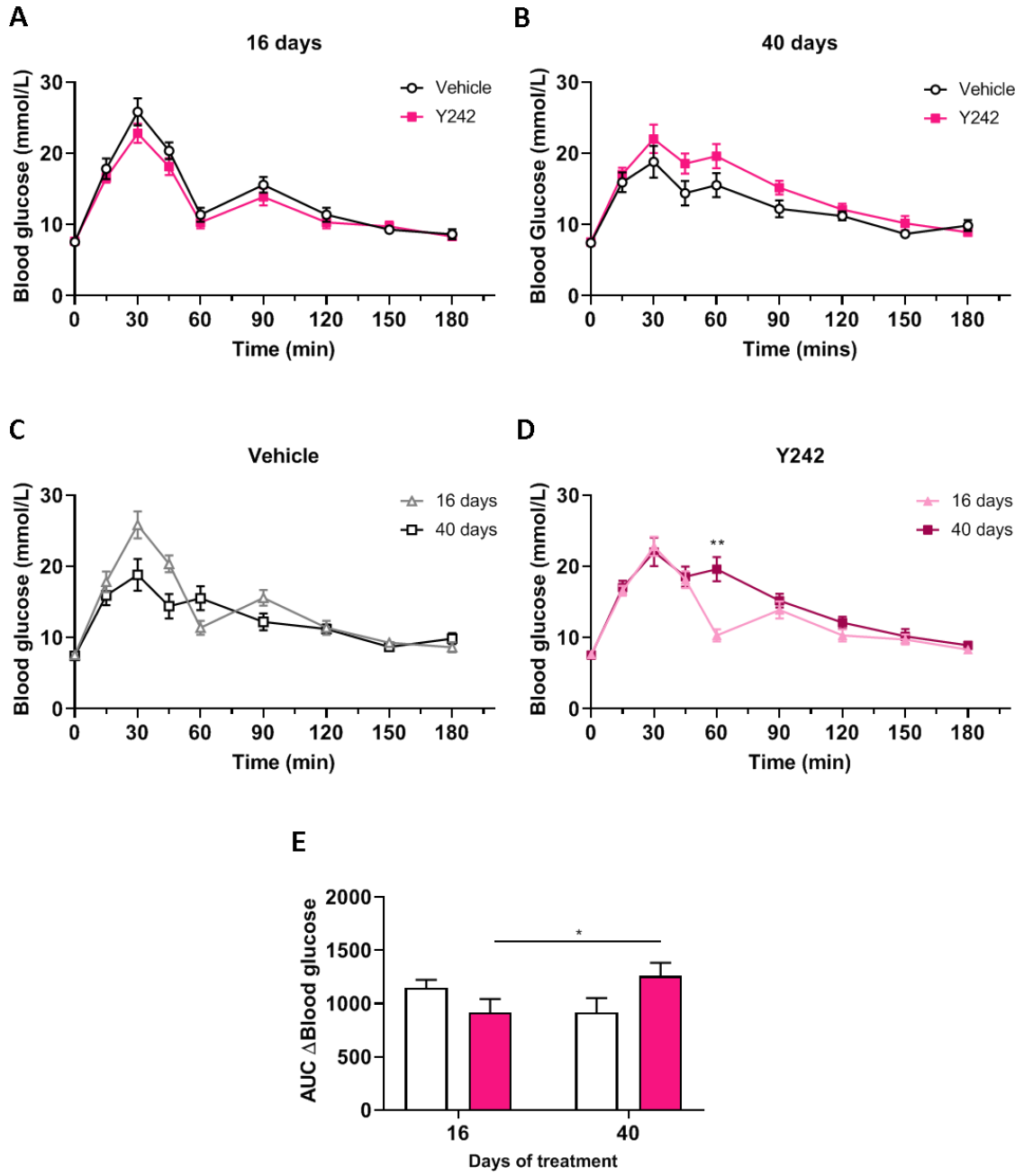

Figure 4.4.4.1. Glucose tolerance during chronic treatment with Y242 in DIO mice.

Blood glucose (mmol/L) during an IPGTT in 5-h fasted DIO mice (n = 8/group) after 16 days (A) and 40 days (B) of daily s.c. injection with Y242 or vehicle. Data is also shown in each treatment group to compare the effect of treatment duration (C, D). AUC of the blood glucose increase (from t=0) is included (E). C: Two-way ANOVA (time x treatment duration: $p<0.0001$, $F(8, 112) = 7.855$) followed by Bonferroni's multiple comparisons test. D: Two-way ANOVA (time x treatment duration: $p<0.0001$, $F(8, 112) = 6.247$) followed by Bonferroni's multiple comparisons test. E: Two-way ANOVA (treatment duration x treatment: $p<0.0001$, $F(8, 112) = 6.247$) followed by Bonferroni's multiple comparisons test (*$p < 0.05$, **$p < 0.01$). C: Unpaired Student's *t* test (****$p < 0.0001$).

4.4.5 Effect of HFD and Y242 in pancreatic islet function

The effect of HFD-induced obesity on islet function was studied by recording calcium dynamics in fluorescence islets implanted in the ACE (Fig. 4.4.5.1, A). During imaging, blood glucose levels were monitored using a glucometer. Blood glucose levels were around 10 mmol/L and animals did not receive any glucose. A trend towards a reduced pan-islet calcium dynamic ($p = 0.124$), as determined by wave index semi-quantification, was observed in the 2nd session (after HFD) compared with the calcium read-out in lean mice (1st session) (Fig. 4.4.5.1, B). In session 1 and 2, animals had not received any treatment yet. As expected, no differences between Y242 and vehicle were observed. Y242 (3rd session) did not reverse the reduction in pan-islet calcium activity.

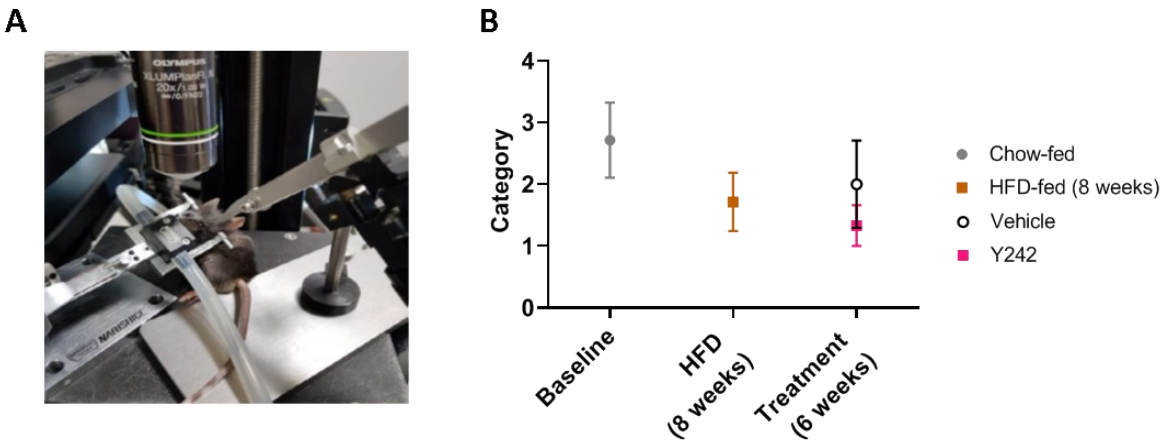

Figure 4.4.5.1. Longitudinal pan-islet calcium activity of GCaMP6f-fluorescence islets implanted in the ACE of DIO mice.

Islets expressing the calcium indicator GCaMP6f in β-cells were transplanted into the ACE of syngeneic recipient mouse eyes. These islets were longitudinally imaged in a confocal microscope (A). Calcium imaging was performed before HFD or treatment (session 1), after 8-week HFD (session 2) and after a 6-week treatment with the PYY_{3-36} analogue Y242 or vehicle (session 3). Semi-quantification (wave category) of calcium activity in session 1 (n = 7 islets), session 2 (n = 7) and of Y242-treated (n = 3 islets) versus vehicle group (n=4 islets) are shown (B). Category indexes are shown as mean±SEM.

Calcium activity is a proxy marker of insulin secretion and the islets in the ACE reflect the activity of endogenous islets, so the recorded calcium fluorescence indicates islet functionality. Calcium fluctuations were also quantified in terms of amplitude, wavelength and FWHM (Fig. 4.4.5.2). After 8 weeks of HFD, amplitude and FWHM were reduced ($p = 0.019$ and $p = 0.026$, respectively), but not wavelength (Fig. 4.4.5.2, A-C). If considering the treatment groups, both Y242 and vehicle groups showed a non-significant reduction in amplitude and FWHM in session 2 versus session 1, but no differences were observed in wavelength (Fig. 4.4.5.2, D-F). After 6 weeks of daily Y242 or vehicle,

amplitude did not significantly change compared to session 2, although there was a slight increase in the Y242 group compared to the vehicle group (Fig. 4.4.5.2, D). After 6 weeks of treatment, FWHM non-significantly increased in both Y242 and vehicle groups after treatment (Fig. 4.4.5.2, F).

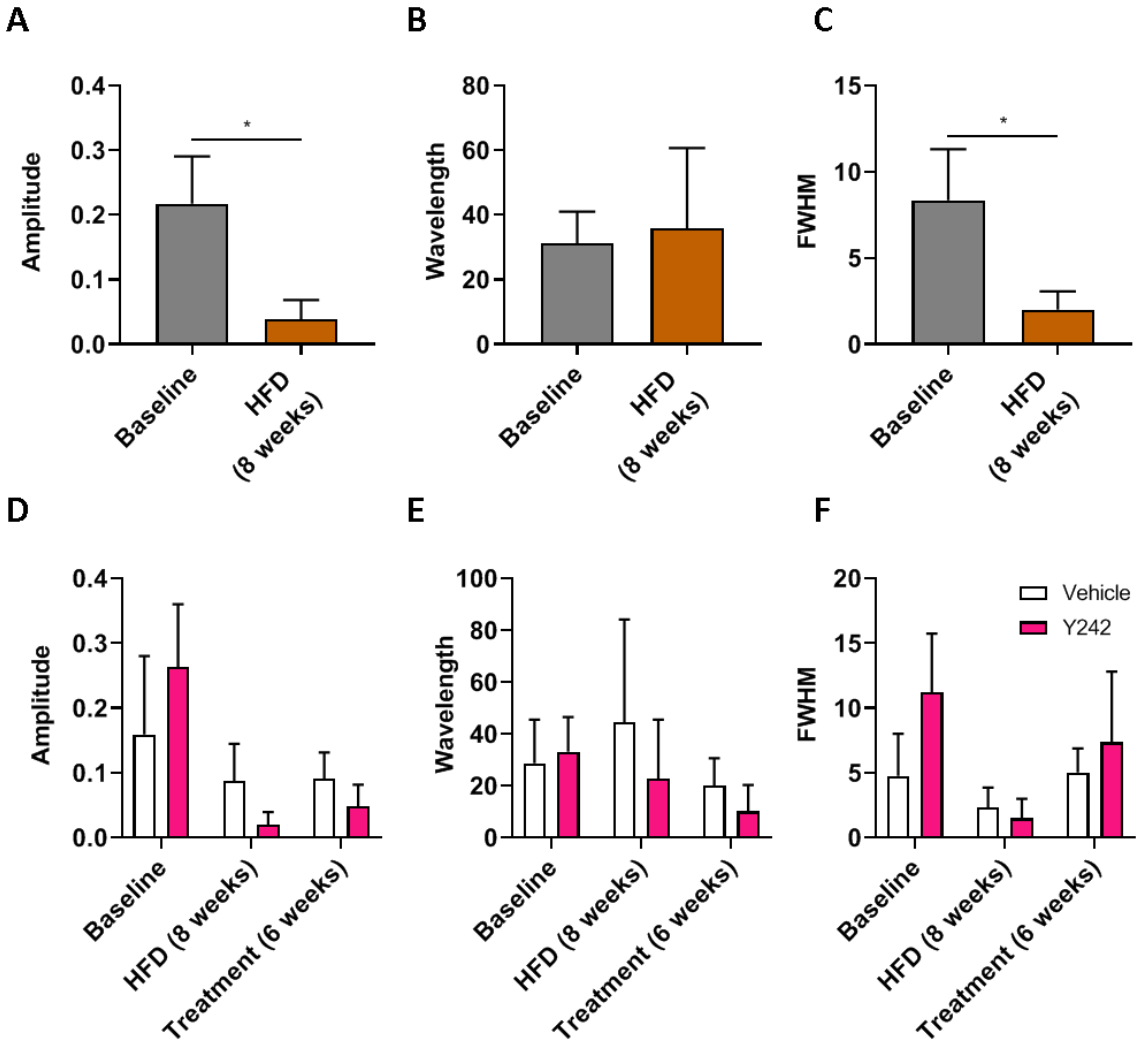

Figure 4.4.5.2. Longitudinal waveform analysis of GCaMP6f-fluorescence islets transplanted into the ACE of DIO mice.

Amplitude (A), wavelength (B) and FWHM (C) are shown at baseline (session 1, n= 9) vs after 8-week HFD (session 2; n = 13-5). Amplitude (D), wavelength (E) and FWHM (F) are shown in Y242 and vehicle groups in session 1 (before diet intervention / start of chronic treatment; n = 5-4 islets/group), session 2 (before start of chronic treatment; n = 6-9 islets/group) and session 3 (after start of treatment; n = 7-10 islets/group). A, C: Student's *t* test (*$p < 0.05$). FWHM, full width at half maximum.

4.5 Discussion

The experiments in this chapter aim to study the effects of chronic treatment with a PYY_{3-36} analogue, named Y242, on energy and glucose homeostasis in DIO mice. Islet function was investigated in response to HFD and Y242 treatment using an islet-in-eye platform. The novelty of this study relies on the application of a novel imaging platform to perform longitudinal functional readouts of the same islets and represents the first study on the effects of chronic Y2R activation on pancreatic islet function.

At the start of the study, obesity was induced by feeding lean mice with HFD. After 8 weeks of HFD, mice showed glucose intolerance and an increased body weight. Mirroring these results, there was a reduction in β-cell calcium activity, in accordance with the hypothesis that β-cell function can be longitudinally measured by *in vivo* imaging of islet in the ACE. We hypothesised that chronic administration of Y242 would reduce body weight. Chronic treatment with Y242 induced mild weight loss that did not reach significance (in part due to the high variation in the vehicle group) and did not alter cumulative food intake. Importantly, in lean wild type animals, food intake was significantly reduced immediately after administration of 25% of the Y242 dose used in the chronic study. This suggests that Y242 produces an acute anorectic effect. We conjectured that Y242 would alter β-cell function in obese mice. Y242 did not alter glucose tolerance at any point after the start of chronic treatment. In addition, islet function was not altered by Y242 treatment. Taken together these results suggest that treatment with the Y2R antagonist Y242 at 200 nmol/kg may cause mild weight loss but did not improve (or worsen) glucose tolerance or alter islet function in DIO mice.

4.5.1 Diet-induced obesity triggers impaired glucose tolerance and a reduced glucose disposal

C57BL/6J mice are widely used to study DIO and, as expected, HFD caused impaired glucose tolerance in these DIO mice. It is well accepted that overnutrition impairs glucose tolerance and induces insulin resistance, which is initially compensated by increasing insulin secretion from β-cells, but subsequently the compensation is insufficient to normalise blood glucose and T2D results. However, eight-week HFD did not induce insulin resistance in an IPITT. It is possible that a longer period after HFD intervention would be needed to observed differences in insulin responsiveness, and differences in mouse strain can also lead to conflicting results (Fergusson *et al.*, 2014; Siersbæk *et al.*, 2020). It has been recently suggested that C57Bl/6J sub-strain fed with 60% fat diet are more insulin sensitive than other C57Bl/6 sub-strains (Siersbæk *et al.*, 2020). Overall, these indicate that the hyperglycaemia

observed in DIO mice in this experiment was probably due to impaired insulin secretion from pancreatic islets.

Insulin secretion was not measured but we indirectly studied islet function by assessing calcium activity of islets transplanted into the ACE. HFD intervention caused a reduction in calcium activity of the transplanted islets. This was observed in wave index analysis as well as in the amplitude and FWHM of calcium traces. This is in agreement with another longitudinal study that showed changes in the calcium activity of GCamp3-expressing islets engrafted in the eyes of DIO mice (Chen *et al.*, 2016). Importantly, a recent study from Benninger's group has shown that HFD reduces the amplitude, and a reduced number of cells are coordinated in the obese state (do Amaral *et al.*, 2020). This was due to a reduced gap junctions-mediated coupling between β-cells as well as in connexin Cx36, a key protein in β-cell coordination (Carvalho *et al.*, 2012; do Amaral *et al.*, 2020). A mechanism involving Cx36 might mediate the impact of diet in islet function in this study but connectivity was not studied in this study.

The mechanisms underlying obesity-induced β-cell failure have not been fully elucidated but lipids are potent stimulators of GSIS and glucagon secretion and they are considered an important link between obesity and diabetes (Imai *et al.*, 2019). Indeed, overnutrition alters islet size (Vernier *et al.*, 2012) and lipotoxicity impairs connectivity and abrogates incretin effect (Hodson *et al.*, 2013). Chronic exposure to HFD triggers β-cell remodelling and impairs insulin secretion and it is a major contributor to T2D (Christensen *et al.*, 2019). Palmitic acid is an abundant lipid in the body and is a potent stimulator of GSIS, but overexposure to this lipid inhibited GSIS due to defects in calcium mobilization (Hoppa *et al.*, 2009). Stress pathways and mitochondrial dysfunction have been suggested to further contribute to impaired β-cell function in overnutrition (Imai *et al.*, 2019; Christensen *et al.*, 2019).

To summarise, chronic exposure to lipids, as occurs in DIO, can impair insulin production and secretion. This study detected this impaired insulin secretion in HFD-fed mice by indirectly measuring calcium dynamics in islet implanted in the ACE. This indicates the opportunities provided by this islet-in-eye platform to study the effect of different nutrient-related states or drugs in the endocrine pancreas.

4.5.2 Long-acting Y2R agonism causes a non-significant reduction in body weight and does not alter total food intake or glucose homeostasis

Chronic treatment with the long acting PYY analogue Y242 in DIO mice did not alter total food intake, and body weight loss was mild (it did not reach significance). In contrast, acute Y242 in lean mice (at

50 nmol/kg) had a strong anorectic effect. Several studies have shown that animals and humans respond to exogenous PYY_{3-36} in both lean and obese states (see section 1.5.3), so this difference is unlikely to be due to the nutritional status.

At the beginning of treatment, all mice are acclimatising daily injections and the loss in body weight is potentially caused by stress. As they get used to it, body weight stabilised in both groups (day 5-10). From that point, the body weight of Y242-treated animals remains low compared to vehicle treated animals. The body weight in vehicle group drops slightly at around day 15 but seems to increase progressively from day 2. Despite we cannot draw conclusions due to the high variability and the subtle effect of Y242 in body weight, we hypothesise that the continuation with Y242 is counteracting the hyperphagia that could be caused by the initial reduction in body weight. We could not measure energy expenditure or activity but this could help explain this data.

The overall reduced body weight in the vehicle group (receiving saline with zinc chloride) as well as the high variability is probably masking the effect of Y242 in body weight. It is possible that the reduction in body weight of the control group is caused by zinc. Zinc has been shown to reduce body weight and insulin resistance in obese subjects (Khorsandi *et al.*, 2019) and inhibits POMC neurons, which would alter feeding and glucose metabolism (Qiu *et al.*, 2014). However, zinc chloride has been used to enhance peptide depot formation and help the sustained release of peptides in human and rodent studies (Ratner *et al.*, 2010; Price, Minnion & Bloom, 2015) and, to my knowledge, there are no reports on zinc chloride causing weight loss in these settings.

PYY_{3-36} can reduce food intake and body weight by causing aversion in rodents depending on the dose (Chelikani, Haver & Reidelberger, 2006; Halatchev & Cone, 2005). In this study a CTA was not performed but it is unlikely that chronic Y242 caused aversion as cumulative food intake was not altered by the treatment and no behavioural effects were observed. Other studies in rats have suggested that PYY_{3-36} reduces caloric intake during the infusion interval, and that compensatory hyperphagia during non-infusion depends on the interval period and dosing pattern (Chelikani *et al.*, 2006; Chelikani, Haver & Reidelberger, 2007). However, the Y242 profile of action lasts 72 hours, much longer than PYY (unpublished data). We do not observe a reduction in food intake in the Y242-treated mice at any point. The effect of chronic Y242 in body weight was mild so it is possible that the differences in food intake were subtle and were not detectable within the limits of our methods. Further investigation on the effects in food intake of acute administration of Y242 for more than 72 hours could help clarifying why we do not observe a reduction in food intake in the chronic study. It is

possible there was a rebound hyperphagia and measuring food intake more frequently (e.g., at 8 h post-injection) would have been useful. For reasons of time, this project was not focussed on the anorectic element of this agent. Instead, this experiment was designed (based on previous observations) to use Y242 chronically to induce mild weight loss in order to establish its weight-loss independent effects on islet function.

Previous studies have tested the effect of exogenous chronic PYY_{3-36} treatment in energy homeostasis in obese rodents and have obtained similar outcomes (Pittner *et al.*, 2004; Adams *et al.*, 2006; Vrang *et al.*, 2006). In *ob/ob* mice, continuous infusion of PYY_{3-36} via osmotic pump reduced body weight without altering food intake or glycemia (Pittner *et al.*, 2004). In DIO C57Bl/6J mice infused with PYY_{3-36} for 28 days, the median effective doses of PYY_{3-36} were 466 µg/kg/day and 297 µg/kg/day to observe a reduction in cumulative food intake and in body weight, respectively (Pittner *et al.*, 2004). In other study in DIO mice, chronic PYY_{3-36} infusion also reduced body weight but only the highest dose (1000 µg/kg/day) altered food intake (and only on the first day of treatment) (Vrang *et al.*, 2006). Several experiments in obese and/or diabetic rodents (Vrang *et al.*, 2006; Adams *et al.*, 2006; Pittner *et al.*, 2004) have observed that PYY_{3-36} reduced body weight but that the effect in food intake was transient. Intermittent i.v. in lean rats (Chelikani *et al.*, 2006) or intermittent i.p. injection of PYY_{3-36} in DIO rats (Chelikani, Haver & Reidelberger, 2007) achieved a more sustained reduction in daily food intake. In this study, Y242 was administered by once-daily s.c. injection so it cannot be directly compared to the protocols used in these previous studies. However, all these studies indicate that chronic exogenous Y2R agonists can decrease body weight in different models and using different doses, but that food intake reduction is highly dependent on the dosage and the administration pattern. These studies might also indicate the difficulty in observing reduced food intake by weighing food once daily in chronic PYY_{3-36} treatments and high-resolution food intake measurements might be needed.

The transient reductions in body weight could be limited by altered appetite signalling or due to a desensitisation of the receptors, which is the reduction in response after prolonged or repeated administration of an agonist. Desensitisation can be homologous or heterologous (Kelly, Bailey & Henderson, 2008; Rajagopal & Shenoy, 2018). Homologous desensitisation occurs when the receptor causes loss of responsiveness to an agonist present at high concentration. In contrast, heterologous mechanisms attenuate receptor responsiveness independently of agonist binding and can affect multiple GPCR subtypes. Phosphorylation of the receptor is key in both mechanisms and can be mediated by different kinases (e.g., G-protein receptor kinases (GRKs) in homologous desensitisation). According to the classical view, the phosphorylated receptor is recognised by arrestins that inhibit

coupling to G-proteins resulting in desensitisation. Arrestins recruit other proteins (e.g., clathrin) and this is followed by internalisation. The receptor is dephosphorylated and recycled to the plasma membrane (resulting in resensitisation). In case of long-term stimulation, the arrestin/phosphorylated-GPCR complex can be targeted to lysosomes resulting in a reduction of receptor expression in the plasma membrane (downregulation). These processes result in tachyphylaxis. Y2R desensitisation was observed in rodent chronically treated with a PYY analogue (Ortiz *et al.*, 2007). It is possible that lower doses and/or less frequent administration of Y242 would be needed to observe an effect in cumulative food intake. Biased agonism is the ability of ligands acting at the same receptor to activate a distinct subset of signalling pathways by stabilising different conformational states of the receptor. Using this approach, drugs could be designed so that arrestin recruitment and internalisation are reduced or that receptor recycling is increased. Biased agonist could allow to increase the efficacy of agonist, as has been suggested for GLP-1R (Jones *et al.*, 2018), and to avoid off-target effects, such as in the case of ghrelin (Nagi & Habib, 2021). Y242 full pharmacological characteristics are not discussed since this peptide is part of a confidential drug discovery line.

In addition, previous studies in my group have shown that chronic treatment with PYY_{3-36} or analogues in obese rodents causes only a temporal reduction in body weight that return to initial body weight overtime and, if treatment is stopped during the period in which body weight is reduced, hyperphagia and increased body weight are observed (unpublished data). This indicates that Y242 alone is not an effective weight loss therapy but in conjunction with other gut hormones can contribute to weight loss.

Mice overexpressing PYY were protected against diet-induced obesity and showed increased thermogenesis (Boey *et al.*, 2008). Importantly, an increase in locomotor activity in PYY_{3-36}-treated DIO rats was also observed, and this could cause the increased weight loss (Vrang *et al.*, 2006). We were not able to measure locomotor activity or energy expenditure in the Y242-treated DIO mice..

We compared glucose tolerance of Y242-treated mice versus vehicle-treated mice at two different times (day 16 and day 40) during chronic treatment. In each of these days, we have not observed an effect of chronic Y242 in glucose tolerance compared to vehicle. This is in agreement with other studies in which chronic infusion with PYY_{3-36} did not have a significant effect in DIO rats and caused an increased in glucose tolerance OGTT only at the highest dose (1000 µg/kg/day) in DIO mice (Vrang *et al.*, 2006). In humans, PYY_{3-36} infusion did not improve glucose homeostasis in the fasted state

(Batterham *et al.*, 2002, 2003a; Sloth *et al.*, 2007). In contrast, Chandarana and colleagues showed that exogenous PYY_{3-36} improved glucose tolerance via acting on the Y2R, albeit this was mediated by post-prandially increasing hepato-portal GLP-1 (Chandarana *et al.*, 2013). We have not measured GLP-1 levels in plasma or in hepatic portal vein but benefits of combining PYY and GLP-1 have been previously observed in humans (Neary *et al.*, 2005; De Silva *et al.*, 2011; Schmidt *et al.*, 2014).

When comparing the effect of time in the chronic treatment, glucose tolerance tests at day 16 and day 40 of Y242 treatment differed only at 60 min after glucose administration suggesting a technical issue at this time point. We expected that blood glucose curves of vehicle treated mice would be similar at day 16 and day 40 of treatment but the glucose profile where slightly different, suggesting that other confounding factors in the experimental procedure (e.g., stress) might influence the results. A longer study with another glucose tolerance test at a later time would be required to confirm if Y242 chronic treatment has a true detrimental effect in glucose tolerance. However, we do not expect that a longer Y242 would alter glucose homeostasis.

After oral glucose, chronic PYY_{3-36}-infused DIO rats showed increased plasma insulin (Vrang *et al.*, 2006). We cannot directly compare our results with this study. However, our islet function data do not indicate an increase in calcium oscillation after 6-week Y242 treatment in DIO mice. This approach has been clearly demonstrated by our group to highlight the effects of raising glucose on islet function, as well as the effects of bariatric surgery and GLP-1 (unpublished). In agreement with this, PYY_{1-36} does not alter cytoplasmic calcium concentration despite inhibiting insulin secretion in perifused islets (Nieuwenhuizen *et al.*, 1994). In addition, no effect in insulin secretion was observed in PYY_{3-36}-treated mouse islet despite an increase in plasma insulin post-injection (Chandarana *et al.*, 2013). The gold standard to measure insulin sensitivity is the hyperinsulinemic-euglycemic clamp technique, which maintains hyperphysiological plasma insulin levels and physiological glucose levels by a variable glucose infusion rate. In diabetic obese rats, chronic PYY_{3-36} infusion showed a trend towards an increased insulin sensitivity (Pittner *et al.*, 2004). HFD-fed mice i.v.-infused with PYY_{3-36} during the clamp showed an improved insulin sensitivity but this was not observed in basal conditions (before the clamp) (Van Den Hoek *et al.*, 2004). However, the postprandial levels of PYY_{3-36} in the mouse are unknown and therefore these data do not confirm that physiologically occurring PYY_{3-36} reinforces insulin action.

Other Y2R agonists have been designed and tested as chronic treatments for obesity and diabetes. A long-acting PEGylated PYY_{3-36} analogue administered once-daily showed a dose-dependent reduction

in body weight in a 14-day period (Ortiz *et al.*, 2007). As observed in other studies, the effect of the PEGylated peptide in food intake during chronic treatment was transitory. More recently, a long-acting antibody-conjugated PYY_{3-36} analogue was shown to reduce body weight and reduce fasting insulin while being more tolerated than a PEGylated analogue (Rangwala *et al.*, 2020).

Studies on the effect of long-acting Y2R agonists not only depend on their design and the pharmacological characteristics of the peptides, but also on the animal model, the diet composition and the route, dose and frequency of administration. While some studies have performed subcutaneous injection others use osmotic pumps, which can infuse continuously or intermittently. Some studies have used *ob/ob*, *db/db* and Zucker diabetic rats, which lack leptin or are insensitivity to leptin. DIO models are a better representation of obesity-diabetes. Taken together, this study has shown that Y242 treatment in DIO mice did not cause changes in cumulative food intake or in glucose tolerance, which agrees with previous reports, and triggered a mild non-significant reduction in body weight. This beneficial effect of Y2R agonism could be amplified by increasing the dose (while avoiding aversion), modifying the peptide structure to increase potency, or by combining it with other gut hormone analogues (e.g., GLP-1 analogues) or other weight-loss approaches, such as inulin proprionate ester.

4.5.3 Limitations of this study and future work

This study has used a longitudinal and direct imaging platform that allows in vivo study of islet insulin secretion. This method successfully detected the diet-induced changes in β-cell activity. Connectivity between β-cells is lost in HFD-fed mice and is recovered after caloric restriction (do Amaral *et al.*, 2020). It would be of interest to assess connectivity by single-cell analysis of calcium fluorescent islets in the ACE (Salem *et al.*, 2019).

Several studies have suggested that exogenous PYY_{3-36} regulates insulin sensitivity and secretion. Although, *in vitro* perifused islet approaches have been used to study the effect of different stimuli in insulin secretion, Y2R expression in islets is controversial and it is more likely that Y2R agonists have an indirect effect in insulin secretion. To overcome this, we used a method based on islets engrafted in the anterior chamber of the eye, where they are vascularised and innervated. We expected that this more physiological approach would detect changes in β-cell secretion after Y242 treatment. However, Y242 treatment did not have a detectable effect on islet secretory activity in the islet-in-eye protocol used in this study. Since PYY regulation of insulin secretion might depend on glucose levels, it is possible that differences in islet activity would be observed after previous administration of a

glucose bolus. These studies should be supplemented with more information about insulin secretion and and insulin action during an *in vivo* clamp experiment.

Previous studies (Pittner *et al.*, 2004; Vrang *et al.*, 2006) have shown stronger effects in food intake (at least transiently) and body weight with continuous infusion of PYY_{3-36}. Therefore, the maximum effect of Y242 might not have been observed at this dose due to the low frequent administration. Future experiments should explore the metabolic effects of other doses and dosage patterns of Y242 or similar peptides, like Y3394 (a PYY analogue more potent than Y242 recently developed by Imperial College London). Future experiments should control the plasma levels, as well as in hepato-portal vein, of the PYY analogue and GLP-1 (Chandarana *et al.*, 2013). Chronic treatment with PYY_{3-36} can reduce adiposity (Pittner *et al.*, 2004; Adams *et al.*, 2006; Vrang *et al.*, 2006; Chelikani, Haver & Reidelberger, 2007) but adiposity could be not be quantified in this study. Therefore, the potential beneficial effects of Y242 in metabolism could be further explored by body composition screening.

Future experiments could assess if chronic exogenous PYY_{3-36} analogues can affect energy expenditure in metabolic cages, which will perform indirect calorimetry as well as monitor activity. This would clarify if compensatory hyperphagia occurs after the effects of Y242 disappear, or if Y242 alters meal patterning without altering total intake.

It is unknown whether Y2R analogues in combination with other long-acting gut hormone analogue could have resulted in a more potent weight loss effect or glycaemic improvement. Future experiments could examine the effects of co-administration of Y242 with a GLP-1 analogue that might supplement the PYY-induced weight loss with a more potent effect on glucose tolerance and insulin responsiveness.

Chapter 5: Final discussion

Gut hormones have been identified as key regulators of glucose metabolism, gastrointestinal secretory function and motility, food intake and long-term energy homeostasis. These hormones are potential targets for weight loss and type 2 diabetes treatments, as exemplified by the licensing of GLP-1 analogues to treat diabetes and latterly obesity in the absence of diabetes (Pi-Sunyer *et al.*, 2015). Since gut hormones are endogenously secreted, and underpin the body's natural mechanisms to limit overconsumption, they are more promising than previous appetite suppressing drugs, such as sibutramine and rimonabant, which have been removed from the market due to dangerous off-target effects. This highlights the complexities of the systems and receptors involved in moderating appetite and energy expenditure and the need for research into these pathways in order to pick out the safest and most effective targets for drug development. Bariatric surgery is still the most effective treatment for obesity but it is costly and involves risks for the patient. Recent research has suggested that increased circulating gut hormones contribute to the beneficial effects of bariatric surgery. This further supports the concept of peripheral administration of gut hormones to mimic the post-bariatric surgery conditions as an effective and safe therapeutical approach.

In order to target the gut hormone system for therapy, we need to better understand the pathways involved. Much of the earliest work into gut hormone signalling focused on the endocrine actions on the central nervous system. Latterly it became apparent that the vagus nerve might be particularly important as a conduit for the neuroendocrine effects of gut hormones and, since vagal afferents are in such close proximity to the site of release of gut hormones, the concept of a paracrine role of gut hormones on nervous activity has grown. Furthermore, whilst many of the aversive (nauseating) effects of high doses of gut hormones are clearly related to activity in central appetite/chemosensory areas, it remains unknown as to whether targeting the vagus may avoid these effects and provide a better site for targeting gut hormone action to maximise food intake reduction without inducing nausea.

The role of the vagus nerve in the gut-brain axis is complex and recent approaches are allowing us to begin to understand the function of different neuronal populations of the afferent vagus nerve. A major advance has been to differentiate afferent and efferent signalling. In this thesis we have developed a model to start to interrogate the interaction between gut hormones and afferent vagal signalling, which transmits sensory information from the gastrointestinal tract to the brain. By genetically altering vagal afferent neurons, we aimed to understand the role of vagus nerve activity in feeding behaviour (Chapter 2), with great focus on the gut hormone PYY_{3-36} (Chapter 2 and 3). The PYY_{3-36}/Y2R signalling in vagal afferents is expected to be involved in the short-term regulation of

feeding. To study the benefits of PYY_{3-36} treatment in long-term energy homeostasis, diet-induced obese mice were treated with a long-acting PYY_{3-36} analogue, Y242, and the effects in body weight and pancreatic islet function were assessed. Apart from its role in feeding and energy homeostasis, the vagus nerve has been linked to other physiological roles. Vagus nerve activity modulation is an interesting therapy for a range of conditions, including obesity, but the mechanisms of action remain unclear. In essence, the use of vagal nerve stimulation is in its infancy, since we still have very little nuanced understanding of the different firing patterns involved with different physiological roles of the vagus and we are not yet able to fine tune vagal nerve manipulation in order to recreate or upregulate certain desired effects. This brings into focus the importance of research aimed providing a more detailed understanding of the actions of the vagus.

With the development of a new microsurgical technique to interrogate vagal function during my research, it became of interest to me to apply this technology to important questions regarding vagal effects on gut physiology. We chose to investigate the effect of chronic vagal afferent activation (using chemogenetics) in lamina propria immune cell populations in order to see whether this technique can be applied to understanding the interaction between afferent vagus nerve and gut immunophenotype. This feeds into a new area of intense research into the immune regulation of the gut, which has been found to be relevant not just in obesity but a broad range of other human disease processes including inflammatory bowel disease and food allergy. If successful this new approach could provide an excellent tool for this type of research. An important limitation of this pilot experiment is the lack of confirmation of hM3Dq expression in the vagus nerve. However, the profound effect of the DREADD ligand in acute food intake, added to the high success rate of viral gene knockdown and GFP expression by injecting in the NG, suggest that most animals have some level of DREADD expression in NG.

Although the low sample size did not provide significant effects, this pilot experiment revealed a convincing trend for vagal afferent activation to reduce the numbers of innate cells, i.e., ILCs, as well as immune cells of the adaptive system, such as T_{reg} cells, which are key in maintaining tolerance within the wall of the gut. Potential underlying mechanism are that vagal activation enhances the number of cells leaving the lamina propria or that it increases apoptosis. In addition, the activation of the vagus nerve might alter the secretion of factors that can inhibit or activate immune cells as well as altered the activity of other neurones, such as the ENS. The role of specific neuropeptides and cytokines in the action of ILC in intestinal barrier is of great interest. Apart from the lamina propria, the muscularis

should also be immunophenotyped as mast cells and resident macrophages in this layer are also potentially altered by vagal neuromodulation.

In addition, it is likely that genetically defined vagal afferent populations have specific roles of genetically defined vagal afferent populations, such as nociceptors (Talbot *et al.*, 2015). Due to the important role of the vagal efferent arm in the anti-inflammatory reflex, this data could be supplemented by assessing the immunophenotype after activating vagal efferents by inducing DREADD expression in the DMX or DVC. It is possible that the effects we have observed are a result of the communication of vagal afferents with the brainstem and the output from the vagal efferents. Since the crosstalk, whether direct or indirect, between vagal afferents and immune cells is likely dependent on the context and the immune challenge, it would be interesting to explore the effect in gut immune cells of vagal chemogenetic modulation in the context of inflammation, such as food allergy models or high-fat diet.

One of the main aims of this project was to investigate the role of the vagus nerve in mediating the anorectic effect of the gut hormone PYY_{3-36}. The vagus nerve is suggested to be involved in the signalling of other anorectic gut hormones secreted from enteroendocrine cells, such as CCK and GLP-1. PYY is released postprandially from L-cells and exogenous peripheral PYY_{3-36} suppresses appetite in humans and rodents. Interestingly, PYY_{3-36} retains its anorectic effect in obese subjects. This suggests that PYY_{3-36} can be a potential target for weight loss but its mechanism of action remains unclear. Although a central pathway of action was originally suggested (Batterham *et al.*, 2002), the receptor of PYY_{3-36} Y2R is also expressed in the vagus nerve suggesting it also plays a role in the mechanism of action of PYY_{3-36}. PYY_{3-36} increased the calcium activity of nodose ganglia neurons in culture. This suggest that vagal Y2R couples to Gq upon PYY_{3-36} binding resulting in IP_3-dependent calcium release. This is in contrast to previous reports that Y2R in the brain works as a presynaptic autoinhibitory receptor. Our observations should be further confirmed in Y2R vagal afferents expressing GCamP as well as by cAMP assays.

For the first time, we have presented a study of the effect of bilateral vagal afferent-specific activation in awake animals using chemogenetics. Activation of all vagal afferent neurones suppressed food intake, as observed in acute feeding studies, and resulted in a reduction in body weight. The effect in food intake after DREADD ligand administration was profound whereas effect of the ligand in non-DREADD control animals showed an attenuated feeding suppression. Future studies could adjust the dose and administration pattern of the DREADD ligand to avoid the off-targets effects. Since

chemogenetic activation of the afferent vagus resulted in such a large effect on food intake, it is unclear whether the lack of any further effect of PYY_{3-36} in this situation is because the PYY_{3-36} vagal afferents were already activated or because any effect was masked. It is possible that afferent vagus activation directly or indirectly (maybe via the brainstem and vagal efferents) caused an increase in anorectic gut hormones levels. An increase in circulating anorectic gut hormones was observed in VNS-treated rodent (Dai, Yin & Chen, 2020). Independently of the potential involvement of other gut hormones, overall, these suggest that PYY_{3-36} suppresses food intake by activating the afferent vagus nerve. Future studies could use this chemogenetic approach to explore the effect of specific Y2R-expressing vagal afferents activation and inhibition, in food intake, gastric emptying and meal pattern, also to supplement our data in models with vagal Y2R disruption.

Vagotomy blunts the anorectic effect of exogenous PYY_{3-36} in rats suggesting a role of vagus nerve in mediating PYY_{3-36} actions (Abbott *et al.*, 2005a; Koda *et al.*, 2005). However, vagal lesioning has many off-target effects and it is unclear if the vagus nerve is truly required for mediating PYY_{3-36} effects. In this work we have used different models to more specifically disrupt the vagal Y2R. One of the mouse models was based on Nav1.8-drived Y2R knockout. However, germline models can develop compensatory mechanisms and this approach was semi-specific (as Nav1.8 is expressed in other parts of the nervous system). To overcome this, we generated a novel mouse model based on the microinjection of Cre-expressing AAV into the nodose ganglia of Y2R floxed adult mice. This allows the super-selective genetic alteration of vagal afferents subpopulations of adult mice as a recovery procedure.

We hypothesized that low doses of peripherally-administered PYY_{3-36} would mirror the effects of endogenous PYY_{3-36} and that it suppresses appetite via the vagus nerve. In contrast, higher doses of PYY_{3-36} would have central actions due to the higher probability of brain penetration and also the aversion effect previously reported (Halatchev & Cone, 2005). We observed a dose response to PYY_{3-36} in terms of a reduction in food intake of freely fed control mice in the early dark phase. The trend for a reduction in food intake with low dose PYY_{3-36} was reproducible although with the numbers used in my experiments this did not consistently reach significance (chapter 2 and 3). It is possible that increasing the sample size or that performing acute feeding studies in fasted animals could result in a more considerable food intake suppression after the low dose of PYY_{3-36}. On the other hand, this low dose did not significantly reduced food intake in any feeding paradigm in other study in mice (Halatchev *et al.*, 2004). Exogenous PYY_{3-36} at the used doses has a moderate anorectic effect and acts

only for a short period of time so stress can mask its effect in food intake, although animals were accustomed to i.p. injections before feeding studies (Halatchev *et al.*, 2004).

Disruption of Y2R in adult mice by injection of Cre-expressing virus in the NG resulted in a reduced Y2R gene expression but there was not a complete disruption and, therefore, some vagal PYY_{3-36} signalling remains. Despite this, we observed a blunted food intake suppression in response to low dose in vagal Y2R KD animals. This phenotype was supported by the similar observation in Nav1.8-driven Y2R KO. Moreover, induction of endogenous PYY release suppressed food intake in control mice but this was attenuated in mice with disrupted vagal Y2R signalling, despite the likely activation of mechanoreceptors as well as secretion of other gut hormones.

Vagal Y2R might be mediating the anorectic effect of low dose PYY_{3-36} by activating neurons of the caudal NTS and AP, as suggested in Nav1.8-driven Y2R KO mice. These neurons could further communicate with higher brain centres and other brainstem centres to generate an output response. However, no definitive conclusions regarding brainstem neuronal activation in response to endogenous or exogenous PYY_{3-36} can be made due to the sample size. Detecting c-Fos increase in brainstem after PYY_{3-36} has shown to be challenging and this might be due to the doses used, the feeding state of the animal, the stress during the procedure or that PYY_{3-36} uses different mechanisms to other satiety hormones (Halatchev *et al.*, 2004). No differences in brainstem neuronal activation were observed after inducing endogenous PYY release. Again, this could be partly due to the low sensitivity of c-fos quantification and the fact that this experiment was underpowered. Oral gavage of a nutrient bolus activates several vagal receptors, both mechanoreceptors and chemoreceptors, and this could potentially mask the PYY-induced increase in c-Fos of brainstem neurons. Future studies should evaluate c-fos expression in other brain centres in the vagal Y2R KD model, such as ARC and other hypothalamic nuclei as well as reward centres previously involved in gut hormone-mediated appetite suppression (Han *et al.*, 2018).

Gut hormone-mediated anorectic effects can also be due to a non-physiological pathway that involves nausea (in humans) or aversion (in rodents), as has been shown for PYY_{3-36} (Halatchev & Cone, 2005). Nausea or aversion are considered at the end of the satiety spectrum and are activated when anorectic stimuli cross a threshold (e.g., high dose of infused gut hormone). Nausea effect is one of the main limitations of gut hormone infusion as an anti-obesity treatment and it is likely due to the access of these gut hormones to central circuits. A conditioned taste aversion study of the doses used in this work showed that the appetite suppression caused by exogenous PYY_{3-36} at the doses used in this work

was not mediated by visceral illness. PYY_{3-36} at high dose might act directly in the hypothalamus or brainstem to suppress food intake but aversion is not induced. Finally, it is worth considering that our assumption of the differential actions of low dose (physiological) and high dose (pharmacological) effects of PYY_{3-36} may be overstated. For example, if we suppose that PYY_{3-36} physiologically acts locally on vagal afferents, then a low dose administered peripherally may not actually be arriving at the nerve terminals of interest.

It is possible that exogenous PYY_{3-36} causes a reduction in food intake at least partly by delaying gastric emptying. Indeed, vagal Y2R disruption accelerated gastric emptying. In addition, vagal Y2R disruption resulted in smaller and shorter meals with shorter time between meals. The mechanism underlying this change in meal patterning needs to be elucidated. However, these data suggest that animals are feeling satiated faster after a food intake start. This is surprising since Y2R is involved in food intake suppression postprandially and vagal Y2R disruption could be expected to delayed meal termination. After a meal, mice with disrupted vagal Y2R signalling are hungry earlier resulting in an increase in shorter inter-meal durations (i.e., more frequent meals) in a mechanism in which gastric emptying might be involved. It is possible that vagal Y2R knockdown alters signalling in other brainstem centres In support of these results, the disruption of other gut hormone receptors, including the vagal GLP-1R, also alters gastric emptying and meal patterning (de Lartigue, Ronveaux & Raybould, 2014; Krieger *et al.*, 2016; Davis *et al.*, 2020). It is also possible that the tendency for more meals is caused by the increased ambulatory activity. However, the mechanism underlying increased ambulatory activity remains to be elucidated. NPY signalling could have increased, maybe via other YRs, resulting in this increased ambulatory activity (Edelsbrunner *et al.*, 2009). Future studies should characterize the expression of other neuropeptides and gut hormone receptors in the vagus nerve as well as in brainstem. In addition, changes in circulating gut hormone levels might also underlie the change in meal patterning.

Although it has been assumed that vagal afferents expressing gut hormone receptors are chemoreceptors by responding to EEC-derived gut hormones, this has been recently challenged by the mechanosensing role of the *Glp1r* vagal afferent population (Williams *et al.*, 2016; Bai *et al.*, 2019). In addition, vagal afferent populations could have unexpected functions, such as the role of *Oxtr* vagal afferents in communicating with GLP-1 secreting PPG neurones of the NTS (rather than the *Glp1r* population) (Brierley *et al.*, 2021). Therefore, the disruption of vagal Y2R could have altered other pathways that are contributing to the altered meal patterning.

The experiments performed in this work are very selective, knocking down signalling in only one portion of a highly complex neuroendocrine circuit, might not be expected to have a large effect on phenotype and these experiments are able to pick out the individual effects on certain parameters. This is also mirrored by the subtle differences observed in acute feeding response to exogenous and endogenous PYY_{3-36}. Importantly, even a mild reduction in food intake can be physiologically or clinically relevant. This work suggests that vagal PYY_{3-36} signalling is involved in the satiety feeling in the short-term but not in the long-term control of energy homeostasis. This is supported by the fact that vagal Y2R disruption in the adult mouse did not alter body composition, body weight (at least after full viral expression), energy expenditure or total food intake. Future experiments should further dissect the roles of left versus right vagal afferents as well as the higher brain centres involved in the signalling pathway of interest. It is possible that is not necessary to inject in both NG sides as well as that distinct pathways can be investigated by targeting left or right vagal afferents (Han *et al.*, 2018).

We have established a surgical technique in mice that allows unprecedented insights into the function of the vagus nerve and that can be used to advance in understanding the role of vagal afferent subpopulations. This concept was previously established in rats at ETH Zurich and we have optimised it in mice. This method it is an advance in terms of the 3Rs principles (Replacement, Reduction and Refinement). In order to minimise harm and improve welfare, minimal manipulation of the vagus nerve during the exposure, tissue retraction and injection. Perioperative care was refined to avoid the effects of vagal over-activation on the heart by administration of atropine, an antagonist of the muscarinic receptors. After surgery, animals were kept in social groups and in an enriched environment. This technique is less invasive than vagal lesioning surgeries (e.g., vagotomy) and, in addition, allows the specific deletion of a gut hormone receptor, in this case the Y2R, without causing neuronal death. Injections in the nodose ganglia were performed in side in two different sessions allowing recovery in between. This was due to the higher mortality rate observed when over-manipulating of the vagus nerve, which can lead to abnormal autonomic function and altered heart rate in the acute postoperative and recovery period. The duration of the surgery was notably reduced also contributing to the high survival rates (almost 100%). In addition, our methodology involves the analysis of expression or knockdown rate in each nodose ganglion, which minimise the number used in each experiment.

PYY_{3-36} is rapidly cleared from the circulation and has a short half-life, e.g., 13 min in mouse (Nonaka *et al.*, 2003). From a therapeutical perspective, this limits the efficacy and makes administration difficult. The development of gut hormone analogues with increased bioactivity or half-life has deserved extensive research. We have focused on the long-term PYY_{3-36} analogue Y242. In lean

animals, Y242 strongly suppressed appetite for more than 8 hours after injection. In obese, glucose intolerant animals, chronic Y242 slightly reduced body weight on the first days (during dose ramping) but 200 nmol/kg/day of Y242 did not achieve a significant weight loss by the end of the chronic treatment (around 40 days). Since PYY_{3-36} retains its anorectic activity in obese subjects we expect that the bioactivity of Y242 is similar in the obese state. Daily food intake did not change. It is likely that there is a compensatory hyperphagic response to Y242 injection (later than 8 h-post injection) that the methodology used in this work could not detect. Measuring food intake more frequently could clarify this. However, the main aim of this project was not to study the effect of Y242 in short-term feeding but its ability as a weight loss agent.

The mechanism underlying the reduction in body weight despite the lack of change in daily food intake needs to be elucidated. Previous studies have shown that the effect in food intake of chronic PYY_{3-36} disappears at the beginning of the treatment while the effect in metabolism persists (Adams *et al.*, 2006; van den Hoek *et al.*, 2007). Chronic PYY_{3-36} increased fat oxidation (van den Hoek *et al.*, 2007) and PYY_{3-36} treatment caused fat loss and increased faecal energy loss in DIO mice (Adams *et al.*, 2006). Therefore, chronic Y242 could cause other changes in energy balance and this caused the mild effect in body weight. Substrate utilization, physical activity, body composition and fecal energy density measurement could help understanding the effect of Y242 in metabolism and body weight loss.

Importantly, the DIO animals receiving subcutaneous injection of the vehicle also lost weight after starting daily injections and there was great variability in this group. These could be due to stress and, consequently, it makes difficult to make definitive conclusions of the ability of Y242 as a weight loss treatment. However, the body weight in this group increases or stabilises whereas the body weight in Y242-treated mice remain low. We hypothesise that continuing the treatment with Y242 avoids the rebound weight gain that would occur following the initial body weight loss. Due to variability, the doses used in this experiment as well as different doses and/or different administration patterns should be explored in another cohort.

Other studies of chronic administration of PYY have shown similar results – chronic treatment, unless delivered in pulses into the portal vein, often does not result in long-term significant reductions in body weight, despite early acute anorectic effects. It remains unclear as to whether this is because of receptor downregulation or the activation of other weight-loss protective pathways. An important observation is that chronic use of PYY_{3-36} as a single agent typically causes minor weight loss and the rebound hyperphagic effect that occurs after withdrawal of an anorectic agent is inhibited with

continued usage (Parkinson *et al.*, 2008). Thus, an anorectic agent like PYY_{3-36}, may not be ideal as a single agent in the treatment of obesity but might be particularly useful in combination therapies with other anorectic or energy expenditure-raising hormones.

There is some evidence that PYY_{3-36} might be beneficial for insulin sensitivity and secretion. On the other hand, other members of the Y-receptor families which share some cross reactivity with PYY may work directly or via autonomic neurones to inhibit insulin secretion. Thus, whether PYY-based agents are used either as monotherapy or in combination with other gut hormones to treat obesity, it is extremely important to ensure that this would not have a deleterious effect on glucose homeostasis. Islet function in response to HFD and Y242 treatment was therefore investigated using a novel imaging platform in the eye of mice that allows longitudinal assessment of calcium activity in the same pancreatic β-cells. This is, to my knowledge, the first experiment to assess *in vivo* islet function in response to chronic Y2R agonism using a direct readout of insulin secretion. HFD intervention increased body weight and caused glucose intolerance, and DIO models of hyperglycaemia in this C57Bl/6J strain are a good model of the diabetic phenotype that occurs as a result of glucolipotoxicity in metabolically unhealthy humans. As a measure of islet function and coordinated insulin secretory behaviour, we measured calcium fluorescence in islets longitudinally. For the first time we provide direct *in vivo* evidence of the effects of HFD-induced diabetes on islet function, as demonstrated by a reduced pan-islet calcium activity. Waveform analysis of calcium oscillations revealed a reduction in amplitude and in the duration of pulse waveform after diet intervention butY2R agonism did not restore calcium activity of islets in DIO mice. Y2R did not improve glucose tolerance, as we expected. However, it is equally important to note that Y242 did not worsen islet calcium readouts either, which supports its use in combination with other agents that may work on other elements of the metabolic syndrome. In brief, if the anorectic effects of PYY are added to another element that better targets insulin secretion, this could be expected to be a successful combination.

Importantly, Y2R is not expressed in pancreatic islets and, therefore, the effect of PYY_{3-36} on islet function is expected to be mainly indirect or via other Y-receptor. Islets transplanted into the eye are rapidly innervated but it is possible that the innervation does not mimic the pancreatic environment. In addition, PYY regulation of insulin secretion might depend on glucose levels and this would not be detected in the imaging experiment setting. Apart from addressing the dosing method and the ambient stress, future experiments should assess the combination of Y242 with other analogues that could potentially restore the islet function and support the Y242-mediated weight loss, such as GLP-1 analogues.

In this work, we have not focused in the role of vagal Y2R in glucose homeostasis but my results showed that vagal Y2R disruption does not alter glucose tolerance. Moreover, global chemogenetic vagal afferent activation also did not have an effect in glucose tolerance. However, the fasting insulin and GSIS was not measured.

In conclusion, we have developed a novel microsurgical technique that will now form an important part of our armamentarium of tools to help dissect the complex effects of the vagus nerve on the gut-brain axis. This is vital for the understanding of neuroendocrine and neuroimmune physiology as well as developing highly targeted and effective treatments for obesity and inflammatory gut conditions. My work showed that afferent vagus nerve activation can alter the immune landscape of the gastrointestinal tract. This opens up a huge field of research to understand the mechanism underling the interaction between vagal afferents and immune cells, as well as if ENS or specific neuromodulators are involved. Vagus nerve modulation, pharmacologically or with electrodes, has huge therapeutic potential for obesity and beyond. This thesis provides more inroads into a better understanding of vagal function in order to realise that potential. In brief, this work is the first to reveal that vagal afferent Y2R mediates the effect of low dose and endogenous PYY_{3-36} and that vagal activation by PYY_{3-36} has a role in short-term feeding regulation. Chronic treatment with a long-acting PYY_{3-36} analogue did not result in an improvement or worsening of the insulin-secretory failure that occurs with DIO and diabetes. In completing this experiment, we have revealed the power of a novel imaging platform capable of longitudinally tracking individual islet function in response to environmental and pharmacological triggers, as well as confirming that the addition of a PYY-based agent to a combination gut-hormone based therapy should not be deleterious to the anti-diabetic goals. Finally, we have shown that the application of the new techniques developed in my thesis are widespread.

References

Abbott, C.R., Monteiro, M., Small, C.J., Sajedi, A., et al. (2005a) The inhibitory effects of peripheral administration of peptide YY 3-36 and glucagon-like peptide-1 on food intake are attenuated by ablation of the vagal-brainstem-hypothalamic pathway. *Brain Research*. [Online] 1044 (1), 127–131. Available from: doi:10.1016/j.brainres.2005.03.011.

Abbott, C.R., Small, C.J., Kennedy, A.R., Neary, N.M., et al. (2005b) Blockade of the neuropeptide Y Y2 receptor with the specific antagonist BIIE0246 attenuates the effect of endogenous and exogenous peptide YY (3-36) on food intake. *Brain Research*. [Online] 1043 (1–2), 139–144. Available from: doi:10.1016/j.brainres.2005.02.065.

Acuna-Goycolea, C., Tamamaki, N., Yanagawa, Y., Obata, K., et al. (2005) Mechanisms of neuropeptide Y, peptide YY, and pancreatic polypeptide inhibition of identified green fluorescent protein-expressing GABA neurons in the hypothalamic neuroendocrine arcuate nucleus. *Journal of Neuroscience*. [Online] 25 (32), 7406–7419. Available from: doi:10.1523/JNEUROSCI.1008-05.2005.

Adams, S.H., Lei, C., Jodka, C.M., Nikoulina, S.E., et al. (2006) PYY[3-36] administration decreases the respiratory quotient and reduces adiposity in diet-induced obese mice. *Journal of Nutrition*. [Online] 136 (1), 195–201. Available from: doi:10.1093/jn/136.1.195.

Adeghate, E. (2002) Pancreatic tissue grafts are reinnervated by neuro-peptidergic and cholinergic nerves within five days of transplantation. *Transplant Immunology*. [Online] 10 (1), 73–80. Available from: doi:10.1016/S0966-3274(02)00051-5.

Adrian, T.E., Ferri, G.L., Bacarese-Hamilton, A.J., Fuessl, H.S., et al. (1985) Human distribution and release of a putative new gut hormone, peptide YY. *Gastroenterology*. [Online] 89 (5), 1070–1077. Available from: doi:10.1016/0016-5085(85)90211-2.

Adrian, T.E., Sagor, G.R., Savage, A.P., Bacarese-Hamilton, A.J., et al. (1986) Peptide YY Kinetics and Effects on Blood Pressure and Circulating Pancreatic and Gastrointestinal Hormones and Metabolites in Man. *The Journal of Clinical Endocrinology & Metabolism*. [Online] 63 (4), 803–807. Available from: doi:10.1210/jcem-63-4-803.

Agostoni, E., Chinnock, J.E., De Daly, M.B. & Murray, J.G. (1957) Functional and histological studies of the vagus nerve and its branches to the heart, lungs and abdominal viscera in the cat. *The Journal of physiology*. [Online] 135 (1), 182–205. Available from: doi:10.1113/jphysiol.1957.sp005703.

Ahrén, B. (2000) Autonomic regulation of islet hormone secretion - Implications for health and disease. *Diabetologia*. [Online] 43 (4), 393–410. Available from: doi:10.1007/s001250051322.

Ahrén, B. & Larsson, H. (1996) Peptide YY does not inhibit glucose-stimulated insulin secretion in humans. *European Journal of Endocrinology*. [Online] 134 (3), 362–365. Available from: doi:10.1530/eje.0.1340362.

Alexiadou, K., Anyiam, O. & Tan, T. (2019) Cracking the combination: Gut hormones for the treatment of obesity and diabetes. *Journal of Neuroendocrinology*. [Online] 31 (5), e12664. Available from: doi:https://doi.org/10.1111/jne.12664.

do Amaral, M.E.C., Kravets, V., Dwulet, J.A.M., Farnsworth, N.L., et al. (2020) Caloric restriction recovers impaired b-cell-b-cell gap junction coupling, calcium oscillation coordination, and insulin secretion in prediabetic mice. *American Journal of Physiology - Endocrinology and Metabolism*. [Online] 319 (4), E709–E720. Available from: doi:10.1152/ajpendo.00132.2020.

Andresen, M.C. & Yang, M. (1990) Non-NMDA receptors mediate sensory afferent synaptic transmission in medial nucleus tractus solitarius. *American Journal of Physiology - Heart and Circulatory Physiology*. [Online] 259 (4 28-4). Available from: doi:10.1152/ajpheart.1990.259.4.h1307.

de Araujo, I.E., Oliveira-Maia, A.J., Sotnikova, T.D., Gainetdinov, R.R., et al. (2008) Food reward in the absence of taste receptor signaling. *Neuron*. [Online] 57 (6), 930–941. Available from: doi:10.1016/j.neuron.2008.01.032.

Asakawa, A., Inui, A., Kaga, T., Yuzuriha, H., et al. (2001) Ghrelin is an appetite-stimulatory signal from stomach with structural resemblance to motilin. *Gastroenterology*. [Online] 120, 337–345. Available from: doi:10.1053/gast.2001.22158.

Asakawa, A., Inui, A., Yuzuriha, H., Ueno, N., et al. (2003) Characterization of the effects of pancreatic polypeptide in the regulation of energy balance. *Gastroenterology*. [Online] 124 (5), 1325–1336. Available from: doi:10.1016/s0016-5085(03)00216-6.

Ashcroft, F.M., Harrison, D.E. & Ashcroft, S.J.H. (1984) Glucose induces closure of single potassium channels in isolated rat pancreatic β-cells. *Nature*. [Online] 312 (5993), 446–448. Available from: doi:10.1038/312446a0.

Astrup, A., Rössner, S., Van Gaal, L., Rissanen, A., et al. (2009) Effects of liraglutide in the treatment of obesity: a randomised, double-blind, placebo-controlled study. *The Lancet*. [Online] 374 (9701), 1606–1616. Available from: doi:https://doi.org/10.1016/S0140-6736(09)61375-1.

Babic, T. & Travagli, R.A. (2016) *Neural Control of the Pancreas*. [Online]. 2016. Pancreapedia: Exocrine Pancreas Knowledge Base. Available from: doi:10.3998/panc.2016.27.

Baggio, L.L., Huang, Q., Brown, T.J. & Drucker, D.J. (2004) Oxyntomodulin and glucagon-like peptide-1 differentially regulate murine food intake and energy expenditure. *Gastroenterology*. [Online] 127 (2), 546–558. Available from: doi:10.1053/j.gastro.2004.04.063.

Bai, L., Mesgarzadeh, S., Ramesh, K.S., Huey, E.L., et al. (2019) Genetic Identification of Vagal Sensory Neurons That Control Feeding. *Cell*. [Online] 179 (5), 1129-1143.e23. Available from: doi:10.1016/j.cell.2019.10.031.

Bain, C.C. & Mowat, A.M. (2014) Macrophages in intestinal homeostasis and inflammation. *Immunological Reviews*. [Online] 260 (1), 102–117. Available from: doi:10.1111/imr.12192.

Bain, C.C., Scott, C.L., Uronen-Hansson, H., Gudjonsson, S., et al. (2013) Resident and pro-inflammatory macrophages in the colon represent alternative context-dependent fates of the same Ly6C hi monocyte precursors. *Mucosal Immunology*. [Online] 6 (3), 498–510. Available from: doi:10.1038/mi.2012.89.

Balthasar, N., Dalgaard, L.T., Lee, C.E., Yu, J., et al. (2005) Divergence of melanocortin pathways in the control of food intake and energy expenditure. *Cell*. [Online] 123 (3), 493–505. Available from: doi:10.1016/j.cell.2005.08.035.

Banni, S., Carta, G., Murru, E., Cordeddu, L., et al. (2012) Vagus nerve stimulation reduces body weight and fat mass in rats.file:///C:/Users/AldaraMA/Downloads/25605682.nbib. *PloS one*. [Online] 7 (9), e44813. Available from: doi:10.1371/journal.pone.0044813.

Baraboi, E.D., Michel, C., Smith, P., Thibaudeau, K., et al. (2010) Effects of albumin-conjugated PYY on food intake: The respective roles of the circumventricular organs and vagus nerve. *European Journal of Neuroscience*. [Online] 32 (5), 826–839. Available from: doi:10.1111/j.1460-9568.2010.07318.x.

Baral, P., Umans, B.D., Li, L., Wallrapp, A., et al. (2018) Nociceptor sensory neurons suppress neutrophil and γδ T cell responses in bacterial lung infections and lethal pneumonia. *Nature Medicine*. [Online] 24 (4), 417–426. Available from: doi:10.1038/nm.4501.

Barrachina, M.D., Martínez, V., Wang, L., Wei, J.Y., et al. (1997) Synergistic interaction between leptin and cholecystokinin to reduce short-term food intake in lean mice. *Proceedings of the National Academy of Sciences of the United States of America*. [Online] 94 (19), 10455–10460. Available from: doi:10.1073/pnas.94.19.10455.

Barsh, G.S. & Schwartz, M.W. (2002) Genetic approaches to studying energy balance: perception and integration. *Nature Reviews Genetics*. [Online] 3 (8), 589–600. Available from: doi:10.1038/nrg862.

Batterham, R.L., Cohen, M.A., Ellis, S.M., Le Roux, C.W., et al. (2003a) Inhibition of food intake in obese subjects by peptide YY3-36. *New England Journal of Medicine*. [Online] 349 (10), 941–948. Available from: doi:10.1056/NEJMoa030204.

Batterham, R.L., Cowley, M.A., Small, C.J., Herzog, H., et al. (2002) Gut hormone PYY3-36 physiologically inhibits food intake. *Nature*. [Online] 418 (6898), 650–654. Available from: doi:10.1038/nature00887.

Batterham, R.L., Ffytche, D.H., Rosenthal, J.M., Zelaya, F.O., et al. (2007) PYY modulation of cortical and hypothalamic brain areas predicts feeding behaviour in humans. *Nature*. [Online] 450 (7166), 106–109. Available from: doi:10.1038/nature06212.

Batterham, R.L., Heffron, H., Kapoor, S., Chivers, J.E., et al. (2006) Critical role for peptide YY in protein-mediated satiation and body-weight regulation. *Cell Metabolism*. [Online] 4 (3), 223–233. Available from: doi:10.1016/j.cmet.2006.08.001.

Batterham, R.L., Le Roux, C.W., Cohen, M.A., Park, A.J., et al. (2003b) Pancreatic polypeptide reduces appetite and food intake in humans. *The Journal of clinical endocrinology and metabolism*. [Online] 88 (8), 3989–3992. Available from: doi:10.1210/jc.2003-030630.

Beckman, L.M., Beckman, T.R., Sibley, S.D., Thomas, W., et al. (2011) Changes in gastrointestinal hormones and leptin after Roux-en-Y gastric bypass surgery. *Journal of Parenteral and Enteral Nutrition*. [Online] 35 (2), 169–180. Available from: doi:10.1177/0148607110381403.

Behary, P., Tharakan, G., Alexiadou, K., Johnson, N., et al. (2019) Combined GLP-1, oxyntomodulin, and peptide YY improves body weight and glycemia in obesity and prediabetes/type 2 diabetes: A randomized, single-blinded, placebo-controlled study. *Diabetes Care*. [Online] 42 (8), 1446–1453. Available from: doi:10.2337/dc19-0449.

Belkaid, Y., Bouladoux, N. & Hand, T.W. (2013) Effector and memory T cell responses to commensal bacteria. *Trends in Immunology*. [Online] 34 (6), 299–306. Available from:

doi:10.1016/j.it.2013.03.003.

Benoit, S.C., Air, E.L., Coolen, L.M., Strauss, R., et al. (2002) The catabolic action of insulin in the brain is mediated by melanocortins. *Journal of Neuroscience*. [Online] 22 (20), 9048–9052. Available from: doi:10.1523/jneurosci.22-20-09048.2002.

Bergman, B.C. & Goodpaster, B.H. (2020) Exercise and muscle lipid content, composition, and localization: Influence on muscle insulin sensitivity. *Diabetes*. [Online] 69 (5), 848–858. Available from: doi:10.2337/dbi18-0042.

Berthoud, H.-R. (2011) Metabolic and hedonic drives in the neural control of appetite: who is the boss? *Current opinion in neurobiology*. [Online] 21 (6), 888–896. Available from: doi:10.1016/j.conb.2011.09.004.

Berthoud, H.-R. (2008a) The vagus nerve, food intake and obesity. *Regulatory Peptides*. [Online] 149 (1), 15–25. Available from: doi:https://doi.org/10.1016/j.regpep.2007.08.024.

Berthoud, H.-R., Lenard, N.R. & Shin, A.C. (2011) Food reward, hyperphagia, and obesity. *American Journal of Physiology-Regulatory, Integrative and Comparative Physiology*. [Online] 300 (6), R1266–R1277. Available from: doi:10.1152/ajpregu.00028.2011.

Berthoud, H.R. (2008b) Vagal and hormonal gut-brain communication: From satiation to satisfaction. *Neurogastroenterology and Motility*. [Online] 20 (SUPPL. 1), 64–72. Available from: doi:10.1111/j.1365-2982.2008.01104.x.

Berthoud, H.R., Blackshaw, L.A., Brookes, S.J.H. & Grundy, D. (2004) Neuroanatomy of extrinsic afferents supplying the gastrointestinal tract. *Neurogastroenterology and Motility*. [Online] 16 (SUPPL. 1), 28–33. Available from: doi:10.1111/j.1743-3150.2004.00471.x.

Berthoud, H.R., Carlson, N.R. & Powley, T.L. (1991) Topography of efferent vagal innervation of the rat gastrointestinal tract. *American Journal of Physiology - Regulatory Integrative and Comparative Physiology*. [Online] 260 (1 29-1), 200–207. Available from: doi:10.1152/ajpregu.1991.260.1.r200.

Berthoud, H.R., Kressel, M. & Neuhuber, W.L. (1992) An anterograde tracing study of the vagal innervation of rat liver, portal vein and biliary system. *Anatomy and Embryology*. [Online] 186 (5), 431–442. Available from: doi:10.1007/BF00185458.

Berthoud, H.R., Kressel, M., Raybould, H.E. & Neuhuber, W.L. (1995) Vagal sensors in the rat duodenal mucosa: distribution and structure as revealed by in vivo DiI-tracing. *Anatomy and embryology*. [Online] 191 (3), 203–212. Available from: doi:10.1007/BF00187819.

Berthoud, H.R. & Neuhuber, W.L. (2000) Functional and chemical anatomy of the afferent vagal system. *Autonomic neuroscience : basic & clinical*. [Online] 85 (1–3), 1–17. Available from: doi:10.1016/S1566-0702(00)00215-0.

Berthoud, H.R. & Neuhuber, W.L. (2019) Vagal mechanisms as neuromodulatory targets for the treatment of metabolic disease. *Annals of the New York Academy of Sciences*. [Online] 1454 (1), 42–55. Available from: doi:10.1111/nyas.14182.

Berthoud, H.R., Patterson, L.M., Neumann, F. & Neuhuber, W.L. (1997) Distribution and structure of vagal afferent intraganglionic laminar endings (IGLEs) in the rat gastrointestinal tract. *Anatomy and Embryology*. [Online] 195 (2), 183–191. Available from: doi:10.1007/s004290050037.

Bischoff, S.C. (2009) Physiological and pathophysiological functions of intestinal mast cells. *Seminars in Immunopathology*. [Online] 31 (2), 185–205. Available from: doi:10.1007/s00281-009-0165-4.

Blevins, J.E., Chelikani, P.K., Haver, A.C. & Reidelberger, R.D. (2008) PYY(3-36) induces Fos in the arcuate nucleus and in both catecholaminergic and non-catecholaminergic neurons in the nucleus tractus solitarius of rats. *Peptides*. [Online] 29 (1), 112–119. Available from: doi:10.1016/j.peptides.2007.11.003.

Blevins, J.E., Schwartz, M.W. & Baskin, D.G. (2004) Evidence that paraventricular nucleus oxytocin neurons link hypothalamic leptin action to caudal brain stem nuclei controlling meal size. *American Journal of Physiology-Regulatory, Integrative and Comparative Physiology*. [Online] 287 (1), R87–R96. Available from: doi:10.1152/ajpregu.00604.2003.

Boey, D., Heilbronn, L., Sainsbury, A., Laybutt, R., et al. (2006a) Low serum PYY is linked to insulin resistance in first-degree relatives of subjects with type 2 diabetes. *Neuropeptides*. [Online] 40 (5), 317–324. Available from: doi:10.1016/j.npep.2006.08.002.

Boey, D., Lin, S., Enriquez, R.F., Lee, N.J., et al. (2008) PYY transgenic mice are protected against diet-induced and genetic obesity. *Neuropeptides*. [Online] 42 (1), 19–30. Available from: doi:10.1016/j.npep.2007.11.003.

Boey, D., Lin, S., Karl, T., Baldock, P., et al. (2006b) Peptide YY ablation in mice leads to the development of hyperinsulinaemia and obesity. *Diabetologia*. [Online] 49 (6), 1360–1370. Available from: doi:10.1007/s00125-006-0237-0.

Bohórquez, D. V., Shahid, R.A., Erdmann, A., Kreger, A.M., et al. (2015) Neuroepithelial circuit formed by innervation of sensory enteroendocrine cells. *Journal of Clinical Investigation*. [Online] 125 (2), 782–786. Available from: doi:10.1172/JCI78361.

Boland, B.B., Mumphrey, M.B., Hao, Z., Townsend, R.L., et al. (2019) Combined loss of GLP-1R and Y2R does not alter progression of high-fat diet-induced obesity or response to RYGB surgery in mice. *Molecular Metabolism*. [Online] 25 (May), 64–72. Available from: doi:10.1016/j.molmet.2019.05.004.

Bonaz, B. (2018) Is-there a place for vagus nerve stimulation in inflammatory bowel diseases? *Bioelectronic Medicine*. [Online] 4 (1), 1–9. Available from: doi:10.1186/s42234-018-0004-9.

Bonaz, B., Bazin, T. & Pellissier, S. (2018) The vagus nerve at the interface of the microbiota-gut-brain axis. *Frontiers in Neuroscience*. [Online] 12 (FEB), 1–9. Available from: doi:10.3389/fnins.2018.00049.

Bonaz, B., Sinniger, V., Hoffmann, D., Clarençon, D., et al. (2016) Chronic vagus nerve stimulation in Crohn's disease: A 6-month follow-up pilot study. *Neurogastroenterology and Motility*. [Online] 28 (6), 948–953. Available from: doi:10.1111/nmo.12792.

Bonaz, B., Sinniger, V. & Pellissier, S. (2016) Anti-inflammatory properties of the vagus nerve: potential therapeutic implications of vagus nerve stimulation. *Journal of Physiology*. [Online] 594 (20), 5781–5790. Available from: doi:10.1113/JP271539.

Borovikova, L. V., Ivanova, S., Zhang, M., Yang, H., et al. (2000) Vagus nerve stimulation attenuates the systemic inflammatory response to endotoxin. *Nature*. [Online] 405 (6785), 458–462. Available from: doi:10.1038/35013070.

Bosmans, G., Appeltans, I., Stakenborg, N., Gomez-Pinilla, P.J., et al. (2019) Vagus nerve stimulation dampens intestinal inflammation in a murine model of experimental food allergy. *Allergy: European Journal of Allergy and Clinical Immunology*. [Online] 74 (9), 1748–1759. Available from: doi:10.1111/all.13790.

Bottcher, G., Ahren, B., Lundquist, L. & Sundler, F. (1989) Peptide yy: Intrapancreatic localization and effects on insulin and glucagon secretion in the mouse. *Pancreas*. [Online] 4 (3), 282–288. Available from: doi:10.1097/00006676-198906000-00002.

Böttcher, G., Ekblad, E., Ekman, R., Håkanson, R., et al. (1993) Peptide YY: A neuropeptide in the gut. Immunocytochemical and immunochemical evidence. *Neuroscience*. [Online] 55 (1), 281–290. Available from: doi:https://doi.org/10.1016/0306-4522(93)90472-R.

Brierley, D.I., Holt, M.K., Singh, A., Araujo, A. De, et al. (2021) Central and peripheral GLP-1 systems independently suppress eating. *Nature Metabolism*. [Online] 3, 258–273. Available from: doi:10.1038/s42255-021-00344-4.

Brissova, M., Fowler, M.J., Nicholson, W.E., Chu, A., et al. (2005) Assessment of human pancreatic islet architecture and composition by laser scanning confocal microscopy. *Journal of Histochemistry and Cytochemistry*. [Online] 53 (9), 1087–1097. Available from: doi:10.1369/jhc.5C6684.2005.

Broberger, C., Holmberg, K., Kuhar, M.J. & Hökfelt, T. (1999) Cocaine- and amphetamine-regulated transcript in the rat vagus nerve: A putative mediator of cholecystokinin-induced satiety. *Proceedings of the National Academy of Sciences of the United States of America*. [Online] 96 (23), 13506–13511. Available from: doi:10.1073/pnas.96.23.13506.

Broberger, C., Landry, M., Wong, H., Walsh, J.N., et al. (1997) Subtypes y1 and y2 of the neuropeptide y receptor are respectively expressed in pro-opiomelanocortin- and neuropeptide-y-containing neurons of the rat hypothalamic arcuate nucleus. *Neuroendocrinology*. [Online] 66 (6), 393–408. Available from: doi:10.1159/000127265.

Browning, K.N., Babic, T., Holmes, G.M., Swartz, E., et al. (2013) A critical re-evaluation of the specificity of action of perivagal capsaicin. *Journal of Physiology*. [Online] 591 (6), 1563–1580. Available from: doi:10.1113/jphysiol.2012.246827.

Browning, K.N. & Travagli, R.A. (2009) Modulation of inhibitory neurotransmission in brainstem vagal circuits by NPY and PYY is controlled by cAMP levels. *Neurogastroenterology and Motility*. [Online] 21 (12), 1309–1319. Available from: doi:10.1111/j.1365-2982.2009.01367.x.

Browning, K.N. & Travagli, R.A. (2003) Neuropeptide Y and peptide YY inhibit excitatory synaptic transmission in the rat dorsal motor nucleus of the vagus. *Journal of Physiology*. [Online] 549 (3), 775–785. Available from: doi:10.1113/jphysiol.2003.042036.

Brumovsky, P., Stanic, D., Shuster, S., Herzog, H., et al. (2005) Neuropeptide Y2 receptor protein is present in peptidergic and nonpeptidergic primary sensory neurons of the mouse. *Journal of Comparative Neurology*. [Online] 489 (3), 328–348. Available from: doi:10.1002/cne.20639.

Bruning, J.C., Gautam, D., Burks, D.J., Gillette, J., et al. (2000) Role of brain insulin receptor in control of body weight and reproduction. *Science*. [Online] 289 (5487), 2122–2125. Available from: doi:10.1126/science.289.5487.2122.

Bugajski, A.J., Gil, K., Ziomber, A., Zurowski, D., et al. (2007) Effect of long-term vagal stimulation on

food intake and body weight during diet induced obesity in rats. *Journal of physiology and pharmacology : an official journal of the Polish Physiological Society*. 58 Suppl 1, 5–12.

Burcelin, R., Brunner, H.R., Seydoux, J., Thorensa, B., et al. (2001) Increased insulin concentrations and glucose storage in neuropeptide Y Y1 receptor-deficient mice. *Peptides*. [Online] 22 (3), 421–427. Available from: doi:10.1016/S0196-9781(01)00357-6.

Burdyga, G., Lal, S., Varro, A., Dimaline, R., et al. (2004) Expression of Cannabinoid CB1 Receptors by Vagal Afferent Neurons, Is Inhibited by Cholecystokinin. *Journal of Neuroscience*. [Online] 24 (11), 2708–2715. Available from: doi:10.1523/JNEUROSCI.5404-03.2004.

Burdyga, G., De Lartigue, G., Raybould, H.E., Morris, R., et al. (2008) Cholecystokinin regulates expression of Y2 receptors in vagal afferent neurons serving the stomach. *Journal of Neuroscience*. [Online] 28 (45), 11583–11592. Available from: doi:10.1523/JNEUROSCI.2493-08.2008.

Burdyga, G., Spiller, D., Morris, R., Lal, S., et al. (2002) Expression of the leptin receptor in rat and human nodose ganglion neurones. *Neuroscience*. [Online] 109 (2), 339–347. Available from: doi:10.1016/S0306-4522(01)00474-2.

Burdyga, G., Varro, A., Dimaline, R., Thompson, D.G., et al. (2006) Ghrelin receptors in rat and human nodose ganglia: Putative role in regulating CB-1 and MCH receptor abundance. *American Journal of Physiology - Gastrointestinal and Liver Physiology*. [Online] 290 (6), 1289–1297. Available from: doi:10.1152/ajpgi.00543.2005.

Burgess, E., Hassmén, P. & Pumpa, K.L. (2017) Determinants of adherence to lifestyle intervention in adults with obesity: a systematic review. *Clinical Obesity*. [Online] 7 (3), 123–135. Available from: doi:10.1111/cob.12183.

Burneo, J.G., Faught, E., Knowlton, R., Morawetz, R., et al. (2002) Weight loss associated with vagus nerve stimulationBurneo, J.G., Faught, E., Knowlton, R., Morawetz, R., et al. (2002) Weight loss associated with vagus nerve stimulation. Neurology. [Online] 59 (3), 463–464. Available from: doi:10.1212/WNL.59.3.463. *Neurology*. [Online] 59 (3), 463–464. Available from: doi:10.1212/WNL.59.3.463.

Cabrele, C. & Beck-Sickinger, A.G. (2000) Molecular characterization of the ligand-receptor interaction of the neuropeptide Y family. *Journal of Peptide Science*. [Online] 6 (3), 97–122. Available from: doi:10.1002/(SICI)1099-1387(200003)6:3<97::AID-PSC236>3.0.CO;2-E.

Cailotto, C., Gomez-Pinilla, P.J., Costes, L.M., Van Der Vliet, J., et al. (2014) Neuro-anatomical evidence indicating indirect modulation of macrophages by vagal efferents in the intestine but not in the spleen. *PLoS ONE*. [Online] 9 (1). Available from: doi:10.1371/journal.pone.0087785.

Cammisotto, P. & Bendayan, M. (2012) A review on gastric leptin: the exocrine secretion of a gastric hormone. *Anatomy & Cell Biology*. [Online] 45 (1), 1. Available from: doi:10.5115/acb.2012.45.1.1.

Campfield, L.A., Smith, F.J., Guisez, Y., Devos, R., et al. (1996) OB protein: A peripheral signal linking adiposity and central neural networks. *Appetite*. [Online] 26 (3), 302. Available from: doi:10.1006/appe.1996.0024.

Campos, C.A., Bowen, A.J., Schwartz, M.W. & Palmiter, R.D. (2016) Parabrachial CGRP Neurons Control Meal Termination. *Cell Metabolism*. [Online] 23 (5), 811–820. Available from:

doi:10.1016/j.cmet.2016.04.006.

Cardoso, V., Chesné, J., Ribeiro, H., Garcia-Cassani, B., et al. (2017) Neuronal regulation of type 2 innate lymphoid cells via neuromedin U. *Nature*. [Online] 549 (7671), 277–281. Available from: doi:10.1038/nature23469.

Carter, M.E., Han, S. & Palmiter, R.D. (2015) Parabrachial calcitonin gene-related peptide neurons mediate conditioned taste aversion. *The Journal of neuroscience : the official journal of the Society for Neuroscience*. [Online] 35 (11), 4582–4586. Available from: doi:10.1523/JNEUROSCI.3729-14.2015.

Carter, M.E., Soden, M.E., Zweifel, L.S. & Palmiter, R.D. (2013) Genetic identification of a neural circuit that suppresses appetite. *Nature*. [Online] 503 (7474), 111–114. Available from: doi:10.1038/nature12596.

Carvalho, C.P.F., Oliveira, R.B., Britan, A., Santos-Silva, J.C., et al. (2012) Impaired β-cell-β-cell coupling mediated by Cx36 gap junctions in prediabetic mice. *American Journal of Physiology - Endocrinology and Metabolism*. [Online] 303 (1), 144–151. Available from: doi:10.1152/ajpendo.00489.2011.

Cegla, J., Troke, R.C., Jones, B., Tharakan, G., et al. (2014) Coinfusion of low-dose GLP-1 and glucagon in man results in a reduction in food intake. *Diabetes*. [Online] 63 (11), 3711–3720. Available from: doi:10.2337/db14-0242.

Challis, B.G., Coll, A.P., Yeo, G.S.H., Pinnock, S.B., et al. (2004) Mice lacking pro-opiomelanocortin are sensitive to high-fat feeding but respond normally to the acute anorectic effects of peptide-YY3-36. *Proceedings of the National Academy of Sciences of the United States of America*. [Online] 101 (13), 4695–4700. Available from: doi:10.1073/pnas.0306931101.

Challis, B.G., Pinnock, S.B., Coll, A.P., Carter, R.N., et al. (2003) Acute effects of PYY3-36 on food intake and hypothalamic neuropeptide expression in the mouse. *Biochemical and Biophysical Research Communications*. [Online] 311 (4), 915–919. Available from: doi:10.1016/j.bbrc.2003.10.089.

Chambers, E.S., Viardot, A., Psichas, A., Morrison, D.J., et al. (2015) Effects of targeted delivery of propionate to the human colon on appetite regulation, body weight maintenance and adiposity in overweight adults. *Gut*. [Online] 64 (11), 1744–1754. Available from: doi:10.1136/gutjnl-2014-307913.

Chandarana, K., Gelegen, C., Irvine, E.E., Choudhury, A.I., et al. (2013) Peripheral activation of the Y2-receptor promotes secretion of GLP-1 and improves glucose tolerance. *Molecular Metabolism*. [Online] 2 (3), 142–152. Available from: doi:10.1016/j.molmet.2013.03.001.

Chang, R.B., Strochlic, D.E., Williams, E.K., Umans, B.D., et al. (2015) Vagal sensory neuron subtypes that differentially control breathing. *Cell*. [Online] 161 (3), 622–633. Available from: doi:10.1016/j.cell.2015.03.022.

Chelikani, P.K., Haver, A.C., Reeve, J.R., Keire, D.A., et al. (2006) Daily, intermittent intravenous infusion of peptide YY(3-36) reduces daily food intake and adiposity in rats. *American Journal of Physiology - Regulatory Integrative and Comparative Physiology*. [Online] 290 (2), 298–305. Available from: doi:10.1152/ajpregu.00674.2005.

Chelikani, P.K., Haver, A.C. & Reidelberger, R.D. (2004) Comparison of the inhibitory effects of PYY(3-

36) and PYY(1-36) on gastric emptying in rats. *American Journal of Physiology - Regulatory Integrative and Comparative Physiology*. [Online] 287 (5 56-5), 1064–1070. Available from: doi:10.1152/ajpregu.00376.2004.

Chelikani, P.K., Haver, A.C. & Reidelberger, R.D. (2006) Dose-dependent effects of peptide YY(3-36) on conditioned taste aversion in rats. *Peptides*. [Online] 27 (12), 3193–3201. Available from: doi:10.1016/j.peptides.2006.08.001.

Chelikani, P.K., Haver, A.C. & Reidelberger, R.D. (2007) Intermittent intraperitoneal infusion of peptide YY(3-36) reduces daily food intake and adiposity in obese rats. *American Journal of Physiology - Regulatory Integrative and Comparative Physiology*. [Online] 293 (1), 39–46. Available from: doi:10.1152/ajpregu.00164.2007.

Chelikani, P.K., Haver, A.C. & Reidelberger, R.D. (2005) Intravenous infusion of glucagon-like peptide-1 potently inhibits food intake, sham feeding, and gastric emptying in rats. *American journal of physiology. Regulatory, integrative and comparative physiology*. [Online] 288 (6), R1695-706. Available from: doi:10.1152/ajpregu.00870.2004.

Chen, C., Chmelova, H., Cohrs, C.M., Chouinard, J.A., et al. (2016) Alterations in β-cell calcium dynamics and efficacy outweigh islet mass adaptation in compensation of insulin resistance and prediabetes onset. *Diabetes*. [Online] 65 (9), 2676–2685. Available from: doi:10.2337/db15-1718.

Chen, C.H. & Rogers, R.C. (1995) Central inhibitory action of peptide YY on gastric motility in rats. *The American journal of physiology*. [Online] 269 (4 Pt 2), R787-92. Available from: doi:10.1152/ajpregu.1995.269.4.R787.

Chen, C.H. & Rogers, R.C. (1997) Peptide YY and the Y2 agonist PYY-(13-36) inhibit neurons of the dorsal motor nucleus of the vagus. *American Journal of Physiology - Regulatory Integrative and Comparative Physiology*. [Online] 273 (1 42-1). Available from: doi:10.1152/ajpregu.1997.273.1.r213.

Chen, H.Y., Trumbauer, M.E., Chen, A.S., Weingarth, D.T., et al. (2004) Orexigenic action of peripheral ghrelin is mediated by neuropeptide Y and agouti-related protein. *Endocrinology*. [Online] 145 (6), 2607–2612. Available from: doi:10.1210/en.2003-1596.

Chen, X., Choo, H., Huang, X.P., Yang, X., et al. (2015) The first structure-activity relationship studies for designer receptors exclusively activated by designer drugs. *ACS Chemical Neuroscience*. [Online] 6 (3), 476–484. Available from: doi:10.1021/cn500325v.

Cheng, H. & Leblond, C.P. (1974) Origin, differentiation and renewal of the four main epithelial cell types in the mouse small intestine. V. Unitarian Theory of the origin of the four epithelial cell types. *The American journal of anatomy*. [Online] 141 (4), 537–561. Available from: doi:10.1002/aja.1001410407.

Cheung, C.C., Clifton, D.K. & Steiner, R.A. (1997) Proopiomelanocortin neurons are direct targets for leptin in the hypothalamus. *Endocrinology*. [Online] 138 (10), 4489–4492. Available from: doi:10.1210/endo.138.10.5570.

Christensen, R.H., Von Scholten, B.J., Hansen, C.S., Jensen, M.T., et al. (2019) Epicardial adipose tissue predicts incident cardiovascular disease and mortality in patients with type 2 diabetes. *Cardiovascular Diabetology*. [Online] 18 (1), 1–10. Available from: doi:10.1186/s12933-019-0917-y.

Chu, C., Parkhurst, C.N., Zhang, W., Zhou, L., et al. (2021) The ChAT-acetylcholine pathway promotes group 2 innate lymphoid cell responses and anti-helminth immunity. *Science immunology*. 3218, 1–11.

ClinicalTrials.gov. (2011) *Identifier: NCT01479452. Effects of Bariatric Surgery in Swedish Obese Subjects (SOS)*. [Online]. 2011. Available from: https://clinicaltrials.gov/ct2/show/NCT01479452.

ClinicalTrials.gov (2012) *Identifier: NCT01515319. Safety and Pharmacokinetic Study of Y242 in adult subjects (Y242-01)*. [Online]. 2012. Available from: https://clinicaltrials.gov/ct2/show/NCT01515319.

Cohen, M.A., Ellis, S.M., Le Roux, C.W., Batterham, R.L., et al. (2003) Oxyntomodulin Suppresses Appetite and Reduces Food Intake in Humans. *Journal of Clinical Endocrinology and Metabolism*. [Online] 88 (10), 4696–4701. Available from: doi:10.1210/jc.2003-030421.

Considine, R. V, Sinha, M.K., Heiman, M.L., Kriauciunas, A., et al. (1996) Serum immunoreactive-leptin concentrations in normal-weight and obese humans. *The New England journal of medicine*. [Online] 334 (5), 292–295. Available from: doi:10.1056/NEJM199602013340503.

Cook, D.L. & Hales, N. (1984) Intracellular ATP directly blocks K+ channels in pancreatic B-cells. *Nature*. [Online] 311 (5983), 271–273. Available from: doi:10.1038/311271a0.

Corcoran, M.P., Lamon-Fava, S. & Fielding, R.A. (2007) Skeletal muscle lipid deposition and insulin resistance: Effect of dietary fatty acids and exercise. *American Journal of Clinical Nutrition*. [Online] 85 (3), 662–677. Available from: doi:10.1093/ajcn/85.3.662.

Cork, S.C. (2018) The role of the vagus nerve in appetite control: Implications for the pathogenesis of obesity. *Journal of Neuroendocrinology*. [Online] 30 (11), 1–10. Available from: doi:10.1111/jne.12643.

Cork, S.C., Richards, J.E., Holt, M.K., Gribble, F.M., et al. (2015) Distribution and characterisation of Glucagon-like peptide-1 receptor expressing cells in the mouse brain. *Molecular metabolism*. [Online] 4 (10), 718–731. Available from: doi:10.1016/j.molmet.2015.07.008.

Corp, E.S., McQuade, J., Krasnicki, S. & Conze, D.B. (2001) Feeding after fourth ventricular administration of neuropeptide Y receptor agonists in rats. *Peptides*. [Online] 22 (3), 493–499. Available from: doi:10.1016/S0196-9781(01)00359-X.

Cowley, M.A., Smart, J.L., Rubinstein, M., Diano, S., et al. (2001) Leptin activates anorexigenic POMC neurons through a neural network in the arcuate nucleus. *Nature Letters*. 411 (May).

Cox, H.M. (2007) Neuropeptide Y receptors; antisecretory control of intestinal epithelial function. *Autonomic neuroscience : basic & clinical*. [Online] 133 (1), 76–85. Available from: doi:10.1016/j.autneu.2006.10.005.

Cummings, D.E., Purnell, J.Q., Frayo, R.S., Schmidova, K., et al. (2001) A preprandial rise in plasma ghrelin levels suggests a role in meal initiation in humans. *Diabetes*. [Online] 50 (8), 1714–1719. Available from: doi:10.2337/diabetes.50.8.1714.

Curry, D.L., Bennett, L.L. & Grodski, G.M. (1968) Dynamics of Insulin Secretion by the Perfused Rat Pancreas. *Endocrinology*. [Online] 83 (3), 572–584. Available from: doi:10.1210/endo-83-3-572.

Dai, F., Yin, J. & Chen, J.D.Z. (2020) Effects and Mechanisms of Vagal Nerve Stimulation on Body Weight in Diet-Induced Obese Rats. *Obesity Surgery*. [Online] 30 (3), 948–956. Available from: doi:10.1007/s11695-019-04365-7.

Dakin, C.L., Small, C.J., Batterham, R.L., Neary, N.M., et al. (2004) Peripheral oxyntomodulin reduces food intake and body weight gain in rats. *Endocrinology*. [Online] 145 (6), 2687–2695. Available from: doi:10.1210/en.2003-1338.

Dalli, J., Colas, R.A., Arnardottir, H. & Serhan, C.N. (2017) Vagal Regulation of Group 3 Innate Lymphoid Cells and the Immunoresolvent PCTR1 Controls Infection Resolution. *Immunity*. [Online] 46 (1), 92–105. Available from: doi:10.1016/j.immuni.2016.12.009.

Daly, D.M., Park, S.J., Valinsky, W.C. & Beyak, M.J. (2011) Impaired intestinal afferent nerve satiety signalling and vagal afferent excitability in diet induced obesity in the mouse. *Journal of Physiology*. [Online] 589 (11), 2857–2870. Available from: doi:10.1113/jphysiol.2010.204594.

Dansinger, M.L., Gleason, J.A., Griffith, J.L., Selker, H.P., et al. (2005) Comparison of the Atkins, Ornish, Weight Watchers, and Zone Diets for weight loss and heart disease risk reduction: A randomized trial. *Journal of the American Medical Association*. [Online] 293 (1), 43–53. Available from: doi:10.1001/jama.293.1.43.

Date, Y., Murakami, N., Toshinai, K., Matsukura, S., et al. (2002) The Role of the Gastric Afferent Vagal Nerve in Ghrelin-Induced Feeding and Growth Hormone Secretion in Rats. *Gastroenterology*. [Online] 123, 1120–1128. Available from: doi:10.1053/gast.2002.35954.

Davis, E.A., Wald, H.S., Suarez, A.N., Zubcevic, J., et al. (2020) Ghrelin Signaling Affects Feeding Behavior, Metabolism, and Memory through the Vagus Nerve. *Current Biology*. [Online] 30 (22), 4510-4518.e6. Available from: doi:10.1016/j.cub.2020.08.069.

Diabetes UK (2019) *Diabetes UK Facts and Figures 2019*. [Online]. 2019. Diabetes UK. Available from: www.diabetes.org.uk.

Diepenbroek, C., Quinn, D., Stephens, R., Zollinger, B., et al. (2017) Validation and characterization of a novel method for selective vagal deafferentation of the gut. *American Journal of Physiology - Gastrointestinal and Liver Physiology*. [Online] 313 (4), G342–G352. Available from: doi:10.1152/ajpgi.00095.2017.

Dirksen, C., Bojsen-Møller, K.N., Jørgensen, N.B., Jacobsen, S.H., et al. (2013) Exaggerated release and preserved insulinotropic action of glucagon-like peptide-1 underlie insulin hypersecretion in glucose-tolerant individuals after Roux-en-Y gastric bypass. *Diabetologia*. [Online] 56 (12), 2679–2687. Available from: doi:10.1007/s00125-013-3055-1.

Dockray, G.J. (2009) Cholecystokinin and gut-brain signalling. *Regulatory Peptides*. [Online] 155 (1–3), 6–10. Available from: doi:10.1016/j.regpep.2009.03.015.

Dockray, G.J. (2014) Gastrointestinal hormones and the dialogue between gut and brain. *Journal of Physiology*. [Online] 592 (14), 2927–2941. Available from: doi:10.1113/jphysiol.2014.270850.

Dolenšek, J., Rupnik, M.S. & Stožer, A. (2015) Structural similarities and differences between the human and the mouse pancreas. *Islets*. [Online] 7 (1), 2–9. Available from: doi:10.1080/19382014.2015.1024405.

Doucet, É., Laviolette, M., Imbeault, P., Strychar, I., et al. (2008) Total peptide YY is a correlate of

postprandial energy expenditure but not of appetite or energy intake in healthy women. *Metabolism - Clinical and Experimental*. [Online] 57 (10), 1458–1464. Available from: doi:10.1016/j.metabol.2008.05.017.

Druce, M.R., Minnion, J.S., Field, B.C.T., Patel, S.R., et al. (2009) Investigation of structure-activity relationships of oxyntomodulin (Oxm) using oxm analogs. *Endocrinology*. [Online] 150 (4), 1712–1721. Available from: doi:10.1210/en.2008-0828.

Dumont, Y., Fournier, A., St-Pierre, S. & Quirion, R. (1995) Characterization of neuropeptide Y binding sites in rat brain membrane preparations using [125I][Leu31,Pro34]peptide YY and [125I]peptide YY3-36 as selective Y1 and Y2 radioligands. *Journal of Pharmacology and Experimental Therapeutics*. 272 (2), 673–680.

Dumont, Y., Moyse, E., Fournier, A. & Quirion, R. (2007) Distribution of peripherally injected peptide YY ([125I] PYY (3-36)) and pancreatic polypeptide ([125I] hPP) in the CNS: enrichment in the area postrema. *Journal of molecular neuroscience : MN*. [Online] 33 (3), 294–304. Available from: doi:10.1007/s12031-007-9007-9.

Eberlein, G.A., Eysselein, V.E., Schaeffer, M., Layer, P., et al. (1989) A new molecular form of PYY: structural characterization of human PYY(3-36) and PYY(1-36). *Peptides*. [Online] 10 (4), 797–803. Available from: doi:10.1016/0196-9781(89)90116-2.

Edelsbrunner, M.E., Painsipp, E., Herzog, H. & Holzer, P. (2009) Evidence from knockout mice for distinct implications of neuropeptide-Y Y2 and Y4 receptors in the circadian control of locomotion, exploration, water and food intake. *Neuropeptides*. [Online] 43 (6), 491–497. Available from: doi:10.1016/j.npep.2009.08.007.

Edfalk, S., Steneberg, P. & Edlund, H. (2008) Gpr40 is expressed in enteroendocrine cells and mediates free fatty acid stimulation of incretin secretion. *Diabetes*. [Online] 57 (9), 2280–2287. Available from: doi:10.2337/db08-0307.

Egerod, K.L., Petersen, N., Timshel, P.N., Rekling, J.C., et al. (2018) Profiling of G protein-coupled receptors in vagal afferents reveals novel gut-to-brain sensing mechanisms. *Molecular Metabolism*. [Online] 12 (April), 62–75. Available from: doi:10.1016/j.molmet.2018.03.016.

Ek, M., Kurosawa, M., Lundeberg, T. & Ericsson, A. (1998) Activation of vagal afferents after intravenous injection of interleukin-1β: Role of endogenous prostaglandins. *Journal of Neuroscience*. [Online] 18 (22), 9471–9479. Available from: doi:10.1523/jneurosci.18-22-09471.1998.

Ekblad, E. & Sundler, F. (2002) Distribution of pancreatic polypeptide and peptide YY. *Peptides*. [Online] 23 (2), 251–261. Available from: doi:10.1016/S0196-9781(01)00601-5.

Ellacott, K.L.J. & Cone, R.D. (2006) The role of the central melanocortin system in the regulation of food intake and energy homeostasis: Lessons from mouse models. *Philosophical Transactions of the Royal Society B: Biological Sciences*. [Online] 361 (1471), 1265–1274. Available from: doi:10.1098/rstb.2006.1861.

Engelstoft, M.S., Egerod, K.L., Holst, B. & Schwartz, T.W. (2008) A Gut Feeling for Obesity: 7TM Sensors on Enteroendocrine Cells. *Cell Metabolism*. [Online] 8 (6), 447–449. Available from: doi:10.1016/j.cmet.2008.11.004.

Epanechnikov, V.A. (1969) Non-Parametric Estimation of a Multivariate Probability Density. *Theory*

of Probability & Its Applications. [Online] 14 (1), 153–158. Available from: doi:10.1137/1114019.

Esterházy, D., Canesso, M.C.C., Mesin, L., Muller, P.A., et al. (2019) Compartmentalized gut lymph node drainage dictates adaptive immune responses. *Nature*. [Online] 569 (7754), 126–130. Available from: doi:10.1038/s41586-019-1125-3.

Faber, C.L., Deem, J.D., Campos, C.A., Taborsky, G.J., et al. (2020) CNS control of the endocrine pancreas. *Diabetologia*. [Online] 63 (10), 2086–2094. Available from: doi:10.1007/s00125-020-05204-6.

Fan, W., Ellacott, K.L.J., Halatchev, I.G., Takahashi, K., et al. (2004) Cholecystokinin-mediated suppression of feeding involves the brainstem melanocortin system. *Nature Neuroscience*. [Online] 7 (4), 335–336. Available from: doi:10.1038/nn1214.

Fergusson, G., Éthier, M., Guévremont, M., Chrétien, C., et al. (2014) Defective insulin secretory response to intravenous glucose in C57Bl/6J compared to C57Bl/6N mice. *Molecular Metabolism*. [Online] 3 (9), 848–854. Available from: doi:10.1016/j.molmet.2014.09.006.

Fernandes, A.B., Alves da Silva, J., Almeida, J., Cui, G., et al. (2020) Postingestive Modulation of Food Seeking Depends on Vagus-Mediated Dopamine Neuron Activity. *Neuron*. [Online] 106 (5), 778-788.e6. Available from: doi:10.1016/j.neuron.2020.03.009.

Forster, E.R., Green, T., Elliot, M., Bremner, A., et al. (1990) Gastric emptying in rats: role of afferent neurons and cholecystokinin. *American Journal of Physiology-Gastrointestinal and Liver Physiology*. [Online] 258 (4), G552–G556. Available from: doi:10.1152/ajpgi.1990.258.4.G552.

Fox, E.A., Phillips, R.J., Baronowsky, E.A., Byerly, M.S., et al. (2001) Neurotrophin-4 deficient mice have a loss of vagal intraganglionic mechanoreceptors from the small intestine and a disruption of short-term satiety. *Journal of Neuroscience*. [Online] 21 (21), 8602–8615. Available from: doi:10.1523/jneurosci.21-21-08602.2001.

Fu-Cheng, X., Anini, Y., Chariot, J., Castex, N., et al. (1997) Mechanisms of peptide YY release induced by an intraduodenal meal in rats: neural regulation by proximal gut. *Pflügers Archiv*. [Online] 433 (5), 571–579. Available from: doi:10.1007/s004240050316.

Fulkerson, P.C. & Rothenberg, M.E. (2008) Origin, regulation and physiological function of intestinal oeosinophils. *Best Practice and Research: Clinical Gastroenterology*. [Online] 22 (3), 411–423. Available from: doi:10.1016/j.bpg.2007.10.023.

Furness, J.B. (2012) The enteric nervous system and neurogastroenterology. *Nature Reviews Gastroenterology and Hepatology*. [Online] 9 (5), 286–294. Available from: doi:10.1038/nrgastro.2012.32.

Gabanyi, I., Muller, P.A., Feighery, L., Oliveira, T.Y., et al. (2016) Neuro-immune Interactions Drive Tissue Programming in Intestinal Macrophages. *Cell*. [Online] 164 (3), 378–391. Available from: doi:10.1016/j.cell.2015.12.023.

Galle-Treger, L., Suzuki, Y., Patel, N., Sankaranarayanan, I., et al. (2016) Nicotinic acetylcholine receptor agonist attenuates ILC2-dependent airway hyperreactivity. *Nature Communications*. [Online] 7, 1–13. Available from: doi:10.1038/ncomms13202.

Garlicki, J., Konturek, P.K., Majka, J., Kwiecien, N., et al. (1990) Cholecystokinin receptors and vagal

nerves in control of food intake in rats. *American Journal of Physiology - Endocrinology and Metabolism*. [Online] 258 (1 21-1), 0–5. Available from: doi:10.1152/ajpendo.1990.258.1.e40.

Gasbjerg, L.S., Helsted, M.M., Hartmann, B., Jensen, M.H., et al. (2019) Separate and Combined Glucometabolic Effects of Endogenous Glucose-Dependent Insulinotropic Polypeptide and Glucagon-like Peptide 1 in Healthy Individuals. *Diabetes*. [Online] 68 (5), 906 LP – 917. Available from: doi:10.2337/db18-1123.

Gautron, L., Elmquist, J.K. & Williams, K.W. (2015) Neural control of energy balance: Translating circuits to therapies. *Cell*. [Online] 161 (1), 133–145. Available from: doi:10.1016/j.cell.2015.02.023.

Gautron, L., Sakata, I., Udit, S., Zigman, J.M., et al. (2011) Genetic tracing of Nav1.8-expressing vagal afferents in the mouse. *Journal of Comparative Neurology*. [Online] 519 (15), 3085–3101. Available from: doi:10.1002/cne.22667.

Ghia, J.E., Blennerhassett, P., Kumar-Ondiveeran, H., Verdu, E.F., et al. (2006) The Vagus Nerve: A Tonic Inhibitory Influence Associated With Inflammatory Bowel Disease in a Murine Model. *Gastroenterology*. [Online] 131 (4), 1122–1130. Available from: doi:10.1053/j.gastro.2006.08.016.

Gibbs, J., Young, R.C. & Smith, G.P. (1973) Cholecystokinin decreases food intake in rats. *Journal of Comparative and Physiological Psychology*. [Online]. 84 (3) pp.488–495. Available from: doi:10.1037/h0034870.

Gil, K., Bugajski, A., Kurnik, M., Zaraska, W., et al. (2009) Physiological and morphological effects of long-term vagal stimulation in diet induced obesity in rats. *Journal of physiology and pharmacology : an official journal of the Polish Physiological Society*. 60 Suppl 3, 61–66.

Di Giovangiulio, M., Bosmans, G., Meroni, E., Stakenborg, N., et al. (2016) Vagotomy affects the development of oral tolerance and ncreases susceptibility to develop colitis independently of α-7 nicotinic receptor. *Molecular Medicine*. [Online] 22 (8), 464–476. Available from: doi:10.2119/molmed.2016.00062.

Godinho-Silva, C., Cardoso, F. & Veiga-Fernandes, H. (2019) Neuro-Immune Cell Units: A New Paradigm in Physiology. *Annual Review of Immunology*. [Online] 37, 19–46. Available from: doi:10.1146/annurev-immunol-042718-041812.

Goehler, L.E., Gaykema, R.P. a., HamMacK, S.E., Maier, S.F., et al. (1998) Interleukin-1 induces c-Fos immunoreactivity in primary afferent neurons of the vagus nerve. *Brain Research*. [Online] 804 (2), 306–310. Available from: doi:10.1016/S0006-8993(98)00685-4.

Goehler, L.E., Gaykema, R.P.A., Hansen, M.K., Anderson, K., et al. (2000) Vagal immune-to-brain communication: A visceral chemosensory pathway. *Autonomic Neuroscience: Basic and Clinical*. [Online] 85 (1–3), 49–59. Available from: doi:10.1016/S1566-0702(00)00219-8.

Goehler, L.E., Relton, J.K., Dripps, D., Kiechle, R., et al. (1997) Vagal paraganglia bind biotinylated interleukin-1 receptor antagonist: A possible mechanism for immune-to-brain communication. *Brain Research Bulletin*. [Online] 43 (3), 357–364. Available from: doi:10.1016/S0361-9230(97)00020-8.

Goldstein, N., McKnight, A.D., Carty, J.R.E., Arnold, M., et al. (2021) Hypothalamic detection of macronutrients via multiple gut-brain pathways. *Cell Metabolism*. [Online] 33 (3), 676-687.e5.

Available from: doi:10.1016/j.cmet.2020.12.018.

Gomez, J.L., Bonaventura, J., Lesniak, W., Mathews, W.B., et al. (2017) Chemogenetics revealed: DREADD occupancy and activation via converted clozapine. *Science*. [Online] 357 (6350), 503–507. Available from: doi:10.1126/science.aan2475.

Goodpaster, B.H., Theriault, R., Watkins, S.C. & Kelley, D.E. (2000) Intramuscular lipid content is increased in obesity and decreased by weight loss. *Metabolism: Clinical and Experimental*. [Online] 49 (4), 467–472. Available from: doi:10.1016/S0026-0495(00)80010-4.

Goumain, M., Voisin, T., Lorinet, A.M. & Laburthe, M. (1998) Identification and distribution of mRNA encoding the Y1, Y2, Y4, and Y5 receptors for peptides of the PP-fold family in the rat intestine and colon. *Biochemical and biophysical research communications*. [Online] 247 (1), 52–56. Available from: doi:10.1006/bbrc.1998.8647.

Goverse, G., Stakenborg, M. & Matteoli, G. (2016) The intestinal cholinergic anti-inflammatory pathway. *Journal of Physiology*. [Online] 594 (20), 5771–5780. Available from: doi:10.1113/JP271537.

Goyal, R.K., Guo, Y. & Mashimo, H. (2019) Advances in the physiology of gastric emptying. *Neurogastroenterology and Motility*. [Online] 31 (4). Available from: doi:10.1111/nmo.13546.

Grandt, D., Schimiczek, M., Beglinger, C., Layer, P., et al. (1994) Two molecular forms of Peptide YY (PYY) are abundant in human blood: characterization of a radioimmunoassay recognizing PYY 1-36 and PYY 3-36. *Regulatory Peptides*. [Online] 51 (2), 151–159. Available from: doi:10.1016/0167-0115(94)90204-6.

Greeley, G.H., Lluis, F., Gomez, G., Ishizuka, J., et al. (1988) Peptide YY antagonizes β-adrenergic-stimulated release of insulin in dogs. *American Journal of Physiology - Endocrinology and Metabolism*. [Online] 254 (4). Available from: doi:10.1152/ajpendo.1988.254.4.e513.

Greenway, F.L. (2015) Physiological adaptations to weight loss and factors favouring weight regain. *International Journal of Obesity*. [Online] 39 (8), 1188–1196. Available from: doi:10.1038/ijo.2015.59.

Gribble, F.M. & Reimann, F. (2016) Enteroendocrine Cells: Chemosensors in the Intestinal Epithelium. *Annual Review of Physiology*. [Online] 78, 277–299. Available from: doi:10.1146/annurev-physiol-021115-105439.

Gribble, F.M. & Reimann, F. (2019) Function and mechanisms of enteroendocrine cells and gut hormones in metabolism. *Nature Reviews Endocrinology*. [Online] 15 (4), 226–237. Available from: doi:10.1038/s41574-019-0168-8.

Gribble, F.M. & Reimann, F. (2021) Metabolic Messengers: glucagon-like peptide 1. *Nature Metabolism*. [Online] 1. Available from: doi:10.1038/s42255-020-00327-x.

Gribble, F.M., Williams, L., Simpson, A.K. & Reimann, F. (2003) A Novel Glucose-Sensing Mechanism Contributing to. *Diabetes*. 52, 1147.

Grill, V., Adamson, U. & Cerasi, E. (1978) Immediate and time-dependent effects of glucose on insulin release from rat pancreatic tissue. Evidence for different mechanisms of action. *Journal of Clinical Investigation*. [Online] 61 (4), 1034–1043. Available from: doi:10.1172/JCI109002.

Grodsky, G.M. (1972) A threshold distribution hypothesis for packet storage of insulin and its mathematical modeling. *The Journal of clinical investigation*. [Online] 51 (8), 2047–2059. Available from: doi:10.1172/JCI107011.

Gromada, J., Holst, J.J. & Rorsman, P. (1998) Cellular regulation of islet hormone secretion by the incretin hormone glucagon-like peptide 1. *Pflugers Archiv European Journal of Physiology*. [Online] 435 (5), 583–594. Available from: doi:10.1007/s004240050558.

Guida, C., McCulloch, L.J., Godazgar, M., Stephen, S.D., et al. (2018) Sitagliptin and Roux-en-Y gastric bypass modulate insulin secretion via regulation of intra-islet PYY. *Diabetes, Obesity and Metabolism*. [Online] 20 (3), 571–581. Available from: doi:10.1111/dom.13113.

Guida, C., Stephen, S.D., Watson, M., Dempster, N., et al. (2019) PYY plays a key role in the resolution of diabetes following bariatric surgery in humans. *EBioMedicine*. [Online] 40, 67–76. Available from: doi:10.1016/j.ebiom.2018.12.040.

Guo, Y., Ma, L., Enriori, P.J., Koska, J., et al. (2006) Physiological evidence for the involvement of peptide YY in the regulation of energy homeostasis in humans. *Obesity (Silver Spring, Md.)*. [Online] 14 (9), 1562–1570. Available from: doi:10.1038/oby.2006.180.

Habib, A.M., Richards, P., Cairns, L.S., Rogers, G.J., et al. (2012) Overlap of endocrine hormone expression in the mouse intestine revealed by transcriptional profiling and flow cytometry. *Endocrinology*. [Online] 153 (7), 3054–3065. Available from: doi:10.1210/en.2011-2170.

Hajnal, A., Smith, G.P. & Norgren, R. (2004) Oral sucrose stimulation increases accumbens dopamine in the rat. *American journal of physiology. Regulatory, integrative and comparative physiology*. [Online] 286 (1), R31-7. Available from: doi:10.1152/ajpregu.00282.2003.

Halaas, J., Gajiwala, K., Maffei, M., Cohen, S., et al. (1995) Weight-reducing effects of the plasma protein encoded by the obese gene. *Science*. [Online] 269 (5223), 543–546. Available from: doi:10.1126/science.7624777.

Halaas, J.L., Boozer, C., Blair-West, J., Fidahusein, N., et al. (1997) Physiological response to long-term peripheral and central leptin infusion in lean and obese mice. *Proceedings of the National Academy of Sciences of the United States of America*. [Online] 94 (16), 8878–8883. Available from: doi:10.1073/pnas.94.16.8878.

Halatchev, I.G. & Cone, R.D. (2005) Peripheral administration of PYY3-36 produces conditioned taste aversion in mice. *Cell Metabolism*. [Online] 1 (3), 159–168. Available from: doi:10.1016/j.cmet.2005.02.003.

Halatchev, I.G., Ellacott, K.L.J., Fan, W. & Cone, R.D. (2004) Peptide YY3-36 inhibits food intake in mice through a melanocortin-4 receptor-independent mechanism. *Endocrinology*. [Online] 145 (6), 2585–2590. Available from: doi:10.1210/en.2003-1754.

Han, W., Tellez, L.A., Perkins, M.H., Perez, I.O., et al. (2018) A Neural Circuit for Gut-Induced Reward. *Cell*. [Online] 175 (3), 665-678.e23. Available from: doi:10.1016/j.cell.2018.08.049.

Hansen, M.K., O'Connor, K.A., Goehler, L.E., Watkins, L.R., et al. (2001) The contribution of the vagus nerve in interleukin-1β-induced fever is dependent on dose. *American Journal of Physiology - Regulatory Integrative and Comparative Physiology*. [Online] 280, 929–934. Available from: doi:10.1152/ajpregu.2001.280.4.r929.

Hao, Z., Townsend, R.L., Mumphrey, M.B., Patterson, L.M., et al. (2014) Vagal Innervation of Intestine Contributes to Weight Loss After Roux-en-Y Gastric Bypass Surgery in Rats. *Obesity Surgery*. [Online] 24 (12), 2145–2151. Available from: doi:10.1007/s11695-014-1338-3.

Harris, G.C., Wimmer, M. & Aston-Jones, G. (2005) A role for lateral hypothalamic orexin neurons in reward seeking. *Nature*. [Online] 437 (7058), 556–559. Available from: doi:10.1038/nature04071.

de Heer, J., Rasmussen, C., Coy, D.H. & Holst, J.J. (2008) Glucagon-like peptide-1, but not glucose-dependent insulinotropic peptide, inhibits glucagon secretion via somatostatin (receptor subtype 2) in the perfused rat pancreas. *Diabetologia*. [Online] 51 (12), 2263–2270. Available from: doi:10.1007/s00125-008-1149-y.

Hernandez, L. & Hoebel, B.G. (1988) Feeding and hypothalamic stimulation increase dopamine turnover in the accumbens. *Physiology & behavior*. [Online] 44 (4–5), 599–606. Available from: doi:10.1016/0031-9384(88)90324-1.

Hodson, D.J., Mitchell, R.K., Bellomo, E.A., Sun, G., et al. (2013) Lipotoxicity disrupts incretin-regulated human β cell connectivity. *Journal of Clinical Investigation*. [Online] 123 (10), 4182–4194. Available from: doi:10.1172/JCI68459.

Van Den Hoek, A.M., Heijboer, A.C., Corssmit, E.P.M., Voshol, P.J., et al. (2004) PYY3-36 reinforces insulin action on glucose disposal in mice fed a high-fat diet. *Diabetes*. [Online] 53 (8), 1949–1952. Available from: doi:10.2337/diabetes.53.8.1949.

van den Hoek, A.M., Heijboer, A.C., Voshol, P.J., Havekes, L.M., et al. (2007) Chronic PYY3-36 treatment promotes fat oxidation and ameliorates insulin resistance in C57BL6 mice. *American journal of physiology. Endocrinology and metabolism*. [Online] 292 (1), E238-45. Available from: doi:10.1152/ajpendo.00239.2006.

Holst, J.J. (2007) The physiology of glucagon-like peptide 1. *Physiological Reviews*. [Online] 87 (4), 1409–1439. Available from: doi:10.1152/physrev.00034.2006.

Holst, J.J., Madsbad, S., Bojsen-Møller, K.N., Svane, M.S., et al. (2018) Mechanisms in bariatric surgery: Gut hormones, diabetes resolution, and weight loss. *Surgery for Obesity and Related Diseases*. [Online] 14 (5), 708–714. Available from: doi:10.1016/j.soard.2018.03.003.

Holt, M.K., Richards, J.E., Cook, D.R., Brierley, D.I., et al. (2019) Preproglucagon Neurons in the Nucleus of the Solitary Tract Are the Main Source of Brain GLP-1, Mediate Stress-Induced Hypophagia, and Limit Unusually Large Intakes of Food. *Diabetes*. [Online] 68 (1), 21 LP – 33. Available from: doi:10.2337/db18-0729.

Holzer, P. & Farzi, A. (2014) Neuropeptides and the microbiota- Gut-brain axis. *Advances in Experimental Medicine and Biology*. [Online] 817, 196–219. Available from: doi:10.1007/978-1-4939-0897-4_9.

Holzer, P., Reichmann, F. & Farzi, A. (2012) Neuropeptide Y, peptide YY and pancreatic polypeptide in the gut-brain axis. *Neuropeptides*. [Online] 46 (6), 261–274. Available from: doi:10.1016/j.npep.2012.08.005.

Hoppa, M.B., Collins, S., Ramracheya, R., Hodson, L., et al. (2009) Chronic Palmitate Exposure Inhibits Insulin Secretion by Dissociation of Ca2+ Channels from Secretory Granules. *Cell Metabolism*. [Online] 10 (6), 455–465. Available from: doi:10.1016/j.cmet.2009.09.011.

Hosoi, T., Okuma, Y., Matsuda, T. & Nomura, Y. (2005) Novel pathway for LPS-induced afferent vagus nerve activation: Possible role of nodose ganglion. *Autonomic Neuroscience: Basic and Clinical*. [Online] 120 (1–2), 104–107. Available from: doi:10.1016/j.autneu.2004.11.012.

Huo, L., Maeng, L., Bjørbaek, C. & Grill, H.J. (2007) Leptin and the control of food intake: neurons in the nucleus of the solitary tract are activated by both gastric distension and leptin. *Endocrinology*. [Online] 148 (5), 2189–2197. Available from: doi:10.1210/en.2006-1572.

Huston, N.J., Brenner, L.A., Taylor, Z.C. & Ritter, R.C. (2019) NPY2 receptor activation in the dorsal vagal complex increases food intake and attenuates CCK-induced satiation in male rats. *American journal of physiology. Regulatory, integrative and comparative physiology*. [Online] 316 (4), R406–R416. Available from: doi:10.1152/ajpregu.00011.2019.

Huszar, D., Lynch, C.A., Fairchild-Huntress, V., Dunmore, J.H., et al. (1997) Targeted disruption of the melanocortin-4 receptor results in obesity in mice. *Cell*. [Online] 88 (1), 131–141. Available from: doi:10.1016/S0092-8674(00)81865-6.

Ibiza, S., García-Cassani, B., Ribeiro, H., Carvalho, T., et al. (2016) Glial-cell-derived neuroregulators control type 3 innate lymphoid cells and gut defence. *Nature*. [Online] 535 (7612), 440–443. Available from: doi:10.1038/nature18644.

Ilegems, E., Dicker, A., Speier, S., Sharma, A., et al. (2013) Reporter islets in the eye reveal the plasticity of the endocrine pancreas. *Proceedings of the National Academy of Sciences of the United States of America*. [Online] 110 (51), 20581–20586. Available from: doi:10.1073/pnas.1313696110.

Imai, Y., Cousins, R.S., Liu, S., Phelps, B.M., et al. (2019) Connecting pancreatic islet lipid metabolism with insulin secretion and the development of type 2 diabetes. *Annals of the New York Academy of Sciences*. [Online] 53–72. Available from: doi:10.1111/nyas.14037.

Imeryüz, N., Yeğen, B.Ç., Bozkurt, A., Coşkun, T., et al. (1997) Glucagon-like peptide-1 inhibits gastric emptying via vagal afferent- mediated central mechanisms. *American Journal of Physiology - Gastrointestinal and Liver Physiology*. [Online] 273 (4 36-4), 920–927. Available from: doi:10.1152/ajpgi.1997.273.4.g920.

Jakob, M.O., Murugan, S. & Klose, C.S.N. (2020) Neuro-Immune Circuits Regulate Immune Responses in Tissues and Organ Homeostasis. *Frontiers in Immunology*. [Online] 11 (March), 1–17. Available from: doi:10.3389/fimmu.2020.00308.

Jarret, A., Jackson, R., Duizer, C., Healy, M.E., et al. (2020) Enteric Nervous System-Derived IL-18 Orchestrates Mucosal Barrier Immunity. *Cell*. [Online] 180 (1), 50–63. Available from: doi:10.1016/j.cell.2019.12.016.

Jendryka, M., Palchaudhuri, M., Ursu, D., van der Veen, B., et al. (2019) Pharmacokinetic and pharmacodynamic actions of clozapine-N-oxide, clozapine, and compound 21 in DREADD-based chemogenetics in mice. *Scientific Reports*. [Online] 9 (1), 1–14. Available from: doi:10.1038/s41598-019-41088-2.

Jesudason, D.R., Monteiro, M.P., McGowan, B.M.C., Neary, N.M., et al. (2007) Low-dose pancreatic polypeptide inhibits food intake in man. *The British journal of nutrition*. [Online] 97 (3), 426–429. Available from: doi:10.1017/S0007114507336799.

Jones, B., Buenaventura, T., Kanda, N., Chabosseau, P., et al. (2018) Targeting GLP-1 receptor

trafficking to improve agonist efficacy. *Nature Communications*. [Online] 9 (1). Available from: doi:10.1038/s41467-018-03941-2.

Jørgensen, N.B., Dirksen, C., Bojsen-Møller, K.N., Jacobsen, S.H., et al. (2013) Exaggerated glucagon-like peptide 1 response is important for improved β-cell function and glucose tolerance after roux-en-Y gastric bypass in patients with type 2 diabetes. *Diabetes*. [Online] 62 (9), 3044–3052. Available from: doi:10.2337/db13-0022.

Kaelberer, M.M., Buchanan, K.L., Klein, M.E., Barth, B.B., et al. (2018) A gut-brain neural circuit for nutrient sensory transduction. *Science*. [Online] 361 (6408). Available from: doi:10.1126/science.aat5236.

Kaelberer, M.M., Rupprecht, L.E., Liu, W.W., Weng, P., et al. (2020) Neuropod Cells: The Emerging Biology of Gut-Brain Sensory Transduction. *Annual Review of Neuroscience*. [Online] 43, 337–353. Available from: doi:10.1146/annurev-neuro-091619-022657.

Kahn, S.E., Hull, R.L. & Utzschneider, K.M. (2006) Mechanisms linking obesity to insulin resistance and type 2 diabetes. *Nature*. [Online] 444 (7121), 840–846. Available from: doi:10.1038/nature05482.

Kamegai, J., Tamura, H., Shimizu, T., Ishii, S., et al. (2001) Chronic central infusion of ghrelin increases hypothalamic neuropeptide Y and Agouti-related protein mRNA levels and body weight in rats. *Diabetes*. 50 (11), 2438–2443.

Kanatani, A., Mashiko, S., Murai, N., Sugimoto, N., et al. (2000) Role of the Y1 receptor in the regulation of neuropeptide Y-mediated feeding: comparison of wild-type, Y1 receptor-deficient, and Y5 receptor-deficient mice. *Endocrinology*. [Online] 141 (3), 1011–1016. Available from: doi:10.1210/endo.141.3.7387.

Karlsson, S., Scheurink, A.J., Steffens, A.B. & Ahrén, B. (1994) Involvement of capsaicin-sensitive nerves in regulation of insulin secretion and glucose tolerance in conscious mice. *The American journal of physiology*. [Online] 267 (4 Pt 2), R1071-7. Available from: doi:10.1152/ajpregu.1994.267.4.R1071.

Karra, E., Chandarana, K. & Batterham, R.L. (2009) The role of peptide YY in appetite regulation and obesity. *The Journal of physiology*. [Online] 587 (1), 19–25. Available from: doi:10.1113/jphysiol.2008.164269.

Kelley, D.E., He, J., Menshikova, E. V. & Ritov, V.B. (2002) Dysfunction of mitochondria in human skeletal muscle in type 2 diabetes. *Diabetes*. [Online] 51 (10), 2944–2950. Available from: doi:10.2337/diabetes.51.10.2944.

Kelly, E., Bailey, C.P. & Henderson, G. (2008) Agonist-selective mechanisms of GPCR desensitization. *British Journal of Pharmacology*. [Online] 153 (S1), S379–S388. Available from: doi:https://doi.org/10.1038/sj.bjp.0707604.

Kentish, S., Li, H., Philp, L.K., O'Donnell, T.A., et al. (2012) Diet-induced adaptation of vagal afferent function. *Journal of Physiology*. [Online] 590 (1), 209–221. Available from: doi:10.1113/jphysiol.2011.222158.

Kentish, S.J., O'Donnell, T.A., Isaacs, N.J., Young, R.L., et al. (2013) Gastric vagal afferent modulation by leptin is influenced by food intake status. *Journal of Physiology*. [Online] 591 (7), 1921–1934. Available from: doi:10.1113/jphysiol.2012.247577.

Kentish, S.J. & Page, A.J. (2014) Plasticity of gastro-intestinal vagal afferent endings. *Physiology and Behavior*. [Online] 136, 170–178. Available from: doi:10.1016/j.physbeh.2014.03.012.

Kerr, B.D., Flatt, P.R. & Gault, V.A. (2010) (d-Ser2)Oxm[mPEG-PAL]: A novel chemically modified analogue of oxyntomodulin with antihyperglycaemic, insulinotropic and anorexigenic actions. *Biochemical Pharmacology*. [Online] 80 (11), 1727–1735. Available from: doi:10.1016/j.bcp.2010.08.010.

Khan, A. & Pessin, J. (2002) Insulin regulation of glucose uptake: A complex interplay of intracellular signalling pathways. *Diabetologia*. [Online] 45 (11), 1475–1483. Available from: doi:10.1007/s00125-002-0974-7.

Khan, D., Vasu, S., Moffett, R.C., Irwin, N., et al. (2016) Islet distribution of Peptide YY and its regulatory role in primary mouse islets and immortalised rodent and human beta-cell function and survival. *Molecular and Cellular Endocrinology*. [Online] 436, 102–113. Available from: doi:10.1016/j.mce.2016.07.020.

Khorsandi, H., Nikpayam, O., Yousefi, R., Parandoosh, M., et al. (2019) Zinc supplementation improves body weight management, inflammatory biomarkers and insulin resistance in individuals with obesity: A randomized, placebo-controlled, double-blind trial. *Diabetology and Metabolic Syndrome*. [Online] 11 (1), 1–10. Available from: doi:10.1186/s13098-019-0497-8.

Kim, B.J., Carlson, O.D., Jang, H.J., Elahi, D., et al. (2005) Peptide YY is secreted after oral glucose administration in a gender-specific manner. *Journal of Clinical Endocrinology and Metabolism*. [Online] 90 (12), 6665–6671. Available from: doi:10.1210/jc.2005-0409.

Klarer, M., Weber-Stadlbauer, U., Arnold, M., Langhans, W., et al. (2019) Abdominal vagal deafferentation alters affective behaviors in rats. *Journal of Affective Disorders*. [Online] 252 (February), 404–412. Available from: doi:10.1016/j.jad.2019.04.015.

Klose, C.S. & Artis, D. (2019) Neuronal regulation of innate lymphoid cells. *Current Opinion in Immunology*. [Online] 56, 94–99. Available from: doi:10.1016/j.coi.2018.11.002.

Klose, C.S.N. & Artis, D. (2016) Innate lymphoid cells as regulators of immunity, inflammation and tissue homeostasis. *Nature Immunology*. [Online] 17 (7), 765–774. Available from: doi:10.1038/ni.3489.

Klose, C.S.N., Mahlakõiv, T., Moeller, J.B., Rankin, L.C., et al. (2017) The neuropeptide neuromedin U stimulates innate lymphoid cells and type 2 inflammation. *Nature*. [Online] 549 (7671), 282–286. Available from: doi:10.1038/nature23676.

Knauf, C., Abot, A., Wemelle, E. & Cani, P.D. (2020) Targeting the Enteric Nervous System to Treat Metabolic Disorders? 'enterosynes' as Therapeutic Gut Factors. *Neuroendocrinology*. [Online] 110 (1–2), 139–146. Available from: doi:10.1159/000500602.

Koda, S., Date, Y., Murakami, N., Shimbara, T., et al. (2005) The role of the vagal nerve in peripheral PYY 3-36-induced feeding reduction in rats. *Endocrinology*. [Online] 146 (5), 2369–2375. Available from: doi:10.1210/en.2004-1266.

Komatsu, M., Sato, Y., Aizawa, T. & Hashizume, K. (2001) KATP channel-independent glucose action: An elusive pathway in stimulus-secretion coupling of pancreatic β-cell. *Endocrine Journal*. [Online] 48 (3), 275–288. Available from: doi:10.1507/endocrj.48.275.

Komatsu, M., Takei, M., Ishii, H. & Sato, Y. (2013) Glucose-stimulated insulin secretion: A newer perspective. *Journal of Diabetes Investigation*. [Online] 4 (6), 511–516. Available from: doi:10.1111/jdi.12094.

Koopmans, S.J., Leighton, B. & DeFronzo, R.A. (1998) Neonatal de-afferentation of capsaicin-sensitive sensory nerves increases in vivo insulin sensitivity in conscious adult rats. *Diabetologia*. [Online] 41 (7), 813–820. Available from: doi:10.1007/s001250050992.

van der Kooy, D., Koda, L.Y., McGinty, J.F., Gerfen, C.R., et al. (1984) The organization of projections from the cortes, amygdala, and hypothalamus to the nucleus of the solitary tract in rat. *Journal of Comparative Neurology*. [Online] 224 (1), 1–24. Available from: doi:https://doi.org/10.1002/cne.902240102.

Koren, M.S. & Holmes, M.D. (2006) Vagus nerve stimulation does not lead to significant changes in body weight in patients with epilepsy. *Epilepsy and Behavior*. [Online] 8 (1), 246–249. Available from: doi:10.1016/j.yebeh.2005.10.001.

Krieger, J.P., Arnold, M., Pettersen, K.G., Lossel, P., et al. (2016) Knockdown of GLP-1 receptors in vagal afferents affects normal food intake and glycemia. *Diabetes*. [Online] 65 (1), 34–43. Available from: doi:10.2337/db15-0973.

Krolczyk, G., Sobocki, J., Laskiewicz, J., Matyja, A., et al. (2001) Effects of continuous microchip (MC) vagal neuromodulation on gastrointestinal functions in rats. *Journal of physiology and pharmacology : an official journal of the Polish Physiological Society*. 52 (4), 705–715.

Kupari, J., Häring, M., Agirre, E., Castelo-Branco, G., et al. (2019) An Atlas of Vagal Sensory Neurons and Their Molecular Specialization. *Cell Reports*. [Online] 27 (8), 2508-2523.e4. Available from: doi:10.1016/j.celrep.2019.04.096.

Lafferty, R.A., Flatt, P.R. & Irwin, N. (2018) Emerging therapeutic potential for peptide YY for obesity-diabetes. *Peptides*. [Online] 100 (November 2017), 269–274. Available from: doi:10.1016/j.peptides.2017.11.005.

de Lartigue, G. (2014) Putative roles of neuropeptides in vagal afferent signaling. *Physiology & behavior*. [Online] 136, 155–169. Available from: doi:10.1016/j.physbeh.2014.03.011.

de Lartigue, G. (2016) Role of the vagus nerve in the development and treatment of diet-induced obesity. *Journal of Physiology*. [Online] 594 (20), 5791–5815. Available from: doi:10.1113/JP271538.

de Lartigue, G., Barbier de la Serre, C., Espero, E., Lee, J., et al. (2012) Leptin resistance in vagal afferent neurons inhibits cholecystokinin signaling and satiation in diet induced obese rats. *PLoS ONE*. [Online] 7 (3), 1–10. Available from: doi:10.1371/journal.pone.0032967.

De Lartigue, G., Dimaline, R., Varro, A. & Dockray, G.J. (2007) Cocaine- and amphetamine-regulated transcript: Stimulation of expression in rat vagal afferent neurons by cholecystokinin and suppression by ghrelin. *Journal of Neuroscience*. [Online] 27 (11), 2876–2882. Available from: doi:10.1523/JNEUROSCI.5508-06.2007.

de Lartigue, G., de la Serre, C.B., Espero, E., Lee, J., et al. (2011) Diet-induced obesity leads to the development of leptin resistance in vagal afferent neurons. *American Journal of Physiology - Endocrinology and Metabolism*. [Online] 301 (1), 187–195. Available from: doi:10.1152/ajpendo.00056.2011.

De Lartigue, G., Lur, G., Dimaline, R., Varro, A., et al. (2010) EGR1 is a target for cooperative interactions between cholecystokinin and leptin, and inhibition by ghrelin, in vagal afferent neurons. *Endocrinology*. [Online] 151 (8), 3589–3599. Available from: doi:10.1210/en.2010-0106.

de Lartigue, G., Ronveaux, C.C. & Raybould, H.E. (2014) Deletion of leptin signaling in vagal afferent neurons results in hyperphagia and obesity. *Molecular Metabolism*. [Online] 3 (6), 595–607. Available from: doi:10.1016/j.molmet.2014.06.003.

Laskiewicz, J. & Sobocki, J. (2003) Effects of vagal neuromodulation and vagotomy on control of food intake and body weight in rats. *Journal of physiology and pharmacology : an official journal of the Polish Physiological Society*. 54 (4), 603–610.

Lay, A.C., Barrington, A.F., Hurcombe, J.A., Ramnath, R.D., et al. (2020) A role for NPY-NPY2R signaling in albuminuric kidney disease. *Proceedings of the National Academy of Sciences of the United States of America*. [Online] 117 (27), 15862–15873. Available from: doi:10.1073/pnas.2004651117.

Lee, S.J., Krieger, J.P., Vergara, M., Quinn, D., et al. (2020) Blunted Vagal Cocaine- and Amphetamine-Regulated Transcript Promotes Hyperphagia and Weight Gain. *Cell Reports*. [Online] 30 (6), 2028-2039.e4. Available from: doi:10.1016/j.celrep.2020.01.045.

Leech, C.A., Chepurny, O.G. & Holz, G.G. (2010) Chapter Ten - Epac2-Dependent Rap1 Activation and the Control of Islet Insulin Secretion by Glucagon-Like Peptide-1. In: Gerald B T - Vitamins & Hormones Litwack (ed.). *Incretins and Insulin Secretion*. [Online]. Academic Press. pp. 279–302. Available from: doi:https://doi.org/10.1016/B978-0-12-381517-0.00010-2.

Leinninger, G.M., Jo, Y.-H., Leshan, R.L., Louis, G.W., et al. (2009) Leptin acts via leptin receptor-expressing lateral hypothalamic neurons to modulate the mesolimbic dopamine system and suppress feeding. *Cell metabolism*. [Online] 10 (2), 89–98. Available from: doi:10.1016/j.cmet.2009.06.011.

Leitch, V.D., Brassill, M.J., Rahman, S., Butterfield, N.C., et al. (2019) PYY is a negative regulator of bone mass and strength. *Bone*. [Online] 127, 427–435. Available from: doi:https://doi.org/10.1016/j.bone.2019.07.011.

Lewis, J.E., Miedzybrodzka, E.L., Foreman, R.E., Woodward, O.R.M., et al. (2020) Selective stimulation of colonic L cells improves metabolic outcomes in mice. *Diabetologia*. [Online] 63 (7), 1396–1407. Available from: doi:10.1007/s00125-020-05149-w.

Lin, H.C., Zhao, X.T., Wang, L. & Wong, H. (1996) Fat-induced ileal brake in the dog depends on peptide YY. *Gastroenterology*. [Online] 110 (5), 1491–1495. Available from: doi:10.1053/gast.1996.v110.pm8613054.

Liu, C., Bookout, A.L., Lee, S., Sun, K., et al. (2014a) Short Article PPAR g in Vagal Neurons Regulates High-Fat Diet Induced Thermogenesis. *Cell Metabolism*. [Online] 19 (4), 722–730. Available from: doi:10.1016/j.cmet.2014.01.021.

Liu, Z., Zhou, J., Li, Y., Hu, F., et al. (2014b) Dorsal raphe neurons signal reward through 5-HT and glutamate. *Neuron*. [Online] 81 (6), 1360–1374. Available from: doi:10.1016/j.neuron.2014.02.010.

Llewellyn-Smith, I.J., Reimann, F., Gribble, F.M. & Trapp, S. (2011) Preproglucagon neurons project

widely to autonomic control areas in the mouse brain. *Neuroscience*. [Online] 180, 111–121. Available from: doi:10.1016/j.neuroscience.2011.02.023.

Lu, V.B., Rievaj, J., O'Flaherty, E.A., Smith, C.A., et al. (2019) Adenosine triphosphate is co-secreted with glucagon-like peptide-1 to modulate intestinal enterocytes and afferent neurons. *Nature Communications*. [Online] 10 (1). Available from: doi:10.1038/s41467-019-09045-9.

Ludwig, D.S., Tritos, N.A., Mastaitis, J.W., Kulkarni, R., et al. (2001) Melanin-concentrating hormone overexpression in transgenic mice leads to obesity and insulin resistance. *The Journal of Clinical Investigation*. [Online] 107 (3), 379–386. Available from: doi:10.1172/JCI10660.

Mace, O.J., Schindler, M. & Patel, S. (2012) The regulation of K- and L-cell activity by GLUT2 and the calcium-sensing receptor CasR in rat small intestine. *Journal of Physiology*. [Online] 590 (12), 2917–2936. Available from: doi:10.1113/jphysiol.2011.223800.

MacLean, D.B. (1985) Abrogation of peripheral cholecystokinin-satiety in the capsaicin treated rat. *Regulatory Peptides*. [Online] 11 (4), 321–333. Available from: doi:10.1016/0167-0115(85)90204-6.

Maffei, M., Halaas, J., Ravussin, E., Pratley, R.E., et al. (1995) Leptin levels in human and rodent: measurement of plasma leptin and ob RNA in obese and weight-reduced subjects. *Nature medicine*. [Online] 1 (11), 1155–1161. Available from: doi:10.1038/nm1195-1155.

Mahler, S. V. & Aston-Jones, G. (2018) CNO Evil? Considerations for the Use of DREADDs in Behavioral Neuroscience. *Neuropsychopharmacology*. [Online] 43 (5), 934–936. Available from: doi:10.1038/npp.2017.299.

Malik, S., McGlone, F., Bedrossian, D. & Dagher, A. (2008) Ghrelin modulates brain activity in areas that control appetitive behavior. *Cell metabolism*. [Online] 7 (5), 400–409. Available from: doi:10.1016/j.cmet.2008.03.007.

Manning, S. & Batterham, R.L. (2014) The role of gut hormone peptide YY in energy and glucose homeostasis: twelve years on. *Annual review of physiology*. [Online] 76, 585–608. Available from: doi:10.1146/annurev-physiol-021113-170404.

Martin, N.M., Small, C.J., Sajedi, A., Patterson, M., et al. (2004) Pre-obese and obese agouti mice are sensitive to the anorectic effects of peptide YY3-36 but resistant to ghrelin. *International Journal of Obesity*. [Online] 28 (7), 886–893. Available from: doi:10.1038/sj.ijo.0802646.

Martinez, V.G. & O'Driscoll, L. (2015) Neuromedin U: a multifunctional neuropeptide with pleiotropic roles. *Clinical chemistry*. [Online] 61 (3), 471–482. Available from: doi:10.1373/clinchem.2014.231753.

Matheis, F., Muller, P.A., Graves, C.L., Gabanyi, I., et al. (2020) Adrenergic Signaling in Muscularis Macrophages Limits Infection-Induced Neuronal Loss. *Cell*. [Online] 180 (1), 64-78.e16. Available from: doi:10.1016/j.cell.2019.12.002.

Matteoli, G., Gomez-Pinilla, P.J., Nemethova, A., Giovangiulio, M. Di, et al. (2014) A distinct vagal anti-inflammatory pathway modulates intestinal muscularis resident macrophages independent of the spleen. *Gut*. [Online] 63 (6), 938–948. Available from: doi:10.1136/gutjnl-2013-304676.

McDole, J.R., Wheeler, L.W., McDonald, K.G., Wang, B., et al. (2012) Goblet cells deliver luminal

antigen to CD103 + dendritic cells in the small intestine. *Nature*. [Online] 483 (7389), 345–349. Available from: doi:10.1038/nature10863.

McGavigan, A.K. & Murphy, K.G. (2012) Gut hormones: the future of obesity treatment? *British journal of clinical pharmacology*. [Online] 74 (6), 911–919. Available from: doi:10.1111/j.1365-2125.2012.04278.x.

Mcgowan, M.K., Andrews, K.M., Fenner, D. & Grossman, S.P. (1993) Chronic intrahypothalamic insulin infusion in the rat: Behavioral specificity. *Physiology and Behavior*. [Online] 54 (5), 1031–1034. Available from: doi:10.1016/0031-9384(93)90320-F.

Mentlein, R., Gallwitz, B. & Schmidt, W.E. (1993) Dipeptidyl-peptidase IV hydrolyses gastric inhibitory polypeptide, glucagon-like peptide-1(7-36)amide, peptide histidine methionine and is responsible for their degradation in human serum. *European journal of biochemistry*. [Online] 214 (3), 829–835. Available from: doi:10.1111/j.1432-1033.1993.tb17986.x.

Meyers, E.E., Kronemberger, A., Lira, V., Rahmouni, K., et al. (2016) Contrasting effects of afferent and efferent vagal nerve stimulation on insulin secretion and blood glucose regulation. *Physiological Reports*. [Online] 4 (4), 1–9. Available from: doi:10.14814/phy2.12718.

Michel, M.C., Beck-Sickinger, A., Cox, H., Doods, H.N., et al. (1998) XVI. International union of pharmacology recommendations for the nomenclature of neuropeptide Y, peptide YY, and pancreatic polypeptide receptors. *Pharmacological Reviews*. 50 (1), 143–150.

Michl, T., Jocič, M., Heinemann, A., Schuligoi, R., et al. (2001) Vagal afferent signaling of a gastric mucosal acid insult to medullary, pontine, thalamic, hypothalamic and limbic, but not cortical, nuclei of the rat brain. *Pain*. [Online] 92 (1–2), 19–27. Available from: doi:10.1016/S0304-3959(00)00467-X.

Mina, A.I., Leclair, R.A., Leclair, K.B., Cohen, D.E., et al. (2018) CalR : A Web-Based Analysis Tool for Indirect Calorimetry Experiments Resource CalR : A Web-Based Analysis Tool for Indirect Calorimetry Experiments. *Cell Metabolism*. [Online] 28 (4), 656-666.e1. Available from: doi:10.1016/j.cmet.2018.06.019.

Misra, S., Murthy, K.S., Zhou, H. & Grider, J.R. (2004) Coexpression of Y1, Y2, and Y4 receptors in smooth muscle coupled to distinct signaling pathways. *Journal of Pharmacology and Experimental Therapeutics*. [Online] 311 (3), 1154–1162. Available from: doi:10.1124/jpet.104.071415.

Moore, C., Jodka, C., Dang, J., Lwin, A., et al. (2002) Chronic administration of PYY [3-36] reduces body weight and improves glycemic control in C57BL/6J mice fed a high fat diet. *Diabetes*. 51.

Moran, T.H. & Kinzig, K.P. (2004) Gastrointestinal satiety signals II. Cholecystokinin. *American journal of physiology. Gastrointestinal and liver physiology*. [Online] 286 (2), G183-8. Available from: doi:10.1152/ajpgi.00434.2003.

Moran, T.H. & McHugh, P.R. (1982) Cholecystokinin suppresses food intake by inhibiting gastric emptying. *The American journal of physiology*. [Online] 242 (5), R491-7. Available from: doi:10.1152/ajpregu.1982.242.5.R491.

Moran, T.H. & Schwartz, G.J. (1994) Neurobiology of cholecystokinin. *Critical reviews in neurobiology*. 9 (1), 1–28.

Moran, T.H., Smith, G.P., Hostetler, A.M. & McHugh, P.R. (1987) Transport of cholecystokinin (CCK) binding sites in subdiaphragmatic vagal branches. *Brain Research*. [Online] 415 (1), 149–152. Available from: doi:10.1016/0006-8993(87)90278-2.

Morgan, D.G., Kulkarni, R.N., Hurley, J.D., Wang, Z.L., et al. (1998) Inhibition of glucose stimulated insulin secretion by neuropeptide Y is mediated via the Y1 receptor and inhibition of adenylyl cyclase in RIN 5AH rat insulinoma cells. *Diabetologia*. [Online] 41 (12), 1482–1491. Available from: doi:10.1007/s001250051095.

Morgan, J.I. & Curran, T. (1991) Stimulus-transcription coupling in the nervous system: Involvement of the inducible proto-oncogenes fos and jun. *Annual Review of Neuroscience*. [Online] 14, 421–451. Available from: doi:10.1146/annurev.ne.14.030191.002225.

Mowat, A.M. & Agace, W.W. (2014) Regional specialization within the intestinal immune system. *Nature Reviews Immunology*. [Online] 14 (10), 667–685. Available from: doi:10.1038/nri3738.

Muller, P.A., Koscsó, B., Rajani, G.M., Stevanovic, K., et al. (2014) Crosstalk between muscularis macrophages and enteric neurons regulates gastrointestinal motility. *Cell*. [Online] 158 (2), 300–313. Available from: doi:10.1016/j.cell.2014.04.050.

Muller, P.A., Matheis, F., Schneeberger, M., Kerner, Z., et al. (2020a) Microbiota-modulated CART+ enteric neurons autonomously regulate blood glucose. *Science*. [Online] 370 (6514), 314–321. Available from: doi:10.1126/science.abd6176.

Muller, P.A., Schneeberger, M., Matheis, F., Wang, P., et al. (2020b) Microbiota modulate sympathetic neurons via a gut–brain circuit. *Nature*. [Online] 583 (7816), 441–446. Available from: doi:10.1038/s41586-020-2474-7.

Mullins, D., Kirby, D., Hwa, J., Guzzi, M., et al. (2001) Identification of potent and selective neuropeptide Y Y1 receptor agonists with orexigenic activity in vivo. *Molecular Pharmacology*. 60 (3), 534–540.

Murray, C.D.R., Booth, C.E., Bulmer, D.C.E., Emmanuel, A. V., et al. (2006) Ghrelin augments afferent response to distension in rat isolated jejunum. *Neurogastroenterology and Motility*. [Online] 18 (12), 1112–1120. Available from: doi:10.1111/j.1365-2982.2006.00848.x.

Nagashima, H., Mahlakõiv, T., Shih, H.Y., Davis, F.P., et al. (2019) Neuropeptide CGRP Limits Group 2 Innate Lymphoid Cell Responses and Constrains Type 2 Inflammation. *Immunity*. [Online] 51 (4), 682–695. Available from: doi:10.1016/j.immuni.2019.06.009.

Nagi, K. & Habib, A.M. (2021) Biased signaling: A viable strategy to drug ghrelin receptors for the treatment of obesity. *Cellular signalling*. [Online] 83, 109976. Available from: doi:10.1016/j.cellsig.2021.109976.

NamKoong, C., Song, W.J., Kim, C.Y., Chun, D.H., et al. (2019) Chemogenetic manipulation of parasympathetic neurons (DMV) regulates feeding behavior and energy metabolism. *Neuroscience Letters*. [Online] 712 (June), 1–7. Available from: doi:10.1016/j.neulet.2019.134356.

National Institute for Health and Care Excellence (2014) *Obesity: identification, assessment and management*. [Online]. 2014. Available from: https://www.nice.org.uk/guidance/cg189.

National Institute of Diabetes and Digestive and Kidney Diseases (2018) *Insulin Resistance &*

Prediabetes. [Online]. 2018. Available from: https://www.niddk.nih.gov/health-information/diabetes/overview/what-is-diabetes/prediabetes-insulin-resistance [Accessed: 15 August 2021].

National Institute of Diabetes and Digestive and Kidney Diseases (2017) *Type 2 diabetes*. [Online]. 2017. Available from: https://www.niddk.nih.gov/health-information/diabetes/overview/what-is-diabetes/type-2-diabetes.

Nauck, M.A., Heimesaat, M.M., Orskov, C., Holst, J.J., et al. (1993) Preserved incretin activity of glucagon-like peptide 1 [7-36 amide] but not of synthetic human gastric inhibitory polypeptide in patients with type-2 diabetes mellitus. *The Journal of clinical investigation*. [Online] 91 (1), 301–307. Available from: doi:10.1172/JCI116186.

Naveilhan, P., Hassani, H., Canals, J.M., Ekstrand, A.J., et al. (1999) Normal feeding behavior, body weight and leptin response require the neuropeptide Y Y2 receptor. *Nature Medicine*. [Online] 5 (10), 1188–1193. Available from: doi:10.1038/13514.

Neary, N.M., Goldstone, A.P. & Bloom, S.R. (2004) Appetite regulation: From the gut to the hypothalamus. *Clinical Endocrinology*. [Online] 60 (2), 153–160. Available from: doi:10.1046/j.1365-2265.2003.01839.x.

Neary, N.M., Small, C.J., Druce, M.R., Park, A.J., et al. (2005) Peptide YY3-36 and glucagon-like peptide-17-36 inhibit food intake additively. *Endocrinology*. [Online] 146 (12), 5120–5127. Available from: doi:10.1210/en.2005-0237.

Nectow, A.R., Schneeberger, M., Zhang, H., Field, B.C., et al. (2017) Identification of a Brainstem Circuit Controlling Feeding. *Cell*. [Online] 170 (3), 429-442.e11. Available from: doi:10.1016/j.cell.2017.06.045.

Nieuwenhuizen, A.G., Karlsson, S., Fridolf, T. & Ahrén, B. (1994) Mechanisms underlying the insulinostatic effect of peptide YY in mouse pancreatic islets. *Diabetologia*. [Online] 37 (9), 871–878. Available from: doi:10.1007/BF00400941.

Niijima, A. (1996) The afferent discharges from sensors for interleukin 1β in the hepatoportal system in the anesthetized rat. *Journal of the Autonomic Nervous System*. [Online] 61 (3), 287–291. Available from: doi:10.1016/S0165-1838(96)00098-7.

Nillni, E.A. (2010) Regulation of the hypothalamic thyrotropin releasing hormone (TRH) neuron by neuronal and peripheral inputs. *Frontiers in neuroendocrinology*. [Online] 31 (2), 134–156. Available from: doi:10.1016/j.yfrne.2010.01.001.

Nonaka, N., Shioda, S., Niehoff, M.L. & Banks, W.A. (2003) Characterization of blood-brain barrier permeability to PYY3-36 in the mouse. *The Journal of pharmacology and experimental therapeutics*. [Online] 306 (3), 948–953. Available from: doi:10.1124/jpet.103.051821.

Nonogaki, K., Strack, A.M., Dallman, M.F. & Tecott, L.H. (1998) Leptin-independent hyperphagia and type 2 diabetes in mice with a mutated serotonin 5-HT2C receptor gene. *Nature Medicine*. [Online] 4 (10), 1152–1156. Available from: doi:10.1038/2647.

Norgren, R. & Smith, G.P. (1994) A method for selective section of vagal afferent or efferent axons in the rat. *American Journal of Physiology - Regulatory Integrative and Comparative Physiology*. [Online] 267 (4 36-4), 1136–1141. Available from: doi:10.1152/ajpregu.1994.267.4.r1136.

Nunemaker, C.S., Wasserman, D.H., McGuinness, O.P., Sweet, I.R., et al. (2006) Insulin secretion in the conscious mouse is biphasic and pulsatile. *American Journal of Physiology - Endocrinology and Metabolism*. [Online] 290 (3), 523–529. Available from: doi:10.1152/ajpendo.00392.2005.

Nussbaum, J.C., Van Dyken, S.J., Von Moltke, J., Cheng, L.E., et al. (2013) Type 2 innate lymphoid cells control eosinophil homeostasis. *Nature*. [Online] 502 (7470), 245–248. Available from: doi:10.1038/nature12526.

Ortiz, A.A., Milardo, L.F., Decarr, L.B., Buckholz, T.M., et al. (2007) A novel long-acting selective neuropeptide Y2 receptor polyethylene glycol-conjugated peptide agonist reduces food intake and body weight and improves glucose metabolism in rodents. *Journal of Pharmacology and Experimental Therapeutics*. [Online] 323 (2), 692–700. Available from: doi:10.1124/jpet.107.125211.

Page, A.J., Martin, C.M. & Blackshaw, L.A. (2002) Vagal mechanoreceptors and chemoreceptors in mouse stomach and esophagus. *Journal of Neurophysiology*. [Online] 87 (4), 2095–2103. Available from: doi:10.1152/jn.00785.2001.

Page, A.J., Slattery, J.A., Milte, C., Laker, R., et al. (2007) Ghrelin selectively reduces mechanosensitivity of upper gastrointestinal vagal afferents. *American Journal of Physiology - Gastrointestinal and Liver Physiology*. [Online] 292 (5), 1376–1384. Available from: doi:10.1152/ajpgi.00536.2006.

Palmiter, R.D. (2018) The Parabrachial Nucleus: CGRP Neurons Function as a General Alarm. *Trends in neurosciences*. [Online] 41 (5), 280–293. Available from: doi:10.1016/j.tins.2018.03.007.

Pan, D.A., Lillioja, S., Kriketos, A.D., Milner, M.R., et al. (1997) Skeletal Muscle Triglyceride Levels Are Inversely Related to Insulin Action. *Diabetes*. [Online] 46 (6), 983 LP – 988. Available from: doi:10.2337/diab.46.6.983.

Pappas, T.N., Debas, H.T., Chang, A.M. & Taylor, I.L. (1986) Peptide YY release by fatty acids is sufficient to inhibit gastric emptying in dogs. *Gastroenterology*. [Online] 91 (6), 1386–1389. Available from: doi:10.1016/0016-5085(86)90191-5.

Parkinson, J.R.C., Dhillo, W.S., Small, C.J., Chaudhri, O.B., et al. (2008) PYY3-36 injection in mice produces an acute anorexigenic effect followed by a delayed orexigenic effect not observed with other anorexigenic gut hormones. *American Journal of Physiology - Endocrinology and Metabolism*. [Online] 294 (4), 698–708. Available from: doi:10.1152/ajpendo.00405.2007.

Pavlov, V.A. & Tracey, K.J. (2012) The vagus nerve and the inflammatory reflex - Linking immunity and metabolism. *Nature Reviews Endocrinology*. [Online] 8 (12), 743–754. Available from: doi:10.1038/nrendo.2012.189.

Payne, S.C., Ward, G., MacIsaac, R.J., Hyakumura, T., et al. (2020) Differential effects of vagus nerve stimulation strategies on glycemia and pancreatic secretions. *Physiological Reports*. [Online] 8 (11), 1–11. Available from: doi:10.14814/phy2.14479.

Pelleymounter, M.A., Cullen, M.J., Baker, M.B., Hecht, R., et al. (1995) Effects of the obese gene product on body weight regulation in ob/ob mice. *Science*. [Online] 269 (5223), 540–543. Available from: doi:10.1126/science.7624776.

Peters, J.H., Karpiel, A.B., Ritter, R.C. & Simasko, S.M. (2004) Cooperative activation of cultured vagal afferent neurons by leptin and cholecystokinin. *Endocrinology*. [Online] 145 (8), 3652–3657.

Available from: doi:10.1210/en.2004-0221.

Peters, J.H., McKay, B.M., Simasko, S.M. & Ritter, R.C. (2005) Leptin-induced satiation mediated by abdominal vagal afferents. *American Journal of Physiology - Regulatory Integrative and Comparative Physiology*. [Online] 288 (4 57-4), 879–884. Available from: doi:10.1152/ajpregu.00716.2004.

Peters, J.H., Ritter, R.C. & Simasko, S.M. (2006) Leptin and CCK selectively activate vagal afferent neurons innervating the stomach and duodenum. *American Journal of Physiology - Regulatory Integrative and Comparative Physiology*. [Online] 290 (6), 1544–1549. Available from: doi:10.1152/ajpregu.00811.2005.

Peterson, L.W. & Artis, D. (2014) Intestinal epithelial cells: Regulators of barrier function and immune homeostasis. *Nature Reviews Immunology*. [Online] 14 (3), 141–153. Available from: doi:10.1038/nri3608.

Phillips, R.J. & Powley, T.L. (1996) Gastric content volume inhibits rather than food intake nutrient. *The American Journal of Physiology*. 271 (3), 766–769.

Pi-Sunyer, X., Astrup, A., Fujioka, K., Greenway, F., et al. (2015) A randomized, controlled trial of 3.0 mg of liraglutide in weight management. *New England Journal of Medicine*. [Online] 373 (1), 11–22. Available from: doi:10.1056/NEJMoa1411892.

Pi-Sunyer, X., Kissileff, H.R., Thornton, J. & Smith, G.P. (1982) C-terminal octapeptide of cholecystokinin decreases food intake in obese men. *Physiology & behavior*. [Online] 29 (4), 627–630. Available from: doi:10.1016/0031-9384(82)90230-x.

Pilichiewicz, A.N., Papadopoulos, P., Brennan, I.M., Little, T.J., et al. (2007) Load-dependent effects of duodenal lipid on antropyloroduodenal motility, plasma CCK and PYY, and energy intake in healthy men. *American journal of physiology. Regulatory, integrative and comparative physiology*. [Online] 293 (6), R2170-8. Available from: doi:10.1152/ajpregu.00511.2007.

Pironi, L., Stanghellini, V., Miglioli, M., Corinaldesi, R., et al. (1993) Fat-induced ileal brake in humans: a dose-dependent phenomenon correlated to the plasma levels of peptide YY. *Gastroenterology*. [Online] 105 (3), 733–739. Available from: doi:10.1016/0016-5085(93)90890-o.

Pittner, R.A., Moore, C.X., Bhavsar, S.P., Gedulin, B.R., et al. (2004) Effects of PYY[3-36] in rodent models of diabetes and obesity. *International Journal of Obesity*. [Online] 28 (8), 963–971. Available from: doi:10.1038/sj.ijo.0802696.

Plamboeck, A., Veedfald, S., Deacon, C.F., Hartmann, B., et al. (2013) The effect of exogenous GLP-1 on food intake is lost in male truncally vagotomized subjects with pyloroplasty. *American Journal of Physiology - Gastrointestinal and Liver Physiology*. [Online] 304 (12), 1117–1127. Available from: doi:10.1152/ajpgi.00035.2013.

Pocai, A., Carrington, P.E., Adams, J.R., Wright, M., et al. (2009) Glucagon-like peptide 1/glucagon receptor dual agonism reverses obesity in mice. *Diabetes*. [Online] 58 (10), 2258–2266. Available from: doi:10.2337/db09-0278.

Pournaras, D.J., Osborne, A., Hawkins, S.C., Mahon, D., et al. (2010) The gut hormone response following roux-en-Y gastric bypass: Cross-sectional and prospective study. *Obesity Surgery*. [Online] 20 (1), 56–60. Available from: doi:10.1007/s11695-009-9989-1.

Powley, T.L., Chi, M.M., Baronowsky, E.A. & Phillips, R.J. (2005) Gastrointestinal tract innervation of the mouse: Afferent regeneration and meal patterning after vagotomy. *American Journal of Physiology - Regulatory Integrative and Comparative Physiology*. [Online] 289, 563–574. Available from: doi:10.1152/ajpregu.00167.2005.

Prechtl, J.C. & Powley, T.L. (1985) Organization and distribution of the rat subdiaphragmatic vagus and associated paraganglia. *Journal of Comparative Neurology*. [Online] 235 (2), 182–195. Available from: doi:https://doi.org/10.1002/cne.902350204.

Prechtl, J.C. & Powley, T.L. (1990) The fiber composition of the abdominal vagus of the rat. *Anatomy and embryology*. [Online] 181 (2), 101–115. Available from: doi:10.1007/BF00198950.

Preibisch, S., Saalfeld, S. & Tomancak, P. (2009) Globally optimal stitching of tiled 3D microscopic image acquisitions. *Bioinformatics (Oxford, England)*. [Online] 25 (11), 1463–1465. Available from: doi:10.1093/bioinformatics/btp184.

Price, S.L., Minnion, J.S. & Bloom, S.R. (2015) Investigating the Glucagon Receptor and Glucagon-Like Peptide 1 Receptor Activity of Oxyntomodulin-Like Analogues in Male Wistar Rats. *Current therapeutic research, clinical and experimental*. [Online] 77, 111–115. Available from: doi:10.1016/j.curtheres.2015.10.003.

Qiu, J., Zhang, C., Borgquist, A., Nestor, C.C., et al. (2014) Insulin excites anorexigenic proopiomelanocortin neurons via activation of canonical transient receptor potential channels. *Cell metabolism*. [Online] 19 (4), 682–693. Available from: doi:10.1016/j.cmet.2014.03.004.

Qu, D., Ludwig, D.S., Gammeltoft, S., Piper, M., et al. (1996) A role for melanin-concentrating hormone in the central regulation of feeding behaviour. *Nature*. [Online] 380 (6571), 243–247. Available from: doi:10.1038/380243a0.

Quatrini, L., Vivier, E. & Ugolini, S. (2018) Neuroendocrine regulation of innate lymphoid cells. *Immunological Reviews*. [Online] 286 (1), 120–136. Available from: doi:10.1111/imr.12707.

Le Quellec, A., Kervran, A., Blache, P., Ciurana, A.J., et al. (1992) Oxyntomodulin-like immunoreactivity: diurnal profile of a new potential enterogastrone. *The Journal of Clinical Endocrinology & Metabolism*. [Online] 74 (6), 1405–1409. Available from: doi:10.1210/jcem.74.6.1592887.

Rajagopal, S. & Shenoy, S.K. (2018) GPCR desensitization: Acute and prolonged phases. *Cellular signalling*. [Online] 41, 9–16. Available from: doi:10.1016/j.cellsig.2017.01.024.

Rakoff-Nahoum, S., Paglino, J., Eslami-Varzaneh, F., Edberg, S., et al. (2004) Recognition of commensal microflora by toll-like receptors is required for intestinal homeostasis. *Cell*. [Online] 118 (2), 229–241. Available from: doi:10.1016/j.cell.2004.07.002.

Ramracheya, R.D., McCulloch, L.J., Clark, A., Wiggins, D., et al. (2016) PYY-Dependent Restoration of Impaired Insulin and Glucagon Secretion in Type 2 Diabetes following Roux-En-Y Gastric Bypass Surgery. *Cell Reports*. [Online] 15 (5), 944–950. Available from: doi:10.1016/j.celrep.2016.03.091.

Rangwala, S.M., Aquino, K.D., Zhang, Y., Bader, L., et al. (2020) *Efficacy with Minimal Emesis in Nonhuman Primates*. [Online] 29 (4), 837–843. Available from: doi:10.1016/j.cmet.2019.01.017.A.

Ratner, R., Nauck, M., Kapitza, C., Asnaghi, V., et al. (2010) Safety and tolerability of high doses of taspoglutide, a once-weekly human GLP-1 analogue, in diabetic patients treated with metformin: a randomized double-blind placebo-controlled study. *Diabetic medicine : a journal of the British Diabetic Association*. [Online] 27 (5), 556–562. Available from: doi:10.1111/j.1464-5491.2010.02990.x.

Raybould, H.E. & Tache, Y. (1988) Cholecystokinin inhibits gastric motility and emptying via a capsaicin-sensitive vagal pathway in rats. *American Journal of Physiology-Gastrointestinal and Liver Physiology*. [Online] 255 (2), G242–G246. Available from: doi:10.1152/ajpgi.1988.255.2.G242.

Richards, P., Parker, H.E., Adriaenssens, A.E., Hodgson, J.M., et al. (2014) Identification and characterization of GLP-1 receptor-expressing cells using a new transgenic mouse model. *Diabetes*. [Online] 63 (4), 1224–1233. Available from: doi:10.2337/db13-1440.

Roberts, L.B., Schnoeller, C., Berkachy, R., Darby, M., et al. (2021) Acetylcholine production by group 2 innate lymphoid cells promotes mucosal immunity to helminths. *Science immunology*. [Online] 6 (57), 1–14. Available from: doi:10.1126/sciimmunol.abd0359.

Röder, P. V., Wu, B., Liu, Y. & Han, W. (2016) Pancreatic regulation of glucose homeostasis. *Experimental & molecular medicine*. [Online] 48 (December 2015), e219. Available from: doi:10.1038/emm.2016.6.

Rosas-Ballina, M., Ochani, M., Parrish, W.R., Ochani, K., et al. (2008) Splenic nerve is required for cholinergic antiinflammatory pathway control of TNF in endotoxemia. *Proceedings of the National Academy of Sciences of the United States of America*. [Online] 105 (31), 11008–11013. Available from: doi:10.1073/pnas.0803237105.

Rosas-Ballina, M., Olofsson, P.S., Ochani, M., Valdés-Ferrer, S.I., et al. (2011) Acetylcholine-synthesizing T cells relay neural signals in a vagus nerve circuit. *Science*. [Online] 334 (6052), 98–101. Available from: doi:10.1126/science.1209985.

Roseberry, A.G., Liu, H., Jackson, A.C., Cai, X., et al. (2004) Neuropeptide Y-mediated inhibition of proopiomelanocortin neurons in the arcuate nucleus shows enhanced desensitization in ob/ob mice. *Neuron*. [Online] 41 (5), 711–722. Available from: doi:10.1016/S0896-6273(04)00074-1.

Roslin, M. & Kurian, M. (2001) The use of electrical stimulation of the vagus nerve to treat morbid obesity. *Epilepsy and Behavior*. [Online] 2 (3 SUPPL. 3), 11–16. Available from: doi:10.1006/ebeh.2001.0213.

Le Roux, C.W., Aylwin, S.J.B., Batterham, R.L., Borg, C.M., et al. (2006) Gut hormone profiles following bariatric surgery favor an anorectic state, facilitate weight loss, and improve metabolic parameters. *Annals of Surgery*. [Online] 243 (1), 108–114. Available from: doi:10.1097/01.sla.0000183349.16877.84.

le Roux, C.W., Batterham, R.L., Aylwin, S.J.B., Patterson, M., et al. (2006) Attenuated peptide YY release in obese subjects is associated with reduced satiety. *Endocrinology*. [Online] 147 (1), 3–8. Available from: doi:10.1210/en.2005-0972.

Le Roux, C.W., Borg, C.M., Murphy, K.G., Vincent, R.P., et al. (2008) Supraphysiological doses of intravenous PYY3-36 cause nausea, but no additional reduction in food intake. *Annals of Clinical Biochemistry*. [Online] 45 (1), 93–95. Available from: doi:10.1258/acb.2007.007068.

Le Roux, C.W., Neary, N.M., Halsey, T.J., Small, C.J., et al. (2005) Ghrelin does not stimulate food intake in patients with surgical procedures involving vagotomy. *Journal of Clinical Endocrinology and Metabolism*. [Online] 90 (8), 4521–4524. Available from: doi:10.1210/jc.2004-2537.

Rüttimann, E.B., Arnold, M., Hillebrand, J.J., Geary, N., et al. (2009) Intrameal hepatic portal and intraperitoneal infusions of glucagon-like peptide-1 reduce spontaneous meal size in the rat via different mechanisms. *Endocrinology*. [Online] 150 (3), 1174–1181. Available from: doi:10.1210/en.2008-1221.

Sainsbury, A., Bergen, H.T., Boey, D., Bamming, D., et al. (2006) Y2Y4 receptor double knockout protects against obesity due to a high-fat diet or Y1 receptor deficiency in mice. *Diabetes*. [Online] 55 (1), 19–26. Available from: doi:10.2337/diabetes.55.01.06.db05-0472.

Sainsbury, A., Schwarzer, C., Couzens, M., Fetissov, S., et al. (2002) Important role of hypothalamic Y2 receptors in body weight regulation revealed in conditional knockout mice. *Proceedings of the National Academy of Sciences of the United States of America*. [Online] 99 (13), 8938–8943. Available from: doi:10.1073/pnas.132043299.

Sainsbury, A., Shi, Y.-C., Zhang, L., Aljanova, A., et al. (2010) Y4 receptors and pancreatic polypeptide regulate food intake via hypothalamic orexin and brain-derived neurotropic factor dependent pathways. *Neuropeptides*. [Online] 44 (3), 261–268. Available from: doi:10.1016/j.npep.2010.01.001.

Sakurai, T., Amemiya, A., Ishii, M., Matsuzaki, I., et al. (1998) Orexins and orexin receptors: a family of hypothalamic neuropeptides and G protein-coupled receptors that regulate feeding behavior. *Cell*. [Online] 92 (4), 573–585. Available from: doi:10.1016/s0092-8674(00)80949-6.

Salem, V., Silva, L.D., Suba, K., Georgiadou, E., et al. (2019) Leader β-cells coordinate Ca2+ dynamics across pancreatic islets in vivo. *Nature Metabolism*. [Online] 1 (6), 615–629. Available from: doi:10.1038/s42255-019-0075-2.

Sam, A.H., Gunner, D.J., King, A., Persaud, S.J., et al. (2012) Selective ablation of peptide YY cells in adult mice reveals their role in beta cell survival. *Gastroenterology*. [Online] 143 (2), 459–468. Available from: doi:10.1053/j.gastro.2012.04.047.

Savage, A.P., Adrian, T.E., Carolan, G., Chatterjee, V.K., et al. (1987) Effects of peptide YY (PYY) on mouth to caecum intestinal transit time and on the rate of gastric emptying in healthy volunteers. *Gut*. [Online] 28 (2), 166–170. Available from: doi:10.1136/gut.28.2.166.

Schmidt, J.B., Gregersen, N.T., Pedersen, S.D., Arentoft, J.L., et al. (2014) Effects of PYY3-36 and GLP-1 on energy intake, energy expenditure, and appetite in overweight men. *American Journal of Physiology - Endocrinology and Metabolism*. [Online] 306 (11), 1248–1256. Available from: doi:10.1152/ajpendo.00569.2013.

Schuster, E.F. (1985) Incorporating support constraints into nonparametric estimators of densities. *Communications in Statistics - Theory and Methods*. [Online] 14 (5), 1123–1136. Available from: doi:10.1080/03610928508828965.

Schwartz, G.J. (2006) Integrative capacity of the caudal brainstem in the control of food intake. *Philosophical Transactions of the Royal Society B: Biological Sciences*. [Online] 361 (1471), 1275–1280. Available from: doi:10.1098/rstb.2006.1862.

Schwartz, G.J., McHugh, P.R. & Moran, T.H. (1993) Gastric loads and cholecystokinin synergistically stimulate rat gastric vagal afferents. *American Journal of Physiology - Regulatory Integrative and Comparative Physiology*. [Online] 265, 872–876. Available from: doi:10.1152/ajpregu.1993.265.4.r872.

Schwartz, G.J., McHugh, P.R. & Moran, T.H. (1991) Integration of vagal afferent responses to gastric loads and cholecystokinin in rats. *The American journal of physiology*. [Online] 261 (1 Pt 2), R64-9. Available from: doi:10.1152/ajpregu.1991.261.1.R64.

Schwartz, G.J. & Moran, T.H. (1994) CCK Elicits and Modulates Vagal Merent Activity Arising from Gastric and Duodenal Sites. *Annals of the New York Academy of Sciences*. 121–128.

Schwartz, G.J. & Moran, T.H. (2002) Leptin and neuropeptide Y have opposing modulatory effects on nucleus of the solitary tract neurophysiological responses to gastric loads: Implications for the control of food intake. *Endocrinology*. [Online] 143 (10), 3779–3784. Available from: doi:10.1210/en.2002-220352.

Schwartz, G.J., Salorio, C.F., Skoglund, C. & Moran, T.H. (1999) Gut vagal afferent lesions increase meal size but do not block gastric preload-induced feeding suppression. *American Journal of Physiology - Regulatory Integrative and Comparative Physiology*. [Online] 276, 1623–1629. Available from: doi:10.1152/ajpregu.1999.276.6.r1623.

Schwartz, M.W., Seeley, R.J., Campfield, L.A., Burn, P., et al. (1996) Identification of targets of leptin action in rat hypothalamus. *Journal of Clinical Investigation*. [Online] 98 (5), 1101–1106. Available from: doi:10.1172/JCI118891.

Schwartz, M.W., Seeley, R.J., Woods, S.C., Weigle, D.S., et al. (1997) Leptin increases hypothalamic pro-opiomelanocortin mRNA expression in the rostral arcuate nucleus. *Diabetes*. [Online] 46 (12), 2119–2123. Available from: doi:10.2337/diab.46.12.2119.

Schwartz, M.W., Sipols, A.J., Marks, J.L., Sanacora, G., et al. (1992) Inhibition of hypothalamic neuropeptide Y gene expression by insulin. *Endocrinology*. [Online] 130 (6), 3608–3616. Available from: doi:10.1210/endo.130.6.1597158.

Scott, V., Kimura, N., Stark, J.A. & Luckman, S.M. (2005) Intravenous Peptide YY3-36 and Y2 Receptor Antagonism in the Rat: Effects on Feeding Behaviour. *Journal of Neuroendocrinology*. [Online] 17 (7), 452–457. Available from: doi:https://doi.org/10.1111/j.1365-2826.2005.01330.x.

Secher, A., Jelsing, J., Baquero, A.F., Hecksher-Sørensen, J., et al. (2014) The arcuate nucleus mediates GLP-1 receptor agonist liraglutide-dependent weight loss. *Journal of Clinical Investigation*. [Online] 124 (10), 4473–4488. Available from: doi:10.1172/JCI75276.

Shechter, A. & Schwartz, G.J. (2018) Gut–brain nutrient sensing in food reward. *Appetite*. [Online] 122, 32–35. Available from: doi:10.1016/j.appet.2016.12.009.

Shi, Y.C., Hämmerle, C.M., Lee, I.C.J., Turner, N., et al. (2012) Adult-onset PYY overexpression in mice reduces food intake and increases lipogenic capacity. *Neuropeptides*. [Online] 46 (4), 173–182. Available from: doi:10.1016/j.npep.2012.04.001.

Shi, Y.C., Loh, K., Bensellam, M., Lee, K., et al. (2015) Pancreatic PYY is critical in the control of insulin secretion and glucose homeostasis in female mice. *Endocrinology*. [Online] 156 (9), 3122–3136. Available from: doi:10.1210/en.2015-1168.

Shields, S.D., Ahn, H.S., Yang, Y., Han, C., et al. (2012) Na v1.8 expression is not restricted to nociceptors in mouse peripheral nervous system. *Pain*. [Online] 153 (10), 2017–2030. Available from: doi:10.1016/j.pain.2012.04.022.

Shikora, S.A., Knudson, M.B., Tweden, K.S., Anvari, M., et al. (2015) Weight Loss Is Durable with Vagal Nerve Blockade (VBLOC) but Not with Sham: 18-Month Results of the ReCharge Trial. *Canadian Journal of Diabetes*. [Online] 39, S36. Available from: doi:10.1016/j.jcjd.2015.01.143.

Shimada, M., Tritos, N.A., Lowell, B.B., Flier, J.S., et al. (1998) Mice lacking melanin-concentrating hormone are hypophagic and lean. *Nature*. [Online] 396 (6712), 670–674. Available from: doi:10.1038/25341.

Shoelson, S.E., Herrero, L. & Naaz, A. (2007) Obesity, Inflammation, and Insulin Resistance. *Gastroenterology*. [Online] 132 (6), 2169–2180. Available from: doi:10.1053/j.gastro.2007.03.059.

Siersbæk, M.S., Ditzel, N., Hejbøl, E.K., Præstholm, S.M., et al. (2020) C57BL/6J substrain differences in response to high-fat diet intervention. *Scientific Reports*. [Online] 10 (1), 1–15. Available from: doi:10.1038/s41598-020-70765-w.

De Silva, A. & Bloom, S.R. (2012) Gut Hormones and Appetite Control: A Focus on PYY and GLP-1 as Therapeutic Targets in Obesity. *Gut and liver*. [Online] 6 (1), 10–20. Available from: doi:10.5009/gnl.2012.6.1.10.

De Silva, A., Salem, V., Long, C.J., Makwana, A., et al. (2011) The gut hormones PYY 3-36 and GLP-1 7-36 amide reduce food intake and modulate brain activity in appetite centers in humans. *Cell Metabolism*. [Online] 14 (5), 700–706. Available from: doi:10.1016/j.cmet.2011.09.010.

Silverman, B.W. (Bernard W. (1986) Includes bibliography and index. *Density estimation for statistics and data analysis*. London, Chapman and Hall.

Sisley, S., Sandoval, D.A., Seeley, R.J., Sisley, S., et al. (2014) *Neuronal GLP1R mediates liraglutide ' s anorectic but not glucose-lowering effect*. [Online] 124 (6), 2456–2463. Available from: doi:10.1172/JCI72434DS1.

Sjölund, K., Sandén, G., Håkanson, R. & Sundler, F. (1983) Endocrine cells in human intestine: an immunocytochemical study. *Gastroenterology*. 85 (5), 1120–1130.

Sjöström, L. (2013) Review of the key results from the Swedish Obese Subjects (SOS) trial - a prospective controlled intervention study of bariatric surgery. *Journal of Internal Medicine*. [Online] 273 (3), 219–234. Available from: doi:10.1111/joim.12012.

Sloth, B., Holst, J.J., Flint, A., Gregersen, N.T., et al. (2007) Effects of PYY1-36 and PYY3-36 on appetite, energy intake, energy expenditure, glucose and fat metabolism in obese and lean subjects. *American Journal of Physiology - Endocrinology and Metabolism*. [Online] 292 (4), 1062–1068. Available from: doi:10.1152/ajpendo.00450.2006.

Smith, G., Jerome, C., Cushin, B., Eterno, R., et al. (1981a) Abdominal vagotomy blocks the satiety effect of cholecystokinin in the rat. *Science*. [Online] 213 (4511), 1036–1037. Available from: doi:10.1126/science.7268408.

Smith, G.P., Gibbs, J., Jerome, C., Pi-Sunyer, F.X., et al. (1981b) The satiety effect of cholecystokinin: A progress report. *Peptides*. [Online] 2 (SUPPL. 2), 57–59. Available from: doi:10.1016/0196-

9781(81)90011-5.

Sonnenberg, G.F. & Hepworth, M.R. (2019) Functional interactions between innate lymphoid cells and adaptive immunity. *Nature Reviews Immunology*. [Online] 19 (10), 599–613. Available from: doi:10.1038/s41577-019-0194-8.

Speier, S., Nyqvist, D., Cabrera, O., Yu, J., et al. (2008a) Noninvasive in vivo imaging of pancreatic islet cell biology. *Nature Medicine*. [Online] 14 (5), 574–578. Available from: doi:10.1038/nm1701.

Speier, S., Nyqvist, D., Köhler, M., Caicedo, A., et al. (2008b) Noninvasive high-resolution in vivo imaging of cell biology in the anterior chamber of the mouse eye. *Nature Protocols*. [Online] 3 (8), 1278–1286. Available from: doi:10.1038/nprot.2008.118.

Srivastava, G. & Apovian, C.M. (2018) Current pharmacotherapy for obesity. *Nature Reviews Endocrinology*. [Online] 14 (1), 12–24. Available from: doi:10.1038/nrendo.2017.122.

Stadlbauer, U., Arnold, M., Weber, E. & Langhans, W. (2013) Possible mechanisms of circulating PYY-induced satiation in male rats. *Endocrinology*. [Online] 154 (1), 193–204. Available from: doi:10.1210/en.2012-1956.

Stadlbauer, U., Woods, S.C., Langhans, W. & Meyer, U. (2015) PYY3-36: Beyond food intake. *Frontiers in neuroendocrinology*. [Online] 38, 1–11. Available from: doi:10.1016/j.yfrne.2014.12.003.

Stakenborg, N., Viola, M.F. & Boeckxstaens, G.E. (2020) Intestinal neuro-immune interactions: focus on macrophages, mast cells and innate lymphoid cells. *Current Opinion in Neurobiology*. [Online] 62, 68–75. Available from: doi:10.1016/j.conb.2019.11.020.

Stanić, D., Brumovsky, P., Fetissov, S., Shuster, S., et al. (2006) Characterization of neuropeptide Y2 receptor protein expression in the mouse brain. I. Distribution in cell bodies and nerve terminals. *Journal of Comparative Neurology*. [Online] 499 (3), 357–390. Available from: doi:https://doi.org/10.1002/cne.21046.

Stauss, H.M., Stangl, H., Clark, K.C., Kwitek, A.E., et al. (2018) Cervical vagal nerve stimulation impairs glucose tolerance and suppresses insulin release in conscious rats. *Physiological Reports*. [Online] 6 (24), 1–10. Available from: doi:10.14814/phy2.13953.

Stirling, C.L., Forlani, G., Baker, M.D., Wood, J.N., et al. (2005) Nociceptor-specific gene deletion using heterozygous NaV1.8-Cre recombinase mice. *Pain*. 113 (1).

Straub, S.G. & Sharp, G.W.G. (2002) Glucose-stimulated signaling pathways in biphasic insulin secretion. *Diabetes/Metabolism Research and Reviews*. [Online] 18 (6), 451–463. Available from: doi:10.1002/dmrr.329.

Takahashi, K.A. & Cone, R.D. (2005) Fasting induces a large, leptin-dependent increase in the intrinsic action potential frequency of orexigenic arcuate nucleus neuropeptide Y/Agouti-related protein neurons. *Endocrinology*. [Online] 146 (3), 1043–1047. Available from: doi:10.1210/en.2004-1397.

Talbot, S., Abdulnour, R.E.E., Burkett, P.R., Lee, S., et al. (2015) Silencing Nociceptor Neurons Reduces Allergic Airway Inflammation. *Neuron*. [Online] 87 (2), 341–354. Available from: doi:10.1016/j.neuron.2015.06.007.

Talsania, T., Anini, Y., Siu, S., Drucker, D.J., et al. (2005) Peripheral exendin-4 and peptide YY3-36 synergistically reduce food intake through different mechanisms in mice. *Endocrinology*. [Online] 146 (9), 3748–3756. Available from: doi:10.1210/en.2005-0473.

Tan, H.-E., Sisti, A.C., Jin, H., Vignovich, M., et al. (2020) The gut–brain axis mediates sugar preference. *Nature*. [Online] 580 (7804), 511–516. Available from: doi:10.1038/s41586-020-2199-7.

Tan, T., Behary, P., Tharakan, G., Minnion, J., et al. (2017) The effect of a subcutaneous infusion of GLP-1, OXM, and PYY on energy intake and expenditure in obese volunteers. *Journal of Clinical Endocrinology and Metabolism*. [Online] 102 (7), 2364–2372. Available from: doi:10.1210/jc.2017-00469.

Tan, T.M., Field, B.C.T., McCullough, K.A., Troke, R.C., et al. (2013) Coadministration of glucagon-like peptide-1 during glucagon infusion in humans results in increased energy expenditure and amelioration of hyperglycemia. *Diabetes*. [Online] 62 (4), 1131–1138. Available from: doi:10.2337/db12-0797.

Tan, T.M., Salem, V., Troke, R.C., Alsafi, A., et al. (2014) Combination of peptide YY3-36 with GLP-17-36 amide causes an increase in first-phase insulin secretion after IV glucose. *Journal of Clinical Endocrinology and Metabolism*. [Online] 99 (11), E2317–E2324. Available from: doi:10.1210/jc.2014-2143.

Tatemoto, K. (1982) Isolation and characterization of peptide YY (PYY), a candidate gut hormone that inhibits pancreatic exocrine secretion. *Proceedings of the National Academy of Sciences of the United States of America*. [Online] 79 (8 I), 2514–2518. Available from: doi:10.1073/pnas.79.8.2514.

Thompson, K.J., Khajehali, E., Bradley, S.J., Navarrete, J.S., et al. (2018) DREADD Agonist 21 is an effective agonist for muscarinic-based DREADDs in vitro and in vivo. *ACS Pharmacology and Translational Science*. [Online] 1 (1), 61–72. Available from: doi:10.1021/acsptsci.8b00012.

Thorens, B. (1992) Expression cloning of the pancreatic β cell receptor for the gluco- incretin hormone glucagon-like peptide 1. *Proceedings of the National Academy of Sciences of the United States of America*. [Online] 89 (18), 8641–8645. Available from: doi:10.1073/pnas.89.18.8641.

Tokunaga, K., Fukushima, M., Kemnitz, J.W. & Bray, G.A. (1986) Comparison of ventromedial and paraventricular lesions in rats that become obese. *American Journal of Physiology-Regulatory, Integrative and Comparative Physiology*. [Online] 251 (6), R1221–R1227. Available from: doi:10.1152/ajpregu.1986.251.6.R1221.

Toräng, S., Bojsen-Møller, K.N., Svane, M.S., Hartmann, B., et al. (2016) In vivo and in vitro degradation of peptide YY3-36 to inactive peptide YY3-34 in humans. *American journal of physiology. Regulatory, integrative and comparative physiology*. [Online] 310 (9), R866-74. Available from: doi:10.1152/ajpregu.00394.2015.

Tracey, K.J. (2002) The inflammatory reflex. *Nature*. [Online] 420, 853–859. Available from: doi:10.1111/j.1365-2796.2004.01440.x.

Travagli, R.A. & Anselmi, L. (2016) Vagal neurocircuitry and its influence on gastric motility. *Nature reviews. Gastroenterology & hepatology*. [Online] 13 (7), 389–401. Available from: doi:10.1038/nrgastro.2016.76.

Tschöp, M., Castañeda, T.R., Joost, H.G., Thöne-Reineke, C., et al. (2004) Physiology: does gut hormone PYY3-36 decrease food intake in rodents? *Nature*. [Online] 430 (6996), 1 p following 165; discussion 2 p following 165. Available from: doi:10.1038/nature02665.

Tschöp, M., Weyer, C., Tataranni, P.A., Devanarayan, V., et al. (2001) Circulating ghrelin levels are decreased in human obesity. *Diabetes*. [Online] 50 (4), 707–709. Available from: doi:10.2337/diabetes.50.4.707.

Turton, M.D., O'Shea, D., Gunn, I., Beak, S.A., et al. (1996) A role for glucagon-like peptide-1 in the central regulation of feeding. *Nature*. [Online] 379 (6560), 69–72. Available from: doi:10.1038/379069a0.

U.S Food and Drug Administration (2020) *FDA requests the withdrawal of the weight-loss drug Belviq, Belviq XR (lorcaserin) from the market | FDA*. [Online]. 2020. Available from: https://www.fda.gov/drugs/drug-safety-and-availability/fda-requests-withdrawal-weight-loss-drug-belviq-belviq-xr-lorcaserin-market.

Unniappan, S. & Kieffer, T.J. (2008) Leptin extends the anorectic effects of chronic PYY(3-36) administration in ad libitum-fed rats. *American journal of physiology. Regulatory, integrative and comparative physiology*. [Online] 295 (1), R51-8. Available from: doi:10.1152/ajpregu.00234.2007.

Unniappan, S., McIntosh, C.H.S., Demuth, H.U., Heiser, U., et al. (2006) Effects of dipeptidyl peptidase IV on the satiety actions of peptide YY. *Diabetologia*. [Online] 49 (8), 1915–1923. Available from: doi:10.1007/s00125-006-0310-8.

Upchurch, B.H., Aponte, G.W. & Leiter, A.B. (1994) Expression of peptide YY in all four islet cell types in the developing mouse pancreas suggests a common peptide YY-producing progenitor. *Development*. 120 (2), 245–252.

Vaisse, C., Clement, K., Guy-Grand, B. & Froguel, P. (1998) A frameshift mutation in human MC4R is associated with a dominant form of obesity. *Nature Genetics*. [Online] 20 (2), 113–114. Available from: doi:10.1038/2407.

Val-Laillet, D., Biraben, A., Randuineau, G. & Malbert, C.H. (2010) Chronic vagus nerve stimulation decreased weight gain, food consumption and sweet craving in adult obese minipigs. *Appetite*. [Online] 55 (2), 245–252. Available from: doi:10.1016/j.appet.2010.06.008.

Veiga-Fernandes, H. & Mucida, D. (2016) Neuro-Immune Interactions at Barrier Surfaces. *Cell*. [Online] 165 (4), 801–811. Available from: doi:10.1016/j.cell.2016.04.041.

Verdich, C., Flint, A., Gutzwiller, J.-P., Näslund, E., et al. (2001) A Meta-Analysis of the Effect of Glucagon-Like Peptide-1 (7–36) Amide on Ad Libitum Energy Intake in Humans. *The Journal of Clinical Endocrinology & Metabolism*. [Online] 86 (9), 4382–4389. Available from: doi:10.1210/jcem.86.9.7877.

Vernier, S., Chiu, A., Schober, J., Weber, T., et al. (2012) B-Cell Metabolic Alterations Under Chronic Nutrient Overload in Rat and Human Islets. *Islets*. [Online] 4 (6), 379–392. Available from: doi:10.4161/isl.22720.

Vrang, N., Madsen, A.N., Tang-Christensen, M., Hansen, G., et al. (2006) PYY(3-36) reduces food intake and body weight and improves insulin sensitivity in rodent models of diet-induced obesity. *American Journal of Physiology - Regulatory Integrative and Comparative Physiology*.

[Online] 291 (2), 367–375. Available from: doi:10.1152/ajpregu.00726.2005.

Wahlestedt, C., Yanaihara, N. & Håkanson, R. (1986) Evidence for different pre-and post-junctional receptors for neuropeptide Y and related peptides. *Regulatory peptides*. [Online] 13 (3–4), 307–318. Available from: doi:10.1016/0167-0115(86)90048-0.

Walker, J.A. & McKenzie, A.N.J. (2018) TH2 cell development and function. *Nature Reviews Immunology*. [Online] 18 (2), 121–133. Available from: doi:10.1038/nri.2017.118.

Wallrapp, A., Riesenfeld, S.J., Burkett, P.R., Abdulnour, R.E.E., et al. (2017) The neuropeptide NMU amplifies ILC2-driven allergic lung inflammation. *Nature*. [Online] 549 (7672), 351–356. Available from: doi:10.1038/nature24029.

Wang, H., Yu, M., Ochani, M., Amelia, C.A., et al. (2003) Nicotinic acetylcholine receptor α7 subunit is an essential regulator of inflammation. *Nature*. [Online] 421 (6921), 384–388. Available from: doi:10.1038/nature01339.

Wang, L., Gourcerol, G., Yuan, P.Q., Wu, S.V., et al. (2010) Peripheral peptide YY inhibits propulsive colonic motor function through Y2 receptor in conscious mice. *American Journal of Physiology - Gastrointestinal and Liver Physiology*. [Online] 298 (1). Available from: doi:10.1152/ajpgi.00349.2009.

Wang, Y.B., de Lartigue, G. & Page, A.J. (2020) Dissecting the Role of Subtypes of Gastrointestinal Vagal Afferents. *Frontiers in Physiology*. [Online] 11 (June). Available from: doi:10.3389/fphys.2020.00643.

Weigle, D.S., Bukowski, T.R., Foster, D.C., Holderman, S., et al. (1995) Recombinant ob protein reduces feeding and body weight in the ob/ob mouse. *The Journal of clinical investigation*. [Online] 96 (4), 2065–2070. Available from: doi:10.1172/JCI118254.

West, D.B., Fey, D. & Woods, S.C. (1984) Cholecystokinin persistently suppresses meal size but not food intake in free-feeding rats. *The American journal of physiology*. [Online] 246 (5 Pt 2), R776-87. Available from: doi:10.1152/ajpregu.1984.246.5.R776.

Wilding, J.P.H., Batterham, R.L., Calanna, S., Davies, M., et al. (2021) Once-Weekly Semaglutide in Adults with Overweight or Obesity. *New England Journal of Medicine*. [Online] 1–13. Available from: doi:10.1056/nejmoa2032183.

Wiley, J.W., Gross, R.A. & Macdonald, R.L. (1993) Agonists for neuropeptide Y receptor subtypes NPY-1 and NPY-2 have opposite actions on rat nodose neuron calcium currents. *Journal of Neurophysiology*. [Online] 70 (1), 324–330. Available from: doi:10.1152/jn.1993.70.1.324.

Williams, D.L., Cummings, D.E., Grill, H.J. & Kaplan, J.M. (2003a) Meal-related ghrelin suppression requires postgastric feedback. *Endocrinology*. [Online] 144 (7), 2765–2767. Available from: doi:10.1210/en.2003-0381.

Williams, D.L., Grill, H.J., Cummings, D.E. & Kaplan, J.M. (2003b) Vagotomy Dissociates Short- and Long-Term Controls of Circulating Ghrelin. *Endocrinology*. [Online] 144 (12), 5184–5187. Available from: doi:10.1210/en.2003-1059.

Williams, E.K.K., Chang, R.B.B., Strochlic, D.E.E., Umans, B.D.D., et al. (2016) Sensory Neurons that Detect Stretch and Nutrients in the Digestive System. *Cell*. [Online] 166 (1), 209–221. Available from: doi:10.1016/j.cell.2016.05.011.

Willing, A.E. & Berthoud, H.R. (1997) Gastric distension-induced c-fos expression in catecholaminergic neurons of rat dorsal vagal complex. *American Journal of Physiology - Regulatory Integrative and Comparative Physiology*. [Online] 272 (1 41-1). Available from: doi:10.1152/ajpregu.1997.272.1.r59.

Woods, S.C., McKay, L.D. & Stein, L.J. (1980) Chronic infusion of insulin reduces food intake and body weight of baboons. *Appetite*. [Online] 1 (1), 89. Available from: doi:10.1016/S0195-6663(80)80014-6.

Woods, S.C. & Porte, D. (1974) Neural control of the endocrine pancreas. *Physiological Reviews*. [Online] 54 (3), 596–619. Available from: doi:10.1152/physrev.1974.54.3.596.

Woods, S.C., Stein, L.J., McKay, L.D. & Porte, D. (1984) Suppression of food intake by intravenous nutrients and insulin in the baboon. *American Journal of Physiology - Regulatory Integrative and Comparative Physiology*. [Online] 16 (2). Available from: doi:10.1152/ajpregu.1984.247.2.r393.

World Health Organisation (2004) *The Global Strategy on Diet, Physical Activity and Health*. [Online]. 2004. Available from: doi:10.1093/acprof:oso/9780195167207.001.0001.

World Health Organization (2020) *Fact sheets: Obesity and overweight*. [Online]. 2020. Available from: https://www.who.int/news-room/fact-sheets/detail/obesity-and-overweight.

World Health Organization (2016) *Global Report on Diabetes*. [Online]. 2016. Available from: http://www.who.int/about/licensing/copyright_form/index.html%0Ahttp://www.who.int/about/licensing/copyright_form/index.html%0Ahttps://apps.who.int/iris/handle/10665/204871%0Ahttp://www.who.int/about/licensing/.

World Obesity (2020) *Obesity: missing the 2025 global targets*. [Online]. 2020. Available from: https://www.worldobesity.org/news/world-obesity-day-all-countries-significantly-off-track-to-meet-2025-who-targets-on-obesity.

Wren, A.M., Seal, L.J., Cohen, M.A., Brynes, A.E., et al. (2001a) Ghrelin Enhances Appetite and Increases Food Intake in Humans. *The Journal of Clinical Endocrinology & Metabolism*. [Online] 86 (12), 5992–5992. Available from: doi:10.1210/jcem.86.12.8111.

Wren, A.M., Small, C.J., Abbott, C.R., Dhillo, W.S., et al. (2001b) Ghrelin Causes Hyperphagia and Obesity in Rats. *Diabetes*. [Online] 50 (11), 2540–2547. Available from: doi:10.2337/diabetes.50.11.2540.

Wynne, K., Park, A.J., Small, C.J., Meeran, K., et al. (2006) Oxyntomodulin increases energy expenditure in addition to decreasing energy intake in overweight and obese humans: A randomised controlled trial. *International Journal of Obesity*. [Online] 30 (12), 1729–1736. Available from: doi:10.1038/sj.ijo.0803344.

Wynne, K., Park, A.J., Small, C.J., Patterson, M., et al. (2005) Subcutaneous oxyntomodulin reduces body weight in overweight and obese subjects. *Diabetes*. 54 (8), 2390–2395.

Yao, G., Kang, L., Li, J., Long, Y., et al. (2018) Effective weight control via an implanted self-powered vagus nerve stimulation device. *Nature Communications*. [Online] 9, 1–10. Available from: doi:10.1038/s41467-018-07764-z.

Yeo, G.S.H., Sadaf Farooqi, I., Aminian, S., Halsall, D.J., et al. (1998) A frameshift mutation in MC4R

associated with dominantly inherited human obesity. *Nature genetics*. 20 (october), 111–112.

Yulyaningsih, E., Loh, K., Lin, S., Lau, J., et al. (2014) Pancreatic polypeptide controls energy homeostasis via Npy6r signaling in the suprachiasmatic nucleus in mice. *Cell Metabolism*. [Online] 19 (1), 58–72. Available from: doi:10.1016/j.cmet.2013.11.019.

Zhang, L., Riepler, S.J., Turner, N., Enriquez, R.F., et al. (2010) Y2 and Y4 receptor signaling synergistically act on energy expenditure and physical activity. *American Journal of Physiology - Regulatory Integrative and Comparative Physiology*. [Online] 299 (6), 1618–1628. Available from: doi:10.1152/ajpregu.00345.2010.

Zhang, S., Guo, W., Wu, J., Gong, L., et al. (2017) Increased β-cell mass in obese rats after gastric bypass: A potential mechanism for improving glycemic control. *Medical Science Monitor*. [Online] 23, 2151–2158. Available from: doi:10.12659/MSM.902230.

Zhang, T., Uchida, T., Gomez, G., Lluis, F., et al. (1993) Neural regulation of peptide YY secretion. *Regulatory Peptides*. [Online] 48 (3), 321–328. Available from: doi:10.1016/0167-0115(93)90160-A.

Zhang, W., Waise, T.M.Z., Toshinai, K., Tsuchimochi, W., et al. (2020) Functional interaction between Ghrelin and GLP-1 regulates feeding through the vagal afferent system. *Scientific Reports*. [Online] 10 (1), 1–12. Available from: doi:10.1038/s41598-020-75621-5.

Zhang, X., Cui, J., Tan, Z., Jiang, C., et al. (2003) The central nucleus of the amygdala modulates gut-related neurons in the dorsal vagal complex in rats. *The Journal of physiology*. [Online] 553 (Pt 3), 1005–1018. Available from: doi:10.1113/jphysiol.2003.045906.

Zhang, X., Fogel, R. & Renehan, W.E. (1995) Relationships between the morphology and function of gastric- and intestine-sensitive neurons in the nucleus of the solitary tract. *The Journal of comparative neurology*. [Online] 363 (1), 37–52. Available from: doi:10.1002/cne.903630105.

Zhang, X., Fogel, R. & Renehan, W.E. (1999) Stimulation of the paraventricular nucleus modulates the activity of gut-sensitive neurons in the vagal complex. *The American journal of physiology*. [Online] 277 (1), G79-90. Available from: doi:10.1152/ajpgi.1999.277.1.G79.

Zhang, X., Shi, T., Holmberg, K., Landry, M., et al. (1997) Expression and regulation of the neuropeptide Y Y2 receptor in sensory and autonomic ganglia. *Proceedings of the National Academy of Sciences of the United States of America*. [Online] 94 (2), 729–734. Available from: doi:10.1073/pnas.94.2.729.

Zhang Y, Proenca R, Maffei M, Barone M, et al. (1994) Positional cloning of the mouse obese gene and its human homologue. *Nature*. 372, 425–432.

Zheng, H., Patterson, L.M., Phifer, C.B. & Berthoud, H.R. (2005) Brain stem melanocortinergic modulation of meal size and identification of hypothalamic POMC projections. *American Journal of Physiology - Regulatory Integrative and Comparative Physiology*. [Online] 289 (1 58-1). Available from: doi:10.1152/ajpregu.00869.2004.

Zheng, H., Patterson, L.M., Rhodes, C.J., Louis, G.W., et al. (2010) A potential role for hypothalamomedullary POMC projections in leptin-induced suppression of food intake. *American Journal of Physiology - Regulatory Integrative and Comparative Physiology*. [Online] 298 (3), 720–728. Available from: doi:10.1152/ajpregu.00619.2009.

Zigman, J.M., Jones, J.E., Lee, C.E., Saper, C.B., et al. (2006) Expression of ghrelin receptor mRNA in the rat and the mouse brain. *The Journal of comparative neurology*. [Online] 494 (3), 528–548. Available from: doi:10.1002/cne.20823.

Zingg, B., Chou, X., Zhang, Z., Mesik, L., et al. (2017) AAV-Mediated Anterograde Transsynaptic Tagging : Mapping Corticocollicular Input-Defined Neural Pathways for Defense Behaviors NeuroResource AAV-Mediated Anterograde Transsynaptic Tagging : Mapping Corticocollicular Input-Defined Neural Pathways for Defen. *Neuron*. [Online] 93 (1), 33–47. Available from: doi:10.1016/j.neuron.2016.11.045.

Appendix I: Preparation of buffers and other reagents

Anti-freeze solution (1 L):

- 200 mL glycerol
- 300 mL ethylene glycol
- 400 mL 0.2M PBS

Distilled water was added up to 1 L and mixed well before use.

Phosphate buffer (0.06 M, 5 L, for radioimmunoassay):

- 48 g Na_2HPO_4-H_2O
- 4.125 g KH_2PO_4
- 18.25 g EDTA
- 2.5 g sodium azide

5 L of boiled distilled water was added, mixed and pH adjusted to 7.2.

Phosphate-buffered saline (PBS, 0.2 M, 1 L):

- 174 g NaCl
- 5.44 g KH_2PO_4
- 28.2 g Na_2HPO_4-H_2O

Distilled water was added to 1 L and mixed well on magnetic stirrer. To make 0.01 M PBS (2 L) from 0.2 M PBS, 100 mL of stock was diluted in 1900 mL of distilled water.

Tris-Acetate EDTA (50X, 1 L):

- 242 g Tris base
- 57.1 mL acetate
- 100 mL 0.5M sodium EDTA

Distilled water was added to 1 L, mixed well on magnetic stirrer and pH adjusted to 8.5. To make 1X TAE (2 L) from 50X TAE stock, 40 mL of stock was diluted in 1960 mL of distilled water.

HEPES-buffered Krebs-ringer bicarbonate (500 mL):

- 0.175 g KCl
- 0.0815 g KH_2PO4
- 3.77 g NaCl
- 0.216 g $NaHCO_3$
- 0.148 g $MgSO_4.7H_2O$
- 0.132 g $CaCl_2.2H_2O$
- 1.192 g HEPES
- 0.5 g glucose

Distilled sterile water was added to 0.5 L and mixed well and pH was adjusted to 7.4 by adding NaOH.

DMEM + 1% P/S + 10% FBS

· 5ml P/S into 500ml DMEM

· 50ml FBS into ^^

50 mM KCl HEPES-buffered Krebs-ringer bicarbonate (500 mL):

- 1.8638 g KCl
- 0.0815 g KH_2PO4
- 2.3084 g NaCl
- 0.216 g $NaHCO_3$
- 0.148 g $MgSO_4.7H_2O$
- 0.132 g $CaCl_2.2H_2O$
- 1.192 g HEPES
- 0.5 g glucose

Distilled sterile water was added to 0.5 L and mixed well and pH was adjusted to 7.4 by adding NaOH.

Appendix II: Genotyping

Y2R floxed:

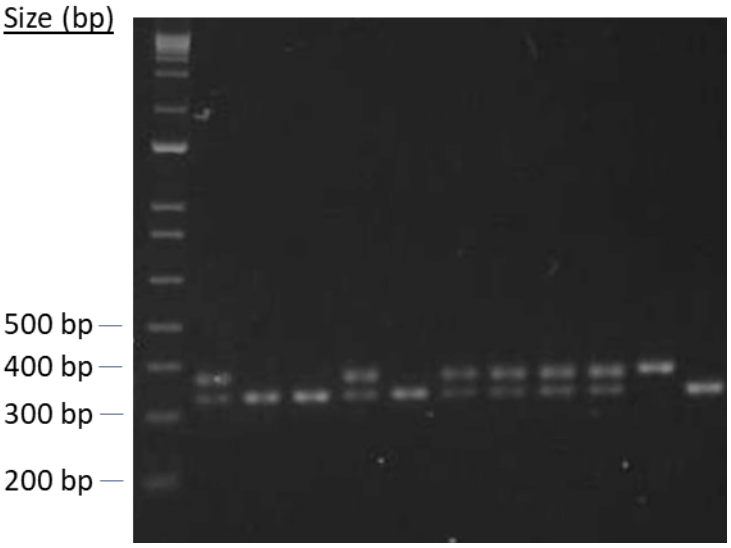

Nav1.8-Cre:

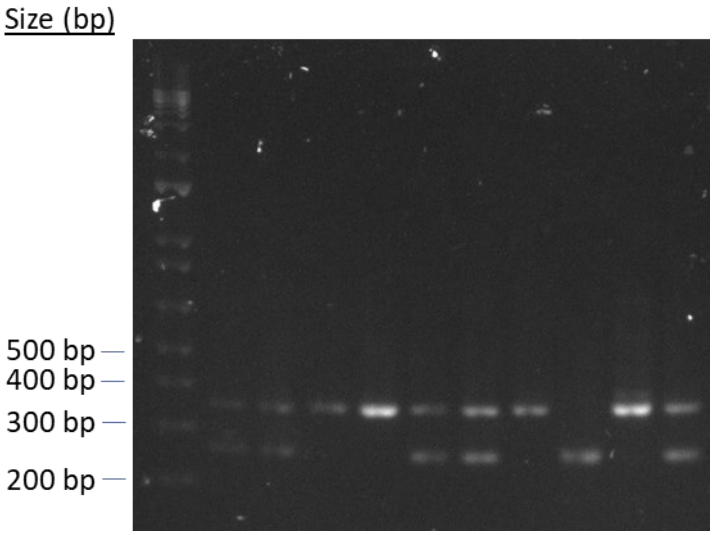

JOHN WILEY AND SONS LICENSE
TERMS AND CONDITIONS

Mar 14, 2021

This Agreement between Imperial College London -- Aldara Martin Alonso ("You") and John Wiley and Sons ("John Wiley and Sons") consists of your license details and the terms and conditions provided by John Wiley and Sons and Copyright Clearance Center.

License Number	5027811342658
License date	Mar 14, 2021
Licensed Content Publisher	John Wiley and Sons
Licensed Content Publication	Clinical Endocrinology
Licensed Content Title	Appetite regulation: from the gut to the hypothalamus
Licensed Content Author	Stephen Robert Bloom, Anthony Peter Goldstone, Nicola Marguerite Neary
Licensed Content Date	Nov 18, 2003
Licensed Content Volume	60
Licensed Content Issue	2
Licensed Content Pages	8
Type of use	Dissertation/Thesis
Requestor type	University/Academic
Format	Print and electronic
Portion	Figure/table
Number of figures/tables	1
Will you be translating?	No
Title	Investigating the physiological and pharmacological effects of the gut hormone peptide YY (PYY)
Institution name	Imperial College London
Expected presentation date	Mar 2021

Portions	Figure 2
	Imperial College London Du Cane Road
Requestor Location	London, W12 0NN United Kingdom Attn: Imperial College London
Publisher Tax ID	EU826007151
Total	0.00 GBP

Terms and Conditions

TERMS AND CONDITIONS

This copyrighted material is owned by or exclusively licensed to John Wiley & Sons, Inc. or one of its group companies (each a"Wiley Company") or handled on behalf of a society with which a Wiley Company has exclusive publishing rights in relation to a particular work (collectively "WILEY"). By clicking "accept" in connection with completing this licensing transaction, you agree that the following terms and conditions apply to this transaction (along with the billing and payment terms and conditions established by the Copyright Clearance Center Inc., ("CCC's Billing and Payment terms and conditions"), at the time that you opened your RightsLink account (these are available at any time at http://myaccount.copyright.com).

Terms and Conditions:

- The materials you have requested permission to reproduce or reuse (the "Wiley Materials") are protected by copyright.
- You are hereby granted a personal, non-exclusive, non-sub licensable (on a stand-alone basis), non-transferable, worldwide, limited license to reproduce the Wiley Materials for the purpose specified in the licensing process. This license, **and any CONTENT (PDF or image file) purchased as part of your order**, is for a one-time use only and limited to any maximum distribution number specified in the license. The first instance of republication or reuse granted by this license must be completed within two years of the date of the grant of this license (although copies prepared before the end date may be distributed thereafter). The Wiley Materials shall not be used in any other manner or for any other purpose, beyond what is granted in the license. Permission is granted subject to an appropriate acknowledgement given to the author, title of the material/book/journal and the publisher. You shall also duplicate the copyright notice that appears in the Wiley publication in your use of the Wiley Material. Permission is also granted on the understanding that nowhere in the text is a previously published source acknowledged for all or part of this Wiley Material. Any third party content is expressly excluded from this permission.
- With respect to the Wiley Materials, all rights are reserved. Except as expressly granted by the terms of the license, no part of the Wiley Materials may be copied, modified, adapted (except for minor reformatting required by the new Publication), translated, reproduced, transferred or distributed, in any form or by any means, and no derivative works may be made based on the Wiley Materials without the prior permission of the respective copyright owner.**For STM Signatory Publishers clearing permission under the terms of the STM Permissions Guidelines only, the terms of the license are extended to include subsequent editions and for editions in other languages, provided such editions are for the work as a whole in situ and does not involve the separate exploitation of the permitted figures or extracts,** You may not alter, remove or suppress in any manner any copyright, trademark or other notices displayed by the Wiley Materials. You may not license, rent, sell, loan, lease, pledge, offer as security, transfer or assign the Wiley Materials on a stand-alone basis, or any of the rights granted to you hereunder to any other person.
- The Wiley Materials and all of the intellectual property rights therein shall at all times remain the exclusive property of John Wiley & Sons Inc, the Wiley Companies, or their respective licensors, and your interest therein is only that of having possession of and the right to reproduce the Wiley Materials pursuant to Section 2 herein during the continuance of this Agreement. You agree that you own no right, title or interest in or to the Wiley Materials or any of the intellectual property rights therein. You shall have no rights hereunder other than the license as provided for above in Section 2. No right, license or interest to any trademark, trade name, service mark or other branding ("Marks") of WILEY or its licensors is granted hereunder, and you agree that you shall not assert any such right, license or interest with respect thereto
- NEITHER WILEY NOR ITS LICENSORS MAKES ANY WARRANTY OR REPRESENTATION OF ANY KIND TO YOU OR ANY THIRD PARTY, EXPRESS, IMPLIED OR STATUTORY, WITH RESPECT TO THE MATERIALS

OR THE ACCURACY OF ANY INFORMATION CONTAINED IN THE MATERIALS, INCLUDING, WITHOUT LIMITATION, ANY IMPLIED WARRANTY OF MERCHANTABILITY, ACCURACY, SATISFACTORY QUALITY, FITNESS FOR A PARTICULAR PURPOSE, USABILITY, INTEGRATION OR NON-INFRINGEMENT AND ALL SUCH WARRANTIES ARE HEREBY EXCLUDED BY WILEY AND ITS LICENSORS AND WAIVED BY YOU.

- WILEY shall have the right to terminate this Agreement immediately upon breach of this Agreement by you.
- You shall indemnify, defend and hold harmless WILEY, its Licensors and their respective directors, officers, agents and employees, from and against any actual or threatened claims, demands, causes of action or proceedings arising from any breach of this Agreement by you.
- IN NO EVENT SHALL WILEY OR ITS LICENSORS BE LIABLE TO YOU OR ANY OTHER PARTY OR ANY OTHER PERSON OR ENTITY FOR ANY SPECIAL, CONSEQUENTIAL, INCIDENTAL, INDIRECT, EXEMPLARY OR PUNITIVE DAMAGES, HOWEVER CAUSED, ARISING OUT OF OR IN CONNECTION WITH THE DOWNLOADING, PROVISIONING, VIEWING OR USE OF THE MATERIALS REGARDLESS OF THE FORM OF ACTION, WHETHER FOR BREACH OF CONTRACT, BREACH OF WARRANTY, TORT, NEGLIGENCE, INFRINGEMENT OR OTHERWISE (INCLUDING, WITHOUT LIMITATION, DAMAGES BASED ON LOSS OF PROFITS, DATA, FILES, USE, BUSINESS OPPORTUNITY OR CLAIMS OF THIRD PARTIES), AND WHETHER OR NOT THE PARTY HAS BEEN ADVISED OF THE POSSIBILITY OF SUCH DAMAGES. THIS LIMITATION SHALL APPLY NOTWITHSTANDING ANY FAILURE OF ESSENTIAL PURPOSE OF ANY LIMITED REMEDY PROVIDED HEREIN.
- Should any provision of this Agreement be held by a court of competent jurisdiction to be illegal, invalid, or unenforceable, that provision shall be deemed amended to achieve as nearly as possible the same economic effect as the original provision, and the legality, validity and enforceability of the remaining provisions of this Agreement shall not be affected or impaired thereby.
- The failure of either party to enforce any term or condition of this Agreement shall not constitute a waiver of either party's right to enforce each and every term and condition of this Agreement. No breach under this agreement shall be deemed waived or excused by either party unless such waiver or consent is in writing signed by the party granting such waiver or consent. The waiver by or consent of a party to a breach of any provision of this Agreement shall not operate or be construed as a waiver of or consent to any other or subsequent breach by such other party.
- This Agreement may not be assigned (including by operation of law or otherwise) by you without WILEY's prior written consent.
- Any fee required for this permission shall be non-refundable after thirty (30) days from receipt by the CCC.
- These terms and conditions together with CCC's Billing and Payment terms and conditions (which are incorporated herein) form the entire agreement between you and WILEY concerning this licensing transaction and (in the absence of fraud) supersedes all prior agreements and representations of the parties, oral or written. This Agreement may not be amended except in writing signed by both parties. This Agreement shall be binding upon and inure to the benefit of the parties' successors, legal representatives, and authorized assigns.
- In the event of any conflict between your obligations established by these terms and conditions and those established by CCC's Billing and Payment terms and conditions, these terms and conditions shall prevail.
- WILEY expressly reserves all rights not specifically granted in the combination of (i) the license details provided by you and accepted in the course of this licensing transaction, (ii) these terms and conditions and (iii) CCC's Billing and Payment terms and conditions.
- This Agreement will be void if the Type of Use, Format, Circulation, or Requestor Type was misrepresented during the licensing process.
- This Agreement shall be governed by and construed in accordance with the laws of the State of New York, USA, without regards to such state's conflict of law rules. Any legal action, suit or proceeding arising out of or relating to these Terms and Conditions or the breach thereof shall be instituted in a court of competent jurisdiction in New York County in the State of New York in the United States of America and each party hereby consents and submits to the personal jurisdiction of such court, waives any objection to venue in such court and consents to service of process by registered or certified mail, return receipt requested, at the last known address of such party.

WILEY OPEN ACCESS TERMS AND CONDITIONS

SPRINGER NATURE LICENSE
TERMS AND CONDITIONS

Mar 24, 2021

This Agreement between Imperial College London -- Aldara Martin Alonso ("You") and Springer Nature ("Springer Nature") consists of your license details and the terms and conditions provided by Springer Nature and Copyright Clearance Center.

License Number	5035560802832
License date	Mar 24, 2021
Licensed Content Publisher	Springer Nature
Licensed Content Publication	Nature Reviews Genetics
Licensed Content Title	Genetic approaches to studying energy balance: perception and integration
Licensed Content Author	Gregory S. Barsh et al
Licensed Content Date	Aug 1, 2002
Type of Use	Thesis/Dissertation
Requestor type	academic/university or research institute
Format	print and electronic
Portion	figures/tables/illustrations
Number of figures/tables/illustrations	1
High-res required	no
Will you be translating?	no
Circulation/distribution	1 - 29
Author of this Springer Nature content	no
Title	Investigating the physiological and pharmacological effects of the gut hormone peptide YY (PYY)
Institution name	Imperial College London
Expected presentation date	Mar 2021
Portions	Figure 2
Requestor Location	Imperial College London

Du Cane Road

London, W12 0NN
United Kingdom
Attn: Imperial College London

Total 0.00 GBP

Terms and Conditions

Springer Nature Customer Service Centre GmbH
Terms and Conditions

This agreement sets out the terms and conditions of the licence (the **Licence**) between you and **Springer Nature Customer Service Centre GmbH** (the **Licensor**). By clicking 'accept' and completing the transaction for the material (**Licensed Material**), you also confirm your acceptance of these terms and conditions.

1. Grant of License

1. 1. The Licensor grants you a personal, non-exclusive, non-transferable, world-wide licence to reproduce the Licensed Material for the purpose specified in your order only. Licences are granted for the specific use requested in the order and for no other use, subject to the conditions below.

1. 2. The Licensor warrants that it has, to the best of its knowledge, the rights to license reuse of the Licensed Material. However, you should ensure that the material you are requesting is original to the Licensor and does not carry the copyright of another entity (as credited in the published version).

1. 3. If the credit line on any part of the material you have requested indicates that it was reprinted or adapted with permission from another source, then you should also seek permission from that source to reuse the material.

2. Scope of Licence

2. 1. You may only use the Licensed Content in the manner and to the extent permitted by these Ts&Cs and any applicable laws.

2. 2. A separate licence may be required for any additional use of the Licensed Material, e.g. where a licence has been purchased for print only use, separate permission must be obtained for electronic re-use. Similarly, a licence is only valid in the language selected and does not apply for editions in other languages unless additional translation rights have been granted separately in the licence. Any content owned by third parties are expressly excluded from the licence.

2. 3. Similarly, rights for additional components such as custom editions and derivatives require additional permission and may be subject to an additional fee. Please apply to Journalpermissions@springernature.com/bookspermissions@springernature.com for these rights.

2. 4. Where permission has been granted **free of charge** for material in print, permission may also be granted for any electronic version of that work, provided that the material is incidental to your work as a whole and that the electronic version is essentially equivalent to, or substitutes for, the print version.

2. 5. An alternative scope of licence may apply to signatories of the STM Permissions Guidelines, as amended from time to time.

3. Duration of Licence

3. 1. A licence for is valid from the date of purchase ('Licence Date') at the end of the relevant period in the below table:

Scope of Licence	Duration of Licence
Post on a website	12 months
Presentations	12 months
Books and journals	Lifetime of the edition in the language purchased

4. Acknowledgement

4. 1. The Licensor's permission must be acknowledged next to the Licenced Material in print. In electronic form, this acknowledgement must be visible at the same time as the figures/tables/illustrations or abstract, and must be hyperlinked to the journal/book's

homepage. Our required acknowledgement format is in the Appendix below.

5. Restrictions on use

5. 1. Use of the Licensed Material may be permitted for incidental promotional use and minor editing privileges e.g. minor adaptations of single figures, changes of format, colour and/or style where the adaptation is credited as set out in Appendix 1 below. Any other changes including but not limited to, cropping, adapting, omitting material that affect the meaning, intention or moral rights of the author are strictly prohibited.

5. 2. You must not use any Licensed Material as part of any design or trademark.

5. 3. Licensed Material may be used in Open Access Publications (OAP) before publication by Springer Nature, but any Licensed Material must be removed from OAP sites prior to final publication.

6. Ownership of Rights

6. 1. Licensed Material remains the property of either Licensor or the relevant third party and any rights not explicitly granted herein are expressly reserved.

7. Warranty

IN NO EVENT SHALL LICENSOR BE LIABLE TO YOU OR ANY OTHER PARTY OR ANY OTHER PERSON OR FOR ANY SPECIAL, CONSEQUENTIAL, INCIDENTAL OR INDIRECT DAMAGES, HOWEVER CAUSED, ARISING OUT OF OR IN CONNECTION WITH THE DOWNLOADING, VIEWING OR USE OF THE MATERIALS REGARDLESS OF THE FORM OF ACTION, WHETHER FOR BREACH OF CONTRACT, BREACH OF WARRANTY, TORT, NEGLIGENCE, INFRINGEMENT OR OTHERWISE (INCLUDING, WITHOUT LIMITATION, DAMAGES BASED ON LOSS OF PROFITS, DATA, FILES, USE, BUSINESS OPPORTUNITY OR CLAIMS OF THIRD PARTIES), AND
WHETHER OR NOT THE PARTY HAS BEEN ADVISED OF THE POSSIBILITY OF SUCH DAMAGES. THIS LIMITATION SHALL APPLY NOTWITHSTANDING ANY FAILURE OF ESSENTIAL PURPOSE OF ANY LIMITED REMEDY PROVIDED HEREIN.

8. Limitations

8. 1. ***BOOKS ONLY*** Where 'reuse in a dissertation/thesis' has been selected the following terms apply: Print rights of the final author's accepted manuscript (for clarity, NOT the published version) for up to 100 copies, electronic rights for use only on a personal website or institutional repository as defined by the Sherpa guideline (www.sherpa.ac.uk/romeo/).

8. 2. For content reuse requests that qualify for permission under the STM Permissions Guidelines, which may be updated from time to time, the STM Permissions Guidelines supersede the terms and conditions contained in this licence.

9. Termination and Cancellation

9. 1. Licences will expire after the period shown in Clause 3 (above).

9. 2. Licensee reserves the right to terminate the Licence in the event that payment is not received in full or if there has been a breach of this agreement by you.

Appendix 1 — Acknowledgements:

For Journal Content:
Reprinted by permission from **[the Licensor]**: **[Journal Publisher (e.g. Nature/Springer/Palgrave)]** **[JOURNAL NAME]** **[REFERENCE CITATION** (Article name, Author(s) Name), **[COPYRIGHT]** (year of publication)

For Advance Online Publication papers:
Reprinted by permission from **[the Licensor]**: **[Journal Publisher (e.g. Nature/Springer/Palgrave)]** **[JOURNAL NAME]** **[REFERENCE CITATION** (Article name, Author(s) Name), **[COPYRIGHT]** (year of publication), advance online publication, day month year (doi: 10.1038/sj.[JOURNAL ACRONYM].)

For Adaptations/Translations:
Adapted/Translated by permission from **[the Licensor]**: **[Journal Publisher** (e.g.

Nature/Springer/Palgrave)] [JOURNAL NAME] [REFERENCE CITATION (Article name, Author(s) Name), [COPYRIGHT] (year of publication)

Note: For any republication from the British Journal of Cancer, the following credit line style applies:

Reprinted/adapted/translated by permission from [the Licensor]: on behalf of Cancer Research UK: : [Journal Publisher (e.g. Nature/Springer/Palgrave)] [JOURNAL NAME] [REFERENCE CITATION (Article name, Author(s) Name), [COPYRIGHT] (year of publication)

For Advance Online Publication papers:
Reprinted by permission from The [the Licensor]: on behalf of Cancer Research UK: [Journal Publisher (e.g. Nature/Springer/Palgrave)] [JOURNAL NAME] [REFERENCE CITATION (Article name, Author(s) Name), [COPYRIGHT] (year of publication), advance online publication, day month year (doi: 10.1038/sj. [JOURNAL ACRONYM])

For Book content:
Reprinted/adapted by permission from [the Licensor]: [Book Publisher (e.g. Palgrave Macmillan, Springer etc) [Book Title] by [Book author(s)] [COPYRIGHT] (year of publication)

Other Conditions:

Version 1.3

Questions? customercare@copyright.com or +1-855-239-3415 (toll free in the US) or +1-978-646-2777.

ELSEVIER LICENSE
TERMS AND CONDITIONS

Mar 24, 2021

This Agreement between Imperial College London -- Aldara Martin Alonso ("You") and Elsevier ("Elsevier") consists of your license details and the terms and conditions provided by Elsevier and Copyright Clearance Center.

License Number	5035550554919
License date	Mar 24, 2021
Licensed Content Publisher	Elsevier
Licensed Content Publication	Cell Metabolism
Licensed Content Title	A Gut Feeling for Obesity: 7TM Sensors on Enteroendocrine Cells
Licensed Content Author	Maja S. Engelstoft,Kristoffer L. Egerod,Birgitte Holst,Thue W. Schwartz
Licensed Content Date	Dec 6, 2008
Licensed Content Volume	8
Licensed Content Issue	6
Licensed Content Pages	3
Start Page	447
End Page	449
Type of Use	reuse in a thesis/dissertation
Portion	figures/tables/illustrations
Number of figures/tables/illustrations	1
Format	both print and electronic
Are you the author of this Elsevier article?	No
Will you be translating?	No
Title	Investigating the physiological and pharmacological effects of the gut hormone peptide YY (PYY)
Institution name	Imperial College London
Expected presentation date	Mar 2021

Portions	Figure 1
Requestor Location	Imperial College London Du Cane Road London, W12 0NN United Kingdom Attn: Imperial College London
Publisher Tax ID	GB 494 6272 12
Total	0.00 GBP

Terms and Conditions

INTRODUCTION

1. The publisher for this copyrighted material is Elsevier. By clicking "accept" in connection with completing this licensing transaction, you agree that the following terms and conditions apply to this transaction (along with the Billing and Payment terms and conditions established by Copyright Clearance Center, Inc. ("CCC"), at the time that you opened your Rightslink account and that are available at any time at http://myaccount.copyright.com).

GENERAL TERMS

2. Elsevier hereby grants you permission to reproduce the aforementioned material subject to the terms and conditions indicated.

3. Acknowledgement: If any part of the material to be used (for example, figures) has appeared in our publication with credit or acknowledgement to another source, permission must also be sought from that source. If such permission is not obtained then that material may not be included in your publication/copies. Suitable acknowledgement to the source must be made, either as a footnote or in a reference list at the end of your publication, as follows:

"Reprinted from Publication title, Vol /edition number, Author(s), Title of article / title of chapter, Pages No., Copyright (Year), with permission from Elsevier [OR APPLICABLE SOCIETY COPYRIGHT OWNER]." Also Lancet special credit - "Reprinted from The Lancet, Vol. number, Author(s), Title of article, Pages No., Copyright (Year), with permission from Elsevier."

4. Reproduction of this material is confined to the purpose and/or media for which permission is hereby given.

5. Altering/Modifying Material: Not Permitted. However figures and illustrations may be altered/adapted minimally to serve your work. Any other abbreviations, additions, deletions and/or any other alterations shall be made only with prior written authorization of Elsevier Ltd. (Please contact Elsevier's permissions helpdesk here). No modifications can be made to any Lancet figures/tables and they must be reproduced in full.

6. If the permission fee for the requested use of our material is waived in this instance, please be advised that your future requests for Elsevier materials may attract a fee.

7. Reservation of Rights: Publisher reserves all rights not specifically granted in the combination of (i) the license details provided by you and accepted in the course of this licensing transaction, (ii) these terms and conditions and (iii) CCC's Billing and Payment terms and conditions.

8. License Contingent Upon Payment: While you may exercise the rights licensed immediately upon issuance of the license at the end of the licensing process for the transaction, provided that you have disclosed complete and accurate details of your proposed use, no license is finally effective unless and until full payment is received from you (either by publisher or by CCC) as provided in CCC's Billing and Payment terms and conditions. If full payment is not received on a timely basis, then any license preliminarily granted shall be deemed automatically revoked and shall be void as if never granted. Further, in the event that you breach any of these terms and conditions or any of CCC's Billing and Payment terms and conditions, the license is automatically revoked and shall be void as if never granted. Use of materials as described in a revoked license, as well as any use of the materials beyond the scope of an unrevoked license, may constitute copyright infringement and publisher reserves the right to take any and all action to protect its copyright in the materials.

9. Warranties: Publisher makes no representations or warranties with respect to the licensed material.

10. Indemnity: You hereby indemnify and agree to hold harmless publisher and CCC, and their respective officers, directors, employees and agents, from and against any and all claims arising out of your use of the licensed material other than as specifically authorized pursuant to this license.

11. No Transfer of License: This license is personal to you and may not be sublicensed, assigned, or transferred by you to any other person without publisher's written permission.

12. No Amendment Except in Writing: This license may not be amended except in a writing signed by both parties (or, in the case of publisher, by CCC on publisher's behalf).

13. Objection to Contrary Terms: Publisher hereby objects to any terms contained in any purchase order, acknowledgment, check endorsement or other writing prepared by you, which terms are inconsistent with these terms and conditions or CCC's Billing and Payment terms and conditions. These terms and conditions, together with CCC's Billing and Payment terms and conditions (which are incorporated herein), comprise the entire agreement between you and publisher (and CCC) concerning this licensing transaction. In the event of any conflict between your obligations established by these terms and conditions and those established by CCC's Billing and Payment terms and conditions, these terms and conditions shall control.

14. Revocation: Elsevier or Copyright Clearance Center may deny the permissions described in this License at their sole discretion, for any reason or no reason, with a full refund payable to you. Notice of such denial will be made using the contact information provided by you. Failure to receive such notice will not alter or invalidate the denial. In no event will Elsevier or Copyright Clearance Center be responsible or liable for any costs, expenses or damage incurred by you as a result of a denial of your permission request, other than a refund of the amount(s) paid by you to Elsevier and/or Copyright Clearance Center for denied permissions.

LIMITED LICENSE

The following terms and conditions apply only to specific license types:

15. **Translation**: This permission is granted for non-exclusive world **English** rights only unless your license was granted for translation rights. If you licensed translation rights you may only translate this content into the languages you requested. A professional translator must perform all translations and reproduce the content word for word preserving the integrity of the article.

16. **Posting licensed content on any Website**: The following terms and conditions apply as follows: Licensing material from an Elsevier journal: All content posted to the web site must maintain the copyright information line on the bottom of each image; A hyper-text must be included to the Homepage of the journal from which you are licensing at http://www.sciencedirect.com/science/journal/xxxxx or the Elsevier homepage for books at http://www.elsevier.com; Central Storage: This license does not include permission for a scanned version of the material to be stored in a central repository such as that provided by Heron/XanEdu.

Licensing material from an Elsevier book: A hyper-text link must be included to the Elsevier homepage at http://www.elsevier.com . All content posted to the web site must maintain the copyright information line on the bottom of each image.

Posting licensed content on Electronic reserve: In addition to the above the following clauses are applicable: The web site must be password-protected and made available only to bona fide students registered on a relevant course. This permission is granted for 1 year only. You may obtain a new license for future website posting.

17. **For journal authors**: the following clauses are applicable in addition to the above:

Preprints:

A preprint is an author's own write-up of research results and analysis, it has not been peer-reviewed, nor has it had any other value added to it by a publisher (such as formatting, copyright, technical enhancement etc.).

Authors can share their preprints anywhere at any time. Preprints should not be added to or enhanced in any way in order to appear more like, or to substitute for, the final versions of articles however authors can update their preprints on arXiv or RePEc with their Accepted Author Manuscript (see below).

If accepted for publication, we encourage authors to link from the preprint to their formal publication via its DOI. Millions of researchers have access to the formal publications on ScienceDirect, and so links will help users to find, access, cite and use the best available version. Please note that Cell Press, The Lancet and some society-owned have different preprint policies. Information on these policies is available on the journal homepage.

Accepted Author Manuscripts: An accepted author manuscript is the manuscript of an article that has been accepted for publication and which typically includes author-incorporated changes suggested during submission, peer review and editor-author communications.

Authors can share their accepted author manuscript:

- immediately
  - via their non-commercial person homepage or blog
  - by updating a preprint in arXiv or RePEc with the accepted manuscript
  - via their research institute or institutional repository for internal institutional uses or as part of an invitation-only research collaboration work-group

- directly by providing copies to their students or to research collaborators for their personal use
- for private scholarly sharing as part of an invitation-only work group on commercial sites with which Elsevier has an agreement

- After the embargo period
  - via non-commercial hosting platforms such as their institutional repository
  - via commercial sites with which Elsevier has an agreement

In all cases accepted manuscripts should:

- link to the formal publication via its DOI
- bear a CC-BY-NC-ND license - this is easy to do
- if aggregated with other manuscripts, for example in a repository or other site, be shared in alignment with our hosting policy not be added to or enhanced in any way to appear more like, or to substitute for, the published journal article.

Published journal article (JPA): A published journal article (PJA) is the definitive final record of published research that appears or will appear in the journal and embodies all value-adding publishing activities including peer review co-ordination, copy-editing, formatting, (if relevant) pagination and online enrichment.

Policies for sharing publishing journal articles differ for subscription and gold open access articles:

Subscription Articles: If you are an author, please share a link to your article rather than the full-text. Millions of researchers have access to the formal publications on ScienceDirect, and so links will help your users to find, access, cite, and use the best available version.

Theses and dissertations which contain embedded PJAs as part of the formal submission can be posted publicly by the awarding institution with DOI links back to the formal publications on ScienceDirect.

If you are affiliated with a library that subscribes to ScienceDirect you have additional private sharing rights for others' research accessed under that agreement. This includes use for classroom teaching and internal training at the institution (including use in course packs and courseware programs), and inclusion of the article for grant funding purposes.

Gold Open Access Articles: May be shared according to the author-selected end-user license and should contain a CrossMark logo, the end user license, and a DOI link to the formal publication on ScienceDirect.

Please refer to Elsevier's posting policy for further information.

18. **For book authors** the following clauses are applicable in addition to the above: Authors are permitted to place a brief summary of their work online only. You are not allowed to download and post the published electronic version of your chapter, nor may you scan the printed edition to create an electronic version. **Posting to a repository:** Authors are permitted to post a summary of their chapter only in their institution's repository.

19. **Thesis/Dissertation:** If your license is for use in a thesis/dissertation your thesis may be submitted to your institution in either print or electronic form. Should your thesis be published commercially, please reapply for permission. These requirements include permission for the Library and Archives of Canada to supply single copies, on demand, of the complete thesis and include permission for Proquest/UMI to supply single copies, on demand, of the complete thesis. Should your thesis be published commercially, please reapply for permission. Theses and dissertations which contain embedded PJAs as part of the formal submission can be posted publicly by the awarding institution with DOI links back to the formal publications on ScienceDirect.

Elsevier Open Access Terms and Conditions:

You can publish open access with Elsevier in hundreds of open access journals or in nearly 2000 established subscription journals that support open access publishing. Permitted third party re-use of these open access articles is defined by the author's choice of Creative Commons user license. See our open access license policy for more information.

Terms & Conditions applicable to all Open Access articles published with Elsevier:

Any reuse of the article must not represent the author as endorsing the adaptation of the article nor should the article be modified in such a way as to damage the author's honour or reputation. If any changes have been made, such changes must be clearly indicated.

The author(s) must be appropriately credited and we ask that you include the end user license and a DOI link to the formal publication on ScienceDirect.

If any part of the material to be used (for example, figures) has appeared in our publication with credit or acknowledgement to another source it is the responsibility of the user to ensure their reuse complies with the terms and conditions determined by the rights holder.

Additional Terms & Conditions applicable to each Creative Commons user license:

CC BY: The CC-BY license allows users to copy, to create extracts, abstracts and new works from the Article, to alter and revise the Article and to make commercial use of the

JOHN WILEY AND SONS LICENSE
TERMS AND CONDITIONS

Mar 08, 2021

This Agreement between Imperial College London -- Aldara Martin Alonso ("You") and John Wiley and Sons ("John Wiley and Sons") consists of your license details and the terms and conditions provided by John Wiley and Sons and Copyright Clearance Center.

License Number	5024150525911
License date	Mar 08, 2021
Licensed Content Publisher	John Wiley and Sons
Licensed Content Publication	Annals of the New York Academy of Sciences
Licensed Content Title	Vagal mechanisms as neuromodulatory targets for the treatment of metabolic disease
Licensed Content Author	Winfried L. Neuhuber, Hans-Rudolf Berthoud
Licensed Content Date	Jul 3, 2019
Licensed Content Volume	1454
Licensed Content Issue	1
Licensed Content Pages	14
Type of use	Dissertation/Thesis
Requestor type	University/Academic

Format	Electronic
Portion	Figure/table
Number of figures/tables	1
Will you be translating?	No
Title	Investigating the physiological and pharmacological effects of the gut hormone peptide YY (PYY)
Institution name	Imperial College London
Expected presentation date	Mar 2021
Portions	Figure 2
Requestor Location	Imperial College London Du Cane Road London, W12 0NN United Kingdom Attn: Imperial College London
Publisher Tax ID	EU826007151
Total	0.00 GBP

Terms and Conditions

TERMS AND CONDITIONS

This copyrighted material is owned by or exclusively licensed to John Wiley & Sons, Inc. or one of its group companies (each a"Wiley Company") or handled on behalf of a society with which a Wiley Company has exclusive publishing rights in relation to a particular work (collectively "WILEY"). By clicking "accept" in connection with completing this licensing transaction, you agree that the following terms and conditions apply to this transaction (along with the billing and payment terms and conditions established by the Copyright Clearance Center Inc., ("CCC's Billing and Payment terms and conditions"), at the time that

you opened your RightsLink account (these are available at any time at http://myaccount.copyright.com).

Terms and Conditions

- The materials you have requested permission to reproduce or reuse (the "Wiley Materials") are protected by copyright.

- You are hereby granted a personal, non-exclusive, non-sub licensable (on a stand-alone basis), non-transferable, worldwide, limited license to reproduce the Wiley Materials for the purpose specified in the licensing process. This license, **and any CONTENT (PDF or image file) purchased as part of your order,** is for a one-time use only and limited to any maximum distribution number specified in the license. The first instance of republication or reuse granted by this license must be completed within two years of the date of the grant of this license (although copies prepared before the end date may be distributed thereafter). The Wiley Materials shall not be used in any other manner or for any other purpose, beyond what is granted in the license. Permission is granted subject to an appropriate acknowledgement given to the author, title of the material/book/journal and the publisher. You shall also duplicate the copyright notice that appears in the Wiley publication in your use of the Wiley Material. Permission is also granted on the understanding that nowhere in the text is a previously published source acknowledged for all or part of this Wiley Material. Any third party content is expressly excluded from this permission.

- With respect to the Wiley Materials, all rights are reserved. Except as expressly granted by the terms of the license, no part of the Wiley Materials may be copied, modified, adapted (except for minor reformatting required by the new Publication), translated, reproduced, transferred or distributed, in any form or by any means, and no derivative works may be made based on the Wiley Materials without the prior permission of the respective copyright owner.**For STM Signatory Publishers clearing permission under the terms of the STM Permissions Guidelines only, the terms of the license are extended to include subsequent editions and for editions in other languages, provided such editions are for the work as a whole in situ and does not involve the separate exploitation of the permitted figures or extracts,** You may not alter, remove or suppress in any manner any copyright, trademark or other notices displayed by the Wiley Materials. You may not license, rent, sell, loan, lease, pledge, offer as security, transfer or assign the Wiley Materials on a stand-alone basis, or any of the rights granted to you hereunder to any other person.

- The Wiley Materials and all of the intellectual property rights therein shall at all times remain the exclusive property of John Wiley & Sons Inc, the Wiley Companies, or their respective licensors, and your interest therein is only that of having possession of and the right to reproduce the Wiley Materials pursuant to Section 2 herein during the continuance of this Agreement. You agree that you own no right, title or interest in or to the Wiley Materials or any of the intellectual property rights therein. You shall have no rights hereunder other than the license as provided for above in Section 2. No right, license or interest to any trademark, trade name, service mark or other branding ("Marks") of WILEY or its licensors is granted hereunder, and you agree that you shall not assert any such right, license or interest with respect thereto

- NEITHER WILEY NOR ITS LICENSORS MAKES ANY WARRANTY OR REPRESENTATION OF ANY KIND TO YOU OR ANY THIRD PARTY, EXPRESS, IMPLIED OR STATUTORY, WITH RESPECT TO THE MATERIALS OR THE ACCURACY OF ANY INFORMATION CONTAINED IN THE MATERIALS, INCLUDING, WITHOUT LIMITATION, ANY IMPLIED WARRANTY OF MERCHANTABILITY, ACCURACY, SATISFACTORY QUALITY, FITNESS FOR A PARTICULAR PURPOSE, USABILITY,

INTEGRATION OR NON-INFRINGEMENT AND ALL SUCH WARRANTIES ARE HEREBY EXCLUDED BY WILEY AND ITS LICENSORS AND WAIVED BY YOU.

- WILEY shall have the right to terminate this Agreement immediately upon breach of this Agreement by you.
- You shall indemnify, defend and hold harmless WILEY, its Licensors and their respective directors, officers, agents and employees, from and against any actual or threatened claims, demands, causes of action or proceedings arising from any breach of this Agreement by you.
- IN NO EVENT SHALL WILEY OR ITS LICENSORS BE LIABLE TO YOU OR ANY OTHER PARTY OR ANY OTHER PERSON OR ENTITY FOR ANY SPECIAL, CONSEQUENTIAL, INCIDENTAL, INDIRECT, EXEMPLARY OR PUNITIVE DAMAGES, HOWEVER CAUSED, ARISING OUT OF OR IN CONNECTION WITH THE DOWNLOADING, PROVISIONING, VIEWING OR USE OF THE MATERIALS REGARDLESS OF THE FORM OF ACTION, WHETHER FOR BREACH OF CONTRACT, BREACH OF WARRANTY, TORT, NEGLIGENCE, INFRINGEMENT OR OTHERWISE (INCLUDING, WITHOUT LIMITATION, DAMAGES BASED ON LOSS OF PROFITS, DATA, FILES, USE, BUSINESS OPPORTUNITY OR CLAIMS OF THIRD PARTIES), AND WHETHER OR NOT THE PARTY HAS BEEN ADVISED OF THE POSSIBILITY OF SUCH DAMAGES. THIS LIMITATION SHALL APPLY NOTWITHSTANDING ANY FAILURE OF ESSENTIAL PURPOSE OF ANY LIMITED REMEDY PROVIDED HEREIN.
- Should any provision of this Agreement be held by a court of competent jurisdiction to be illegal, invalid, or unenforceable, that provision shall be deemed amended to achieve as nearly as possible the same economic effect as the original provision, and the legality, validity and enforceability of the remaining provisions of this Agreement shall not be affected or impaired thereby.
- The failure of either party to enforce any term or condition of this Agreement shall not constitute a waiver of either party's right to enforce each and every term and condition of this Agreement. No breach under this agreement shall be deemed waived or excused by either party unless such waiver or consent is in writing signed by the party granting such waiver or consent. The waiver by or consent of a party to a breach of any provision of this Agreement shall not operate or be construed as a waiver of or consent to any other or subsequent breach by such other party.
- This Agreement may not be assigned (including by operation of law or otherwise) by you without WILEY's prior written consent.
- Any fee required for this permission shall be non-refundable after thirty (30) days from receipt by the CCC.
- These terms and conditions together with CCC's Billing and Payment terms and conditions (which are incorporated herein) form the entire agreement between you and WILEY concerning this licensing transaction and (in the absence of fraud) supersedes all prior agreements and representations of the parties, oral or written. This Agreement may not be amended except in writing signed by both parties. This Agreement shall be binding upon and inure to the benefit of the parties' successors, legal representatives, and authorized assigns.
- In the event of any conflict between your obligations established by these terms and conditions and those established by CCC's Billing and Payment terms and conditions,

these terms and conditions shall prevail.

- WILEY expressly reserves all rights not specifically granted in the combination of (i) the license details provided by you and accepted in the course of this licensing transaction, (ii) these terms and conditions and (iii) CCC's Billing and Payment terms and conditions.
- This Agreement will be void if the Type of Use, Format, Circulation, or Requestor Type was misrepresented during the licensing process.
- This Agreement shall be governed by and construed in accordance with the laws of the State of New York, USA, without regards to such state's conflict of law rules. Any legal action, suit or proceeding arising out of or relating to these Terms and Conditions or the breach thereof shall be instituted in a court of competent jurisdiction in New York County in the State of New York in the United States of America and each party hereby consents and submits to the personal jurisdiction of such court, waives any objection to venue in such court and consents to service of process by registered or certified mail, return receipt requested, at the last known address of such party.

WILEY OPEN ACCESS TERMS AND CONDITIONS

Wiley Publishes Open Access Articles in fully Open Access Journals and in Subscription journals offering Online Open. Although most of the fully Open Access journals publish open access articles under the terms of the Creative Commons Attribution (CC BY) License only, the subscription journals and a few of the Open Access Journals offer a choice of Creative Commons Licenses. The license type is clearly identified on the article.

The Creative Commons Attribution License

The Creative Commons Attribution License (CC-BY) allows users to copy, distribute and transmit an article, adapt the article and make commercial use of the article. The CC-BY license permits commercial and non-

Creative Commons Attribution Non-Commercial License

The Creative Commons Attribution Non-Commercial (CC-BY-NC)License permits use, distribution and reproduction in any medium, provided the original work is properly cited and is not used for commercial purposes.(see below)

Creative Commons Attribution-Non-Commercial-NoDerivs License

The Creative Commons Attribution Non-Commercial-NoDerivs License (CC-BY-NC-ND) permits use, distribution and reproduction in any medium, provided the original work is properly cited, is not used for commercial purposes and no modifications or adaptations are made. (see below)

Use by commercial "for-profit" organizations

Use of Wiley Open Access articles for commercial, promotional, or marketing purposes requires further explicit permission from Wiley and will be subject to a fee.

Further details can be found on Wiley Online Library
http://olabout.wiley.com/WileyCDA/Section/id-410895.html

Other Terms and Conditions:

v1.10 Last updated September 2015

Questions? customercare@copyright.com or +1-855-239-3415 (toll free in the US) or +1-978-646-2777.